THE ROLE OF PDZ DOMAIN-CONTAINING PROTEINS IN FRIZZLED-7 RECEPTOR SIGNALLING

by

IZABELA AGNIESZKA BOMBIK

A thesis submitted to the University of Birmingham for the degree of

DOCTOR OF PHILOSOPHY

School of Cancer Sciences

College of Medical and Dental Sciences

University of Birmingham

October 2014

ABSTRACT

Wnt signalling is one the most important pathways involved in embryonic development. It controls a number of processes including cellular proliferation, stem cell maintenance, cell fate decisions and establishment of tissue polarity. It is also frequently deregulated in human cancers. Frizzled-7 (Fz7) is a member of the Frizzled family of receptors responsible for the signal transduction in Wnt signalling. Frizzled-7 has been reported to be upregulated in several types of cancer. Furthermore, recent reports suggest that endocytosis of Frizzled may play a critical role in enhancing role in Wnt signal transduction, thus facilitating cancer development. We demonstrate here that the C-terminal PDZ binding motif (PDZ-BM) of Frizzled-7 contributes to signalling triggered by the receptor. We also explore the interaction between Frizzled-7 and syntenin-1, a PDZ domain containing protein that controls endocytic trafficking of various transmembrane proteins. We demonstrate that syntenin-1 regulates Frizzled-7 cell distribution and also modulates canonical Wnt signalling in epithelial breast cancer cells. Further, we report that the C-terminal PDZ-BM of Fz7 is indispensable for the receptor interaction with a number of PDZ proteins that control protein trafficking and cell polarity. Among these PDZ proteins are LNX1 and LNX2, E3 ubiquitin ligases which are known to control trafficking of transmembrane proteins. In this study we characterize the interaction between Frizzled-7 and LNX2. We demonstrate that LNX2 influences ubiquitylation of Frizzled-7 and has the ability to moderate signal transduction within the canonical Wnt pathway in breast cancer cells.

To my parents,

for their love, endless support

and encouragement

ACKNOWLEDGEMENTS

I would like to express my gratitude to my supervisor, Dr Fedor Berditchevski, who welcomed me in his laboratory and made this thesis possible. I am thankful for all his help and advice throughout this project. Further, I would like to thank my co-supervisors, Dr Neil Hotchin and Dr Chris Tselepis, for their constructive advice during my studies and guidance. I extremely appreciate all your help, support and effort put into my progress. It was a great privilege to work with all of you. A special thanks to Dr Rajesh Sundaresan for providing the NMR data, to Dr Douglass Ward for his help in producing and analysing mass spectrometry data and to Dr Elena Odintsova for her help with confocal microscopy. Additionally, I would like to extend my gratitude to Cancer Research UK for funding my research.

I wish to express my profound thanks to all my dear friends and colleagues with whom I had the pleasure of working. For their help, encouragement and never being too busy whenever I needed their help. Especially I would like to thank Vera for helping me to stand on my feet when I first arrived to Birmingham; Ruzica for her patience with my endless questions; Eva and Michael for their good humour and always being there for me. Thank you to Tijs, Kamil, Kiren, Anna and everyone else on the fifth floor, for making my short stay in Biosciences a wonderful experience. It wouldn't have been the same without all of you.

I am also thankful to all my friends who made my time in Birmingham unforgettable. Special thanks to Kasia, for being an amazing housemate and friend for the past three years. Also thank you to Fiona, Natalie, Glenys and Angela, for their invaluable friendship and great times we spent together.

Finally, I also would like to thank my family, Mum, Dad, Natalia and Przemek, for their love, belief and support of all my choices. Without you I wouldn't be who I am today.

This work would not have been done without all those mentioned above and thus I extend my deepest appreciation to you all.

TABLE OF CONTENTS

LIST OF FIGURES

LIST OF TABLES

ABBREVIATIONS

AJ	adherens junction
ALL	acute lymphoblastic leukaemia
APC	adenomatosis polyposis coli
aPKC	atypical PKC
Arf6	ADP-ribosylation factor 6
AR-JP	autosomal recessive juvenile Parkinsonism
BRCA1	breast cancer type 1 susceptibility protein
BSA	bovine serum albumin
CAFs	cancer associated fibroblasts
CAMKII	calmodulin-dependent kinase II
cAMP	cyclic adenosine monophosphate
CAR	coxsackie and adenovirus receptor
CAST	calpastatin
cGMP	cyclic guanosine monophosphate
CK2	casein kinase 2
CKIα	casein kinase Iα
CLIC/GEEC	clathrin-independent carrier/GPI-AP-enriched early endosomal compartment
CLL	chronic lymphocytic leukaemia
CM	conditioned medium
CPZ	carboxypeptidase Z
CRD	cysteine-rich domain
CSKP	Peripheral plasma membrane protein CASK
CYLD	Ubiquitin carboxyl-terminal hydrolase CYLD
DAAM	DVL-associated activator of morphogenesis 1
Dab2	disabled-2
DAPI	4',6-diamidino-2-phenylindole
DDX17	probable ATP-dependent RNA helicase DDX17
DDX5	probable ATP-dependent RNA helicase DDX5
DEP	Dishevelled, Egl-10 and Pleckstrin domain
Div	diversin
DIX	Dishevelled and axin domain
Dkk	Dickkopf
DLG1	discs large 1
DLG2	discs large 2
DLG4	discs large 4
DMEM	Dulbecco's modified Eagle's medium
DMSO	dimethyl sulfoxide
DNA	deoxyribonucleic acid

dNTP	deoxyribonucleotide triphosphate
dPatj	Pals-1 associated tight junction protein
DTNA	dystrobrevin alpha
DTNB	dystrobrevin beta
DTT	ditiotreitol
DUB	deubiquitylating enzyme
DVL	Dishevelled
ECM	extracellular matrix
EDTA	ethylenediaminetetraacetic acid
EGFR	epidermal growth factor receptor
EIF4A	eukaryotic translation initiation factor 4A
EMT	epithelial-to-mesenchymal transition
ER	endoplasmic reticulum
ERK1/2	extracellular signal-regulated kinase 1
ES	embryonic stem cells
ESCRT	endosomal sorting complex required for transport
FACS	fluorescent activated cell sorting
FC	flow cytometry
FCS	Fetal Calf Serum
FGF	fibroblast growth factor
FHA	forkhead associated domain
FITC	fluorescein-5-isothiocyanate
FRIED	Frizzled interaction and ectoderm defects
Fz	Frizzled
FZD	Frizzled
GFP	green fluorescent protein
GOPC	Golgi associated PDZ and coiled-coil motif containing
GPC3	Glypican-3
GPCR	G protein-coupled receptor
GRIP	glutamate receptor-interacting protein
GSK3β	glycogen synthase kinase3β
GTP	guanosine triphosphate
HA	hemagglutinin
HCC	hepatocellular carcinoma
HDAC	histone deacetylase
HI-BSA	heat inactivated BSA
HMEC	human mammary epithelial cells
HNRPQ	heterogeneous nuclear ribonucleoprotein Q
HRP	horseradish peroxidise
HS	heparan sulphate
ICAT	Inhibitor of β-catenin and TCF
ICD	intracellular domain
IF	immunofluorescence
IFNγ	interferon γ

IL-5Rα	interleukin-5 receptor α
INADL	InaD-like protein
JAM4	junctional adhesion molecule 4
JNK	JUN-N-terminal kinase
KCNA4	shaker-type voltage-gated K+ channel
KLHL12	Kelch-like 12
KU70	ATP-dependent DNA helicase 2 subunit 1
KU86	ATP-dependent DNA helicase 2 subunit 2
LB	Luria Bertani broth
LGR5	leucine-rich repeat-containing G-protein coupled receptor 5
LGS	legless
LNX1	ligand of Numb protein X 1
LNX2	ligand of Numb protein X 2
LRP5/6	low-density lipoprotein receptor-related protein 5/6
LS-MS	liquid chromatography and mass spectrometry
mAb	monoclonal antibody
MAGE-B18	melanoma-associated antigen B18
MAGI1	membrane-associated guanylate kinase, WW and PDZ domain-containing protein 1
MAGI3	membrane-associated guanylate kinase, WW and PDZ domain-containing protein 3
MAPK	mitogen-activated protein kinase
MCCA	methylcrotonoyl-CoA carboxylase subunit alpha, mitochondrial
MDCK	Madin-Darby canine kidney
Mdm2	double minute 2 protein
MMP	matrix metalloproteinases
MMTV	mouse mammary tumour virus
MPDZ	Multiple PDZ domain protein
MPP5	MAGUK p55 subfamily member 5
MPP7	MAGUK p55 subfamily member 7
M-RIP	myosin phosphatase Rho interacting protein
MS	mass spectrometry
mTOR	mammalian target of rapamycin
MUPP1	multiple PDZ domain protein
MuSK	muscle skeletal receptor Tyr kinase
MVB	multivesicular bodies
MYH9	Myosin-9
NaCl	sodium chloride
NaF	sodium fluoride
NaN_2	sodium azide
$NaVO_3$	sodium orthovanadate
NEDL1	NEDD4-like E3 ubiquitin-protein ligase 1
NES	nuclear export signal

NFAT	nuclear factor of activated T cells
NF-κB	nuclear factor kappa-light-chain-enhancer of activated B cells
NHERF1	Na+/H+ exchange factor 1
Nkd2	Naked2
NLS	nuclear localization signal
NMR	nuclear magnetic resonance
OCT4	octamer-binding protein 4
pAb	polyclonal antibody
PAK6	p21-activated kinase 6
PALS	protein associated with Lin-7 1
PBK	PDZ-binding kinase
PBS	phosphate buffer saline
PCP	planar cell polarity
PCR	polymerase chain reaction
PDE	phosphodiesterase
PDZ	Postsynaptic density-95, Disc large, ZO-1
PDZ-BM	PDZ binding motif
PDZRN	PDZ and RING
PEI	polyethyleimine
PIP2	phosphatidylinositol 4,5-bisphosphate
PIPs	phosphatidylinositol phosphates
PIST	PDZ protein interacting specifically with TC10
PKC	protein kinase C
PKG	cGMP-dependent kinase G
PLC	phospholipase C
PLEKHG5	pleckstrin homology domain-containing family G member 5
PLOD1	procollagen-lysine,2-oxoglutarate 5-dioxygenase 1
PLOD3	procollagen-lysine,2-oxoglutarate 5-dioxygenase 3
PMSF	phenylmethylsulfonyl fluoride
PP2	protein phosphatase 2
PSD-93	postsynaptic density protein-93
PSD-95	postsynaptic density protein-95
PTEN	phosphatidylinositol 3,4,5-trisphosphate 3-phosphatase and dual-specificity protein phosphatase
PTHR1R	type I parathyroid hormone receptor
PTK7	protein Tyr kinase 7
PX	Phox homology domain
PYC	Pyruvate carboxylase, mitochondrial
RAB8B	Ras-related protein Rab-8B
Rbc3a	rabconnectin-3a
RhoA	RAS homologue-gene family member A
RhoC	RAS homologue-gene family member C
RING	Really Interesting New Gene domain
RKIP	Raf kinase inhibitor protein

RNF43	ring finger 43
ROCK	Rho-associated coiled-coil containing protein kinase
ROR	receptor Tyr kinase-like orphan receptor
RPM	rates per minute
RYK	receptor Tyr kinase
SAP97	synapse associated protein 97
SCC	sporadic colorectal cancer
SCRIB	Protein scribble homolog
SDCBP	syndecan binding protein
SDS-PAGE	sodium dodecyl sulphate-poliacrylamide gel electrophoresis
SFRP	secreted Frizzled-related protein
SH2	Src homology 2
SH3	Src homology 3
shRNA	small hairpin RNA
Sim1	single-minded homolog 1
siRNA	Small interfering RNA
SIRT1	NAD-dependent protein deacetylase sirtuin-1
SMO	Smoothened
SNX27	Sorting nexin-27
SOST	Sclerostin
SSTR5	somatostatin receptor subtype 5
Stbm	Strabismus
TCF/LEF	T-Cell Factor/Lymphoid Enhancer Factor
TGFα	transforming growth factor alpha
TGN	trans-Golgi network
TJ	tight junction
TMEN46	Transmembrane protein 46
TNBC	triple negative breast cancer
TP4A3	Protein tyrosine phosphatase type IVA 3
TSHR	thyroid stimulating hormone receptor
Ulk1	Unc-51-like kinase 1
USP8	ubiquitin specific protease 8
Vangl2	van Gogh-like 2
VEGF	vascular endothelial growth factor
VSDs	ventricular septal defects
WB	western blot
WIF	Wnt inhibitory factors
WRE	Wnt response elements
ZNRF3	zinc and ring finger 3
ZO-1	Tight junction protein ZO-1
ZO-2	Tight junction protein ZO-2

1. INTRODUCTION

1.1. Wnt signalling overview

Wnt signalling pathways evolved in multicellular organisms to mediate complex cell-cell communication during development and in adult tissue homeostasis. Wnt signalling plays an important role in the regulation of many biological processes, such as development, proliferation, stem cell maintenance, cell movement and establishment of tissue polarity (Fuerer et al. 2008). Deregulation of Wnt signalling contributes significantly to the development of cancer and emerges as a central mechanism in cancer biology (Polakis 2012).

Wnt signalling is extremely complex. It involves numerous components regulated in many steps and involves cross-talk with other pathways. There are three major pathways of Wnt signalling: the canonical pathway, also known as β-catenin-dependent pathway, and two noncanonical (β-catenin independent) pathways: the planar cell polarity (PCP) pathway and the Wnt/Ca^{2+} pathway. Activation of signal transduction in all of these pathways requires binding of a protein from the Wnt family to Frizzled receptors and co-receptors (Rao et al. 2010). A simplified overview of Wnt signalling pathways is presented in the Figure 1. 1.

Wnt ligands are glycoproteins belonging to a large family of cysteine-rich secreted growth factors. In humans, there are 19 genes encoding evolutionarily conserved Wnt proteins (Miller 2002). They can bind to different receptors and activate various downstream pathways. Several Wnts preferentially activate either canonical (Wnt1, Wnt3a, Wnt8) or non-

canonical pathways (Wnt5a and Wnt11). Nonetheless, Wnt activity depends on the cellular context and receptors on the cell surface, so Wnt proteins can not be strictly divided into subgroups based on the pathway they activate (Niehrs 2012).

There are more than 15 Wnt receptors and co-receptors, and their various combinations with Wnt proteins determine the nature and extent of downstream pathway activation. Wnt receptors and co-receptors include 10 Frizzled receptors, low-density lipoprotein receptor-related protein 5/6 (LRP5/6), receptor Tyr kinase-like orphan receptor (ROR), protein Tyr kinase 7 (PTK7), receptor Tyr kinase (RYK), muscle skeletal receptor Tyr kinase (MuSK) and proteoglycan families. This allows for a number of ligand-receptor combinations (Kikuchi et al. 2007). Additionally, Frizzled can act as a receptor for both, canonical and non-canonical pathways. The outcome depends on the co-receptor expressed in the cells; for example, LRP5/6 allows engagement of the canonical pathway, whereas ROR1/2 the non-canonical pathway (Niehrs 2012;van Amerongen R. et al. 2009). Figure 1.2. summarizes reported Wnt/Frizzled interactions.

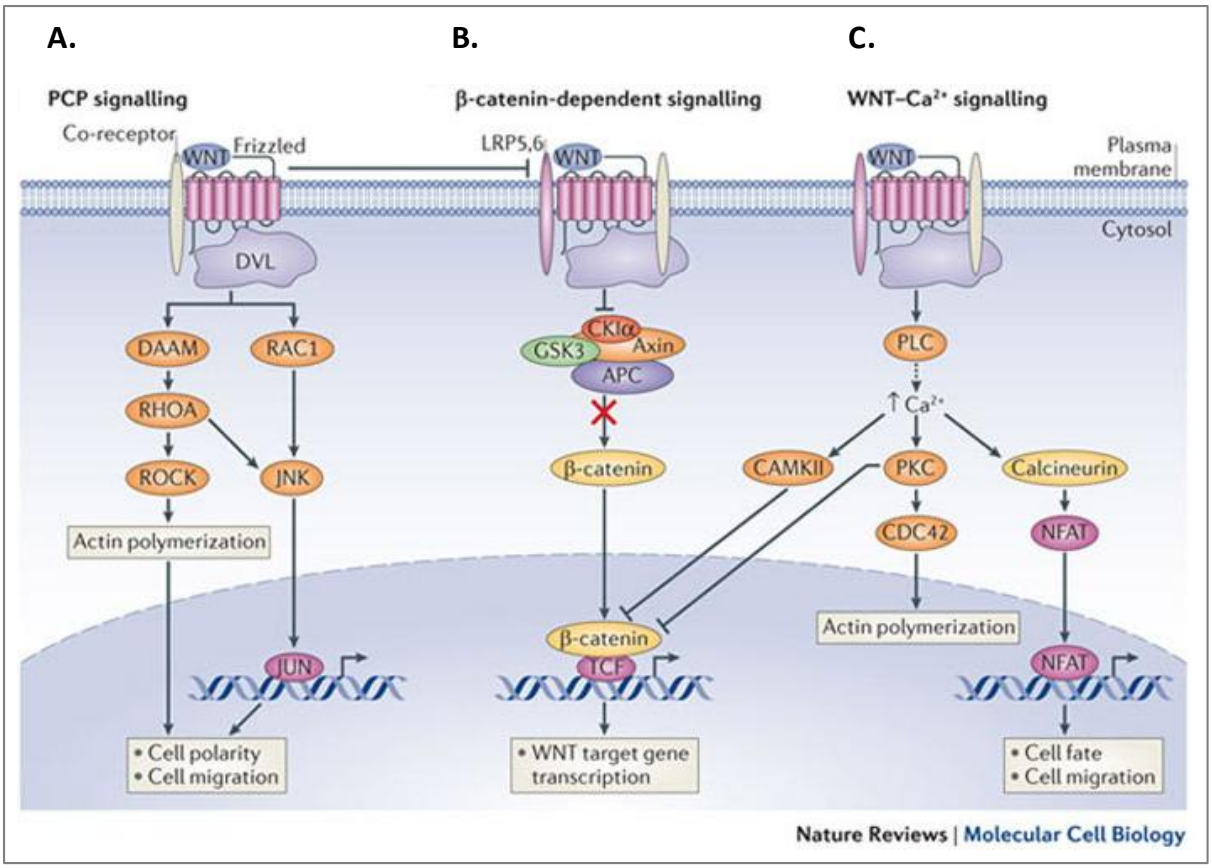

Figure 1. 1. Wnt signalling pathways.

A simplified diagram showing the main pathways mediated by Wnt proteins, Frizzled receptors and Wnt co-receptors interactions. (A) Noncanonical planar cell polarity (PCP) signalling triggers activation RHO kinase (ROCK) and JUN-N-terminal kinase (JNK), leading to actin polymerization and microtubule stabilization. This pathway is involved in the cell polarity regulation, cell motility and morphogenetic movements. (B) Canonical Wnt signalling pathway. Upon stimulation with Wnt ligand, the β-catenin destruction complex (glycogen synthase kinase3β (GSK3β), casein kinase Iα (CKIα), Axin and adenomatosis polyposis coli (APC)) is recruited to the Wnt–Frizzled complex and inactivated. This leads to β-catenin accumulation and translocation to the nucleus, where it initiates the transcription of Wnt target genes under the control of T cell factor (TCF). (C) The Wnt/Ca2+ pathway activates Ca2+- and calmodulin-dependent kinase II (CAMKII), protein kinase C (PKC) and calcineurin. Calcineurin activates nuclear factor of activated T cells (NFAT), which regulates the transcription of genes involved in regulation of cell fate and cell migration. PCP and Ca2+ pathways antagonize β-catenin signalling at various levels. PLC, phospholipase C; DAAM, DVL-associated activator of morphogenesis 1; DVL, Dishevelled; LRP, low-density lipoprotein receptor-related protein. Figure reproduced and modified from (Niehrs 2012).

WNT	1	2	2B	3	3A	4	5A	5B	6	7A	7B	8A	8B	9A	9B	10A	10B	11	16
FZD_1	x	x		o	x		x	o		o	x								
FZD_2		o		o	o		x		o	o	o		o						
FZD_3		x			x		x												
FZD_4		x	x		o		o				x								
FZD_5		o			x		x			x					o		o		
FZD_6					x	x	x	o		o									
FZD_7				x	x		o			o									
FZD_8					x										o				
FZD_9		x																	
FZD_{10}											x								

Figure 1. 2. Wnt/Frizzled interactions.

An overview of reported human Wnt/Frizzled combinations and their possible interaction. Crosses (x) indicate evidence for direct binding based on immunoprecipitation, whereas circles (o) indicate colocalization, signalling outcomes such as TCF reporter activity, TOPFlash or internalization. Green indicates data already present in the IUPHAR Database. Figure is reproduced from (Dijksterhuis et al. 2014).

1.1.1. Molecular mechanism of Wnt canonical pathway

The best-characterized Wnt pathway described in the literature is the so-called canonical Wnt pathway. It is also known as the β-catenin dependent pathway, as it involves a multifunctional protein β-catenin. β-catenin was discovered as a part of adherens junction complex, where it interacts with E-cadherin and α-catenin (McCrea et al. 1991). It has an important function in cadherin-based cell adhesion. It is also a central component of the canonical Wnt signalling pathway, and serves as a transcription co-factor through interacting with TCF/LEF (T-Cell Factor/Lymphoid Enhancer Factor) proteins in the nucleus (Behrens et al. 1996). It was proposed that dissociation of β-catenin from the cadherin complex (E-

cadherin-β-catenin-α-catenin) causes loss of cell adhesion and promotes the migration of cancer cells (Xu et al. 2007).

In the absence of Wnt ligand, the cellular levels of β-catenin are strictly controlled by a multi-protein destruction complex composed of axin, adenomatous polyposis coli (APC), glycogen synthase kinase 3β (GSK3β) and casein kinase 1α (CK1α). This complex phosphorylates β-catenin on the N-terminus, leading to its subsequent ubiquitylation and degradation by theproteosome. β-catenin can be phosphorylated on Ser33, Ser37, Thr41 and Ser45. Firstly, Ser45 is phosphorylated by CK1α (Amit et al. 2002). Other sites are phosphorylated later by GSK3β (Liu et al. 2002). All four residues have to be phosphorylated to allow ubiquitylation. Mutation in any of these sites leads to β-catenin stabilization in the cytoplasm. Axin serves as a scaffold protein to bring kinases and β-catenin together. Phosphorylated β-catenin is recognized by β-TrCP (β-transducin repeat-containing protein), an E3 ubiquitin ligase, that triggers the ubiquitylation process (Marikawa et al. 1998). Thus, the intracellular level of β-catenin remains low and TCF/LEF mediated expression of Wnt response genes is repressed by Grouchos (Rao et al. 2010).

The canonical Wnt pathway is activated by binding of Wnt ligands to Frizzled receptors and LRP5/6 co-receptors, which leads to the phosporylation of LRP5/6 by CK1γ and GSK3β (Zeng et al. 2005). The phosphoprotein Dishevelled (Dvl) is recruited to the plasma membrane, where it interacts with Frizzled via its PDZ domain, self-polymerizes via DIX domain and serves as a mediator for recruitment of axin-GSK3β to the plasma membrane (Schwarz-Romond et al. 2007;Wong et al. 2003). Activation of LRP5/6 co-receptors leads to their redistribution in the plasma membrane to the caveolin-rich areas. This results in the formation of Wnt-Fz-LRP5/6-Dvl-Axin platform, called LRP5/6 signalosome (Bilic et al.

2007). Axin recruitment to the plasma membrane leads to disassembly of the destruction complex and stabilization of β-catenin, which accumulates in the cytoplasm and finally enters the nucleus. It is suggested that the main route of β-catenin nuclear transport is independent of the classical Ran-GTPase/importin import mechanism, as it does not possess a classical nuclear localization signal (NLS) or a nuclear export signal (NES) sequence. β-catenin is able to directly interact with the nuclear pore complex (nucleoporin Nup358 on cytoplasmic tail, Nup62 in central channel and Nup98 and Nup153 on the nuclear end). β-catenin can also self-regulate its own entry into the nucleus (Jamieson et al. 2014). In the nucleus β-catenin associates with transcription factors from the TCF/LEF family and activates the transcription of Wnt response genes. Among them are genes that play role in cell differentiation (siamois and brachyury (protein T), cell signalling (*VEGF* (vascular endothelial growth factor), *FGF4* (fibroblast growth factor 4) and *FGF18*), proliferation (cyclin D1, *c-MYC*), adhesion (E-cadherin) (Klaus et al. 2008). An overview of the Wnt/β-catenin pathway is presented in the Figure 1. 3.

The canonical Wnt pathway is regulated by a number of proteins. Secreted Frizzled-related proteins (SFRPs) and Wnt inhibitory factors (WIFs) can bind Wnt proteins, because they contain a domain that resembles the cysteine-rich domain (CRD) domain of Frizzled receptors. SOST and Wise proteins bind LRP5/6 and in consequence inhibit signalling. Dickkopf (Dkk) triggers LRP5/6 internalization and inactivation, as a result of enhancing LRP5/6 interaction with Kremen (Staal et al. 2008). Protein phosphatase 2 (PP2) is responsible for dephosporylation of β-catenin. Inhibitor of β-catenin and TCF (ICAT) and protein Chibby bind β-catenin inside the nucleus and prevent it from forming a complex with TCF (Klaus et al. 2008).

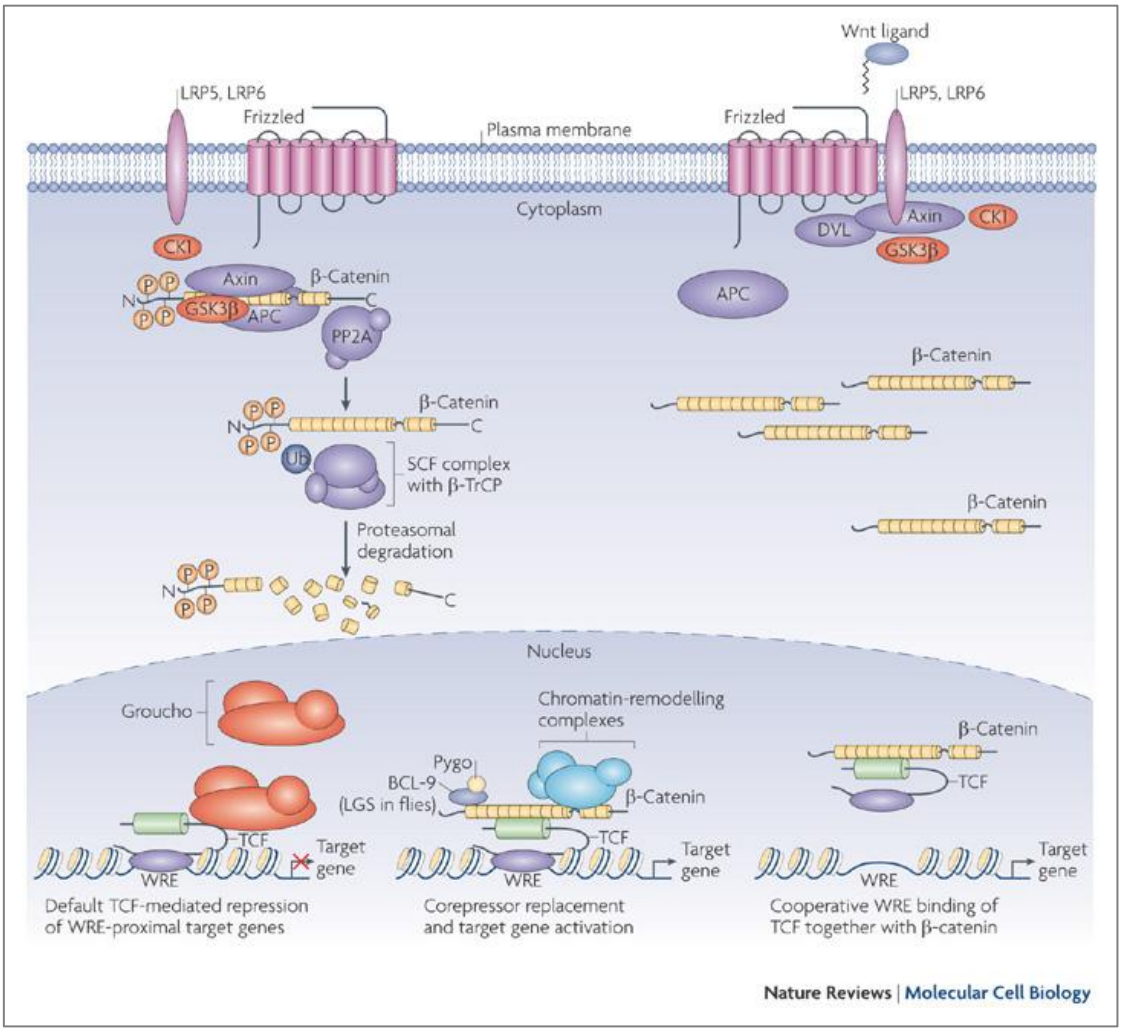

Figure 1. 3. The canonical Wnt pathway.

In the default state (left panel), β-catenin is degraded by the cytoplasmic degradation complex, which comprises glycogen synthase kinase 3β (GSK3β), casein kinase Iα (CKIα), axin and adenomatosis polyposis coli (APC). Phosphorylation of β-catenin by this complex triggers SCF (SKP1, Cullin, F-box)/ β-TrCP-mediated polyubiquitylation and proteasomal degradation of β-catenin. After Wnt ligand binding to the Frizzled receptor and LRP5/6 co-receptor, the degradation complex is recruited to the plasma membrane and inhibited by Dishevelled (Dvl). β-catenin translocates then to the nucleus, where it replaces TCF (T cell factor)-bound corepressors (such as groucho; middle panel) or co-imports additional TCF to the Wnt response elements (WREs; right panel) and activates target gene expression. LGS, Legless; LRP, low-density lipoprotein receptor. Figure reproduced from (Mosimann et al. 2009).

1.1.2. Molecular mechanisms involved in non-canonical Wnt pathway signalling

Non-canonical Wnt pathways are defined as routes independent of β-catenin transcriptional activity. There are many non-canonical pathways reported. However, due to a high level of cross-talk between receptors and secondary messengers from different signalling branches, it is difficult to separate individual pathways completely. For the sake of simplification, the following branches of the non-canonical Wnt pathways can be distinguished: PCP, Wnt/Ca^{2+}, Wnt/RAP, Wnt/cAMP, Wnt/GSK3-microtubules, Wnt/aPKC, Wnt/mTOR, Wnt/ROR and Wnt/RYK (Schulte 2010;Semenov et al. 2007). Of these, the best described are the PCP and Wnt/Ca^{2+} pathways.

Planar Cell Polarity (PCP) refers to cell polarization within two-dimensional epithelium. It occurs during hair orientation and gastrulation (Wu et al. 2009). PCP signalling is often activated by Wnt5a or Wnt11 through various Frizzled receptors (e.g. Fz6, Fz7 and Fz8 (Dijksterhuis et al. 2014)) and Dvl, but instead of LRP5/6, ROR and PTK7 are involved, and signals are transmitted without involving β-catenin. In *Drosophila melanogaster*, two complexes relocate to the opposite sites of the cell during the process. Frizzled-Dishevelled-Diversin (Div) complex localizes distally and Strabismus (Stbm, Vangl in vertebrates)-Prickle (Pk) localizes proximally, which leads to planar cell polarization (Veeman et al. 2003a). Dvl together with DAAM (Dishevelled-Associated Activator of Morphogenesis) activates the small GTPase RhoA (RAS homologue-gene family member A)-ROCK (Rho-associated coiled-coil containing protein kinase) and JUN-N-terminal kinase (JNK) routes, which results in actin cytoskeleton reorganization (Endo et al. 2005). PCP and Wnt canonical pathway are

known to antagonize each other and inhibiting one pathway will usually upregulate the other (Niehrs 2012).

The Wnt/Ca^{2+} pathway is activated by interaction of Wnt5a with Frizzled-2 (Sheldahl et al. 2003). The Frizzled receptor activates phosphodiesterase (PDE) via heterotrimeric G protein. As a result, the cellular levels of cGMP (cyclic guanosine monophosphate) are decreased, which inactivates the cGMP-dependent kinase G (PKG) and increases the cellular concentration of calcium. Wnt/Fz also activates phospholipase C (PLC). It initiates a cascade of events that results in the generation of diacylglycerol (DAG) and inositol trisphosphate (IP_3), followed by calcium fluxes. This leads to activation of the protein kinase C (PKC), which induces changes in actin cytoskeleton (Kuhl et al. 2000). Increased Ca^{2+} concentration also activates calcium-calmodulin-dependent kinase II (CamKII) and calcium-sensitive phosphatase calcineurin, which leads to activation of NFAT (nuclear factor of activated T cells) transcription factor. Wnt/Ca^{2+} signalling through CamKII inhibits Wnt/β-catenin pathway (Kohn et al. 2005;Semenov et al. 2007).

1.1.3. Wnt signalling in diseases

Deregulation of Wnt signalling during development leads to developmental defects (van Amerongen R. et al. 2009). In adult organisms, Wnt signalling is often associated with loss of growth control and impaired cell differentiation. Mutations or altered expression of Wnt signalling pathway components are associated with development of different types of cancers, such as colon carcinoma. Somatic mutations of Wnt pathway components identified in cancer are summarized in the table 1.1. Wnt signalling proteins associated with distinct patient outcomes in a cancer-subtype-specific manner are presented in the table 1.2. Aberrant Wnt signalling has also been reported in breast cancer, lung cancer, kidney disease, inflammatory bowel disease, diabetes type II and sarcoidosis (Herr et al. 2012). Furthermore, Wnt signalling is also involved in maintaining bone mass and is important for bone healing; findings which may have implications in osteoporosis (Canalis 2013).

Activation of the canonical Wnt pathway, evidenced by stabilization and nuclear accumulation of β-catenin, has been observed in colorectal, lung, breast, cervical, skin and liver tumours. β-catenin accumulation is linked with poor differentiation, high proliferative activity and poor prognosis (Endo et al. 2000). Stabilization of β-catenin may occur as a result of mutations in components of signalling pathway or due to epigenetic events. Mutations of APC lead to an inability to downregulate β-catenin (Polakis 2000). Mutations of *APC* rarely occur outside of the gastrointestinal tract, but have been found in the majority of sporadic colorectal cancers (SCC) (Polakis 2007). The acquisition of *APC* mutations is an initial step in colorectal carcinogenesis and facilitates and accelerates tumour development (Kinzler et al. 1996). Gain-of-function mutations of the *CTNNB1* gene, which encodes β-catenin, occur in

approximately 1% of SCC and more frequently in sporadic cancers outside of the intestines, for example in brain tumours, ovarian, prostate and hepatocellular cancers (Camilli et al. 2010;Klaus et al. 2008).

The Wnt pathway can be regulated by epigenetic mechanisms, such as hypermethylation. Silencing by hypermethylation was reported in different types of tumours for inhibitory Wnt ligands SFRPs (Caldwell et al. 2006;Jost et al. 2009;Nojima et al. 2007;Suzuki et al. 2008) and DKK (Sato et al. 2007). Overexpression of several Wnt pathway components in cancer is also common. It was shown for Wnt proteins (Katoh et al. 2001), Frizzleds (Kirikoshi et al. 2001;Saitoh et al. 2002) and Dishevelled (Okino et al. 2003).

Recent developments showed antagonistic crosstalk between Wnt and Notch signalling. It was reported that the expansion of intestinal progenitor cells by constitutively active Notch pathway was contingent to Wnt signalling in the intestine (Fre et al. 2009). The Notch receptor intracellular domain (ICD) was shown to bind unphosphorylated (active) β-catenin, making it inaccessible for transcription activity. Notch1 depletion, upregulated Wnt signalling, whereas expression of non-cleavable Notch1 receptor or inhibition of γ-secretase led to downregulation of the Wnt pathway. The authors concluded that association of β-catenin with the Notch receptor leads to its degradation in the lysosomes in a Numb-dependent fashion (Kwon et al. 2011).

The role of non-canonical pathways in cancer is less well studied, but there is evidence for their involvement in cancer development. Wnt5a is the main object in studies of β-catenin independent signalling in cancer. It was shown that, depending on the type of cancer; it can have either a suppressive or an oncogenic role. The suppressive function results from antagonizing the β-catenin dependent pathway. Wnt5a expression is

downregulated in colorectal cancer (Dejmek et al. 2005a;Ying et al. 2008), neuroblastoma (Blanc et al. 2004), ductal breast cancer (Dejmek et al. 2005b), esophageal squamous cell carcinoma (Li et al. 2010) and haematological malignancies (Ying et al. 2007). On the other hand, it is overexpressed in gastric (Kurayoshi et al. 2006), pancreatic (Ripka et al. 2007), prostate (Wang et al. 2007) and non-small cell lung cancer (Huang et al. 2005). It enhances cell motility and tumour invasion in breast cancer (Pukrop et al. 2006). It was reported that Wnt5a-induced migration of melanoma cells depends on signalling through Frizzled 5 and PKC (Weeraratna et al. 2002). Wnt5a and β-catenin in gastric cancer are expressed in mutually exclusive manner. Moreover, Wnt5a activates focal adhesion kinase and small GTP-binding protein Rac. Both play a role in the regulation of cell migration (Kurayoshi et al. 2006).

Recent data have revealed roles for the Wnt/PCP pathway in cancer progression, invasion, metastasis and in cancer angiogenesis (Wang 2009). It was shown that Frizzled-7 promotes migration of human hepatocellular carcinoma and invasion of colon cancer cells (Merle et al. 2004;Ueno et al. 2009;Vincan et al. 2007b). There is also evidence that Wnt signalling plays a significant role in angiogenesis (Masckauchan et al. 2006;Zhang et al. 2006) and it was reported that Wnt5a mediated signalling regulates endothelial cell growth and migration (Cheng et al. 2008;Cirone et al. 2008). The latter study by Cirone and colleagues showed that impaired non-canonical Wnt signalling leads to vascular defects in vertebrate model.

Table 1. 1. Somatic mutations of Wnt pathway components in cancer.

Table is reproduced from (Anastas et al. 2013)

Gene	Type of mutation	Primary tissues	Number of mutated samples	% mutated	Total samples
APC	Primarily frameshift and deletion mutations leading to compromised ability to degrade CTNNB1	Large intestine	2152	39%	5517
		Stomach	129	15%	214
		Soft tissue	50	12%	430
		Small intestine	34	16%	214
		Pancreas	26	14%	184
		Liver	11	12%	94
CTNNB1	Mutations in CTNNB1 cluster around the amino-terminus and prevent the phosphorylation of amino acids, S33, S37, T41 and S45, resulting in impaired degradation of CTNNB1	Liver	907	23%	3933
		Soft tissue	673	42%	1601
		Endometrium	218	20%	1098
		Kidney	168	14%	1225
		Pancreas	125	26%	476
		Ovary	104	11%	913
		Adrenal gland	100	19%	534
		Pituitary	86	24%	360
		Biliary tract	43	10%	433
AXIN1	Many mutations prevent AXIN1 from acting as a scaffold to degrade CTNNB1	Biliary tract	10	38%	26
		Liver	49	11%	448
WTX (also known as *FAM123B*)	Predicted to be loss-of-function mutations	Kidney	125	13%	949
		Large intestine	19	13%	151
TCF7L2	Unknown	Large intestine	13	28%	47

*Curated from the Catalogue of Somatic Mutations in Cancer (COSMIC) database. Genes that are mutated in at least 10% of the analysed samples for each cancer type are included in the table. *APC*, adenomatous polyposis coli; *CTNNB1*, β-catenin; *WTX*, Wilms tumour gene on the X chromosome.

Table 1. 2. Wnt signalling proteins are associated with distinct patient outcomes in a cancer-subtype-specific manner.

Table is reproduced from (Anastas et al. 2013)

Protein	Cancer	Clinical relevance
APC	Breast	APC expression was decreased in grade 1 breast tumours compared with normal breast, yet was increased in grade 3 tumours
CTNNB1	Adrenocortical	High nuclear CTNNB1 levels were associated with reduced overall and disease-free survival
	AML	CTNNB1 is expressed in a subset of primary AML samples and correlates with decreased relapse-free and overall survival
	Breast	Nuclear CTNNB1 is associated with reduced metastasis-free and overall survival in breast cancer. Cancer subtype differences have been observed. Invasive ductal carcinomas exhibited membranous but not nuclear CTNNB1 staining, lobular carcinomas lacked any CTNNB1 expression, and basal-like breast cancers exhibited strong nuclear CTNNB1 levels and high expression of CTNNB1 target genes
	Colorectal	High nuclear CTNNB1 expression was associated with patient deaths, particularly when found at the invasive front of tumours. However, CTNNB1 levels were not prognostic in obese patients
	Oesophageal carcinoma	Nuclear CTNNB1 was increased in malignant tumours and correlates with poor one-year survival but not with lymph node metastases
	Gastric cancer	Decreased nuclear CTNNB1 expression was observed in high-grade gastric cancers
	Glioblastoma	High nuclear and cytoplasmic CTNNB1 levels were associated with poor survival in glioblastoma
	Lung	Cytoplasmic or nuclear CTNNB1 expression predicts increased patient survival in non-small-cell lung carcinomas and non-squamous-cell lung carcinomas
	Prostate	Nuclear CTNNB1 correlates with decreased relapse-free survival, and nuclear CTNNB1 was decreased in metastases
	Melanoma	High levels of nuclear CTNNB1 in primary tumours predicted patient deaths
	HCC	High levels of CTNNB1 were predictive of decreased overall survival and increased risk of recurrence
TCF/LEF family	Colorectal	High LEF1 but low TCF4 expression were correlated with a better prognosis in colorectal carcinoma. However, in another study, high levels of LEF1 were associated with reduced patient survival in colorectal cancer, and the reasons for this discrepancy are unclear
	ALL	High *LEF1* transcript expression was associated with poor relapse-free survival in B cell ALL
ROR1 and ROR2	Breast	ROR1 expression was increased in high-grade and triple-negative breast cancer, and high levels of ROR1 correlated with decreased patient survival
	Sarcoma	ROR2 is expressed in a subset of soft tissue sarcomas, including leiomyosarcoma and gastrointestinal stromal tumours, and predicts patient deaths
SFRP4	Prostate	Decreased membranous expression of SFRP4 was associated with decreased patient survival in prostate cancer
WNT1	Breast	WNT1 protein expression was increased in tumour tissue compared with non-cancerous adjacent tissue. However, there was no significant difference in WNT1 expression in high-grade breast tumours, indicating that WNT1 may be particularly important during the early stages of tumorigenesis
	Glioblastoma	Increased WNT1 staining was associated with poor survival in glioma
WNT2	Oesophageal	Overexpression of WNT2 was correlated with poor survival in oesophageal squamous cell carcinoma. WNT2 was highly overexpressed in tumour-associated fibroblasts, indicating that it might function non-cell-autonomously
WNT5A	Gastric	Increased levels of WNT5A protein were associated with high-grade tumours and with decreased patient survival
	Prostate	Low WNT5A, especially in combination with high Ki67 staining or high androgen receptor protein levels, was predictive of reduced relapse-free survival
	Ovarian	High WNT5A was correlated with poor survival in ovarian carcinoma, yet low expression of WNT5A is observed during progression in the epithelial subtype of ovarian cancer, and loss of WNT5A correlates with decreased overall survival in patients with epithelial ovarian cancer
	Colorectal	High levels of WNT5A protein were correlated with increased patient survival in locally invasive colon cancer
WNT7A	Ovarian	WNT7A was overexpressed in ovarian carcinoma and was significantly associated with patient deaths
WIF1	HCC	Loss of *WIF1* mRNA expression was associated with decreased overall survival in HCC

*A full table with references can be found in Supplementary information S1 (table). ALL, acute lymphoblastic leukaemia; AML, acute myeloid leukaemia; APC, adenomatous polyposis coli; CTNNB1, β-catenin; HCC, hepatocellular carcinoma; ROR, receptor tyrosine kinase-like orphan receptor; SFRP4, secreted frizzled-related protein 4; WIF1, WNT inhibitory factor 1.

1.2. Wnt/Frizzled signalling in breast cancer

Breast cancer is the most invasive form of cancer in women and the second leading cause of death in women in industrialized nations. Evidence shows that Wnt signalling is essential in the development of normal mammary gland and also plays an important role in mammary oncogenesis. Mouse mammary carcinoma was the first known example of a Wnt-related disease. An insertion of the MMTV (mouse mammary tumour virus) was found in *Wnt1* locus, which resultantly was continuously driving Wnt1 expression (van 't Veer et al. 1984). Later, Wnt3 and Wnt10b were also found to carry the insertion of MMTV in breast cancer (Tekmal et al. 1997).

Numerous reports have shown the deregulation of Wnt signalling in breast cancer. Mutations in genes encoding components of Wnt signalling pathway, such as APC, β-catenin or Axin, are rare in breast cancer. Yet, upregulation of the pathway is evident, especially in basal-like and triple negative breast cancer (TNBC), where nuclear and cytosolic accumulation of β-catenin is associated with poor outcome (Geyer et al. 2011;Khramtsov et al. 2010;Lopez-Knowles et al. 2010). Cyclin D1 and c-Myc, well-known targets of canonical pathway, are also overexpressed in breast tumours (Lin et al. 2000). Recent report by Dey and colleagues provides additional evidence for preferential activation of Wnt signalling in TNBC and increased risk for brain and lung metastases (Dey et al. 2013). The mechanisms underlying activation of Wnt signalling pathways in breast cancer still remain unclear. However, it seems that it is mainly achieved through upregulation of potentially oncogenic receptors and co-receptors, such as Frizzled-7 and LRP5/6 (Liu et al. 2010;Yang et al. 2011).

Promoter hypermethylation of Wnt antagonist genes, like *APC*, *WIF1* and *SFRP1* was also reported (Klarmann et al. 2008;Suzuki et al. 2008).

1.2.1. Frizzled-7 in TNBC

Activation of Wnt signalling pathway is particularly associated with triple-negative (TNBC) basal-like breast cancer, which is one of the six major breast cancer subtypes. It represents approximately 10-20% of all breast cancers, and is more frequent in premenopausal women, especially of African-American and Hispanic descent (Carey et al. 2010). TNBC is characterized by a very aggressive clinical behaviour, demonstrated by lack or limited expression of estrogen receptor (ER), progesterone receptor (PR) and human epidermal growth factor receptor 2 (HER2/ERBB2). That makes TNBC cells resistant to therapeutic protocols based on pharmaceutical targeting of mentioned receptors (Gusterson 2009). TNBC was subdivided into six subtypes. Three of them (basal-like, mesenchymal-like, mesenchymal stem-like) were characterized by constitutive activation of Wnt signalling. Even though Herceptin (anti-HER2 antibodies), ER antagonists and aromatase inhibitors improved treatment of other breast cancer subtypes, the treatment of TNBC still remains a great challenge (Lehmann et al. 2011).

Frizzled-7 (Fz7) emerges as the most important Frizzled receptor involved in breast cancer, where it activates the canonical Wnt pathway. Expression of Fz7 is characteristic for basal-like and triple-negative breast cancer. Fz7 is the only member of Frizzled family of receptors significantly overexpressed in triple-negative breast cancer (TNBC) and TNBC-derived cell lines (Yang et al. 2011). Yang and colleagues demonstrated that Fz7 plays

a crucial role in cell proliferation in TNBC. Its depletion reduces cell growth and expression of Wnt target genes (Cyclin D1 and c-Myc), inhibits tumourigenesis *in vitro*, and decreases the ability of the MDA-MB-231 cell line to form tumours in athymic nude mice. Additionally, in the same study it has been shown that tumour growth could be reduced by the use of FZD7shRNA in mice with xenografts of triple negative breast cancer cells (Yang et al. 2011). These findings indicate that Fz7 is a key factor involved in TNBC cell transformation, evidenced by changes in cell invasion, motility and clonogenicity.

Recently, it has been shown that SIRT1, a class III histone deacetylase (HDAC) positively regulates Fz7 mRNA and protein levels in breast cancer cells (Simmons, Jr. et al. 2014)

1.2.2. Autocrine Wnt signalling

Autocrine Wnt signalling has been reported in 25% of human breast and ovarian cancer cell lines (Bafico et al. 2004) and 50% of human non-small lung carcinoma cell lines (Akiri et al. 2009). It was suggested that autocrine Wnt signalling contributes to the proliferation of breast cancer cells in a manner that depends on EGFR activity (Schlange et al. 2007). Recently, Luga and colleagues showed that exosomes derived form human breast cancer associated fibroblasts (CAFs) are involved in mobilizing autocrine Wnt-PCP signalling in breast cancer cells and stimulate their invasive behaviour and metastasis in animal models in tetraspanin CD81 dependent manner (Luga et al. 2012).

1.2.3. Crosstalk with other pathways

Several reports have shown evidences for crosstalk between Wnt signalling and other pathways in breast cancer. It was reported that TGFα and Wnt cooperatively induce mammary tumourigenesis, through the interaction between β-catenin and EGFR/ErbB2 heterodimers (Schroeder et al. 2000;Schroeder et al. 2002). Wnt1 and Wnt5a binding to Frizzled transactivates ErbB1, which leads to MAPK activation and overexpression of Cyclin D1 (Civenni et al. 2003). Furthermore, Schlange and colleagues suggested that Wnt1 induces c-Src-dependent EGFR transactivation, which in turn stimulates ERK1/2 signalling and cell proliferation (Schlange et al. 2007). Recent report has also shown that Wnt3 expression in breast cancer cells leads to activation of canonical Wnt signalling, upregulation of EGFR and promotion of epithelial-to-mesenchymal-like transition. Consequently it results in reduction of the growth-inhibiting effects of Herceptin in HER2-overexpressing cells. This finding indicates a role for Wnt3 in the development of Herceptin resistance in patients with breast cancer tumours overexpressing HER2 receptor (Wu et al. 2012). Interestingly, upregulated Wnt signalling was also associated with breast cancer resistance to Tamoxifen (Loh et al. 2013). Furthermore, it was reported that increased expression of Wnt1 in human mammary epithelial cells (HMEC) activates Notch signalling pathway, what leads to tumourigenic transformation of the HMEC cells (Ayyanan et al. 2006).

1.2.4. Epigenetic modifications

Gene hypermethylation has been widely documented in several types of cancer including breast cancer. In relation to the Wnt canonical pathway, DNA methylation of the *WIF1* (Wnt Inhibitory Factor 1) promoter was observed in 60% of breast carcinomas (Ai et al. 2006;Wissmann et al. 2003). Expression of *SFRP1*, another protein that antagonizes Wnt signalling, was found to be silenced in breast cancer. 60% of samples from primary breast cancers displayed methylation of *SFRP1* promoter and *SFRP1* gene hypermethylation is associated with shorter survival of patients with invasive breast cancer (Shulewitz et al. 2006;Veeck et al. 2006). It was shown that *SFRP1* is methylated in 64%, *SFRP2* in 100% and *SFRP5* in 90% of breast cell lines (Suzuki et al. 2008). Furthermore, several studies revealed that *APC* gene promoter is hypermethylated in 35-50% of breast cancer tumours and cell lines (Jin et al. 2001). Downregulation of APC protein leads to activation of β-catenin. Accumulation of β-catenin can be also a result of E-cadherin downregulation caused by methylation of *CDH1* gene. E-cadherin is a membrane receptor and a main part of adherens junction complex. It binds β-catenin and decreases its cytoplasmic concentration (Yang et al. 2001).

1.3. Frizzled-7: member of Wnt receptor family

1.3.1. Frizzled receptors

Frizzled's were originally identified as Wingless receptors in *D. melanogaster* (Bhanot et al. 1996). They are highly conservative in animal kingdom (Schioth et al. 2005). In mammals, 10 Frizzled isoforms have been identified. The amino acid sequence analysis revealed that Frizzled share 20 to 40% identity. The level of similarity is higher within particular clusters: Fz1, Fz2 and Fz7 share 75% amino acid identity, Fz5 and Fz8 share 80% identity, Fz4, Fz9 and Fz10 share 65% identity, and Fz3 and Fz6 share 50% identity with each other, as presented in the Figure 1. 4.A. (Fredriksson et al. 2003). The major characteristics of human Frizzled receptor are summarized in the table 1.3.

Receptors from Frizzled family are seven-transmembrane-spanning proteins. Although they are G protein-coupled receptors (GPCRs), they differ significantly from other GPCRs and represent a separate class surface receptors (Foord et al. 2005). Three regions can be distinguished within Frizzled structure: the extracellular N-terminal portion (224 amino acids), the transmembrane domains, and intracellular C-terminal cytoplasmic tail (25 amino acids) (Figure 1.4.B).

The extracellular region consists of a signal sequence, which ensures correct protein insertion into the membrane, followed by the Cysteine-Rich Domain (CRD), responsible for binding of Wnt proteins. Ten cysteines present in CRD are highly conserved and form five disulfide bond (Xu et al. 1998). The three dimensional structure was solved for mFzd8-CRD (Dann et al. 2001). It revealed a new protein fold, which consists mainly of α-helical structure

(Figure 1.4.C). Moreover, the existence of CRD dimers was reported. A similar Cysteine-Rich Domain is also found in SMO (Smoothened), a protein closely related to Frizzled, which does not bind Wnts (Wu et al. 2002), SFRPs (Secreted Frizzled Related Proteins), collagen α1(XVIII), carboxypeptidase Z (CPZ), Ror family of receptor tyrosine family kinase and muscle-specific kinase (MuSK) family (Xu et al. 1998). CRD domain of Frizzled receptors contains also Asn residues that are predicted to be glycosylated (Schulte 2010). The structure of *X.leavis* Wnt8 in complex with mouse CRD of Frizzled8 has been recently resolved (Figure 1.4.D). It revealed a new two-domain Wnt structure, not related to any known protein folds, with two finger-like domains (N-terminal "lipid thumb" and C-terminal "index finger") grasping CRD of Fz8 at two distinct binding sites. The conservation of amino acids in both Wnt domains facilitates ligand-receptor cross-reactivity, which is important for understanding functionality of Wnt proteins (Janda et al. 2012).

Transmembrane domain consists of seven membrane-spanning regions, three intracellular and three extracellular loops. In the extracellular loops 1 and 2 conserved cysteines are present. They are thought to stabilize an overall structure of the receptors (Lagerstrom et al. 2008).

The intracellular domain is involved in extensive protein-protein interactions. It also contains sites for posttranslational modifications, such as phosphorylation, ubiquitylation, nitrosylation and hydroxylation (Schulte 2010). Cytosolic tails of most Frizzled receptors have two Postsynaptic density-95, Disc large, ZO-1 (PDZ) binding motifs, PDZ-BM. They are 4-6 amino acid motifs that interact with PDZ domains of partner proteins. Frizzled proximal PDZ-BM (K-T-xxx-W) interacts with the PDZ domain of the phoshoprotein Dishevelled (Dvl). This atypical, internal PDZ-BM is placed very close to the plasma membrane and is

conserved within all Frizzleds (Umbhauer et al. 2000;Wallingford et al. 2005). Dvl is a cytoplasmic scaffold of which three homologs exist in vertebrates (Dvl1, Dvl2, Dvl3). Their functional redundancy is evidenced by overlapping expression patterns and high degree of conserved structures (Gao et al. 2010b). The interaction between Frizzled and Dvl is essential for different Wnt-induced signalling pathways. Recently, Tauriello and colleagues presented a model of Frizzled-Dishevelled interaction involving a three-segmented discontinuous binding surface on the Frizzled receptor. They have shown that the DEP domain and C-terminal region of Dvl binds cooperatively to the motifs I and II in the third intracellular loop and to the C-terminal motif III of mouse Frizzled-5 and *Xenopus* Frizzled-7 (Figure 1.4.D). That allows forming a stable Fz-Dvl complex at the plasma membrane and initiating canonical Wnt signalling. Whether Frizzled interaction with Dishevelled requires PDZ and DEP domains to act cooperatively or sequentially needs to be established (Tauriello et al. 2012).

The distal PDZ-BM (x-S/T-x-φ, where φ represents a hydrophobic residue) is a standard, terminal class I PDZ ligand (Jelen et al. 2003). It can bind a range of different PDZ proteins (GOPC, MAGI-3, Syntenin, Kermit, PSD-95) (Wawrzak et al. 2009). So far, the interactions involving the distal PDZ-BM have been shown for Fz1,-2,-3,-4,-5,-7,-8, but not for Fz6, -9 and -10 (Schulte 2010).

Table 1. 3. Characteristics of Frizzled receptors

(+) or (–) in the C-terminus column indicates experimental evidence for or against, respectively, the functionality of the class Frizzled receptor C terminus as PDZ ligand domain.

Receptor	Human Gene Name	NCBI Accession No.	Chromosomal Location	Protein Length	Molecular Mass	Transcripts	Exons	C-Terminus
				aa	*kDa*			
Frizzled-1	*FZD1*	NP_003496	7q21	647	71,158	1	1	ETTV (+)
Frizzled-2	*FZD2*	NP_001457	17q21.1	565	63,554	1	1	ETTV (+)
Frizzled-3	*FZD3*	NP_059108	8p21	666	76,263	1	8	GTSA (+)
Frizzled-4	*FZD4*	NP_036325	11q14.2	537	59,881	1	2	ETVV (+)
Frizzled-5	*FZD5*	NP_003459	2q33-q34	585	64,507	1	2	LSHV (+)
Frizzled-6	*FZD6*	NP_003497	8q22.3-q23.1	706	79,292	1	7	HSDT (–)
Frizzled-7	*FZD7*	NP_003498	2q33	574	63,620	1	1	ETAV (+)
Frizzled-8	*FZD8*	NP_114072	10p11.22	694	73,300	1	1	LSQV (+)
Frizzled-9	*FZD9*	NP_003499	7q11.23	591	64,466	1	1	PTHL (–)
Frizzled-10	*FZD10*	NP_009128	12q24.33	581	65,336	1	1	PTCV (+)

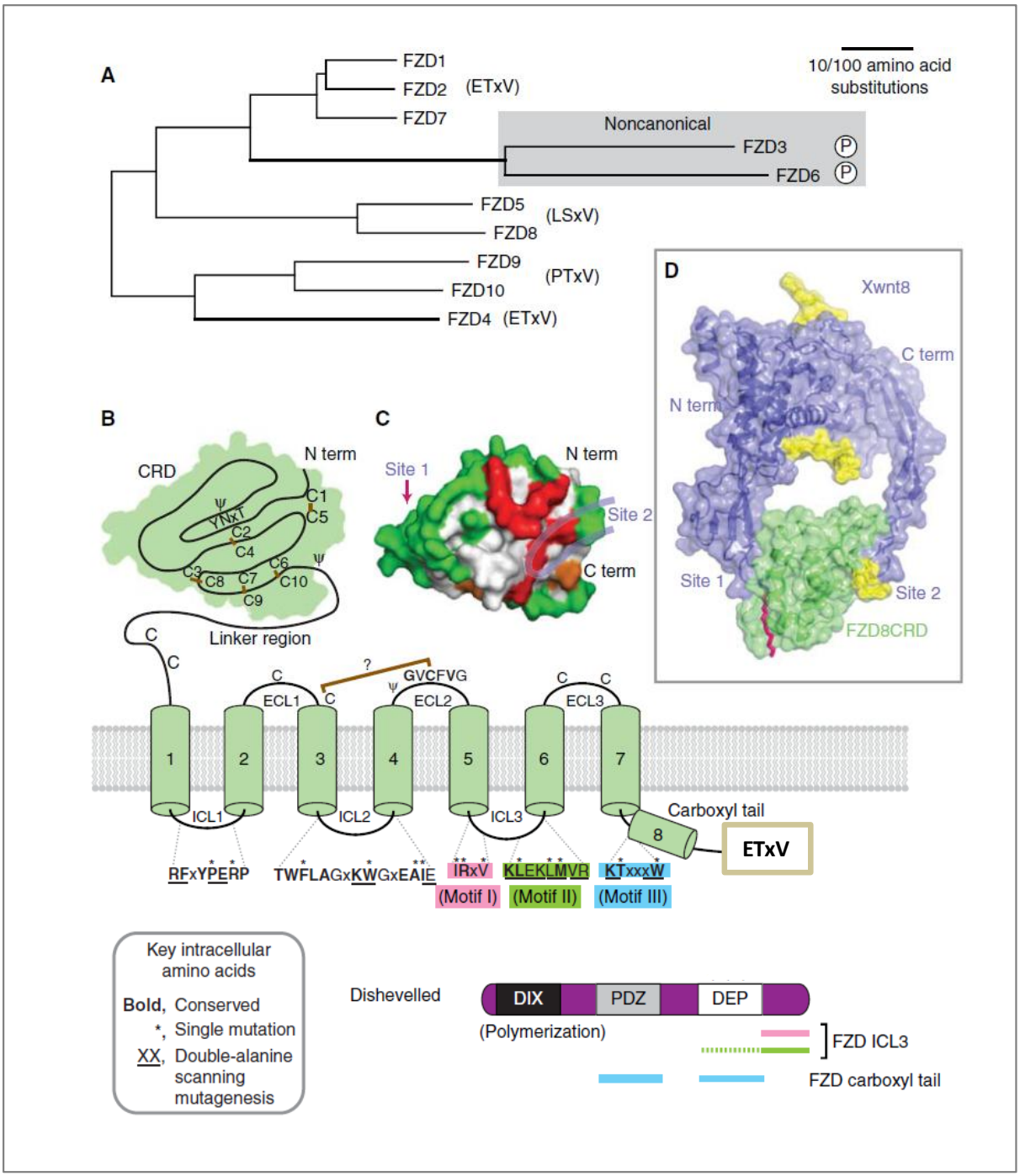

Figure 1. 4. Structure of Frizzled receptors

(A) Phylogeny comparing human Frizzled (FZD) receptors. Consensus sequences of C-terminal tails are presented in the brackets. (B) Topology of a Frizzled receptor on the plasma membrane, with cysteine rich domain (CRD), seven transmembrane domains (1-7) and cytoplasmic domain (8) with C-terminal PDZ binding motif. Ten conserved cysteines „C" forming five disulfide bonds are highlighted in CRD. Ψ depicts potential N-glycosylation sites. Dishevelled (DVL) is presented schematically with DIX, PDZ, and DEP domains. Two discontinuous regions of Frizzled-ICL3 (motif I „pink" and motif II

„green") bind to the C-terminus of Dvl. The cytoplasmic tail of Frizzled contains the KTxxxW motif („blue"), which interacts strongly with Dishevelled-PDZ domain. (C) Crystal structure of Fz8-CRD. Residues in red are suggested to be a Wnt-binding interface. Residues in green when altered did not affect Wnt activity (PDB:1IJY). (D) Wnt8–Fz8-CRD co-crystal structure, shown as a ribbon diagram superimposed on surface representation. Site 1 and site 2, mediate contacts between Wnt8 and Fz8-CRD. Palmitoleic acid adduct from the Wnt8 thumb at site 1 (red); N-glycans of Wnt8 and Fz8-CRD (yellow). N-term, amino terminal; C-term, carboxyl terminal; ICL, intracellular loop; ECL, extracellular loop. Figure reproduced and modified from (MacDonald et al. 2012).

1.3.2. Frizzled-7

Human FZD7 gene is located on chromosome 2q.3317. Another form of Fz7, FzE3, was isolated from esophageal carcinoma tissue. FzE3 shares 98% homology with Fz7 and their sequences differ by 9 amino acids (Tanaka et al. 1998). Frizzled-7 is the only member of Frizzled family that regulates development of the gastric tract (King et al. 2012b). In recent years several reports have indicated that Fz7 is an important receptor governing Wnt signalling in cancer cells.

1.3.2.1. Functions of Frizzled-7

Frizzled-7 is a unique receptor that can activate canonical and noncanonical pathways. Human Wnt3a, *Xenopus* Wnt8b and mouse Wnt6 were reported to activate canonical Wnt signalling through interactions with Fz7 orthologs (Kim et al. 2008b;Linker et al. 2005;Medina et al. 2000). On the other hand, zebrafish and *Xenopus* Wnt11, as well as *Xenopus* Wnt5a are proposed to bind to Fzd7 to activate noncanonical Wnt pathways (Swain et al. 2001).

Frizzled-7 activates the canonical signalling upon interaction with Wnt3a, which was shown in liver cancer cells (Kim et al. 2008b). Frizzled-7 was also found necessary for the mesenchymal-to-epithelial transition in the human colorectal cancer LIM1863-*Mph* cell line (Vincan et al. 2007a)

PCP pathway activation by Frizzled-7 is responsible for regulation of cell movements via activation of JNK and Rho (Kinoshita et al. 2003;Tanegashima et al. 2008). Frizzled-7 was also reported to regulate bone morphogenesis through PCP signalling (Li et al. 2009).

Frizzled-7 interaction with Wnt11 activates PKC-Cdc42 and PKCδ-JNK signalling pathways that regulate convergent extension movements during gastrulation, as well as migration of neural crest cells in *Xenopus* and zebrafish (De Calisto et al. 2005;Djiane et al. 2000;Kinoshita et al. 2003;Knowlton et al. 2004;Penzo-Mendez et al. 2003). *Xenopus* Frizzled-7 signalling has been also shown to activate the PKC and Ca^{2+}/calmodulin kinase signalling during cardiac development (Sheldahl et al. 2003). Furthermore, Frizzled-7 has been reported in the PCP pathway-dependent repair of mouse muscle. Receptor interaction with Wnt7a was shown to activate PCP pathway, in the mechanism involving Vangl2, which resulted in the expansion of satellite stem cells, and muscle repair (Le Grand et al. 2009).

Recently Frizzled-7 has implicated in the maintenance of embryonic stem cell self-renewal capacity (Takahashi-Yanaga et al. 2010). Dormeyer and colleagues have reported that *FZD7* mRNA levels are 200-fold higher in human embryonic stem cells, when compared to differentiated cell types. They have also shown that Fz7 depletion by shRNA in human embryonic stem cells leads to dramatic changes in the morphology of embryonic stem cell colonies and loss of expression of the embryonic stem cell-specific transcription factor OCT4 (Dormeyer et al. 2008). Furthermore, Frizzled-7 expression is upregulated in colonic crypt stem cells, but its expression level decreases when cells differentiate into mature epithelial cells (Gregorieff et al. 2005).

Frizzled knockout mice ($Fz7^{-/-}$) display tail truncation and kinking with 100% penetrance and ventricular septal defects (VSDs) with 15% penetrance. Furthermore, $Fz2^{+/-}$; $Fz7^{-/-}$ mice display VSDs with 50% penetrance and $Fz2^{-/-}$; $Fz7^{-/-}$ mice display convergent extension defects and mid-gestational lethality with 100% penetrance. It was suggested that

cross-talk events between different signalling pathways in development are susceptible to disruptions in Frizzled signalling (Yu et al. 2012).

Taken together, Frizzled-7 is involved in canonical and non-canonical Wnt signalling during embryogenesis, adult-tissue homeostasis and carcinogenesis.

1.3.2.2. Ligands and binding partners of Frizzled-7

Frizzled-7 has been reported to activate the canonical Wnt pathway upon interaction with *Xenopus* Wnt8b, mouse Wnt6, and human Wnt3 (Kim et al. 2008b;Linker et al. 2005;Medina et al. 2000). As direct interaction between Wnt3a and Fz7-CRD has been shown in L-cells (Kemp et al. 2007). Frizzled-7 is also able to bind *Xenopus* Wnt11 and mouse Wnt7a. This, however leads to activation of noncanonical Wnt signalling (Bentzinger et al. 2014;Kim et al. 2008a).

Frizzled-7 interacts with a number of PDZ (postsynaptic density protein (PSD)-95, Discs-large and ZO-1) domain-containing proteins. The PDZ domain of DVL family of proteins binds to the internal PDZ binding motif, KTxxxW, in the C-terminal cytoplasmic region of Frizzled-7 (Umbhauer et al. 2000;Wong et al. 2003), while other PDZ proteins, such as discs large 1/synapse associated protein 97 (DLG1/SAP97), DLG2/PSD-93, DLG4/SAP90/PSD-95, MAGI3 and Syntenin-1 (syndecan binding protein, SDCBP) bind to the C-terminal PDZ binding motif, ETxV, of the receptor (Hering et al. 2002;Luyten et al. 2008;Schulte et al. 2007;Yao et al. 2004). MAGI3-mediated assembly of Fz7 together with van Gogh-like 2 (Vangl2) has been shown to activate the Rac–JNK signalling cascade (Yao et al. 2004), while syntenin-dependent assembly of the Fz7–Dishevelled–Syndecan complex was

reported to activate the Cdc42 signalling pathway (Luyten et al. 2008). Syntenin-1 has been shown to facilitate interaction between *Xenopus* Frizzled-7 and Syndecan-2 or Syndecan-4 (Luyten et al. 2008). The interaction between Frizzled-7 and Syndecan-4 leads to the recruitment of fibronectin in the extracellular matrix and cytoplasmic Dvl to the Fz7–Syndecan-4 and activation of noncanonical Wnt signalling (Munoz et al. 2006).

There are also proteins involved in regulation of Fz7 trafficking. One of them is Transmembrane protein 46 (TMEM46; also called Shisa). Immature Fz7 after synthesis in the endoplasmic reticulum (ER) translocates to the trans-Golgi network (TGN) for further modification to generate mature Fz7, before being trafficked to the plasma membrane. TMEM46 is an ER protein with a Cysteine-rich region that associates with Fz7 and mediates its retention within the ER. It was shown that TMEM46 negatively regulates Fz7 post-translational maturation and cell-surface delivery (Katoh et al. 2005;Yamamoto et al. 2005).

1.3.2.3. Biosynthetic and endocytic trafficking of Frizzled-7

Synthesized native Fz7 (about 50 kDa) is modified in the endoplasmic reticulum (ER) to immature Fz7 via Asn-linked glycosylation at two sites (Asn63 and Asn164) within the N-terminal extracellular region (Katoh et al. 2007;Struewing et al. 2007). Immature Frizzled-7 (about 54 kDa) is then further modified to mature Frizzled-7 (about 64 kDa) with complex oligosaccharides in the TGN, prior to trafficking to the cell surface. Glycosylation sites on the extracellular loops of Frizzled-7 could be involved in interactions with ligands. Glycosylation has also been shown to be important for receptor maturation in the ER, regulated by the protein Shisa, which mediates Fz7 retention in ER (Yamamoto et al. 2005). Mature Fz7 on the

plasma membrane is internalized in complex with Dishevelled via clathrin-mediated or caveolin-mediated endocytosis and can be found in endosomes (Blitzer et al. 2006;Gagliardi et al. 2008;Yu et al. 2007). Detailed information about endocytic trafficking of Frizzled receptors is presented in the section 1.4.1 and 1.4.2.2.

1.3.2.4. Major sites of expression of Frizzled-7

Human *FZD7* is expressed in the blastocyst and in undifferentiated embryonic stem (ES) cells. Fz7 mRNA was also detected in ES-derived endodermal and neural progenitors, as well as in fetal cochlea and regenerating liver (Katoh et al. 2007). Frizzled-7 is relatively highly expressed in fetal kidney, lung, adult skeletal muscle and heart, and weakly expressed in adult brain, kidney and placenta (Sagara et al. 1998). It was also found in the gastrointestinal tract (the esophagus, stomach, duodenum, jejunum, ileum, cecum, colon and rectum) (Kirikoshi et al. 2001). Boland and colleagues found that Frizzled-7 expression is downregulated in mesenchymal stem cells during osteogenesis (Boland et al. 2004).

Frizzled-7 mRNA is upregulated in gastric cancer (Kirikoshi et al. 2001;Sagara et al. 1998), esophageal cancer (Tanaka et al. 1998), colorectal cancer (Sagara et al. 1998;Vincan et al. 2007b) , hepatocellular cancer (Merle et al. 2004;Merle et al. 2005), nasopharyngeal cancer (Zeng et al. 2007), and in triple negative breast cancer (Yang et al. 2011).

1.3.2.5. Frizzled-7 in cancer

As already mentioned in the previous section, Frizzled-7 is upregulated in a number of cancer types, and becomes recognized as a potential therapeutic target for various cancers (King et al. 2012b).

Frizzled-7 is abundantly expressed in colon cancer tissues and cell lines, also in those with mutations in genes encoding APC or β-catenin (Ueno et al. 2008). Fz7 is mainly expressed in well differentiated tumour cells in the centre of cancerous tissue where it is predominantly restricted to the proliferative regions (Vincan et al. 2007b;Vincan et al. 2010). Fz7 overexpression in colon cancer cell lines with *APC* and/or *CTNNB1* mutations upregulates canonical Wnt signalling. Moreover, Fz7 depletion with siRNA downregulates β-catenin dependent pathway and decreases cell viability, migration and invasion. Furthermore, high expression of Frizzled-7 is correlated with a significantly shorter survival time in colon and gastric cancer (Ueno et al. 2009). It was also found that Fz7 is a downstream target of β-catenin in colorectal cancer cells that may explain its high expression level in colon cancer. This finding indicates the existence of a feed-forward mechanism that enhance canonical Wnt signalling in colorectal cancer and facilitate its progression and metastasis (Vincan et al. 2010). Recently, it was reported that interaction between Fz7 and Wnt11 might be also involved in progression of colorectal cancer. The authors suggested that Fz7 might be involved in Wnt11-induced migration of HCT-116 cells. They have also found a correlation between Wnt11 and Fz7 mRNAs expression in human colon cancer cell lines and primary tissues of colorectal cancer. The prognostic significance of Wnt11 and Fz7

expression in primary tissues has been suggested, as Fz7-high and Wnt11-high group had worse disease free survival than Fz7-low and Wnt11-low group (Nishioka et al. 2013).

Canonical Wnt signalling plays role in normal liver development, and its aberrant regulation has been reported in hepatocellular carcinoma (HCC) (Fatima et al. 2011;Whittaker et al. 2010). Frizzled-7 mRNA levels has been found elevated in hepatitis B and C, as well as in non-viral-induced HCC cell lines. Furthermore, Frizzled-7 and/or Wnt3a are upregulated in 60-90% of human HCCs and in 35-60% of the surrounding pre-neoplastic liver tissues. Increased expression of Frizzled-7 has been reported to correlate with increased level of cytosolic/nuclear β-catenin and cell migration (Bengochea et al. 2008;Merle et al. 2004;Merle et al. 2005). A recent report showed that pharmacological inhibition of Fz7 with small interfering peptides, disrupting its interaction with Dishevelled, displayed anti-tumour properties against hepatocellular cancer (Nambotin et al. 2011)

Frizzled-7 is also associated with gastric cancer and chronic lymphocytic leukaemia (CLL). Patients with Fz7-positive gastric cancers have poorer prognosis when compared with Fz7-negative cancers (Schmuck et al. 2011). Increased Frizzled-7 expression is also associated with less favourable clinical prognosis in patients with CLL (Kaucka et al. 2013). Increased Frizzled-7 expression has been also observed in acute lymphoblastic leukaemia (ALL) (Khan et al. 2007).

Frizzled-7 is the main Wnt receptor implicated in triple-negative breast cancer, where it plays a crucial role in regulation of cell proliferation (Yang et al. 2011).

1.4. Regulation of Frizzled signalling

1.4.1. Endocytosis

Endocytosis is a biological process in which cells uptake particles and macromolecules, such as proteins, into transport vesicles derived from plasma membrane. It is crucial in development, intercellular communication, signal transduction and cellular homeostasis. There are different mechanisms of endocytosis. The best studied is the clathrin-dependent pathway. Beside that, there are several clathrin-independent pathways including the CLIC/GEEC (clathrin-independent carrier/GPI-AP-enriched early endosomal compartment) endocytic pathway, arf6-dependent endocytosis, flotillin-dependent endocytosis, macropinocytosis, circular doral ruffles, phagocytosis, trans-endocytosis and caveolin-mediated endocytosis (Doherty et al. 2009).

Internalized by varied endocytic pathways, material is directed to different destinations within mammalian cells. There are two major sorting compartments: the early and late endosome. The early endosomes (marked by Rab5 GTPase) receive cargo from the plasma membrane and from the trans-Golgi. They direct the molecules back to the cell surface by rapid recycling pathway controlled by Rab4 or through recycling endosomes in Rab11-dependent manner, to the trans-Golgi network by retrograde transport or to the late endosome/lysosome. The early endosomes also regulate cell signalling, through the downregulation of internalized receptors, which are packaged into intralumenal vesicles. These multivesicular regions mature to become the multivesicular body, which transports cargoes to late endosomes. The transition from early to late endosomes is driven by the

replacement of Rab5 to Rab7. Rab factors are GTP-binding proteins that play a regulatory role in vesicle trafficking. The late endosome serves as a compartment gathering molecules from the endocytic, biosynthetic and autophagic pathways and directing them to the lysosomes, the Golgi complex or the plasma membrane (Scott et al. 2014). To direct cargoes to the lysosomes, the ESCRT (endosomal sorting complex required for transport) machinery assembles on the late endosome membrane. The ESCRT complex is composed of three subcomplexes, ESCRT I, II and III, recognizing in sequence ubiquitylated proteins and directing them into inner vesicles of multivesicular bodies and lysosomes. (Gagliardi et al. 2008). Alternatively, some intraluminal vesicles can be released as exosomes into the extracellular space after fusion of secretory endo-lysosomes with the plasma membrane (Scott et al. 2014). Recently, some reports have shown that the relationship between endocytosis and signalling is more complex and it is possible for endocytosis to contribute positively to signalling.

The inhibition of clathrin mediated endocytosis by different reagents leads to downregulation of Wnt3a induced canonical signalling in mouse fibroblast L cells (Blitzer et al. 2006). It was also shown that Dishevelled-1 and Dishevelled-2 proteins bind β-arrestin, a clathrin adaptor, and these proteins activate synergistically Wnt-dependent transcriptional activity of TCF factor (Chen et al. 2001). Lack of β-arrestin affects the phosphorylation process of Dvl-2 and consequently β-catenin fails to be stabilized in response to Wnt (Bryja et al. 2007).

In addition to these findings, it is proposed that caveolin-dependent route is also involved in the activation of β-catenin dependent pathway. Wnt3a induces phosphorylation of LRP6 and subsequently axin is recruited to the Wnt-receptor complex on the plasma

membrane, which is called LRP6-signalosome, and is highly dynamic. Signalosome is assembled by Dvl-2 mediated recruitment of axin, GSK3β and β-catenin to the activated receptors and partially disassembled by endocytosis (Bilic et al. 2007). It was shown that phosphorylated LRP6 forms intracellular aggregates, which do not co-localize with any endocytic markers except caveolin. In response to Wnt3a, LRP6 binds to caveolin and is internalized (Yamamoto et al. 2006). It is suggested that caveolin-mediated endocytosis plays an important role in inducing internalization of LRP6 and accumulation of β-catenin. The model of interactions was proposed where the binding of Wnt3a to LRP6 in the lipid rafts triggers a conformational change of LRP6. This leads to its phosphorylation and association with axin, Frizzled and Dishevelled. In the next step, the vesicles with phosphorylated LRP6, in complex with axin and caveolin, are severed from the plasma membrane by dynamin and transported to the early endosome by Rab5. When forming the vesicle, the complex between proteins and/or lipids on the vesicle can be altered, what may result in the inhibition of GSK3 and dissociation of β-catenin from axin. This leads to the stabilization of β-catenin (Kikuchi et al. 2009). It was recently reported that after internalization the Wnt/Fz/LRP6 complex and the transducer complex (Dvl-2, axin, GSK3β and β-catenin) take separate routes. The first complex follows a Rab-positive path, whereas the latter forms intracellular aggregates (Hagemann et al. 2014). Zebrafish Rabconnectin-3a (Rbc3a), a protein associated with the vacuolar-ATPase (v-ATPase) proton pump control, was recently implied to control intracellular trafficking events required for Wnt signalling during neural crest migration. It was shown that loss of Rbc3a in zebrafish embryos disrupts the maturation of endocytic vesicles which leads to inhibition of Wnt signalling in neural crest cells before migration and

to increase of the Wnt signalling after the migration, as evidenced by accumulation of Fz7 in plasma membrane and increased level of β-catenin(Tuttle et al. 2014).

There are several proteins implicated in the regulation of Wnt-induced endocytosis. It has been shown recently, that the tumour suppressor and endocytic adaptor protein, disabled-2 (Dab2) selectively recruits LRP6 to the clathrin-mediated endocytic pathway and sequesters it from the caveolin-dependent route. It was shown that LRP6 phosphorylation by casein kinase 2 (CK2), upon Wnt stimulation, promotes Dab2 binding and internalization with clathrin, which has inhibitory effect on canonical Wnt signalling. It is suggested that Dab2 expression levels influence canonical Wnt signalling by modulating LRP6 endocytic fate (Jiang et al. 2012). On the other hand, Rab GTPase RAB8B was identified as a positive regulator of the canonical pathway by promoting LRP6 internalization and rescuing caveolar inhibition of LRP6 endocytosis. RAB8B was also shown to be involved in regulation of Wnt signalling during vertebrate development and modulation of Wnt target genes (Demir et al. 2013). Glypican-3 (GPC3) is a membrane bound proteoglycan, associated with hepatocellular carcinomas. It has been reported to promote canonical Wnt signalling by increasing the amount of Wnt at the cell surface, but also by direct interaction with Frizzled receptors through glycosaminoglycan chains. It is suggested that glypican stimulates the formation of complexes between Wnt and Frizzled. GPC3 was also found in complexes with Frizzled, Wnt and presumably LRP6, that were internalized after Wnt stimulation (Capurro et al. 2014).

The importance of endocytosis in the non-canonical Wnt pathway is well documented. As already mentioned, Dishevelled is a part of canonical and PCP pathways. Dishevelled enhances endocytosis of Frizzled through its interactions with β-arrestin, a

protein known to recruit clathrin to activated GPCRs and thus to promote receptor internalization. Frizzled are not able to bind β-arrestin directly, but the interaction can occur through Dvl. It was shown that is Dvl-2, upon Wnt5a stimulation, recruits β-arrestin to Frizzled-4 and initiates clathrin-mediated endocytosis (Chen et al. 2003). The importance of β-arrestin-Dvl-Frizzled interaction was shown in *Xenopus*, where downregulation of β-arrestin significantly affected PCP signalling (Kim et al. 2007).

It was also reported that the region of Dishevelled-2 (Dvl-2), that corresponds to the DEP domain and is required for the PCP signalling, interacts with the μ2-adaptin subunit of AP-2. This interaction is essential for Frizzled-4 internalization. Moreover, authors suggest that it is crucial for the PCP signalling, but not for the canonical pathway. When Dvl-2 is mutated and unable to bind AP-2, there is no noticeable signalling via PCP pathway, but canonical pathway is not disturbed (Yu et al. 2007).

Wnt5a and Wnt3a can induce the endocytosis of Frizzled-5, when the co-receptor LRP6 is not expressed ectopically. This process is clathrin dependent. Furthermore, Ryk, co-receptor that plays role in activation of RhoA and JNK, also interacts with β-arrestin-2 and promotes internalization of Frizzled-7 and Dishevelled upon Wnt-11 treatment in *Xenopus*. Although there is no evidence that clathrin-dependent internalization of Frizzled-4 or Frizzled-5 is directly linked with activation of PCP or Ca^{2+} pathways, it is suggested that Frizzleds are endocytosed in response to Wnts and different endocytic pathways determine whether activated is canonical or noncanonical signalling (Kikuchi et al. 2009).

Recently, it was reported that Frizzled-3 undergoes endocytosis via filipodia tips upon Wnt5a stimulation. It was also discovered that in filipodia with active PCP signalling pathway Dvl2 blocks Dvl1-induced Fz3 hyperphosphorylation and membrane accumulation.

Furthermore, Fz3 hyperphosphorylation is was found to correlate with loss of PCP signalling *in vivo*. It was also reported that small GTPase Arf6 is required for Fz3 endocytosis and crucial for Wnt-induced outgrowth, indicating the importance of Fz3 recycling in PCP signalling in growth cone guidance (Onishi et al. 2013)

1.4.2. Ubiquitin

1.4.2.1. Ubiquitin in Wnt signalling regulation

Wnt signalling is regulated by several ubiquitin-mediated mechanisms. Ubiquitylation is one of the most important posttranslational modification, as it regulates many biological processes, including proteasome degradation, intracellular trafficking, DNA repair and signal transduction (Tauriello et al. 2010b). Diverse ubiquitin modifications link to distinct cellular mechanism. Ubiquitin can be recognized by specific ubiquitin-binding domains within proteins, thus it can serve as signalling device. Ubiquitylation occurs as a cascade of reactions catalyzed by three types of enzymes (E1, E2 and E3). The process leads to the covalent attachment of ubiquitin to the ε-amino group of a lysine residue in the target protein. Proteins can be mono- or multi-ubiquitylated, i.e. they can have single or multiple monomers of ubiquitin attached, respectively. Mono-ubiquitylation is associated with receptor endocytosis, lysosomal targeting, chromatin remodelling and DNA repair (Di Fiore et al. 2003;Haglund et al. 2003). In addition, very often, protein poliubiquitylation is observed. It occurs when ubiquitin moieties, added to a protein, form a chain. Ubiquitin has seven lysines (K6, K11, K27, K29, K33, K48, K63) and each of them can be used to form various poliubiquitin chains, generating different molecular signals (Acconcia et al.

2009;Komander et al. 2012). The fate of an ubiquitylated protein depends on the type of ubiquitin linkage. K48-linked ubiquitin chains target proteins for degradation by proteosomes, whereas other types of linkages also mediate non-proteolytic functions (Haglund et al. 2005;Ikeda et al. 2008).

The core components of canonical Wnt pathway, APC, Axin and β-catenin, are regulated by ubiquitylation. As described in details in the section 1.1.1., phospho-β-catenin undergoes poliubiquitylation by β-TrCP E3 ligase and subsequent proteosomal degradation (Marikawa et al. 1998). Furthermore, β-catenin levels are controlled independent of Wnt signalling by Jade-1, a ubiquitin ligase found primarily in the nucleus, and Siah-1, a p53-activated ubiquitin ligase, induced in response to DNA damage (Chitalia et al. 2008;Dimitrova et al. 2010). Also, APC and Axin are subjected to ubiquitin-mediated proteolysis (Tauriello et al. 2010b). Regulation of Dishevelled involves ubiquitylation in at least two different manners. K48-linked ubiquitylation by the E3 ligases KLHL12 (Kelch-like 12), NEDL1 and inversin targets Dishevelled for degradation and downregulates canonical Wnt pathway (Angers et al. 2006;Miyazaki et al. 2004;Simons et al. 2005). On the other hand, K63 poliubiquitylation of Dishevelled-DIX domain positively regulates Wnt signalling. Inhibition of Dishevelled K63-ubiquitylation by CYLD, tumour suppressor and DUB, was shown to negatively regulate Wnt signalling (Tauriello et al. 2010a). Recently, Usp14 was identified as a major DUB of Dishevelled. It was shown that Usp14 regulates Dishevelled ubiquitylation and subsequent phosphorylation, essential for activation of Wnt pathway (Jung et al. 2013).

1.4.2.2. Ubiquitin and Frizzled

Targeting transmembrane proteins to their destinations requires specific mechanisms. Studies have revealed that ubiquitylation acts as a signal for endocytosis and sorting of plasma membrane proteins. Addition of ubiquitin changes the properties of target proteins. It affects their stability, associations with other proteins, enzymatic activity and subcellular localization.

Removal and recycling of ubiquitin moieties from ubiquitylated substrates is catalized by specific deubiquitylating enzymes (DUBs). They serve to balance the ubiquitination reactions within a cell and regulate different processes, such as endosomal sorting. In mammals deubiquitylation is carried out DUBs enzymes, such as USP8 (ubiquitin specific protease 8) also called UBPY. It is recruited to endosomes by interaction with ESCRT III complex and deubiquitylates cargo proteins (Clague et al. 2006). Ubiquitin plays a role in sorting of internalized receptors to multivesicular bodies and lysosomes. In early endosomes, proteins without attached ubiquitin are recycled to the plasma membrane or directed to other intracellular compartments. In contrast, ubiquitylated proteins are directed into late endosomes and finally lysosomes (Mukhopadhyay et al. 2007).

It was discovered recently that the level of Frizzled receptors on the plasma membrane is controlled by a cycle of monoubiquitylation and deubiquitylation. The amount of Frizzled receptors on the cell surface seems to be an important factor that determines cell responsiveness to Wnt. The information comes from a study on Frizzled and UBPY/USP8 both in mammalian cells and *Drosophila*. Mukai et al. found that the deubiquitinating enzyme UBPY/USP8 is a positive regulator of Wnt/β-catenin pathway. While inactivated, it

downregulates canonical Wnt pathway. Whereas a constitutive active variant of UBPY/USP8 enhances the expression of β-catenin dependent genes. A model was proposed, whereby Frizzled (Fz8, but also Fz4, Fz5 and Fz6) in the plasma membrane is ubiquitylated by RING-type ubiquitin ligase ZNRF3 or RNF43 and internalized (Hao et al. 2012;Koo et al. 2012). Afterwards, there are two possible scenarios. Frizzled receptor can be deubiquitylated by UBPY/USP8 and recycled to the cell surface via Rab11-positive recycling endosomes, or it can be trafficked to Rab7-positive multivesicular bodies, and subsequently degraded in a lysosome (Figure 1.5.). No evidence were found that the cycle of Frizzled monoubiquitylation – deubiquitylation is influenced by binding of Wnt. It is proposed that Frizzled recycling is crucial for setting the level of responsiveness of cells to the Wnt ligand (Cadigan 2010;Mukai et al. 2010).

Recently, two studies have shown that two transmembrane RING finger ubiquitin ligases, ZNRF3 (zinc and ring finger 3) and RNF43 (ring finger 43), are involved in Wnt signalling modulation, through their interaction with Wnt receptors. ZNRF3 and RNF43 are highly homologous Wnt targets (they are both targets of β-catenin – dependent transcription), detected in LGR5 crypt stem cells and colon cancer (Hao et al. 2012;Koo et al. 2012). Both reports demonstrated that ZNRF3 and RNF43 regulate the stability and cell-surface levels of Frizzled receptors (Fz5 and Fz8) via multiubiquitylation of lysines in the cytoplasmic loops and subsequent internalization and lysosomal degradation. A similar mechanism was recently found for the *C.elegans* ortholog PLR-1 E3 ligase (Moffat et al. 2014). Due to the fact that *ZNRF3* and *RNF43* are Wnt target genes, it is suggested that these ubiquitin ligases function as a negative feedback regulators of Wnt signalling. However the structural basis for specific targeting of Frizzled receptors by ZNRF3, RNF43 and PLR-1

remains unknown (de Lau et al. 2014). Hao and colleagues also provide evidence that R-spondins stabilize Frizzled receptors levels on the plasma membrane by tethering a complex of LGR family member (LGR4/5) and ZNRF3/RNF43 (Hao et al. 2012). A model was proposed whereby formation of the R-spondin-LGR4/5-ZNRF3/RNF43 complex would lead to membrane clearance of the ubiquitin ligase, increased Frizzled level on the cell surface and enhanced Wnt signalling (Fearon et al. 2012).

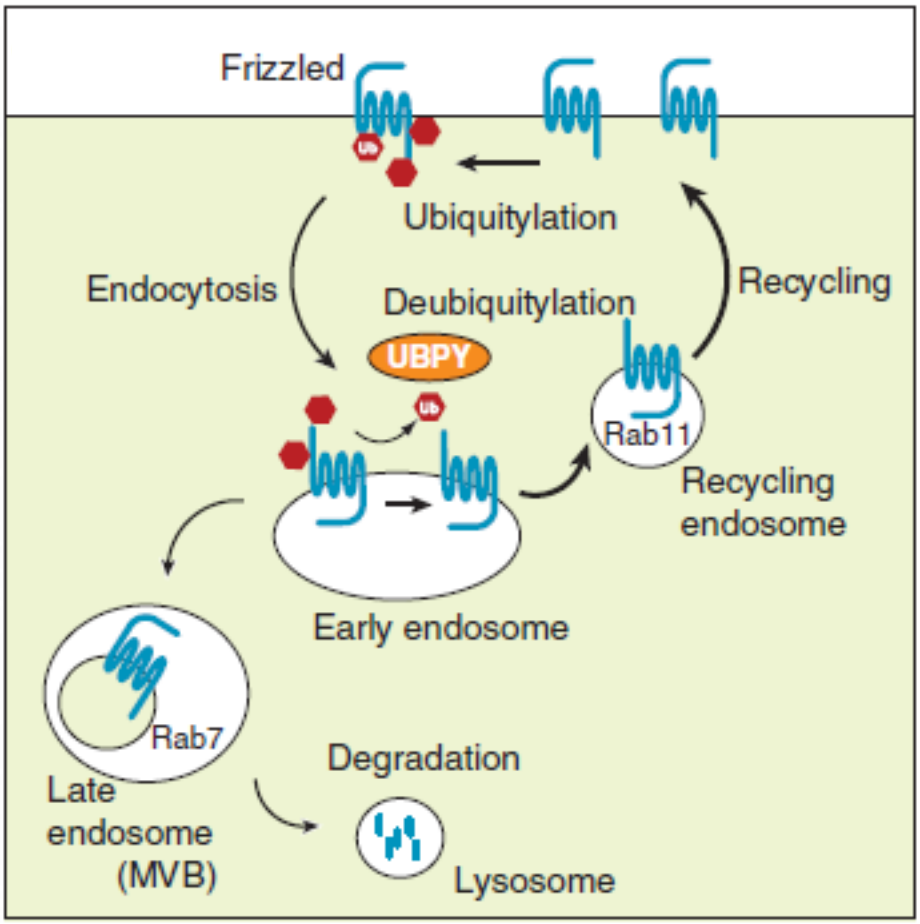

Figure 1. 5. A model for the regulation of the cell surface level of Frizzled.

Frizzled in the plasma membrane is ubiquitylated by an E3 ubiquitin ligase and internalized. Afterwards, it can be deubiquitylated by UBPY/USP8 and recycled to the cell surface via Rab11-positive recycling endosomes, or it can be trafficked to Rab7-positive multivesicular bodies, and subsequently degraded in a lysosome. UBPY/USP, ubiquitin specific protease 8; MVB, multivesicular bodies; Ub, ubiquitin. Figure reproduced and modified from (Mukai et al. 2010).

1.4.3. PDZ domain containing proteins

PDZ (PSD95/Dlg/ZO-1) domains are common in multicellular organisms. So far over 250 PDZ domains have been identified in the human proteome (Finn et al. 2006). They facilitate protein-protein and protein-lipid interactions and play an important role in cell signalling, maintenance of cell polarity, stabilization of adhesion structures, organization of signalling complexes, trafficking and clustering of receptors (Wawrzak et al. 2009). PDZ domains consist of 80-100 residues forming a globular structure with six β-strands and two α-helices (Figure 1.6.). Initially, they have been described as interacting with C-terminal tail of target proteins (Doyle et al. 1996;Jemth et al. 2007). Later, PDZ domains have been shown to bind other PDZ domains, internal binding sites and phosphoinositides (Gallardo et al. 2010;Harris et al. 2001;Wong et al. 2003;Zimmermann 2006).

Traditionally, PDZ domains have been classified into four classes, depending on the consensus sequence of the binding motif: class 1 (x-S/T-x-φ$_{COOH}$), class 2 (x-φ-x-φ$_{COOH}$), class 3 (x-D/E/K/R-x-φ$_{COOH}$) and class 4 (x-x-ψ-φ$_{COOH}$), where φ is a hydrophobic amino acid and ψ is an aromatic amino acid (Song et al. 2006). More recent analysis showed that binding to a PDZ domain may involve more than four amino acids and the current classification distinguishes 16 subclasses (Tonikian et al. 2008).

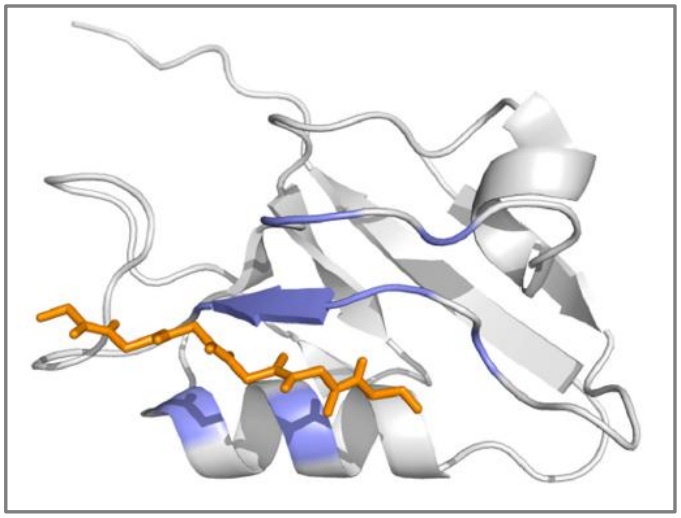

Figure 1. 6. 3D structure of a bound PDZ domain.

The PDZ domain is a globular structure built of six β-strands and two α-helices. Canonical interaction occurs through C-terminal tail of target proteins and the hydrophobic binding pocket formed between strand β2 and helix α2 of the PDZ domain. The core binding sites of PDZ domain are highlighted in blue, and the bound peptide is orange (RREQV). PDB:2OQS (NMR first model). Figure reproduced from (Hui et al. 2013).

PDZ domains are often present in proteins containing other modular domains and most of the PDZ proteins function as scaffold proteins.

Many PDZ domain-containing proteins are involved in signal transduction. It is particularly striking in the case of Wnt signalling, where the PDZ protein Dishevelled plays a central role in the signalling cascade, as it was already discussed in previous sections. Dishevelled binds to the internal, membrane proximal PDZ binding motif of Frizzled receptors. Other PDZ proteins interact with membrane distal PDZ-BM of Frizzled (with consensus sequence (x-S/T-x-φ_{COOH}) and also play role in regulation of Wnt signalling (Figure 1.7.) (Wawrzak et al. 2009).

GOPC/PIST (Golgi associated PDZ and coiled-coil motif containing) is a Golgi protein containing one PDZ domain. GOPC was reported to bind the C-terminal PDZ-BM of

mammalian Fz5 and Fz8. It was shown that GOPC trafficked together with Frizzled through Golgi to the plasma membrane, which implies its role in vesicular transport of the receptors (Yao et al. 2001). GOPC/PIST was implicated in regulation of trafficking of several other transmembrane proteins. GOPC/PIST overexpression leads to different surface expression patterns of β1-adrenergic receptor, the somatostatin receptor subtype 5 (SSTR5) and Cadherin 23, by holding them back in the Golgi (He et al. 2004;Wente et al. 2005;Xu et al. 2010). It also regulates membrane expression of cystic fibrosis transmembrane conductance regulator (CFTR), by facilitating its targeting to lysosomes (Cheng et al. 2005)

Another PDZ protein involved in Frizzled trafficking is dGRIP (glutamate receptor-interacting protein). It has been shown to co-localize with DFrizzled-2 in trafficking vesicles and to play role in transporting the receptor from neuromuscular junctions to the perinuclear area in *Drosophila* (Ataman et al. 2006).

MAGI3 (Membrane-associated guanylate kinase, WW and PDZ domain-containing protein 3) is a protein with six PDZ domains, usually enriched in cell junctions. The second PDZ domain of the protein has been shown to bind Frizzled-4 and Frizzled-7. MAGI3 co-localizes with Fz4 and Ltap protein, transmembrane protein supporting noncanonical Wnt signalling, at cell contact sites in MDCK cells. Complexing of Fz4 with Ltap by MAGI3 has been reported to enhance noncanonical Wnt/JNK pathway (Yao et al. 2004).

Pals-1 associated tight junction protein (dPatj), also known as InaD-like protein (INADL), is a protein with four PDZ domains, involved in the establishment of cell polarity. It forms a subapical complex together with Crumbs and Stardust/Pals-1 proteins. dPatj has been shown to interact with dFz1 (mediating PCP signalling), but not with DFz2 (mediating

canonical signalling), via Frizzled C-terminal PDZ-BM. It was proposed that dPatj facilitate the phosphorylation of dFz1 by atypical PKC (aPKC), what consequently inhibits PCP signalling, without compromising receptor localization or interaction with Dishevelled (Djiane et al. 2005).

Kermit, the *X. laevis* ortholog of GIPC/Synectin, was shown to interact with C-terminal PDZ-BM of XFz3 and XFz7, but not with XFz8. It has been reported that downregulation and high overexpression of Kermit blocks XFz3 mediated induction of neural crest, but discrete overexpression of Kermit enhances it. This led to a conclusion that Kermit is involved in regulation of canonical Wnt signalling in neural crest development, probably functioning as a scaffold for XFz3 and another unidentified component of the pathway (Tan et al. 2001).

Proteins from the PSD-95 family (PSD-95/SAP90/Dlg4, PSD93/chapsyn-110/Dlg2 and SAP97/Dlg1) also have been shown to interact with Frizzled receptors. Proteins from this family contain three PDZ domains and function in synapses by organizing signalling complexes. PSD-95 has been shown to bind C-terminal PDZ-BM of Frizzled-1, -2, -4 and -7, whereas PSD-93 and SAP97 interact with Frizzled-1, -4 and -7. Based on the observation that PSD-95 form a complex with Fz2 and APC, it was suggested that it may serve as an adaptor protein recruiting components of the canonical Wnt pathway (Hering et al. 2002).

FRIED (Frizzled interaction and ectoderm defects), an ortholog of mammalian PTP-BL and a six PDZ domain containing tyrosine phosphatase, has been identified to interact with XFz8 in *X. laevis*. It was shown that FRIED can inhibit induction of secondary axis in frog embryos mediated by XWnt8, as well as modulate XWnt5a mediated reorganization of the actin cytoskeleton in a Dishevelled-independent manner (Itoh et al. 2005).

Finally, NHERF1(Na^+/H^+ exchange factor 1), adaptor protein highly expressed in normal mammary epithelium, was reported to regulate canonical Wnt signalling due to a direct interaction between its second PDZ domain and C-terminal PDZ-BM of Frizzled receptors (Fz4, Fz2 and Fz7). It was shown that Frizzled binding to NHERF1 modulates Dishevelled recruitment and Wnt-induced β-catenin activation. Furthermore, the loss of NHERF1 in breast cancer cell lines enhances Wnt signalling and cell proliferation, which imply that NHERF1 is involved in breast cancer pathogenesis (Wheeler et al. 2011).

Syntenin-1 is another PDZ domain-containing adaptor protein implicated in the regulation of Frizzled signalling, and it will be discussed separately in the section 1.6.3.3.

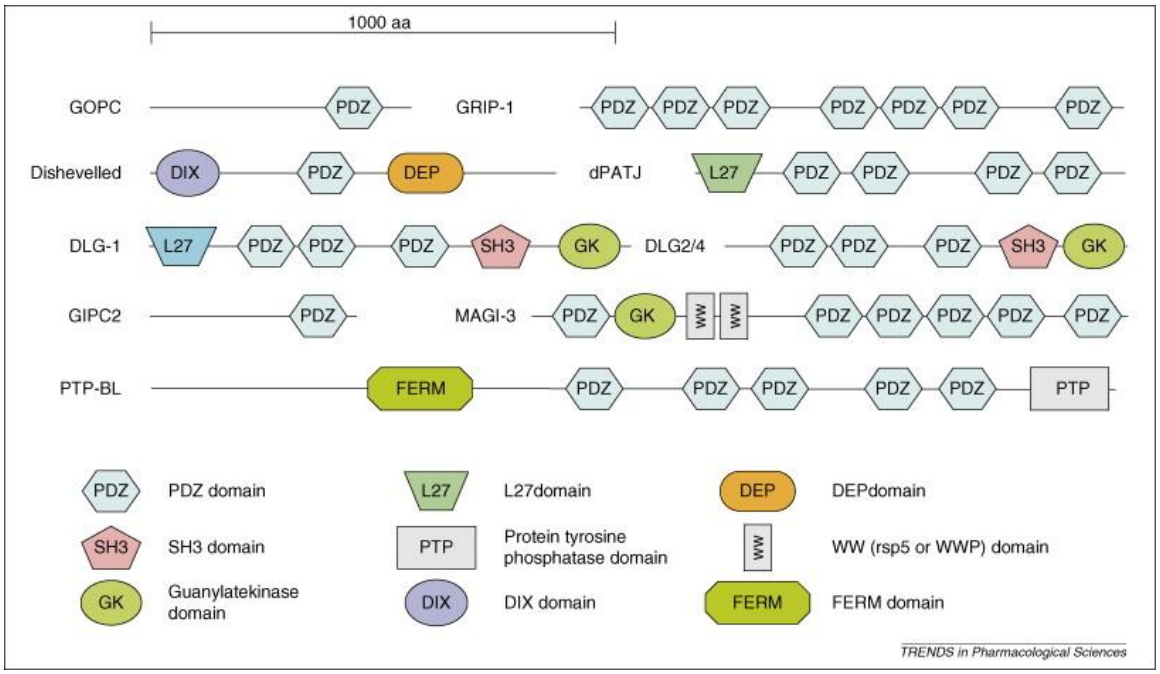

Figure 1. 7. Schematic domain structure of proteins directly interacting with Frizzled. Figure reproduced from (Schulte et al. 2007).

1.5. Syntenin-1

Syntenin-1 is a protein containing two PDZ domains, originally identified as a syndecan binding protein (Grootjans et al. 1997) and as a melanoma differentiation gene (*mda-9)*, expression of which was induced by interferon γ (IFNγ) (Lin et al. 1998). It is widely present in all adult tissues (Zimmermann et al. 2001) and especially robustly expressed in developing skin, spinal cord, heart and lung during development of mouse embryo (Jeon et al. 2013). Currently, many reports describe numerous interactions between syntenin-1 and different proteins. It is suggested that syntenin-1 can serve as a scaffold for a number of intracellular interactions.

1.5.1. Subcellular localization of syntenin-1

Analysis of the syntenin-1 distribution in epithelial cells revealed its localization at cell-cell contact sites. Syntenin-1 co-localizes with F-actin, syndecan-1, E-cadherin, β-catenin and α-catenin. In fibroblasts, it was shown that syntenin-1 localizes to focal adhesions and in stress fibres (Zimmermann et al. 2001). Syntenin-1 also localizes in the early secretory pathway, e.g. endoplasmic reticulum, intermediate compartment, *cis*-Golgi and apical endosomes (Sarkar et al. 2008). Thus, it is implicated that syntenin-1 facilitates trafficking of transmembrane proteins (Fernandez-Larrea et al. 1999). Furthermore, syntenin-1 interactions with phosphatidylinositol 4,5-bisphosphate (PIP_2) and phospholipase Cδ facilitates its membrane anchorage (Zimmermann et al. 2002).

1.5.2. Molecular structure and binding partners of syntenin-1

Syntenin-1 is a 32 kDa protein. It contains N-terminal domain (NTD), followed by two PDZ domains (PDZ1 and PDZ2) and C-terminal domain (CTD) (Figure 1.8).

NTD contains 113 amino acids and does not display any structural motifs. However, it contains three conserved L-Y-P-x-L sequences, where X stands for any amino acid residue. The first one has a conserved serine residue at the "X" position, and was shown to be involved in ubiquitin binding to syntenin-1 (Rajesh et al. 2011). Recently, the L-Y-P-x-L motifs were implicated in syntenin-1 binding to ALIX protein during syndecan-lead cargo recruitment to exosomes and syntenin-1-syndecan-ALIX complex has been reported to regulate the biogenesis of exosomes (Baietti et al. 2012). The NTD domain recruits the transcription factor SOX4 and eukaryotic translation initiation factor 4A (EIF4A) into signalling complexes (Beekman et al. 2008). It is also important for homo-dimerization and hetero-dimerization with syntenin-2, protein homologous to syntenin-1 (Koroll et al. 2001). It was shown that endogenous syntenin-1 is phosphorylated within its NTD domain. Five conserved tyrosine's were found (Y4, Y46, Y50, Y56 and Y91), which are potential phosphorylation sites. Tyrosine phosphorylation within NTD might be an important factor in the regulation of syntenin-1 functions (Beekman et al. 2008). Indeed, Wawrzyniak and colleagues showed that phosphorylation of Y56 of syntenin-1 decreases membrane localization of the protein (Wawrzyniak et al. 2012). It has been also shown that Src-dependent Tyr4 phosphorylation of syntenin-1 leads to binding of the protein to myosin

phosphatase Rho interacting protein (M-RIP). By that it regulates Rac GTPAse-dependent actin polymerization (Sala-Valdes et al. 2012).

CTD is a short, 24 amino acid long domain. CTD domain is required, but not sufficient, for syntenin-1 interaction with CD63 (Latysheva et al. 2006). Negative charges of the K280 and R281 residues present in CTD increase syntenin-1 localization at the plasma membrane (Wawrzyniak et al. 2012).

Syntenin-1 contains two PDZ domains (PDZ1 and PDZ2). They do not bind a unique sequence, but different peptide motifs (PDZ-BM class 1, 2 and 3, but also to unconventional PDZ-BMs) with low-to-medium affinity (Grembecka et al. 2006). PDZ1 displays 26% of sequence similarity with PDZ2 domain. However both domains closely resemble each other structurally. They are linked by a conserved peptide built of five residues and extensive contact site between two PDZ domains have been observed in syntenin-1 crystals (Cierpicki et al. 2005). PDZ2 domain binds peptides in canonical orientation (Cierpicki et al. 2005). Whereas in case of PDZ1, backbone of the interacting peptide is nearly in perpendicular orientation to the PDZ1 domain, when compared to the peptide-PDZ2 interaction (Grembecka et al. 2006). Recently, syntenin-1-PDZ2 has been found to bind internal PDZ-BM. Two types of motifs were identified. The consensus sequence of the first one was φ-A-I-x-(ALV)-(IV), which can be regarded as two tandem canonical class II PDZ-BM, i.e. φ-A-I and I-x-(ALV). The consensus of the second motif was identified as φ-R-φ-φ-φ, which includes two canonical class II PDZ-BM, i.e. φ-R-φ and φ-φ-φ (Mu et al. 2014).

Most protein ligands show preference for PDZ2 (for example syndecans and ephrinB). PDZ1 binds with higher affinity to IL-5Rα (interleukin-5 receptor α), neurexin, merlin and CD63 (Beekman et al. 2008). It was also reported that PDZ1 can bind

phosphoinositol lipids in the plasma membrane (Zimmermann 2006). Even though PDZ domains of syntenin-1 can interact separately with their ligands, most of the interactions depend on cooperative ligand binding to the PDZ1-PDZ2 tandem (Grembecka et al. 2006;Grootjans et al. 2000). Furthermore, it is suggested that PDZ1 plays a chaperone-like role in stabilizing of PDZ2 domain folding (Boukerche et al. 2010).

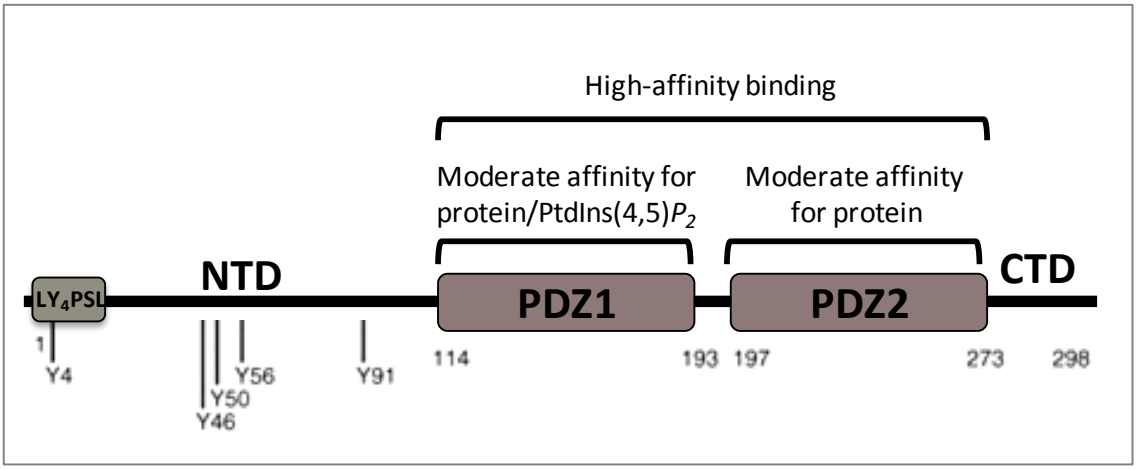

Figure 1. 8. The domain structure of syntenin-1

Syntenin-1 contains N-terminal domain (NTD), followed by two PDZ domains (PDZ1 and PDZ2) and C-terminal domain (CTD). Five tyrosine residues within the NTD are conserved, as indicated in the lower part of the figure. LY4PSL motif is implicated in the ubiquitin binding. Figure is reproduced and modified from (Beekman et al. 2008).

1.5.3. Functions of syntenin-1

1.5.3.1. Syntenin-1 and receptor trafficking

Syntenin-1 plays an important role in receptor trafficking. Endocytosis of receptors leads to signal attenuation, as internalized receptors are targeted for degradation. However it can also positively influence signalling output, as receptors at endocytic compartments can interact with different downstream effectors, within the plasma membrane.

The first reported functional interaction of syntenin-1 was with syndecans, membrane proteins with heparan sulphate (HS) side chains in the extracellular domain. HS chains allow syndecans to act as co-receptors. They bind and concentrate growth factors at the cell surface and facilitate their interactions with receptors. It was reported that syntenin-1 mutants, defective in phosphoinositol lipid PtdIns(4,5)P_2 binding, trap syndecans in perinuclear recycling endosomes, characterized by the presence of Rab11 and Arf6, small GTPases involved in endosome recycling (Zimmermann et al. 2005). Thus, the interaction with syntenin-1 plays role in syndecans recycling to the plasma membrane. Furthermore, it has been shown that membrane receptors associated with syndecans, such as FGF receptor, can be recycled to the cell surface together with syndecans and syntenin-1 (Zimmermann et al. 2005). Recently, it has been demonstrated that ternary complex syndecan-syntenin-1-ALIX is able to recruit syndecan associated proteins to the intraluminal vesicles of multivesicular endosomes and exosomes (Baietti et al. 2012).

Pro-TGFα is membrane bound and functions as a ligand for EGFR (epithelial growth factor receptor). It was reported that syntenin-1 binds to the C-terminus of the protein and

both PDZ domains of syntenin-1 are required for optimal interaction. It was shown that mutations of pro-TGFα, that disrupt its association with syntenin-1, result in retention of the protein in the endoplasmic reticulum (Fernandez-Larrea et al. 1999).

It was suggested that syntenin-1 plays a role in maintaining Delta1 expression on the cell surface. Delta1 is a ligand for Notch receptor. Estrach et al. (2007) reported that Delta1 interacts with syntenin-1 and its membrane expression is decreased by syntenin-1 depletion. Delta1 contains PDZ-BM on its C-terminus and a mutation of C-terminal valine leads to activation of Notch signalling (Estrach et al. 2007).

Syntenin-1 was also reported to regulate endocytosis of tetraspanin CD63. Tetraspanins regulate maturation and processing of associated transmembrane proteins, their activity and internalization. CD63 directly binds syntenin-1 and it has been proposed that the interaction may have a negative effect on AP2-clathrin mediated endocytosis of CD63, by inhibiting CD63-AP2 association (Latysheva et al. 2006).

1.5.3.2. Syntenin-1 and metastasis

Syntenin-1 was reported to be involved in cancer metastasis. Ability to metastasize is the major characteristic of malignant tumours. Metastasis is a complex process that requires attachment of tumour cell to matrix proteins, degradation of extracellular matrix (ECM) by matrix metalloproteinases (MMP) and migration of cancer cells into surrounding stroma. Overexpression of syntenin-1 was observed in a number of metastatic breast and gastric cell lines. Breast cancer cell line MCF7 and gastric cancer cell line Az-521 showed increased invasion rate and migration properties after transfection with syntenin-1. Moreover,

syntenin-1 overexpression in MCF7 was associated with pseudopodia formation. Further analysis showed that PDZ2 domain of syntenin-1 is responsible for the stimulatory effect of the protein on cell migration (Koo et al. 2002). It was also observed that syntenin-1 expression increases during melanoma progression from primary to metastatic melanoma (Helmke et al. 2004).

Syntenin-1 displays preferential link with fibronectin signalling. In melanoma cells, after cell interaction with fibronectin, syntenin-1 facilitates phosphorylation of FAK (focal adhesion kinase) what leads to activation of p38, JNK (c-jun NH_2-terminal kinase) and NF-κB (nuclear factor κB) activation. NF-κB was shown to induce expression of MMP-2 in melanoma cells (Boukerche et al. 2005;Boukerche et al. 2007). This pathway can be inhibited by RKIP (Raf kinase inhibitor protein), which prevents syntenin-1 binding to FAK and c-Src kinases (Das et al. 2012). Nonetheless, syntenin-1-induced expression of MMP-2 or MMP-9 was not observed in breast cancer cell lines (Koo et al. 2002). Recently, it was reported that syntenin-1 interaction with c-Src also positively regulates NF-κB activation (Boukerche et al. 2010). Furthermore, activation of c-Src mediated by syntenin-1 induces activation of EGFR (epidermal growth factor receptor) in uroepithelial cells, and in consequence increases their proliferation and invasion properties (Dasgupta et al. 2013)

1.5.3.3. Syntenin-1 and Frizzled receptors

Syntenin-1 was identified as an intracellular ligand for Frizzled receptors. It was shown that it interacts with the C-terminal PDZ-BM of human Frizzled-3,-7 and -8, but not with Frizzled-2, -5 and -6. Luyten et al. reported that association with Frizzled-7 requires PDZ1 domain of syntenin-1, whereas Frizzled-3 and Frizzled-8 prefer the second PDZ domain. However, the tandem of syntenin-1's PDZ domains mediates higher affinity binding than the isolated domains. Syntenin-1 was reported to stimulate noncanonical Wnt/JNK pathway. Further investigation revealed that in *Xenopus leavis* Xsyntenin interacts with XFrizzled-7. Overexpression of Xsyntenin blocks convergent extension in animal cap assay, while its downregulation affects gastrulation movements and shortens body axis of embryos, process controlled by noncanonical Wnt signalling. It was also established that syntenin-1 stimulates Frizzled-7 dependent activation of the PKCα/CDC42 signalling (Luyten et al. 2008). Syndecans, syntenin-1 binding partners, are Wnt co-receptors and were shown to stimulate PKCα and CDC42 activities. Xsyndecan-4 functionally and physically interacts with XFrizzled-7 and XDvl, and a model was proposed where syntenin-1 acts as an intracellular scaffold protein between Frizzled and syndecans. This function of syntenin-1 would support noncanonical Wnt signalling. In addition, as syntenin-1 was reported to interact with PIP_2 and that this association stimulates syndecan and syndecan cargo recycling, it is possible that syntenin-1 plays role in joined recycling of Frizzled and syndecans (Wawrzak et al. 2009).

1.5.3.4. Other functions of syntenin-1

Syntenin-1 plays several other important roles in cells. It interacts with IL-5Rα (interleukin-5 receptor α) and the transcription factor Sox4, thus mediates IL-5 dependent activation of Sox4. IL-5 and SOX4 are implicated in B-cell development and differentiation and syntenin-1 may also be involved in these processes (Geijsen et al. 2001).

Syntenin-1 interacts with ephrinBs and ephrin receptors (Eph), thus may regulate ephrin-Eph signalling. It has been shown that syntenin-1 interaction with ephrinB ligands is important for the pre-synaptic machinery recruitment during development of presynaptic and postsynaptic compartments in neurons (McClelland et al. 2009). Syntenin also functions in regulation of axon outgrowth. It interacts with Unc51.1, which is a serine/threonine kinase important for neurite extension, and Rab5, a marker of early endosomes. This interaction creates a scaffold for Unc51.1 and endocytic machinery, what is important for the regulation of axon extension (Tomoda et al. 2004).

Recently syntenin-1 was implicated in ubiquitin-dependent sorting of transmembrane proteins and facilitating recruitment of ubiquitylated proteins to transmembrane partners. Syntenin-1 was shown to bind ubiquitin via unconventional pocket in its N-terminal domain, in a process regulated by Ulk1, a serine/threonine kinase, known to control different trafficking pathways in cells (Rajesh et al. 2011).

1.6. LNX family of ubiquitin ligases

1.6.1. RING-type E3 ligases

E3 ubiquitin ligases catalyse the transfer of ubiquitin from an E2 enzyme to the target protein and also ensure the specificity of ubiquitin modification. E3 ubiquitin ligases function by one of the two mechanisms. HECT (Homologous to E6-AP Carboxy Terminus)-type E3s serve as catalytic intermediates in ubiquitination. Ubiquitin is transferred from E2 enzyme to the catalytic cysteine of HECT domain, and later to a lysine in the substrate. Alternatively, really interesting new gene (RING)-type E3s mediate the transfer of ubiquitin directly from E2~ubiquitin to the target protein. (Budhidarmo et al. 2012;Metzger et al. 2014).

LNX proteins belong to the RING-type family of E3 ubiquitin ligases, defined by the presence of RING domain. RING type ubiquitin ligases are conserved from yeast to humans, and over 400 different ligases were identified in mammalian cells. RING domain binds Zn^{2+} ion through a cross-braced arrangement of cysteine and histidine amino acids with a characteristic spacing. The consensus sequence of this domain is $C\text{-}X_2\text{-}C\text{-}X_{(9\text{-}39)}\text{-}C\text{-}X_{(1\text{-}3)}\text{-}H\text{-}X_{(2\text{-}3)}\text{-}C\text{-}X_2\text{-}C\text{-}X_{(4\text{-}48)}\text{-}C\text{-}X_2\text{-}C$ (where X means any amino acid). Ligases use RING domain to recruit and activate an E2~ubiquitin enzyme, which in turn transfers ubiquitin to the substrate (Pickart 2001;Satija et al. 2013).

RING-type E3s were described to function as both tumour suppressors and oncogenes. At the cellular level they play critical roles in endocytic trafficking, DNA repair and activation of NF-κB signalling (Metzger et al. 2014). The interaction between E3 ligase and substrate is often mediated via protein-binding domains on the E3, such as SH2 (Src

homology 2), SH3 (Src homology 3), FHA (forkhead associated domain), ankyrin repeats or PDZ domains. Indeed, bioinformatics analysis revealed that 75% of human RING-type E3 ligases contain at least one other domain or binding motif (Deshaies et al. 2009)

Mutations or impaired modulation of RING-type E3s activity are often linked with human disease. Mutations of BRCA1, an E3 ubiquitin ligase involved in DNA repair, are associated with familial breast and ovarian cancers (Welcsh et al. 2001). FANC ubiquitin ligase, which also plays role in DNA repair, is mutated in the multisystemic Fanconi anemia syndrome, cause of severe developmental defects (Moldovan et al. 2009). Another RING-type E3, FBXO11 is often mutated or deleted in diffuse large B-cell lymphomas (Duan et al. 2012). The malignant von Hippel–Lindau syndrome is associated with mutations in VHL protein, the component of the $CRL2^{VHL}$ E3 (Lipkowitz et al. 2011). Mutations in the RING–IBR (in between RING)–RING (RBR) E3 ubiquitin ligase Parkin were reported in autosomal recessive juvenile Parkinsonism (AR-JP) (Kitada et al. 1998). Finally, increased expression of Mdm2 (double minute 2 protein) E3 ligase or loss of its negative modulator, leads to the upregulation of Mdm2 activity towards the tumour suppressor p53, and is associated with human cancers, especially those with wild type p53 (Lipkowitz et al. 2011;Metzger et al. 2014).

1.6.2. Ligand of Numb Protein-X (LNX) family

LNX (Ligand of Numb Protein-X) family of proteins, also known as PDZRN (PDZ and RING) family, consists of five members (LNX1 – LNX5) as presented in the Figure 1.9. Proteins belonging to this group are characterized by the presence of RING domain followed by one to four PDZ domains. Within the family, LNX1 and LNX2 share identical domain structure, consisting of one RING domain and four PDZ domains. There is a high degree of similarity between LNX3 and LNX4 (PDZRN3 and PDZRN4), and they are more distantly related to LNX1 and LNX2. They both contain one RING domain and two PDZ domains. LNX5 (PDZK4, PDZRN4L) lacks RING domain, but due to its high sequence homology to LNX3 and LNX4, it was also included in the family. The LNX proteins are unique in vertebrates as they are the only proteins characterized by the presence of both RING and PDZ domains. Combination of these two types of domains suggests that PDZ domains might be involved in substrate recognition and targeting the ubiquitin ligase activity of the proteins (Flynn et al. 2011).

LNX1 was initially discovered as a protein interacting with Numb, a component of Notch signalling (Dho et al. 1998). Subsequently, LNX2 was also shown to interact with Numb and its paralog Numb-like (Rice et al. 2001). Apart from Numb, several other binding partners of LNX1 and LNX2 were discovered, and they will be further discussed in following sections.

LNX3 was identified as a binding partner of Semaphorin (Sema4C) in yeast two-hybrid screen (Wang et al. 1999). Its high expression was detected in heart and muscle. LNX3 was shown to be involved in differentiation of C2C12 cells into myotubes (Ko et al. 2006) and

into osteoblasts (Honda et al. 2010). It served as a negative regulator of osteoblast differentiation through inhibition of canonical Wnt signalling. Furthermore, LNX3 was found to regulate formation of neuromuscular junction, as it interacts and ubiquitylates the muscle specific tyrosine kinase (MuSK), a key regulator of postsynaptic assembly. LNX3 promotes MuSK endocytosis thus negatively regulates its cell surface expression (Lu et al. 2007).

LNX4 and LNX5 were identified *in silico* based on homology to LNX3, and they remain virtually uncharacterized. LNX4 was found to be down regulated in the hypothalamus of Sim1 (single-minded homolog 1) knockout mice. Whereas LNX5 was identified as up-regulated in synovial sarcomas. Their physiological functions remain unknown (Flynn et al. 2011).

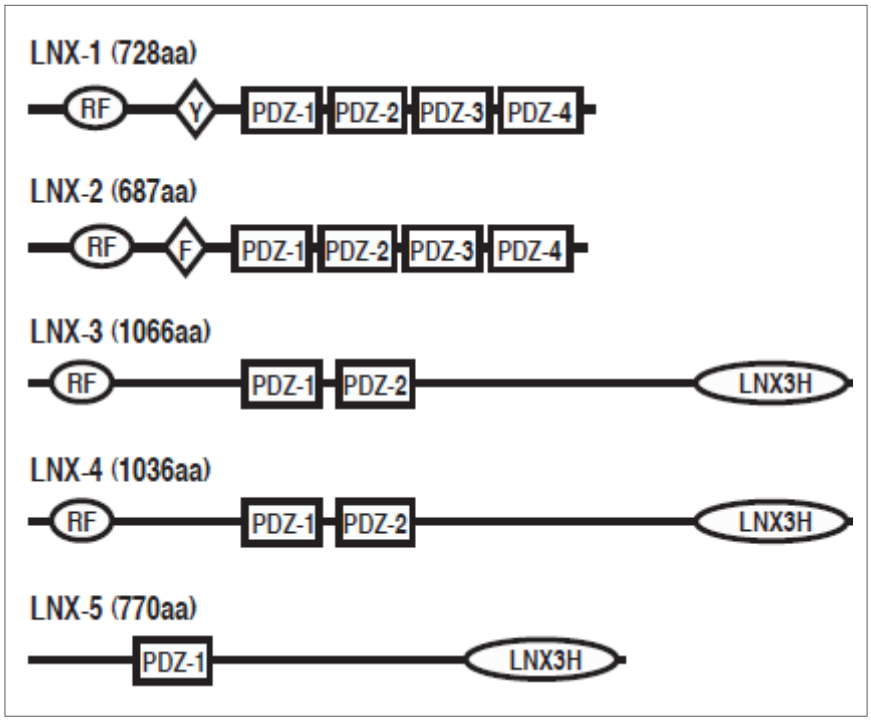

Figure 1. 9. Domain structures of mammalian LNX family members.

LNX1 and LNX2 share a similar domain structure, as do LNX3 and LNX4. The number of amino acids the murine LNX protein is indicated. Alternative splicing variants of LNX1, LNX3 and LNX4 are not presented. RF, RING finger domain; Y, NPxY motif; F, NPxF motif; PDZ, post synaptic density protein (PSD95), Drosophila disc large tumour suppressor (Dlg1), and zonula occludens-1 protein (ZO-1) domain; LNX3H, homology domain with a significant sequence similarity between LNX family members. Figure reproduced from (Flynn et al. 2011).

1.6.3. Molecular structure of LNX1 and LNX2

LNX1 and LNX2 display similar domain organisation, one RING domain followed by NPXY motif and four PDZ domains. RING finger-domains function as a catalytic component of E3 ubiquitin ligases, whereas NPXY motif (NPAY in LNX1, or NPAF in LNX2) serves a binding place for Numb protein. Amino acid sequences of LNX1 and LNX2 are identical in 50%. Orthologs of both proteins were found in all vertebrates with available genome sequences. Additionally, fish, marsupial, amphibian and bird genomes contains a LNX-2-related protein, called LNX-like or LNX2b (Flynn et al. 2011).

BLAST analysis of the NCBI GenPept protein sequence database showed that corresponding PDZ domains of LNX1 and LNX2 display sequence identity in range of 56% to 63%. Sequence identity of 17 amino acids identified as PDZ domain binding site sequence was also examined. PDZ2 and PDZ4 of LNX1 were found to share over 70% identity with PDZ2 and PDZ4 of LNX2, respectively (Wolting et al. 2011).

Furthermore, LNX1, but not LNX2, exists in two splice variants. Two cDNAs were isolated, 2.8 kb and 2.6 kb, encoding 80 and 70 kDa proteins. The 80 kDa protein (LNX1 p80) encodes the RING domain and four PDZ domains, whereas the 70 kDa protein (LNX1 p70) lacks the RING domain but contains all four PDZ domains (Figure 1.10.) (Dho et al. 1998).

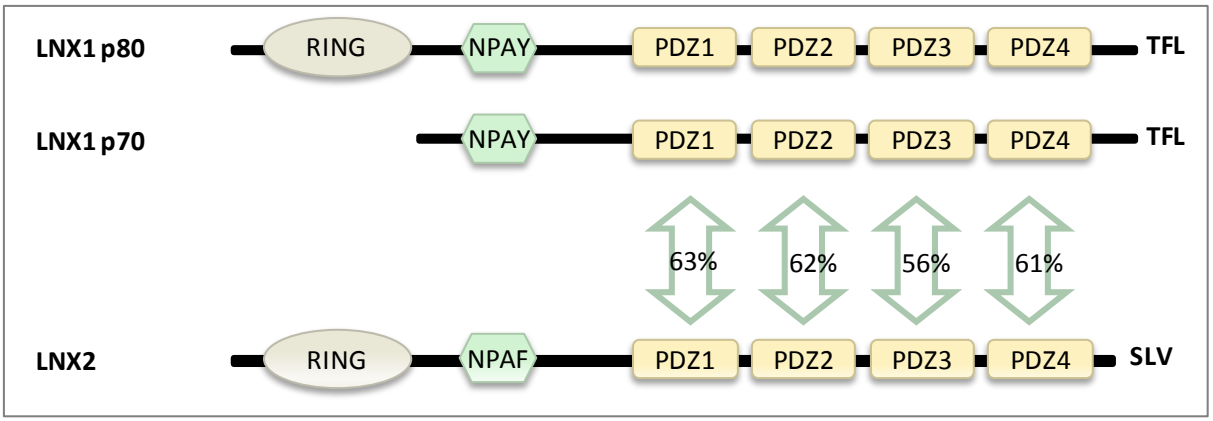

Figure 1. 10. Ligand of Numb Protein X 1 and 2.

LNX1 and LNX2 share a similar domain organisation: one RING domain followed by NPXY motif and four PDZ domains. RING finger-domains function as a catalytic component of E3 ubiquitin ligases, whereas NPXY motif (NPAY in LNX1, or NPAF in LNX2) serves a binding place for Numb protein. LNX1 exists in two splice variants, p80 and p70. Figure based on (Wolting et al. 2011).

1.6.4. Binding partners of LNX1 and LNX2

LNX1 interacts with a number of proteins, predominantly those with a PDZ binding motif. Predicted functional partners of human LNX1, retrieved from the STRING database (www.string-db.org), are presented in the Figure 1.11. A total of 166 binding partners of LNX1 have been discovered in different yeast two-hybrids and proteomics studies (Guo et al. 2012;Rice et al. 2001;Rual et al. 2005;Wolting et al. 2011). LNX1 was initially identified to interact with the cell fate determinant NUMB in a yeast two-hybrid screen (Dho et al. 1998), and subsequently it was shown to interact with all four isoforms of human NUMB as the NUMB PTB domain binds the NPAY motif in LNX1 (Dho et al. 1999). In addition, the first PDZ domain of LNX1 binds to the PTB domain of NUMB (Nie et al. 2004).

LNX1 interacts with RhoC, a small GTPase playing role in reorganization of the actin cytoskeleton. Efficient binding of RhoC to LNX1 requires the first PDZ domain of LNX1 (Zheng et al. 2010). KCNA4, a shaker-type voltage-gated K^+ channel and PLEKHG5 (pleckstrin homology domain-containing family G member 5) are also recognized by the PDZ1 of LNX1 via their carboxy terminal tails (Wolting et al. 2011). PLEKH5 can also bind to PDZ3 of LNX1. Similarly to PLEKH5, LNX1-PDZ1 and PDZ3 can both recognize the carboxy termini of the proto-oncogene c-Src, a cytoplasmic protein kinase (Weiss et al. 2007). PDZ-binding kinase (PBK) also binds to LNX1-PDZ1 (Guo et al. 2012).

LNX1-PDZ2 is involved in binding to the pre-synaptic active zone protein CAST (Higa et al. 2007), junctional adhesion molecule 4 (JAM4) (Kansaku et al. 2006) and to Coxsackie and adenovirus receptor (CAR) (Sollerbrant et al. 2003) via their C-terminus. However efficient binding to the latter requires not only C-terminal PDZ binding motif of the

receptor, but also upstream sequences. Protein kinases Tyk2, PAK6 and PKC-α1 also interact with the second PDZ domain of LNX1. Additionally PAK6 and PKC-α1 also bind to LNX1-PDZ4. Tyk2 is a member of Janus kinase (JAK) family of cytoplasmic protein tyrosine kinases, whereas PAK6 and PKC-α1 are serine/threonine kinases involved in signal transduction, cell proliferation and apoptosis (Wolting et al. 2011). LNX1-PDZ4 was also shown to bind numerous PIPs (phosphatidylinositol phosphates). PDZ4 is the only PDZ domain of LNX1 found to interact with membrane phospholipids and it may regulate LNX1 subcellular localization (Wolting et al. 2011).

Several other ligands have been identified for LNX1, including: CD8α, the T-cell co-receptor (D'Agostino et al. 2011); Claudin-1, a tight junction protein (Takahashi et al. 2009); ErbB2, a member of the epidermal growth factor receptor family (Young et al. 2005); SKIP, the transcription and splicing factor Ski-interacting protein (Chen et al. 2005) and the human endogenous retrovirus protein NP9 (Armbruester et al. 2004). Additionally, MAGE-B18, a melanoma antigen family member has been shown to bind to a basic region between the RING and first PDZ domain of LNX1 via the MAGE homology domain (MHD) (Doyle et al. 2010).

LNX2 has been shown so far to interact only with Numb protein (Nie et al. 2002), CAR receptor (Sollerbrant et al. 2003) and with CD8α (D'Agostino et al. 2011).

LNX1 and LNX2 contain consensus type I PDZ domain-binding motifs (T-x-L in LNX1 and S-x-V in LNX2) at their C-termini that can also bind PDZ domains. Indeed, in yeast two-hybrid assays, LNX1 has been shown to homo-oligomerize and hetero-oligomerize with LNX2, indicating the possibility that LNX proteins may be able to form large oligomeric networks in the cell (Rice et al. 2001). In the latest proteomics study Guo and colleagues

discovered that PDZ domains of LNX can interact with each other and form dimers (Guo et al. 2012). They have found three pairs of PDZ-PDZ interactions: LNX1-PDZ1 and LNX1-PDZ4, LNX1-PDZ1 and LNX2-PDZ4, and LNX2-PDZ1 ad LNX2-PDZ4. Using LNX1-PDZ1 and LNX2-PDZ1 as baits in Y2H, they have also discovered that neither of these domains interact with their own C-termini. However, the interaction of LNX1-PDZ1 with C-terminus binding motif of LNX2 was detected. Recent study by Mu and colleagues revealed that the first PDZ domain of LNX2 (LNX2-PDZ1) is able to bind internal PDZ-BM. 17 unique internal binding motifs were identified, with consensus sequence φ-Tx-φ-Tx- φ, which can be regarded as two canonical class II C-terminal PDZ-BM in tandem (Mu et al. 2014).

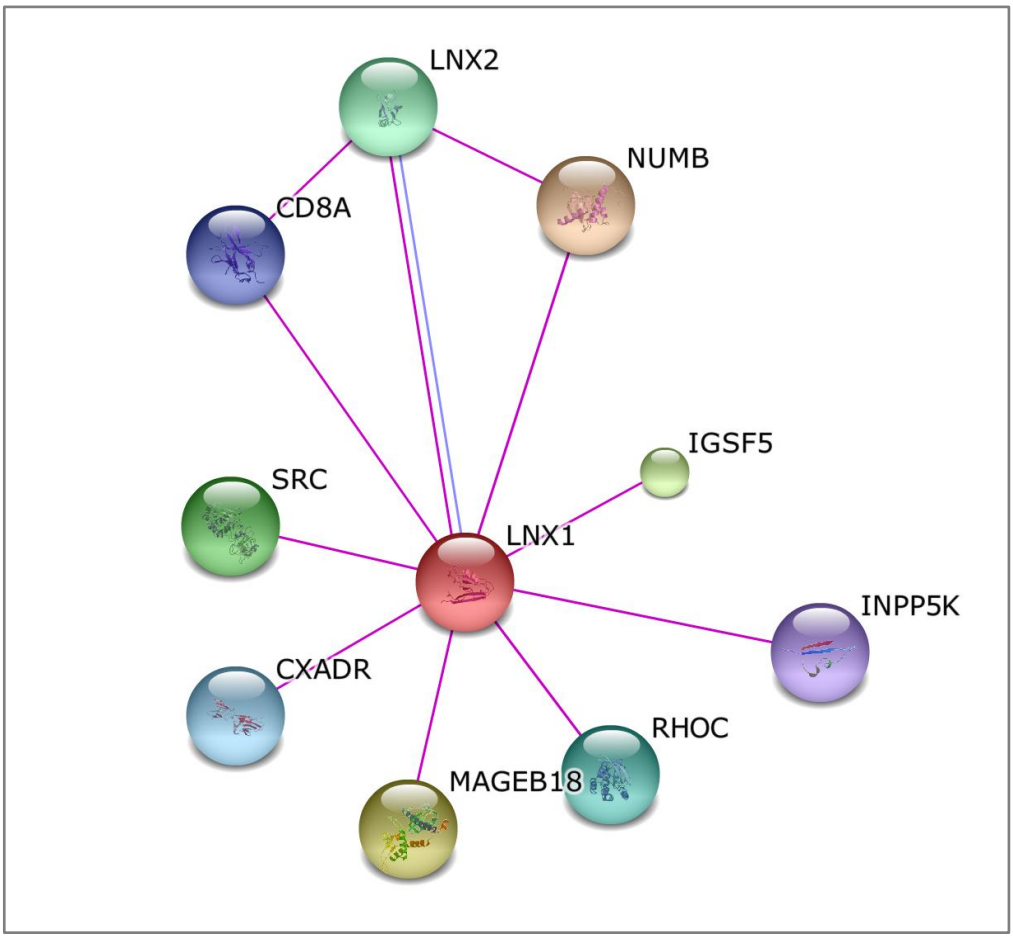

Figure 1. 11. Functional partners of LNX1.

Network of binding partners of LNX1 based on experimental evidence, retrieved from the STRING database (www.string-db.org). LNX1, ligand of numb protein X1; LNX2, ligand of numb protein X2; NUMB, numb homolog; MAGEB18, melanoma antigen family B 18; IGSF5, immunoglobulin super family member 5; SRC, c-Src sarcoma viral oncogene homolog; RHOC, Ras homolog gene family member C; CXADR, coxsackie virus and adenovirus receptor; CD8A, CD8α molecule; INPP5K, inositol polyphospate-5-phosphatase K.

1.6.5. Functions of LNX1 and LNX2

The functional significance of many interactions presented in the previous section remains unclear. Nevertheless LNX1 and LNX2 have been shown to function as both E3 ubiquitin ligases and molecular scaffolds in regulation of the activity, stability, or subcellular localization of their interacting partners. LNX proteins are involved in several different biological process, such as Notch signalling, tight junction reorganization and Wnt signalling.

1.6.5.1. Notch signalling

The E3 ligase activity of LNX1 p80 and LNX2 is possible due to the RING domain, which has been shown to have the ubiquitin ligase activity *in vitro* and *in vivo.* The first protein identified as a target of LNX1 ubiquitylation was Numb protein, a component of Notch signalling pathway. Numb is an endocytic adapter, shown to control cell fate during development by suppressing Notch receptor. LNX1 can ubiquitilate two isoforms of Numb (p66 and p72), containing the eleven amino acid insert in the PTB domain, and target them for proteasomal degradation. LNX1 functions as a positive regulator of Notch signalling by promoting Numb degradation and reducing its ability to antagonize Notch (Nie et al. 2002;Nie et al. 2004). Homologous LNX2 was also shown to interact with Numb and is also likely to ubiquitilate the protein and thereby modulate Notch signalling (Nie et al. 2002;Rice et al. 2001). Finally, LNX2 siRNA-mediated silencing leads to downregulation of NOTCH1 expression. Also, following LOF (loss-of-function mutation) of LNX2, the protein level of

Numb and expression of JAGGED1, a ligand for the receptor Notch1, were significantly reduced in colorectal cell line SW480 (Camps et al. 2013).

1.6.5.2. Tight junction reorganization

Both LNX1 and LNX2 play a crucial role in tight junction (TJ) reorganization, as they have been shown to interact with multiple TJ components, namely CAR, JAM4 and claudins. LNX1 and LNX2 bind to the Coxsackie and adenovirus receptor (CAR) and might function together at intercellular junctions (Sollerbrant et al. 2003). LNX1 was also reported to interact with junctional adhesion molecule 4 (JAM4), an immunoglobulin superfamily member present at TJs. LNX1 is involved in JAM4 endocytosis and redistribution after transforming growth factor (TGF) β induction. Numb protein was found to be involved in this process and to form a tripartite complex with JAM4 and LNX1, important for the LNX1-mediated endocytosis of JAM4. This suggests that LNX1 provides an endocytic scaffold for JAM4 (Kansaku et al. 2006). Finally, claudin-1, claudin-2 and claudin-4 had been reported to be polyubiquitylated by LNX1, followed by their internalization and degradation in lysosomes. Overexpression of LNX1 in MDCK (Madin-Darby canine kidney) cells led to downregulation of claudins from TJs and reduced the number of tight junctions (Takahashi et al. 2009). Recently, LNX1 has been shown to interact also with claudin-17 (Guo et al. 2012).

1.6.5.3. Wnt signalling

Recently, several reports have implicated the role of LNX family members in Wnt signalling. Wnt signalling regulators Naked2 (Nkd2) and Dishevelled-3 (Dvl3) have been identified to interact with LNX1 PDZ domains (Wolting et al. 2011). Additionally, LNX3 was found in a high-throughput siRNA screen designed to identify novel Wnt regulators, as required for Wnt signal transduction (Major et al. 2008). LNX3 has been shown to be an antagonist of Wnt signalling transmission in osteoblast precursor cells (Honda et al. 2010) and also to ubiquitylated Dishevelled-3 to promote PCP signalling in endothelial cells (Sewduth et al. 2014). Furthermore, LNX2b (an LNX zebrafish ortholog) has been implicated in canonical Wnt signalling in the developing zebrafish embryo. LNX2b was shown to bind and ubiquitylate the Wnt inhibitor Bozozok, followed by its degradation. Also, altered dorso-ventral patterning in the LNX2b knockdown embryos coincided with increased stabilization of Bozozok. As a consequence LNX2b-mediated degradation of Bozozok, the β-catenin Wnt signalling was upregulated (Ro et al. 2009). Finally, it was reported that siRNA-mediated silencing of LNX2 downregulated the transcription factor TCF7L2 and its targets, and reduced Wnt signalling in colorectal cancer cells. TCF7L2 is an important effector of the Wnt pathway and is responsible for transcriptional regulation of genes involved in Wnt signalling (Camps et al. 2013).

1.6.5.4. Other functions

LNX1 p80 and LNX2 are also involved in ubiquitylation, internalization and degradation in lysosomes of CD8α, a T-cell co-receptor (D'Agostino et al. 2011). Authors also suggested that LNX2 might be involved in the regulation of CD8α transport to, through, or from Golgi complex.

LNX1 also ubiquitilates the non-receptor tyrosine kinase c-Src. In addition to acting as a substrate for LNX1 ubiquitylation, c-Src was shown to phosphorylate LNX1. That suggests that c-Src may have a role in regulation of LNX1 activity (Weiss et al. 2007).

Guo and colleagues reported that LNX1 mediates ubiquitylation and degradation of PBK, what leads to inhibition of cell proliferation and enhances cell sensitivity to doxorubicin-induced apoptosis. It indicates the role of LNX1 in regulation of cell growth and apoptosis, thus it may act as a tumour suppressor (Guo et al. 2012). Furthermore, a separate genomic study demonstrated that LNX1 knockdown leads to cell cycle arrest in the G_0/G_1 phase (Zheng et al. 2011).

1.6.6. Major sites of expressions of LNX1 and LNX2

Murine LNX1 mRNA is widely expressed. It was found in brain, lung, heart, kidney and skeletal muscle. LNX1 p80 was specifically reported in heart, skeletal muscle and lunges, whereas LNX1 p70 expression was restricted to brain and heart (Dho et al. 1998). Human LNX1 mRNA is similarly expressed in brain, heart, kidney, skeletal muscle and lunges as well as placenta and pancreas (Xie et al. 2001). Murine LNX2 mRNA was detected in liver, spleen, lung, heart, kidney, thymus, skeletal muscle and brain. Interestingly, expression of LNX1 and LNX2 overlaps in some brain regions and differs in others (Rice et al. 2001).

1.6.7. Subcellular localization of LNX1 and LNX2

Several studies have examined the subcellular localization of LNX1 and LNX2 in different cell lines by fluorescence microscopy and reported its diffuse distribution throughout the cytoplasm and nucleus. In HEK293 cells LNX1 colocalizes with CAR at cell-cell contacts (Sollerbrant et al. 2003). In HeLa cells, LNX1 was shown to localize in the plasma membrane proximity, as well as diffuse in the cytoplasm and nucleus. It also localizes to the microtubule-like structures (Weiss et al. 2007). Sometimes LNX1 distribution is altered by co-expression with its interacting partners. Interaction with NP9 leads to LNX1 recruitment to punctuate nuclear structures (Armbruester et al. 2004). Additionally, LNX1 and LNX2 were recruited from the cytoplasm to the plasma membrane by the human glycoprotein CD8α (D'Agostino et al. 2011). On the other hand, RhoC was redistributed from the cytoplasm to the nucleus by LNX1 (Zheng et al. 2010). In MDCK cells, endogenous LNX1

co-localizes with JAM4 to TJs along with JAM4 (Kansaku et al. 2006). However overexpressed LNX1 localizes to the cytoplasm and to the apical junctional complex, where it colocalizes with ZO-1 at TJs. Furthermore, LNX1 was reported to colocalize with claudin-2 in late endosomes and lysosomes of MDCK cells (Takahashi et al. 2009)

1.6.8. LNX1 and LNX2 in diseases

LNX1 has been implicated in brain tumourigenesis. LNX1 mutations were found in a number of human gliomas (Blom et al. 2008) and the protein was reported to be downregulated in all gliomas (Chen et al. 2005). Susceptibility to Kawasaki disease, an infectious inflammatory vasculitis has also been linked to alterations in LNX1 expression (Burgner et al. 2009). Additionally, interactions of LNX1 with proto-oncogene NP9 and c-Src indicate its role in tumourigenesis (Armbruester et al. 2004;Weiss et al. 2007). High levels of LNX1 and LNX2 mRNAs were found in endocarditis, the principal manifestation of chronic Q fever, but not in acute Q fever (Mehraj et al. 2012). Finally, LNX2 overexpression was linked with chromosome 13 amplification and activation of the Wnt and Notch signalling pathways in colorectal cancer (Camps et al. 2013).

1.7. Research objectives

Frizzled-7, a member of Frizzled family of Wnt receptors, emerges as a key component involved in activation of Wnt signalling in breast cancer cells. It is a transmembrane receptor containing two PDZ binding motifs (PDZ-BM) in its cytoplasmic tail. The membrane proximal PDZ-BM is a binding site for Dishevelled, a crucial component of Wnt signalling pathways. Whereas the contribution of the C-terminal PDZ-BM of Frizzled receptors to Wnt signalling remains poorly studied. PDZ domains are very common in multicellular organisms and present in structures of many scaffolding proteins. They facilitate protein interactions and are implicated in regulation of cell signalling, maintenance of cell polarity, as well as in modulation of trafficking and clustering of membrane receptors. We hypothesized that PDZ proteins interacting with the C-terminal PDZ-BM of Frizzled receptors are involved in these processes. In this study we focused on Frizzled-7 and the role of the C-terminal PDZ-BM in the receptor functionality. Specific aims of this study were as follow:

- To determine the importance of Frizzled-7 interactions via the C-terminal PDZ-BM for transduction of canonical Wnt signalling
- To determine the role of syntenin-1, an established Frizzled-7 PDZ partner in canonical Wnt signalling
- To identify novel Frizzled-7 partners interacting with the C-terminal PDZ-BM of the receptor and examining their role in canonical Wnt signalling

2. MATERIALS AND METHODS

2.1. Materials

2.1.1. Antibodies

Table 2. 1. Primary antibodies used in this study.

Abbreviations: mAb, monoclonal antibody; pAb, polyclonal antibody; WB, western blotting; IF, immunofluorescence; FC, flow cytometry;

Primary Antibody	Species	Target antigen	Supplier	Catalogue number	Dilution
anti-beta actin mAb	mouse	human beta-actin	Sigma Aldrich	A5316	WB: 1:40 000
anti-beta-catenin mAb	mouse	human beta-catenin	BD Laboratories	610153	WB: 1:2000
anti-FLAG M2 mAb	mouse	FLAG tag sequence	Sigma Aldrich	F1804	IF: 1:1000; FC: 1:300
anti-FLAG pAb	rabbit	FLAG tag sequence	Sigma Aldrich	F7425	WB: 1:3000; IF: 1:1000
anti-GFP pAb	rabbit	GFP	Invitrogen	A6455	WB: 1:1000
anti-HA pAb	rabbit	HA tag sequence	Santa Cruz Biotechnology	sc-805	WB: 1:500
anti-HA mAb	mouse	HA tag sequence	Santa Cruz Biotechnology	sc-7392	IF:1:25
anti-LNX2 pAb	rabbit	human LNX2	ProteinTech	13719-1-AP	WB 1:500
anti-Myc mAb (9E10)	mouse	Myc tag sequence	Santa Cruz Biotechnology	sc-40	WB: 1:500; IF:
anti-Myc pAb (A-14)	rabbit	Myc tag sequence	Santa Cruz Biotechnology	sc-789	WB: 1:200; IF:1:100
anti-Syntenin 1 mAb	rabbit	human syntenin-1	Abcam	ab133267	WB: 1:1000
anti-V5 pAb	rabbit	V5 tag sequence	Sigma Aldrich	V8137	WB: 1:2000

Table 2. 2. Secondary antibodies used in this study.

Abbreviations: HRP, horseradish peroxidise; FITC, fluorescein-5-isothiocyanate;

Antibody against	Conjugation	Host species	Supplier	Catalogue number
mouse IgG	HRP	goat	Dako	P0447
rabbit IgG	HRP	goat	Dako	P0448
mouse IgG	IRDye 680RD	goat	Licor	926-68078
rabbit IgG	IRDye 800CW	goat	Licor	926-32211
mouse IgG	FITC	goat	Sigma-Aldrich	F2012
mouse IgG (H+L)	Alexa Fluor® 488	goat	Life Technologies	A-11017
mouse IgG (H+L)	Alexa Fluor® 546	goat	Life Technologies	A-11003
rabbit IgG (H+L)	Alexa Fluor® 488	goat	Life Technologies	A-11008
rabbit IgG (H+L)	Alexa Fluor® 594	goat	Life Technologies	A-11012

2.1.2. DNA oligonucleotides

Table 2. 3. DNA oligonucleotides used for cloning, sequencing or mutagenesis.

All DNA oligonucleotides were purchased from Sigma-Aldrich and were designed to amplify human genes. Abbreviations: Fw, forward primer; Rv, reverse primer;

Primer	Sequence (5'-3')	Application
P1	GTCATTGAATTCGCCACCATGCGGGACCCCGGCGC	Fw Fz7, cloning
P2	GATCTCGGATCCGTCATACCGCAGTCTCC	Rv Fz7, cloning
P3	GATTATAAAGATGATGATGATAAAGGTAGTTACCACGGAGAGAAGG	Fw Fz7, cloning, FLAG insert
P4	TTTATCATCATCATCTTTATAATCACTACCCGGCTGCGCCCCGGCG	Rv Fz7, cloning, FLAG insert
P5	TACCGGTCGTTATTATGAAGTCCGGAGGTAGTTACCACGGAGAGAAGG	Fw Fz7, cloning, linker sequence insert
P6	TCCGGACTTCATAATAACGACCGGTAGACTACCCGGCTGCGCCCCGGCG	Rv Fz7, cloning, linker sequence insert
P7	GATCTCGGATCCGTCA TCC CGC AGT CTC CCC CTT G	Rv Fz7, cloning, V574G
P8	GATCTCGGATCCGTCA TTC CGC AGT CTC CCC CTT G	Rv Fz7, cloning, V574E
P9	AGAACACGTCGGACGGC	Fw Fz7, sequencing
P10	CCATGGCCAGGATAGTG	Rv Fz7, sequencing
T7	TAATACGACTCACTATAGGG	sequencing
As	TAGAAGGCACAGTCGAGG	Rv pcDNA3, sequencing

2.1.3. DNA plasmids

DNA constructs were generated according to cloning procedures, as described in 2.3.2. These are listed in Table 2.4. The DNA constructs provided by other scientists and used for transfections or as templates for cloning are listed in Table 2.5.

Table 2. 4. Cloned DNA constructs.

Construct	Cloning details
pcDNA™3.1-FLAG-Fz7	FLAG epitope was introduced at position 34 of human Fz7; cloned into pcDNA3.1 plasmid using EcoRI and BamHI sites
pcDNA™3.1-Myc-Fz7	Myc epitope was introduced at the position 34 of human Fz7; cloned into pcDNA3.1 plasmid using EcoRI and BamHI sites
pcDNA™3.1-GFP-Fz7	GFP was introduced at the position 34 of human Fz7; cloned into pcDNA3.1 plasmid using EcoRI and BamHI sites
pcDNA™3.1-FLAG-Fz7 V574G	Mutagenised Flag-tagged human Fz7 cloned into pcDNA3.1 plasmid using EcoRI and BamHI sites
pcDNA™3.1-FLAG-Fz7 V574E	Mutagenised Flag-tagged human Fz7 cloned into pcDNA3.1 plasmid using EcoRI and BamHI sites
pcDNA™3.1-Myc-Fz7 V574G	Mutagenised Myc-tagged human Fz7 cloned into pcDNA3.1 plasmid using EcoRI and BamHI sites
pcDNA™3.1-GFP-Fz7 V574G	Mutagenised GFP-tagged human Fz7 cloned into pcDNA3.1 plasmid using EcoRI and BamHI sites
pcDNA™3.1-GFP-Fz7 V574E	Mutagenised GFP-tagged human Fz7 cloned into pcDNA3.1 plasmid using EcoRI and BamHI sites

Table 2. 5. Other plasmids.

The plasmids listed in the table contain sequences of human genes, unless otherwise stated.

Plasmid encoding:	Kindly provided by:
FLAG-GIPC1	Dr Fedor Berditchevski
FLAG-MAGI1	Dr Lawrence Banks
FLAG-MPP5	Dr Fedor Berditchevski
FLAG-MPP7	Dr Scott Vande Pol
FLAG-NHERF	Dr Maria-Magdalena Georgescu
FLAG-Syntenin 1	Dr Fedor Berditchevski
GFP-GOPC	Dr Fedor Berditchevski
GFP-LNX1 p70	Dr Yutaka Hata
GFP-LNX1 p80	Dr Massimo D'Agostino
GFP-LNX2	Dr Massimo D'Agostino
HA-Dlg1	Dr Lawrence Banks
HA-LNX2	Dr Massimo D'Agostino
HA-LNX2 PDZ1-2	Dr Massimo D'Agostino
HA-LNX2 PDZ1-4	Dr Massimo D'Agostino
HA-LNX2 PDZ3-4	Dr Massimo D'Agostino
HA-Scribble	Dr Lawrence Banks
HA-Syntenin 1	Dr Fedor Berditchevski
HA-Syntenin 1-PDZ1* (G126D)	Dr Fedor Berditchevski
HA-Syntenin 1-PDZ1*-PDZ2* (G126D, G210E)	Dr Fedor Berditchevski
HA-Syntenin 1-PDZ2* (G210E)	Dr Fedor Berditchevski
M50 Super 8x TOPFlash	Addgene, plasmid 12456
M51 Super 8x FOPFlash (TOPFlash mutant)	Addgene, plasmid 12457
Myc-Fz7-V5-His; Fz7-V5-His	Dr Catherine Mao
Myc-INADL	Dr Fedor Berditchevski
Myc-LNX2	Addgene, plasmid 37010
Myc-PSD95	Dr Karen Sommer
Myc-Syntenin-1	Dr Fedor Berditchevski
pcDNA™3.1 (puromycin resistant)	Dr Fedor Berditchevski
pcDNA™3.1-GFP	Dr Fedor Berditchevski
pEGFP-C1	Dr Fedor Berditchevski
pRenilla	Dr Chris Dawson
V5-MAGI3	Dr Lawrence Banks

2.1.4. siRNA duplexes

The siRNAs used included siLNX2 (ON-TARGETplus Human LNX2 siRNA – SMART pool) purchased from ThermoScientific Dharmacon, siSyntenin-1 purchased from Eurofins MWG Operon, and siNEG (negative control siRNA) purchased from Qiagen.

Table 2. 6. siRNA duplexes.

	Sequence (5′-3′)
ON-TARGETplus SMARTpool Human LNX2 siRNA	CCAAGUGGCUCUUCAUAAA
	GGACAUACAUUCUGCUACA
	CUUCAUAGCUGCCACGAUA
	CAACGAAACACCUUUGAUU
Syntenin-1 siRNA	GGAUGGAGCUCUGAUAAAGTT
Negative siRNA	UUCUCCGAACGUGUCACGUdTdT

2.2. Cell culture methods

2.2.1. Mammalian cell lines

Origin and characteristics of cell lines used in the study are listed in the Table. HEK293T, SKBr3, MDA-MB-231, T47D and MCF7 were obtained from Cancer Research UK, L cells and L-Wnt3a from ATCC.

Table 2. 7. Mammalian cell lines used in this study.

Cell line	Tissue	Cell type	Tumour
HEK293T	Human Embryonic Kidney	Epithelial	NA
MCF7	Human Breast	Epithelial	Adenocarcinoma
MDA-MB-231	Human Breast	Epithelial	Adenocarcinoma
SKBr3	Human Breast	Epithelial	Adenocarcinoma
T47D	Human Breast	Epithelial	Ductal Carcinoma
L cells	Mouse Subcutaneous Connective Tissue	Fibroblast	NA
L Wnt3a	Mouse Subcutaneous Connective Tissue	Fibroblast	NA

2.2.2. Maintenance of mammalian cell lines

All mammalian cells were cultured in sterile tissue culture dishes or flasks (Corning). HEK293T, SKBr3, MDA-MB-231, MCF7 and L cells were grown in high glucose (4500 mg/l) Dulbecco's Modified Eagle's Medium (DMEM) (Gibco), supplemented with 10% (v/v) Fetal Calf Serum (FCS) (Gibco) and 50 U/ml Penicillin / 50 μg/ml Streptomycin (Gibco). L Wnt3a cells were grown in medium as mentioned above, supplemented with 0.4 mg/ml G418 (Sigma-Aldrich). Stably transfected SKBr3 cells were maintained in the presence of 2 μg/ml

puromycin (Sigma-Aldrich). All cell lines were cultivated at 37°C, in humidified incubator (Galaxy R CO2 Incubators, RS Biotech) in 5% CO_2 atmosphere. When passaging, cells were split in the ratio 1:5 (SKBr3, MDA-MB-231, MCF7) or 1:10 (HEK293T, L cells, L Wnt3a) twice a week. Growth medium was removed, and a confluent monolayer of cells was washed with sterile phosphate buffer saline (PBS) to remove all traces of serum that contains trypsin inhibitors. To detach cells from a plastic surface, they were incubated with 0.05% Trypsin-EDTA (Gibco) for 5 min at 37°C to facilitate dispersal. Subsequently, cells were collected from plate in a fresh growth medium and pelleted by centrifuging at 900 RPM for 3 min. After resuspension in complete growth medium, cells were plated at required density. Cell growth and condition were monitored using Nikon TMS microscope.

2.2.3. Cryopreservation and recovery of cell lines

Detached cells, as described in section 2.2.2, were resuspended in freezing solution (10% (v/v) dimethyl sulfoxide (DMSO) (Sigma-Aldrich) and 90% (v/v) Fetal Calf Serum (FCS)). The suspension was subsequently frozen in 1 ml CryoTube™ vials (Nunc) at -80°C for at least 24h before transferring to liquid nitrogen for long term storage.

Cells were recovered by thawing in a water bath for 2 min at 37°C. Thawed cell suspension was transferred to a tube with 9 ml of pre-warmed, complete growth medium and pelleted by centrifugation at 900 RPM for 3 min. Pellet was resuspended in fresh medium and cells were seeded in T25 tissue culture flask. Cells were incubated at 37°C, in humidified 5% CO_2 atmosphere for at least 48h before further manipulation.

2.2.4. Counting cells

When a specified number of cells was required for an experiment, cells were trypsinized (Section 2.2.2), resuspended in fresh complete medium and counted. 10 µl of cell suspension was used to count cell in Neubauer haemocytometer counting chamber (Marienfeld) according to the manufacturer's instructions.

2.2.5. Mycoplasma testing

Cultured cell lines were routinely tested to ensure they were mycoplasma free. Mycoalert® Mycoplasma Detection Kit (Lonza) was used, according to the manufacturer's instructions.

2.2.6. Cell transfection

2.2.6.1. Polyethyleimine (PEI)

HEK293T cells were transfected with DNA plasmids using polyethyleimine (PEI) (Sigma-Aldrich). PEI working solution (1 mg/ml) was prepared by warming up stock solution at 55°C and dissolving appropriate amount in dH_20. After cooling down to room temperature, PEI was neutralized with HCl to pH 7.0 and filter sterilized (0.22 µm syringe filters (Appleton Woods)). Aliquots were stored at -20°C.

To transfect cells, DNA and PEI were mixed in Opti-MEM® I reduced-serum medium (Gibco) (without FCS), in the amounts indicated in the Table 2.8. Prepared mix was

vortexed, briefly centrifuged and incubated at room temperature for 45-60 min. Cell growth medium was removed from culture dishes, and changed for DMEM (without FCS). Transfection mix was gently added to the dishes with cells and incubated for 3h at 37°C. After that time, cell medium was changed for complete growth medium (DMEM supplemented with 10% FCS and pen/strep). Experiments were performed 24h after transfection, unless stated otherwise.

Table 2. 8. Transfection guidelines for PEI transfection reagent.

Container	Opti-MEM® [µl]	DNA [µg]	PEI [µl]	Number of cells
6 well (1 well)	100	2.5	3.75	0.5*106
6 cm	200	7.3	11	1.5*106
10 cm	600	20.0	30.0	4*106

2.2.6.2. FuGENE®6 Transfection Reagent

MCF7 and SKBr3 cells were transfected using FuGENE®6 Transfection Reagent (Promega), according to the manufacturer's protocol. 24h prior transfection, cells were trypsinized and plated on a required dish in numbers adequate to obtain 50-70% cell confluency on the day of transfection. FuGENE®6 Transfection Reagent and plasmid DNA ratio of 3:1 (3µl of transfection reagent for 1 µg of plasmid DNA) was maintained throughout all experiments. FuGENE®6 was brought to room temperature, added drop wise to Opti-MEM® I reduced-serum medium and incubated for 5 minutes at room temperature. Subsequently, plasmid DNA was added to FuGENE®6-OptiMEM, mixed immediately and incubated for further 20 minutes at room temperature to allow formation of lipo-complexes with DNA. Volumes and amounts of required reagents are summarized in the Table 2.9.

Transfection mix was added directly to cells cultured in full growth medium and gently mixed to obtain even distribution of complexes. Cells were returned to the incubator (37°C, 5% CO_2) for 24-48h before performing further assays.

Table 2. 9. Transfection guidelines for FuGENE®6 transfection reagent.

Container	Opti-MEM® [µl]	FuGENE®6 [µl]	DNA [µg]	Number of cells
48-well (1 well)	10	0.3	0.1	$0.25*10^5$
24-well (1 well)	20	0.6	0.2	$0.5*10^5$
12-well (1 well)	50	1.5	0.5	$1*10^5$
6-well (1 well)	100	3.0	1.0	$1.5*10^5$
35 mm	100	3.0	1.0	$1.5*10^5$
60 mm	200	6.0	2.0	$7.5*10^5$
10 cm	600	18.0	6.0	$1.8*10^6$

2.2.6.3. Lipofectamine™ RNAiMAX Reagent

SKBr3 and HEK293T were transfected with siRNA duplexes using Lipofectamine™ RNAiMAX Reagent (Invitrogen), according to the manufacturer's protocol. Reverse transfection procedure was employed, where the complexes are prepared inside the wells of culture dishes, after which cells and medium are added. To prepare siRNA-Lipofectamine™ RNAiMAX complexes, siRNA was diluted in Opti-MEM® I Medium without serum. Then Lipofectamine™ RNAiMAX was added, mixed gently and incubated for 10-20 minutes at room temperature. Trypsinized cells were resuspended in complete growth medium without antibiotics and added to each well containing siRNA-Lipofectamine™ RNAiMAX complexes. Cell density should be 50% confluent on the next day after plating. The final volume of Opti-MEM® I Medium transfection mix together with the volume of cell

suspension was calculated to obtain a final RNA concentration of 10 nM. All amounts and volumes are summarized in the Table 2.10.

Table 2. 10. Transfection guidelines for Lipofectamine™ RNAiMAX Reagent.

Culture vessel	Volume of plating medium [µl]	Number of cells plated per well	Dilution medium (Opti-MEM®) [µl]	siRNA [pmol]	Final siRNA conc. [nM]	Lipofectamine™ RNAiMAX [µl]
48-well (1 well)	200	$0.25*10^5$	40	2.4	10	0.4
24-well (1 well)	500	$0.5*10^5$	100	6	10	1
12-well (1 well)	1000	$1*10^5$	200	12	10	2
6-well (1 well)	2500	$1.5*10^5$	500	30	10	5
60 mm	5000	$7.5*10^5$	1000	60	10	10

2.2.7. Generation of SKBr3 cell lines with stable expression of Frizzled 7

As described in Section 2.2.6.2., parental SKBr3 cell were transfected plasmids pcDNA™3.1-FLAG-Fz7, pcDNA™3.1-FLAG-Fz7 V574G or pcDNA™3.1(-) using FuGENE®6 Transfection Reagent. The first plasmid encodes the wild type human Frizzled-7 cDNA with N-terminal FLAG-tag. Second encodes FLAG-tagged human Frizzled-7 cDNA with the mutation of the last Valine to Glycine (V574G). Both constructs were cloned into pcDNA™3.1 (-) mammalian expression vector encoding puromycin resistance gene (procedure described in details in the section 2.3.2.2.). pcDNA™3.1(-) plasmid was used to

generate SKBr3-control cell line. 48h after transfection with DNA plasmids, cells medium was changed for the regular growth medium containing puromycin (Sigma-Aldrich) (2μg/ml) to select for stable transfectants. Puromycin containing medium was replaced every 3-4 days, until isolated colonies started to appear. After selection (2-3 weeks) cells were sorted two times using anti-Flag mouse mAb and fluorescent activated cell sorting (FACS) (Section 2.6.1.) to obtain SKBr3-FLAG-Fz7 and SKBr3-FLAG-Fz7 V574G stable cell lines.

2.2.8. Production of Wnt3a conditioned medium

Mouse fibroblast, L cells, were transfected for stable expression of Wnt3a (Willert et al. 2003). L Wnt3a cells are cultivated in DMEM complete growth medium supplemented with 0.4 mg/ml G418. To prepare Wnt3a conditioned medium (Wnt3a CM) cells were split and replated into 15 cm culture dish, without G418 if conditioned was to be used with a cell line sensitive to G418. For 15 cm dish, $4*10^6$ cells were seeded. Cells were grown until almost confluent, for approximately 48h. Each plate was washed with PBS and 25 ml of complete growth medium was added. Cells were then incubated for 4 days (37°C, 5% CO_2). Conditioned media were collected into 50 ml tubes and centrifuged at 1000 RPM for 5 minutes. Supernatants were filter sterilized and stored at 4°C. In all experiment conditioned medium was used in dilution 1:2. Since the conditioned medium contains also other factors than Wnt3a, it was important to control all experiments with control conditioned medium from the parental cell line (L cell), prepared in similar way as Wnt3a conditioned medium.

2.2.9. Bacteria strains, media and antibiotics

The chemically competent *Escherichia Coli* (*E.Coli*) DH5α (NEB) were used for transformation with various DNA plasmids. Bacteria were cultured in Luria Bertani (LB) broth or LB agar (Invitrogen) with appropriate antibiotics. Final concentrations of used antibiotics were as follow: ampicillin (Sigma-Aldrich) 100 μg/ml and kanamycin (Sigma-Aldrich) 30 μg/ml. Bacteria were grown on LB agar plates at 37°C in incubator (Heraeus) or in liquid LB media at 37°C in the orbital shaking incubator (Gallenkamp).

2.3. Manipulation of DNA material.

2.3.1. Molecular cloning

The DNA cloning was performed as summarised in the figure. 2.1. All the steps are described in detailed in the next sections. Tagged Fz7 constructs were generated using Myc-Fz7-V5-His or Fz7-V5-His plasmids as the templates (Struewing et al. 2007). Amino acid sequences corresponding FLAG and Myc epitopes, and GFP were introduced at the position 34, after the signal peptide, on the N-terminus of the receptor. Tagged Fz7 WT, Fz7 V574G and Fz7 V574E were generated using a standard PCR technique and cloned into pcDNA™3.1 plasmid using EcoRI and BamHI sites. Sequences of all DNA oligonucleotides (primers) used in this study are listed in the Table 2.3.

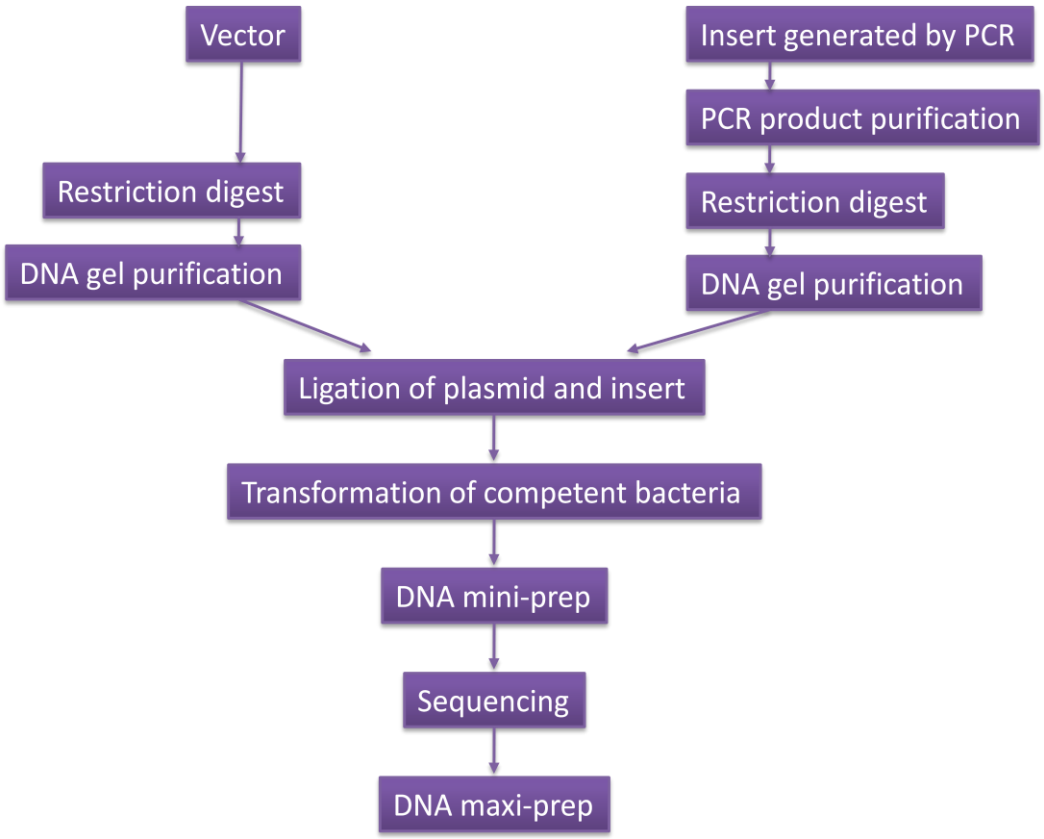

Figure 2. 1. Cloning process.

The DNA sequence of interest (insert) was generated by PCR with forward and reverse primers which contained specific restriction sites. The insert and plasmid were then digested with restriction enzymes, resolved by agarose gel electrophoresis, purified and ligated together. The ligation mixtures were subsequently introduced into competent bacteria by transformation. Bacteria from the antibiotic-resistant colonies were further cultivated for small scale DNA preparation (DNA mini-prep). Purified DNA plasmids were screened by diagnostic digest to identify positive clones and subsequently sequenced. Plasmids with correctly introduced inserts were produced on large scale (DNA maxi-prep).

2.3.2. Amplification of DNA insert by Polymerase Chain Reaction (PCR)

2.3.2.1. Myc-Frizzled-7

Myc-Frizzled-7 cDNA was amplified in a PCR reaction on the template of Myc-Fz7-V5-His. For the reaction forward primer P1 containing restriction site for enzyme EcoRI and reverse primer P2 containing restriction site for enzyme BamHI were used. PCR reactions were conducted using Expand High Fidelity PCR System (Roche) following manufacturer's guidelines. 50 µl reaction mixes were prepared by adding 40.25 µl of water, 5 µl of 10x concentrated Expand High Fidelity buffer with $MgCl_2$, 1 µl of 10 mM deoxyribonucleotide triphosphate (dNTP) mix (New England Biolabs), 1 µl of each 100 µM primer (Sigma-Aldrich), 0,75 µl of Expand High Fidelity Enzyme Mix and 1 µl of DNA template (10 ng). The PCR reaction involved initial denaturation (94°C, 2 min), then 40 cycles of denaturation (94°C, 30 sec), annealing (56°C, 1 min) and elongation (72°C, 2 min). A final DNA elongation step of 72°C for 7 minutes was added when all cycles were completed. Amplified PCR products were separated and purified using agarose gel electrophoresis.

2.3.2.2. FLAG-Frizzled-7

In order to generate FLAG-Frizzled-7 construct a two-step PCR protocol was utilised (Figure 2.2. schematically summarises this experiment). In the 1st round of PCR, two fragments of Frizzled 7 cDNA were amplified using the Fz7-V5-His:pcDNA3 construct as a template of. Fragment A was amplified with primers: forward P1 with restriction site for EcoRI and reverse P4 with FLAG-tag sequence (GATTATAAAGATGATGATGATAAA, encoding DYKDDDDK). Fragment B was amplified with primers: P3 with FLAG tag sequence (as above) and P2 with restriction site for BamHI. After the first round of PCR two products were generated: PCR product A ('leader') contained EcoRI site, Fz7 leader sequence (1-102bp) and FLAG-tag; PCR product B ('sequence') contained FLAG-tag, Fz7 sequence (103-1725bp) and BamHI site. PCR reactions were conducted using Expand High Fidelity PCR System (Roche) following manufacturer's guidelines. 50 µl reaction mixes were prepared by adding 40.25 µl of water, 5 µl of 10x concentrated Expand High Fidelity buffer with $MgCl_2$, 1 µl of 10 mM deoxyribonucleotide triphosphate (dNTP) mix, 1 µl of each 100 µM primer, 0,75 µl of Expand High Fidelity Enzyme Mix and 1 µl of DNA template (10 ng). The PCR reaction involved initial denaturation (94°C, 2 min), then 40 cycles of denaturation (94°C, 30 sec), annealing (56°C, 2 min) and elongation (72°C, 2 min). A final DNA elongation step of 72°C for 7 minutes was added when all cycles were completed. Amplified PCR products were separated and purified using agarose gel electrophoresis (Section 2.3.4).

The PCR products A ('leader') and B ('sequence') were subsequently used as templates for 2nd round of PCR. Sequence encoding FLAG-tag present on the 5' end of 'leader' and 3' end of 'sequence' was used as a linker to join two fragments into one DNA

template during the PCR reaction. To achieve this, Expand High Fidelity PCR System was used. 50 µl reaction mix was prepared by adding 42 µl of water, 5 µl of 10x concentrated Expand High Fidelity buffer with $MgCl_2$, 1 µl of 10 mM dNTP mix, 0.75 µl of Expand High Fidelity Enzyme Mix, 10 ng of template A 'leader' (0.5 µl) and 100 ng of template B 'sequence' (1 µl). First step of PCR reaction involved initial denaturation (94°C, 2 min), then 15 cycles of denaturation (94°C, 30 sec), annealing (56°C, 1 min) and elongation (72°C, 2 min), and a final elongation step (72°C, 7 min). Primers were not included in this step to create the ssDNA. Obtained ssDNA was used as a template for the final amplification with forward primer P1 and reverse P2. 50 µl reaction mixes were prepared by adding 31.25 µl of water, 5 µl of 10x concentrated Expand High Fidelity buffer with $MgCl_2$, 1 µl of 10 mM dNTP mix, 1 µl of each 100 µM primer (Sigma-Aldrich), 0.75 µl of Expand High Fidelity Enzyme Mix and 10 µl of ssDNA template. The PCR reaction involved initial denaturation (94°C, 2 min), then 35 cycles of denaturation (94°C, 30 sec), annealing (56°C, 1 min) and elongation (72°C, 2 min). A final DNA elongation step of 72°C for 7 minutes was added when all cycles were completed. Final PCR product contained EcoRI and BamHI restriction sites, and FLAG-tag introduced at the position 34, after signal peptide ('leader').

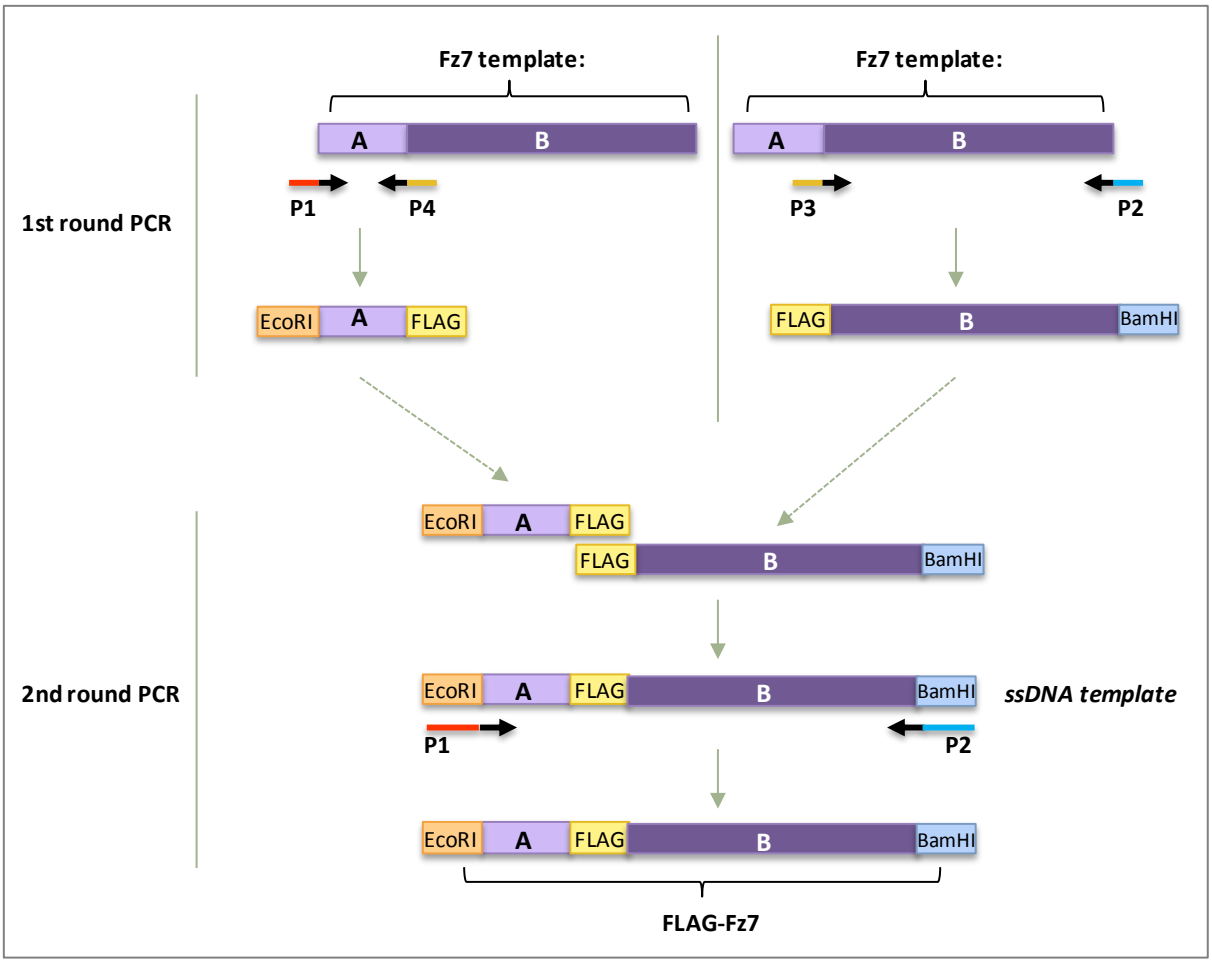

Figure 2. 2. A two-step PCR protocol utilised to generate FLAG-Frizzled-7.

Details of the protocol are presented in the section 2.3.2.2. „A", Fz7 leader sequence (1-102bp); „B", Fz7 sequence (103-1725bp); P1; forward primer with restriction site for EcoRI; P4, reverse primer with FLAG-tag sequence; P3, forward primer with FLAG-tag sequence; P2, reverse primer with restriction site for BamHI; ssDNA, single-stranded DNA;

2.3.2.3. GFP-Frizzled 7

In order to generate GFP- tagged Fz7 construct a similar two-step PCR protocol was used with slight modifications (summarised in Figure 2.3.). Initially, a linker with two restriction sites for AgeI and BspEI enzymes was introduced into Fz7 sequence at the position 34. The experimental PCR conditions were similar to those described in Section 2.3.2.2. As a result Frizzled-7 construct was obtained with the introduced linker sequence, containing two restrictions, after the leader peptide. These two sites were used for insertion of GFP into Fz7. GFP sequence was cut out from plasmid pEGFP-C1, using restriction enzymes AgeI and BspEI. This process is described in details in the section 2.3.3. Digested Fz7 and GFP fragments were gel purified (Section 2.3.5) and ligated together (Section 2.3.7).

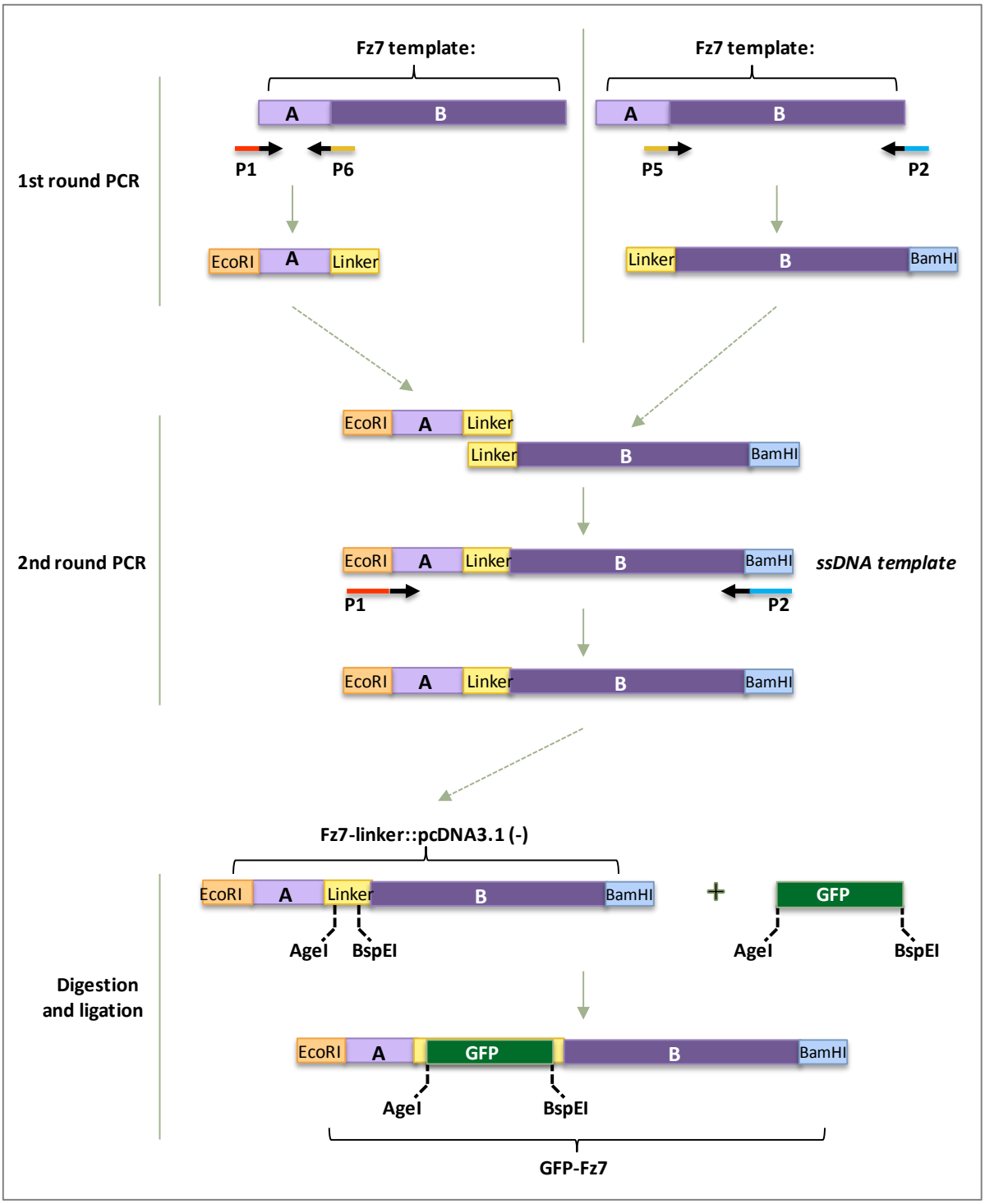

Figure 2. 3. A two-step PCR protocol utilised to generate GFP-Frizzled-7.

Details of the protocol are presented in the section 2.3.2.3. When Fz7-linker:pcDNA3.1 construct was prepared, GFP was ligated into the linker using AgeI and BspEI restriction sites. „A", Fz7 leader sequence (1-102bp); „B", Fz7 sequence (103-1725bp); P1; forward primer with restriction site for EcoRI; P6, reverse primer with linker sequence; P5, forward primer with linker sequence; P2, reverse primer with restriction site for BamHI;

2.3.2.4. Frizzled 7 V574G and V574E

In order to generate constructs of Frizzled-7 with mutation of the last amino acid, V574G or V574E, PCR reactions were set up with forward primer P1 and reverse P7 or P8, respectively. As templates Myc-Fz7, FLAG-Fz7 and GFP-Fz7 constructs were used. Amplified PCR products were Fz7 V574G or Fz7 V574 with restrictions sites for EcoRI and BamHI. Conditions for PCR reaction were the same as in Section 2.3.2.1.

2.3.3. DNA digestion with endonuclease (restriction) enzymes

Frizzled-7 PCR products and vector pcDNA3.1 were digested with restriction enzymes EcoRI and BamHI (Roche) according to manufacturer's guidelines. The digestion was performed as follows. Purified PCR product (from 50 µl reaction) or vector DNA (3 µg) were incubated in 50 µl of digestion solution containing dH_2O, 1x buffer A (Roche) and 10 units of each enzyme. Digestion was carried out overnight at 37°C.

To generate GFP-Fz7, Fz7-linker construct (Section 2.3.2.3) in pcDNA3.1 and pEGFP-C1 were sequentially digested with AgeI and BspEI endonucleases. In the first step both constructs were incubated in 50 µl digestion mixes containing dH_2O, 1x buffer 1 (NEB) and 10 units of AgeI enzyme, overnight at 37°C. Subsequently, AgeI digested constructs were purified and incubated in second 50 µl digestion mix containing dH_2O, 1x buffer 3 (NEB) and 10 units of BspEI endonuclease (NEB), overnight at 37°C.

Restriction digest reactions for diagnostic purposes were scaled down appropriately to the volume of 10 μl, and carried out for 1h at 37°C.

2.3.4. Agarose gel electrophoresis

PCR products or DNA restriction digest were mixed with 6xDNA Loading buffer (Qiagen) and subjected to horizontal electrophoresis (Geneflow). Gels were prepared by boiling agarose, 1% (w/v) (Invitrogen), in H2O and subsequently supplementing the solution with the appropriate volume of 10xTAE buffer and SYBR Safe (Invitrogen). The samples were resolved by electrophoresis at 100V, and subsequently gels were visualized and recorded by UV gel documentation system (InGenius® Syngene).

2.3.5. DNA extraction from agarose gel (DNA gel purification)

DNA bands were cut from the agarose gels and DNA was extracted using the Qiagen Gel Extraction Kit, following manufacturer's guidelines. Efficiency of purification was assessed by loading 1/10 of obtained DNA on 1% agarose gel and visualised as described above.

2.3.6. DNA ligation

Ligation reactions were performed using T4 DNA ligase (NEB) as follows. 1 µl of T4 DNA ligase (400 000 U/ml) and 2 µl of T4 DNA ligase buffer (NEB) were added to the 17 µl of insert:vector mixture, prepared in ratio 3:1. Before adding T4 ligase, DNA mixture was preincubated for 2 minutes at 60°C. Ligation was performed for 2h at room temperature. Reactions were stopped by incubating samples for 10 minutes at 65°C.

2.3.7. Heat-shock transformation of competent bacteria

Chemically competent *5-α I^{q} E.coli* cells (18 µl; NEB) were mixed with 10 µl of ligation mix or 500 pg of DNA plasmid and incubated for 30 minutes on ice. Afterwards bacteria were heat-shocked at 42°C for 30 seconds and incubated on ice for further 2 minutes. Transformation mixed was diluted with 250 µl of antibiotic-free LB medium and bacteria were allowed to recover for 1h at 37°C in an orbital shaker incubator. Subsequently bacteria were plated on LB-agar plates with appropriate antibiotic for overnight incubation.

2.3.8. Preparation of plasmid DNA from transformed bacteria

Large scale production of DNA plasmid was performed using Qiagen Plasmid Maxi Kit (Qiagen) according to the manufacturer's protocol. For small scale DNA purification Mini-Prep DNA Purification Kit (Qiagen) was used. Final DNA concentration was measured with the Nanodrop ND-1000 Spectrophotometer (Labtech).

2.3.9. DNA sequencing

All the constructed plasmids were verified by sequencing at the Functional Genomics and Proteomics Laboratory (School of Biosciences, University of Birmingham). Briefly, 150 ng of plasmid DNA, 3.2 pmol of an appropriate primer and dH_2O were mixed up to the final volume of 10 μl. Samples were then sent for sequencing analysis.

2.3.10. Preparation of glycerol stocks

All constructs were stored in glycerol stock in -80 °C. Bacterial cultures were mixed with glycerol (Fisher Scientific) to obtain its final concentration of 30% (v/v).

2.4. Protein analysis

2.4.1. Preparation of mammalian cell lysates

Unless specified otherwise, procedure described in this section was used to obtain mammalian cellular lysates. Proteins were extracted from cells growing in 60 mm dishes, 24h (HEK293T) or 48h (SKBr3; MCF7) after transfection. Cells were lysed using 500 µl of 1% v/v Triton X-100 (150 mM NaCl, 50 mM Tris pH 7.4), 0.5% v/v Brij98- 0.5% v/v Triton X-100 (150 mM NaCl, 50 mM Tris pH 7.4) or 0.8% v/v Brij98- 0.2% v/v Triton X-100 (150 mM NaCl, 50 mM Tris pH 7.4), supplemented with 2 mM phenylmethylsulfonyl fluoride (PMSF), 10 µg/ml aprotinin, 10 µg/ml leupeptin, 2 mM $NaVO_3$ (sodium orthovanadate) and 10 mM NaF (sodium fluoride). Cells were scraped quickly with a cell scraper and cell lysates were transferred into a 1,5 ml eppendorf tube. The tubes were subsequently placed on a rotary wheel for 30 minutes at 4°C. The insoluble material was pelleted at 13,000 rpm for 10 min. Supernatants were used directly for different assays or stored in -80°C. If needed for SDS-PAGE (Section 2.4.3.) cell lysates were mixed in ratio 3:1 (v/v) with 4x concentrated Laemmli loading buffer (0.5M Tris pH 6.8 2.1 ml, 4.4 ml glycerol, 2.2 ml 20% SDS, 1 ml dH_2O and 0,05 g bromophenol blue).

2.4.2. Protein concentration determination

Protein concentration was determined using Bio-Rad DC Protein Assay Kit according to the manufacturer's protocol. In 96-well plate (BD-Falcon) 5 µl of cell lysate was mixed with 25 µl of Bio-Rad mixture (20 µl of reagent S in 1 ml of reagent A) and with 200 µl reagent B. Samples were incubated at room temperature for 15 minutes and absorbance was measured at 630 nm wavelength using microplate reader (Bio-Rad). To obtain standard curve, bovine serum albumin (BSA, Sigma-Aldrich) was serially diluted in an appropriate lysis buffer in a range of 0.4 – 3.2 mg/ml. Based on the absorbance values for the known concentrations of BSA standards the protein standard curve was created in MS Excel Software and the protein concentration in lysate samples was determined. The protein samples and BSA samples were measured in triplicate to obtain more accurate values.

2.4.3. SDS-PAGE and Western Blot analysis

Lysate samples, with equal amount of proteins, along with prestained protein ladder, were resolved in SDS-PAGE (sodium dodecyl sulphate-poliacrylamide gel electrophoresis). If required samples were reduces by adding β-mercaptoethanol in dilution 1:20. Samples were loaded on 10% polyacrylamide gel (unless stated otherwise) and resolved at 120V using Bio-Rad electrophoretic equipment and 1x SDS/Tris/Glycine running buffer (GeneFlow). Table 2.11. shows recipes for preparation 5% stacking and 10% resolving SDS-PAGE: .

The proteins resolved by SDS-PAGE were stained with InstantBlue (Expedeon) or transferred to a nitrocellulose membrane, using Trans-Blot® Turbo™ Transfer System (Bio-

Rad) and Trans-Blot® Turbo™ Transfer System RTA Transfer Kit (Bio-Rad) according to the manufacturer's protocol. To block non-specific binding of antibodies, membranes were incubated with 5% dry skimmed milk (Marvel) (dissolved in TBST) for 1h at room temperature. Subsequently, membranes were incubated overnight with specific primary antibodies (diluted in solution containing 5% (w/v) skimmed milk, 3 mM NaN_2 and TBST). After washing with TBST (3x10 min), membranes were incubated with secondary antibody conjugated with fluorescent dye, goat anti-mouse Ab IRDye 680LT, or goat anti-rabbit Ab IRDye 800CW (LI-COR), for 1 hour at room temperature. After another washing with TBST (3x10 min), proteins were visualized and quantified using Odyssey®CLx Infrared Imaging System (LI-COR). If blots were developed using a Chemiluminescence-based protocol, membranes were incubated with a secondary antibody conjugated with HRP (horseradish peroxidase), goat anti-mouse or goat anti-rabbit (Dako). Afterwards proteins were detected using Enhanced Chemiluminescence Plus reagents (ECL Plus) (Biological Industries). Protein bands were visualized onto Amersham Hyperfilm™ X-ray film using Kodak X-OMAT 1000 developer. All primary and secondary antibody used in this study are summarized in Tables 2.1. and 2.2, respectively.

Table 2. 11. Components of a single mini SDS-PAGE running gel.

	5% stacking gel	10% resolving gel
30% w/v Acrylamide:Bis	1.3 ml	6.7 ml
1.5 M Tris-HCl pH 8.8	-	5.0 ml
1 M Tris-HCl pH 6.8	1.0 ml	-
dH_2O	5.5 ml	7.9 ml
10% w/v SDS	80 µl	200 µl
10% w/v Ammonium Persulphate	80 µl	200 µl
Temed	8 µl	12 µl

2.4.4. Quantitative analysis of Western blot images

Densytometric analysis was carried out on images obtain by Odyssey CLx infrared imaging system (LI-COR) using Image Studio Lite Software (LI-COR). Rectangular shapes of equal size were drawn separately around bands of interest and the fluorescent absorbance within the shapes was calculated. The background absorbance of the blot was subtracted from the shapes using the software to obtain consistent data. The Median Method was chosen to subtract the median value of the pixels in the background segment of each shape. Absorbance values representing the densitometric values were used to quantify protein expression level in this study.

2.4.5. Immunoprecipitation

For immunoprecipitation experiments, lysates prepared as described in section 2.4.1., were incubated for 1h or overnight on a rotary wheel at 4°C with 18 µl of agarose or magnetic beads conjugated with mouse anti-FLAG M2 mAb (Sigma-Aldrich) or magnetic GFP-Trap® beads (Chromotek). Subsequently, beads were washed 3 times with 700 µl of ice-cold TBS –Tween and retained proteins were eluted by adding 15 µl of 2x concentrated Laemmli sample buffer and boiling for 10 minutes at 60°C. If necessary, beads were pre-incubated with 0.5% BSA/PBS before adding lysates, to prevent unspecific binding of proteins to the beads.

2.4.6. Pull-down with peptides

For pulldown experiments lysates, prepared as described in section 2.4.1., were incubated with NeutrAvidin™-conjugated agarose resins (Pierce) with immobilized custom synthesised biotinylated peptides corresponding to the C-terminal cytoplasmic tails of Fz7, Fz3 and Fz8 (Alta Bioscience, sequences of peptides are summarized in the Table 2.12.). In several experiments the Fz7-V574G peptide (Table Table 2.12.) was used alongside of the Fz7 wild-type peptide. NeutrAvidin™ beads (50% slurry solution) were transferred into 1.5 ml tubes (30 µl/sample for analytical (A) or 50 µl/ sample for preparative (P) purposes) and washed twice with 500 µl (A) or 1000 µl (P) of ice cold PBS. Beads were incubated with 6 µg (A) or 20 µg (P) of peptides in ice cold PBS at 4°C on a rotary wheel for at least an hour. Subsequently, NeutrAvidin™ beads with immobilized peptides were washed twice with ice cold PBS.

Lysates of mammalian cells were prepared as described in section 2.4.1. (500 µl/6 cm dish (A), or 3 ml/15 cm dish (P)). An aliquot from each lysate was kept for WB to serve as a positive control. Lysates were then incubated with NeutrAvidin™ beads for pre-clearance for 1h at 4°C on a rotary wheel. Subsequently, pre-cleared cell lysates were incubated with peptide-conjugated NeutrAvidin™ resins over night at 4°C on a rotary wheel.

Beads were washed 3 times with ice-cold TBS–Tween 0.1% and retained proteins were eluted by adding 15 µl (A) or 25 µl (P) of 2x concentrated Laemmli sample buffer and boiling for 5 minutes at 95°C.

Table 2. 12. Biotinylated peptides used in this study.

Peptide	Sequence
Fz7 WT	Biotin-SGKTLQSWRRFYHRLSHSSKGETAV
Fz7 V574G	Biotin-SGKTLQSWRRFYHRLSHSSKGETAG
Fz3	Biotin-SNNPMTHITHGTSMNRVIEEDGTSA
Fz8	Biotin-STGLTWRSGTASSVSYPKQMPLSQV

2.4.7. Preparation of samples for Mass-Spectrometry

Proteins were resolved by SDS-PAGE using gradient 4-20% Mini-PROTEAN® TGX™ Precast Gel (Bio-Rad), which subsequently was stained with InstantBlue (Expedeon) according to the manufacturer's instruction. Briefly, gel was incubated with InstantBlue for 1h and then washed several times with de-ionized Millipore H_2O. Bands of interest were cut and placed in 1.5 ml sterile tube and destained by incubation in 500 µl of 50% (v/v) acetonitrile (Sigma-Aldrich) in 50 mM ammonium bi-carbonate (Sigma-Aldrich) an a shaker for 30 minutes at room temperature. Afterwards gel slices were reduced by incubation in 500 µl of 50 mM DTT (ditiotreitol; USB Corporation) in 50 mM ammonium bi-carbonate for 1 h at 56°C, and alkalyted with 300 µl of 100 mM iodoacetamide (Sigma-Aldrich) for 30 minutes at room temperature, in the dark. Finally they were dehydrated in 100% acetonitrile for 10 min. Solution was removed and gel slices were dried at room temperature. Proteins were in-gel digested with 25 µl of trypsin (1.25 mg/ml) (Promega) in 10% acetonitrile in 50 mM ammonium bi-carbonate overnight at 37°C. Next day, peptides were extracted from the gel slices by incubating twice in 50 µl of 1% (w/v) formic acid for 1 h at room temperature on a shaker. Supernatants were transferred to new 1.5 tubes and placed in Speedivac for 30-60

min at 45°C in order to diminish sample volumes to 40-50 μl. Retained peptides were analyzed by mass spectrometry.

2.4.8. Mass spectrometry

Proteomic analysis was performed at Proteomics Facility (University of Birmingham) by Dr Doug Ward. Samples prepared in Section 2.4.7. were used in liquid chromatography and mass spectrometry analysis, performed on Bruker micrOTOF II (LC-MS). To identify proteins encompassing detected peptide sequences, data base SwissProtDecoy was used (Species: Human). During peptide analysis following parameters were applied: Missed Cleavage: 1; Accurance search: 50 ppm; Fragment searching: 0.1 Da; Peptide score Mascot : 25.

2.5. Assays on live cells (functional studies)

2.5.1. Luciferase TOP-Flash assay

TOPFlash luciferase reporter assay was designed to demonstrate activation of canonical Wnt pathway. It is a read-out for β-catenin transcription activation, the end-point of canonical Wnt pathway (Korinek et al. 1997).

Cells were plated at the density 2.5×10^4 per well in 48-well plate. If protein knock-down was required during the assay, cells were transfected, in triplicates, with 2.4 pmol of siRNA per well, using Lipofectamine RNAiMAX using reverse protocol during plating cells (section 2.2.6.3). 24 hours later cells were transfected with DNA plasmids using FuGENE6 (section 2.2.6.2), indicated as a total amount per well in a 48-well plate: SKBr3 with 50 ng luciferase plasmid (M50 Super 8x TOPFlash or M51 Super 8x FOPFlash; Addgene), 25 ng pRenilla and 50 ng pcDNA™3.1 plasmids encoding the respective cDNA inserts; HEK293T with 22.5 ng luciferase plasmid, 2.5 ng pRenilla, 5 ng of pcDNA™3.1 plasmids encoding the respective cDNA inserts and supplemented with 95 ng pcDNA™3.1. M50 Super 8x TOPFlash is a β-catenin reporter plasmid, containing TCF/LEF sites upstream of a luciferase reporter. M51 Super 8x FOPFlash is a control for β-catenin reporter plasmid, containing mutated TCF/LEF sites upstream of a luciferase reporter. Both constructs were generated at Randall Moon's laboratory (Veeman et al. 2003b), based on original TOPFlash constructed at laboratory of Hans Clevers (Korinek et al. 1997).

At 48h following plating, cells were treated for 24 hours with 50% Wnt3a-conditioned medium or 50% control medium produced by L-cells (Section 2.2.9). Subsequently, cells were

washed with PBS and lysed by incubating with Passive Lysis Buffer (Promega) overnight at -20°C, 50 µl/well. 20 µl of lysate from each well was transferred to 96-well plate. Firefly (*Photinus pyralis)* and Renilla (*Renilla reniformis)* luminescence signals were measured sequentially from the same sample, using the Dual-Glo luciferase assay system (Promega). Briefly, the luminescence signal of the firefly luciferase expressed from TOPFlash or FOPFlash plasmid was quantitatively measured first by the addition of Luciferase Assay Reagent II (LARII). Afterwards, the firefly signal was quenched by addition of Stop & Glo® reagent to the same sample, and Renilla luciferase signal was measured and quantified. Luminesence signal was measured using Orion L Microplate Luminometer (Berthold Detection Systems).

Firefly luminescence signal values were normalized according to their corresponding Renilla signal values. TOP-flash signal was standardized to the background signal (FOP-flash). Histograms were constructed to show the relative fold change in the levels of promoter reporter activity. Statistical significance was determined using MS Excel software using the relevant Student's t-test after determining whether the sample variance is equal or unequal by performing an F-test.

2.5.2. *In vivo* ubiquitylation assay

HEK293T cells, plated on 6 cm dish, were co-transfected with HA-Ubiquitin, FLAG-Fz7 and GFP-LNX2 (GFP-LNX1 p70; GFP-LNX1 p80) or GFP. 48h after transfection cells were lysed using 100 µl of SDS lysis buffer (containing 0.5% SDS, 50 mM NaF, 1 mM EDTA in PBS), supplemented with 2 mM PMSF, 10 µg/ml aprotinin, 10 µg/ml leupeptin and 20 mM iodoacetemide. Samples were incubated at 60°C for 15 minutes, and diluted with 900 µl of 1% v/v Triton X-100 (150 mM NaCl, 50 mM Tris pH 7.4) supplemented with 2 mM PMSF, 10 µg/ml aprotinin, 10 µg/ml leupeptin and 20 mM iodoacetemide. Subsequently samples were sonicated and the insoluble material was pelleted at 13,000 rpm for 10 min. Supernatants were incubated for 1h with magnetic beads conjugated with anti-FLAG M2 mAb (Sigma-Aldrich). Later, beads were washed three times with TBS-Tween. Proteins retained by the magnetic resins were eluted by incubating with 15 µl of 2x Laemmli buffer for 10 minutes at 60°C. Eluates were analysed by the SDS-PAGE and Western Blotting as described in Section 2.4.3. Frizzled-7 ubiquitylation level was assessed by incubating membranes with rabbit antibodies against HA-tag, to detect HA-ubiquitin.

2.6. Staining and imaging methods

2.6.1. Flow cytometry

Cells growing in monolayer were detached using enzyme-free dissociation buffer (Gibco) and counted. 3-5 x 10^5 cells was centrifuged at 1000 RPM for 3 minutes and resuspended in 50 µl of ice cold 1% HI-BSA/PBS. All the following steps were performed on ice. To block non-specific binding of antibodies, 1% HI-BSA/PBS was aliquoted into U-shaped 96-well plate (50 µl/well) and placed on ice for 20 minutes. Then, the blocking solution was removed and replaced with 150 µl of specific primary antibody diluted in 1% HI-BSA/PBS or hybridoma supernatant. Subsequently, 50 µl of cell suspension was added to each well and incubated on ice for 1h. The cells were pelleted by centrifugation at 1000 RPM for 5 minutes at 4°C and washed twice with 200 µl of ice cold PBS. The last wash was followed by incubation of cells with secondary FITC- or PE-conjugated antibody (Sigma), diluted in 1% HI-BSA/PBS for 1h. The incubation with fluorescently labelled secondary antibodies was carried out under the aluminium foil to prevent sample exposure to light. Cells were washed again twice with ice cold PBS, as described above. Finally cells were resuspended in 250 µl of ice cold PBS and transferred into FACS tubes containing 250 µl of 4% paraformaldehyde (PFA). Stained cells were analyzed using Accuri C6 Flow Cytometer (BD Biosciences) and FlowJo v7.6 software. All antibodies used in this study are listed in Tables 2.1. and 2.2.

2.6.2. Fluorescent Activated Cell Sorting (FACS)

Homogenous population of cells stably expressing Flag-tagged Frizzled proteins (SKBr3-FLAG-Fz7 and SKBr3-FLAG-Fz7 V574G, section 2.2.7) was established using Fluorescent Activated Cell Sorting (FACS). The day before cell sorting, cells were trypsinized and replated at ~50-60% confluency. The sample preparation and all subsequent procedures were conducted under sterile conditions. On the day of sorting, cells were detached using enzyme-free dissociation buffer (Gibco) and pelleted by centrifugation at 1200 RPM for 3 min at 4°C. Subsequently cells were resuspended in 1.5 ml of ice-cold complete growth medium containing primary antibody, the anti-FLAG M2 mAb (Sigma-Aldrich) was diluted at 1:300 and sterilised by filtration. After incubation for 1 hour, cells were pelleted by centrifugation at 1200 RPM for 3 min at 4°C, and washed twice with 2 ml of ice-cold complete growth medium. Then cells were resuspended in 1.5 ml of ice cold complete growth medium containing secondary, fluorescent labelled antibody (FITC (fluorescein isothiocyanate)-conjugated goat anti-mouse pAb, (Sigma-Aldrich) in dilution 1:300) and incubated on ice for one hour in dark. Cells were pelleted, and washed twice with ice-cold complete growth medium. Finally they were resuspended in 2 ml of ice cold complete growth medium and passed through Cell Trics filters (Partec) to remove cellular aggregates. Cell suspension was transfered to sterile FACS tubes (BD Falcon). Cells were sorted using a Beckman Coulter MoFlo Legacy FACS machine and positive and negative cell populations were separated. After sorting cells were resuspended in complete growth medium containing double amount of penicillin/streptomycin to prevent sample contamination. 48h later medium was changed

for a regular complete growth medium and cells were cultivated in humidified incubator (37°C, 5% CO_2) until they were ready to use.

2.6.3. Immunofluorescence

Cells grown on glass coverslips or Nunc™ Lab-Tek™ II Chamber Slide™ System (Thermo Scientific) were transfected with appropriate DNA plasmids using FuGENE6 (Roche). Staining was performed 48h after transfection. Cells were fixed with 4% paraformaldehyde/PBS for 15 min at room temperature and permeabilized with 0.1% v/v Triton X-100 for 2 minutes. Coverslips or chambered slides were incubated with blocking buffer (20% heat inactivated goat serum/PBS) for 1h, followed by 1 h incubation with a primary antibody, diluted in blocking solution. Cells were washed three times with PBS for 10 minutes, with agitation. Subsequently coverslips or Lab-Tek™ chambered slides were incubated with appropriate secondary antibodies conjugated with fluorochrome (diluted in blocking solution), for 1h in darkness. After removing secondary antibody, cells were incubated with Hoechst33342 (1μg/ml in PBS) for 10 min at room temperature to stain cell nuclei. Finally cells were washed again with PBS, as described earlier. Coverslips were air dried and mounted on glass slides, whereas chambers from Lab-Tek™ slides were removed and slides were mounted with appropriate size coverslips, using anti-fade fluorescence mounting medium (SlowFade® Gold Antifade Mountant with DAPI, Molecular Probes®). Coverslips were sealed on the edges using nail polish and stored at -20°C in darkness. The images were captured using Zeiss LSM510 META confocal system with 63X oil immersion objective. All antibodies used in this study are summarized in Tables 2.1. and 2.2.

3. RESULTS AND DISCUSSION

3.1. Establishing a model system to study Fz7 biology

Frizzled-7 (Fz7) is a transmembrane receptor that transduces signals from secreted glycoproteins known as Wnts. Activation of Wnt signalling pathway frequently occurs in colorectal cancer, but also in breast cancer. Activation of canonical Wnt signalling is well studied in colorectal cancer cells, and it is predominantly associated with mutations in APC or β-catenin proteins (Polakis 2012). However, the mechanism of Wnt pathway activation in breast cancer remains unclear. Recent reports suggested that Fz7 is involved in breast cancer malignancy (King et al. 2012a;Simmons, Jr. et al. 2014;Yang et al. 2011)

However, the contribution of the C-terminal PDZ-BM in signalling triggered by Fz7 remains unknown. The work described in this chapter covers characterization of Fz7 expression vectors and identification of a suitable breast cancer cell line to use as a model in further the study.

3.1.1. Characterization of Fz7 expression vectors

There is no suitable antibody available to detect endogenous Fz7. Therefore, to be able to monitor Fz7 expression throughout the functional experiments, a molecular tag had to be introduced into the Fz7 sequence. The procedure is described in details in the section 2.3. of Materials and Methods. In the vast majority of the following experiments FLAG-Fz7 was used, but Myc- and GFP-Fz7 constructs were also generated.

Fz7 contains a PDZ binding motif on the C-terminal end that enables interactions of the receptor with PDZ domain containing proteins. Given that the main objective of this study was to investigate the role of Fz7 interactions with PDZ proteins, the molecular tag was introduced at the N-terminal extracellular portion of the protein. Employing molecular biology techniques, FLAG-, Myc- or GFP-sequences were introduced at the position 34, after the leader peptide, to ensure correct topology of the protein on the plasma membrane. A schematic representation of Fz7 structure with introduced tag is shown in Figure 3.1.A.

In order to assess FLAG-Fz7 expression in transfected cells, SDS-PAGE and western blot analysis was used. Samples for the analysis were prepared by mixing cellular lysates with 4xLaemmli loading buffer containing β-mercaptoethanol, and subsequently boiled at 100°C for 5 minutes. Anti-FLAG pAb were used to detect FLAG-Fz7. While analysing samples by western blot, it was observed that Fz7 forms aggregates of a high molecular mass and monomers of the receptor were not detected. Aggregate formation might be a consequence of Fz7 being a transmembrane receptor with seven hydrophobic regions. Therefore the procedure of sample preparation for SDS-PAGE-western blot analysis was modified. In order to do find an alternative protocol several conditions were examined. Cell

lysates, obtained from HEK293Ts transfected with FLAG-Fz7, were mixed with 4xLaemmli loading buffer, with or without a reducing agent (β-mercaptoethanol), and incubated at 100°C for 5 minutes or at 60°C for 10 minutes. Results of these experiments are shown in the Figure 3.1.B. When samples were boiled (100°C), Fz7 formed aggregates and receptor monomers were impossible to detect (reduced conditions; lane 1) or they were barely detectable (non-reduced conditions; lane 3). Decreasing the denaturation temperature to 60°C prevented formation of protein aggregates. Separated Fz7 forms included two monomeric forms with apparent sizes 50 kDa and 60 kDa, (in reduced, lane 5, and non-reduced conditions, lane 7). These forms are likely to represent a different degree of *N*-glycosylation of Fz7 and were observed in both HEK293T and SKBr3 cells (see below). Under non-reduced conditions (lanes 3 and 7), Fz7 dimers (around 130 kDa) and higher oligomers with sized exceeding 200 kDa, were also observed.

In order to determine cell localization of Fz7, immunofluorescence analysis was performed on MCF7s transiently transfected with FLAG-Fz7 expression vector. Cells were fixed and stained using anti-FLAG antibody. DAPI was used to visualize nuclei. Analysis by confocal microscopy showed that Fz7 immunoreactivity is mostly detected on the plasma membrane (Figure 3.1.C). Similar, plasma membrane localization of Fz7 was observed in SKBr3 cells (see below).

As mentioned at the beginning of this section, in addition to FLAG-Fz7 expression vector, Myc-Fz7 and GFP-Fz7 expression vectors were generated. Both of them were subjected to a similar analysis as FLAG-Fz7 construct. Both Myc- and GFP-Fz7 were found to be expressed in transfected cells and localize on the plasma membrane. Western blot analysis showed that Myc-Fz7 and GFP-Fz7 are also expressed as two monomers with a different

degree of *N*-glycosylation (50 kDa and 60 kDa for Myc-Fz7; 80 kDa and 90 kDa for GFP-Fz7), but also form dimers and aggregates of higher molecular weight, as seen for FLAG-Fz7. Summary of this work is presented in the Supplementary Figure S.1.

Taken together, western blot and immunofluorescence experiments showed that generated construct allows for FLAG-Fz7, Myc-Fz7 and GFP-Fz7 expression on the surface of transfected cells.

A.

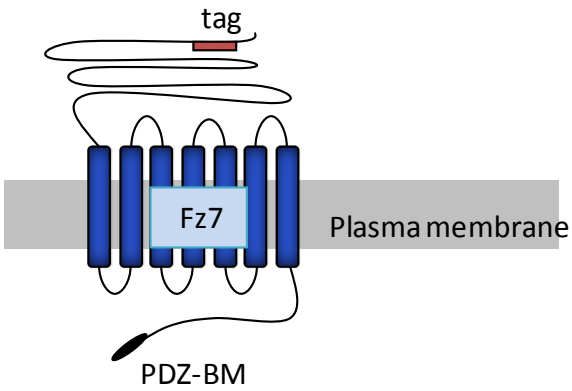
tag
Fz7
Plasma membrane
PDZ-BM

B.

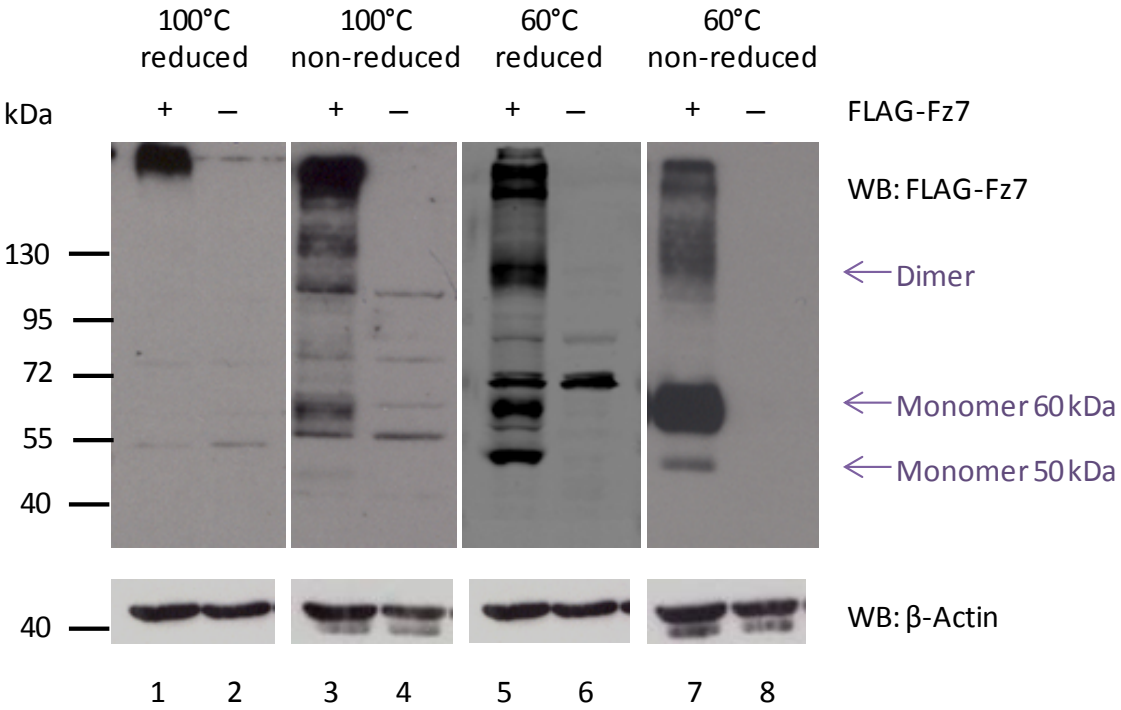
100°C reduced
100°C non-reduced
60°C reduced
60°C non-reduced
kDa
+ – + – + – + –
FLAG-Fz7
WB: FLAG-Fz7
130
95
72
55
40
Dimer
Monomer 60 kDa
Monomer 50 kDa
40
WB: β-Actin
1 2 3 4 5 6 7 8

C.

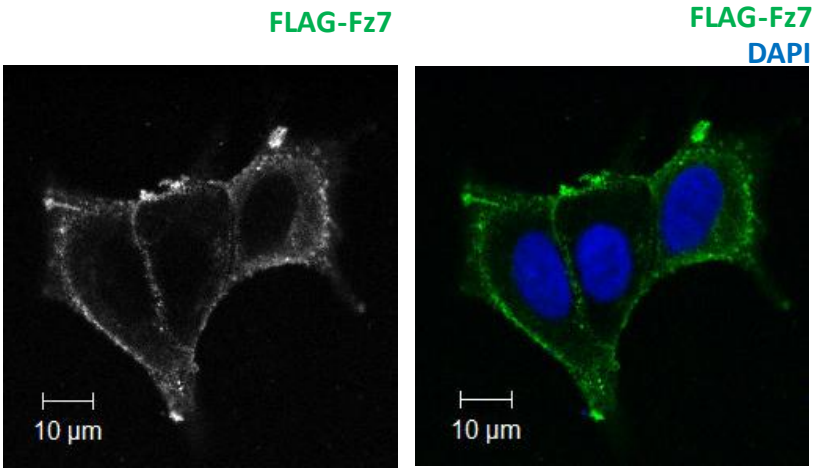
FLAG-Fz7
FLAG-Fz7
DAPI
10 µm
10 µm

Figure 3. 1. Characterization of the FLAG-Fz7 expression construct.

(A) Schematic representation of Fz7 structure with PDZ-binding motif at the C-terminus and molecular tag introduced at the position 34, after the leader peptide. PDZ-BM, PDZ domain binding motif. (B) Western blot analysis of whole cell lysates of HEK293T cells transiently transfected with FLAG-Fz7 expression vector. Cells were lysed in 1% Triton X-100 and equal amounts of protein were resolved by SDS-PAGE under indicated conditions, followed by detection with rabbit anti-FLAG antibodies. β-actin served as a loading control. (C) MCF7 cells transiently transfected with FLAG-Fz7 expression vector display membrane immunoreactivity. 48h after transfection cells were fixed and stained with mouse anti-FLAG (M2) mAb and Alexa Fluor 488-conjugated goat-anti mouse Ab (green). DAPI was used to visualize nuclei.

3.1.2. Assessing functionality of FLAG-Fz7

Fz7 is a membrane receptor which contains a ligand binding site within the N-terminal extracellular domain. It was important to confirm that insertion of the molecular tag (FLAG sequence) in the N-terminus did not alter receptor functionality and its ability to bind Wnt ligands. In order to assess functionality of constructed tagged-Fz7 a luciferase-based reporter assay, called TOP-Flash, was used. It is a widely used method that allows the measurement of canonical Wnt signalling activity. HEK293T cells were transfected with two reporter plasmids: (pRenilla and TOPFlash (or FOPFlash)) and stimulated with Wnt3a conditioned medium. "TOP" is a read-out for β-catenin transcription activation, the end-point of the canonical Wnt pathway, whereas "FOP" is a read-out for a background signal. The TOP-Flash assay procedure is described in details in the section 2.5.1. of Materials and Methods.

The ability of FLAG-Fz7 to transduce signals after binding to the Wnt3a ligand, and to activate canonical Wnt signalling pathway was examined. HEK293T cells were transfected with reporter plasmids and with FLAG-Fz7 or pcDNA™3.1 plasmids. Cells were incubated with Wnt3a conditioned medium, or with control conditioned medium for 24h, and TOP-Flash activity measured 48h post-transfection. Control HEK293T cells, transfected only with reporter plasmids, but not with Fz7 plasmid, were used as a reference sample. Reporter activity was compared in control cells and cells expressing FLAG-Fz7 upon stimulation with Wnt3a, as presented in the Figure 3.2. Due to the fact that the parental HEK293T cells express endogenous Frizzled receptors, they are able to transduce signals after incubation with Wnt3a. As expected, control HEK293T cells showed activation of Wnt signalling pathway

upon stimulation with Wnt3a ligand, as evidenced by a 20 fold increased signal of the TOPFlash reporter when compared with FOPFlash reporter. Canonical Wnt pathway activation was significantly stronger in HEK293T cells expressing Fz7 than in control cells, as evidenced by four times increased signal of the TOPFlash reporter. Hence, the generated FLAG-Fz7 is functional.

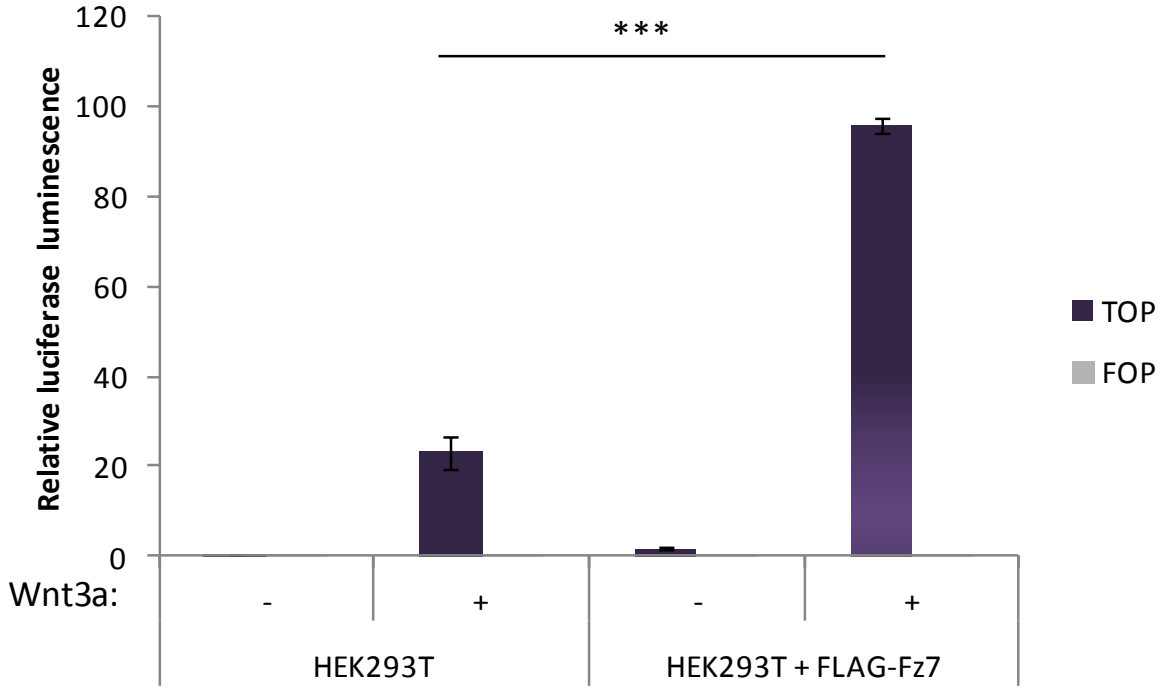

Figure 3. 2. Verification of FLAG-Fz7 functionality.

Wnt3a-induced signalling was analysed using TOP-Flash luciferase assay. HEK293T cells were transfected with reporter plasmids and with plasmid encoding FLAG-Fz7 or mock transfected. Cells were stimulated for 24h with Wnt3a conditioned medium and TOP/FOP activity was analysed 48h after the transfection. Test was done in triplicates and three independent experiments were performed. Statistical significance was determined by two-tailed, unpaired Student's t-test (* p<0.001)**

Functionalities of other generated Fz7 constructs (Myc-Fz7 and GFP-Fz7) were also assessed in HEK293T cells in similar experiments. The activation level of Wnt canonical pathway was two fold higher in cells expressing Myc-Fz7 and almost three fold higher in cells expressing GFP-Fz7, when compared with control samples, as presented in the Supplementary Figure S.2. Therefore both Myc-Fz7 and GFP-Fz7 appear to be functional.

Wnt pathway activation was also assessed in HEK293T cells expressing Fz7-V5-His. V5- and His-tag were introduced at the C-terminal end of Fz7 receptor, leaving the N-terminus intact. Transfection of HEK293T cells with different amounts of DNA encoding Fz7-V5-His (80 ng, 40 ng, 20 ng, 10ng, 5 ng or 2,5 ng as per one well of 48-well plate) showed that signal transduction depends on expression level of Fz7. High level of the receptor expression prevents activation of canonical Wnt signalling pathway by endogenous Frizzled receptors in HEK293Ts, as was observed in cells transfected with 80 ng to 10 ng of Fz7-V5-His. The highest activation of Wnt signalling was found in HEK293Ts transfected with 5 ng of Fz7-V5-His plasmid. Yet, even in the sample with the highest activation of the pathway, it wasn't significantly higher then in the control cells, thus demonstrating that insertion of the molecular tag at the C-terminus of Fz7 receptor attenuates its capability to transduce signals (Figures 3.2. and 3.3). Furthermore, our results seems to indicate that the Fz7-V5-His construct have a dominant negative properties.

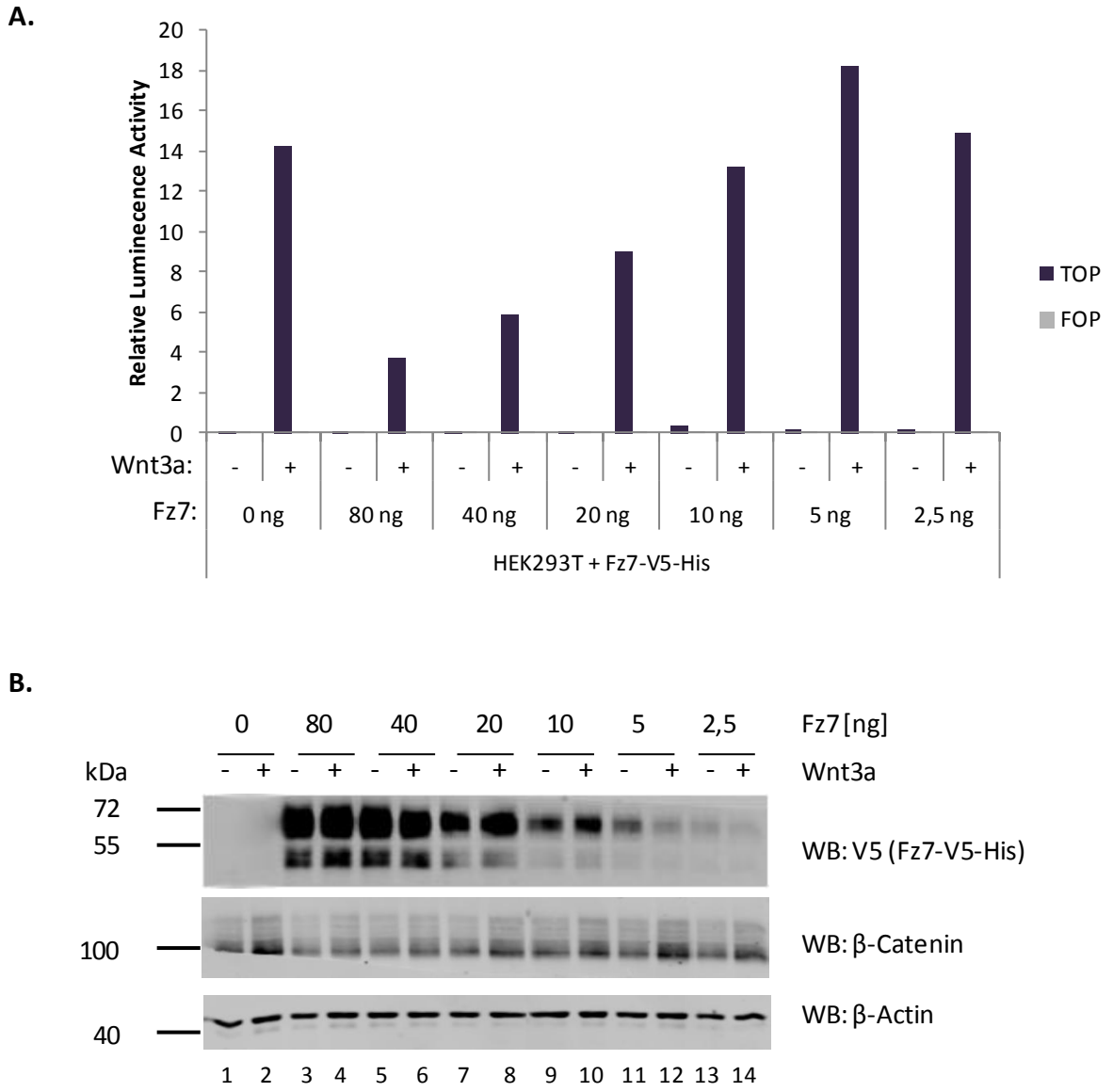

Figure 3. 3. Activation of canonical Wnt signalling in Fz7-V5-His expressing cells.

(A) HEK293T cells were transfected with TOPFlash or FOPFlash luciferase plasmid, pRenilla plasmid and different amount of plasmid DNA encoding Fz7-V5-His, and stimulated with Wnt3a conditioned medium for 24h. TOP and FOP activity was analysed 48h after transfection with reporter plasmids. (B) Lysates obtained in the assay were analysed by western blotting. Anti-V5 pAb were used to detect Fz7-V5-His and anti-β-catenin to detect endogenous β-catenin. β-actin served as a loading control.

Taken together, insertion of molecular tags within the N-terminus of Fz7 (at the position 34) does not affect the receptor functionality. However, inserting a tag at the C-terminus, behind the PDZ binding motif, leads to loss of receptor ability to transduce the canonical Wnt signalling. This indicates the importance of Fz7 interactions with PDZ proteins, via the C-terminal binding motif, in the activation of the canonical Wnt signalling.

3.1.3. Identifying a suitable epithelial breast cancer model

Having generated a functional epitope-tagged Fz7 construct, we proceeded to identify a suitable breast cancer cell line to use as a model for signalling studies. To investigate activation of canonical Wnt signalling pathway by Fz7, we have decided to find a model system in which we could establish a stable expression of the Fz7. For that purpose several well-characterized epithelial breast cancer cell lines were initially screened using TOP-Flash reporter assay. The aim of these experiments was to find cells with low responsiveness to Wnt3a, indicating low expression of endogenous receptors. At the same time, we were looking for cells in which all the components of the canonical Wnt signalling pathway downstream of the receptor were intact (i.e. be able to transduce signals upon activation).

In order to identify a suitable cell line, activation of the canonical Wnt signalling pathway was analysed in cells stimulated with Wnt3a or when treated with SB216763, an inhibitor of GSK3,. Wnt3a activates Wnt signalling through the interaction with Frizzled receptor. TOP-Flash activity, after Wnt3a stimulation, would reflect on expression of the receptors and an overall functionality of the pathway. SB216763 is a small molecule that inhibits GSK3 by competing with ATP. Inhibition of GSK3 kinase activates β-catenin dependent Wnt pathway downstream of Wnt receptor and allows testing functionality of the pathway in cells deficient in the expression of the receptors. Four epithelial breast cancer cell lines were tested in these experiments: MDA-MB-231, T47D, MCF7 and SKBr3. HEK293T cell were used as a control cell line. Cells were transfected with reporter plasmids and incubated for 24h with Wnt3a conditioned medium or with control conditioned medium (Figure 3.4.A).

In parallel experiments, cells were treated for 24h with 10 μM SB216763 or vehicle (DMSO) (Figure 3.4.B). 48h after the transfection activity of TOP-Flash reporter was analysed and activation of the Wnt pathway was evaluated in samples treated with Wnt3a and GSK3 inhibitor. In order to compare results in different cell lines, obtained TOPFlash reporter values were standardized to the corresponding FOPFlash reporter values for each of the tested cell lines. We found that in MDA-MB-231 cells, the canonical Wnt pathway could be activated by both Wnt3a (two fold increase), and GSK3i (four fold increase), compared to control samples. These results indicate that canonical Wnt pathway is functional in MDA-MB-231, but also that these cells express endogenous Frizzled receptors. On the contrary, T47D and MCF7 cell lines did not display pathway activation upon stimulation with Wnt3a or GSK3i thus suggesting that the β-catenin-dependent pathway is not functional in these cells. This may be due to mutations in pathway components downstream of Frizzled, or interference of other proteins involved in regulation of the pathway (Wheeler et al. 2011). Finally, analysis of the Wnt signalling pathway in SKBr3 cell line showed that it was not activated by Wnt3a, but could be induced by GSK3i (more than seven fold stronger when compared with the control). Whilst these results indicate that SKBr3 cells express no (or low levels) of endogenous Wnt3a receptors, the β-catenin-dependent pathway remains functional. That makes the SKBr3 cell line a suitable model to establish stable cell lines and to study Fz7-dependent signalling.

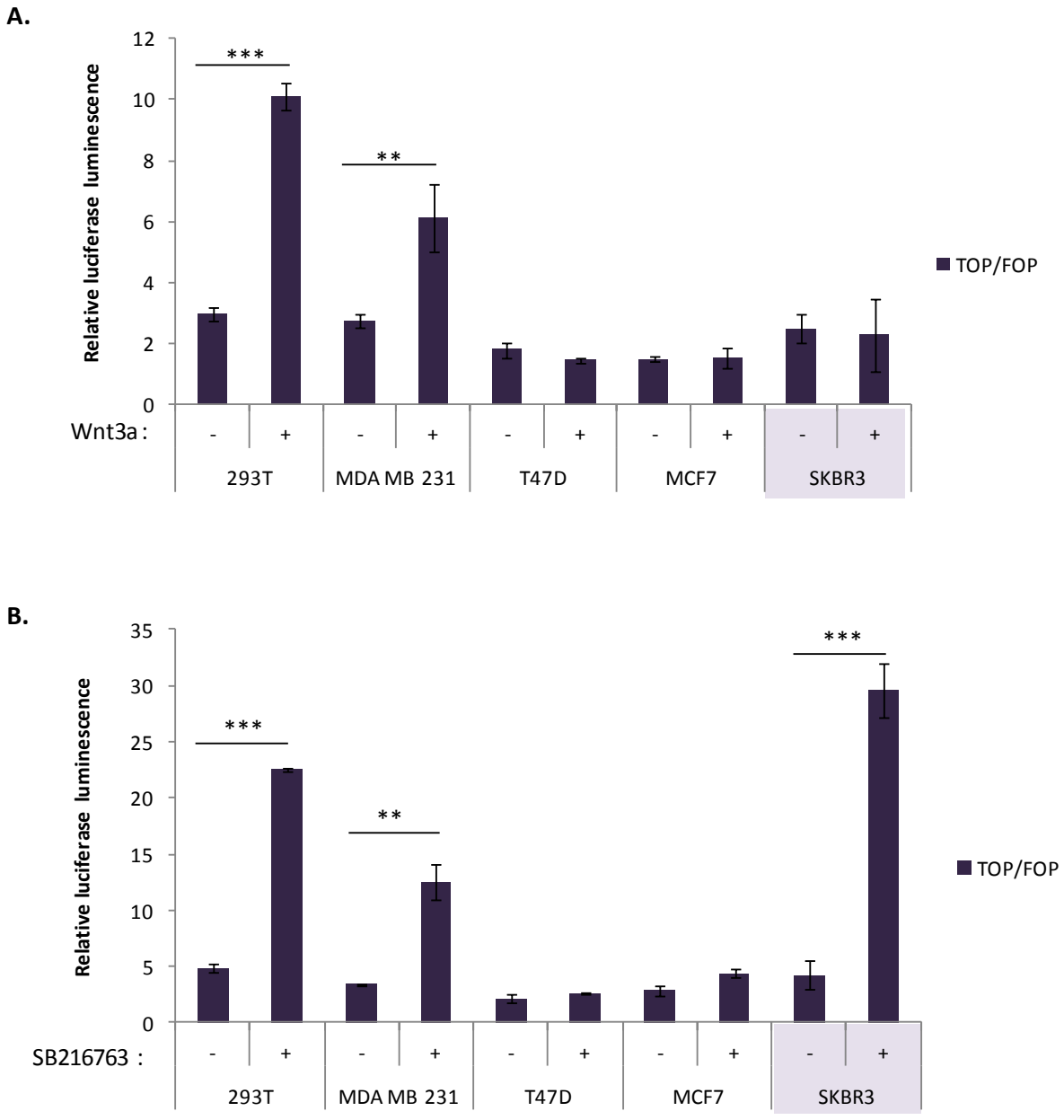

Figure 3. 4. Analysis of canonical Wnt signalling pathway activation in epithelial breast cell lines.

(A) Wnt3a-induced signalling or (B) SB216763 (10 µM) (GSK3 inhibitor)-induced signalling was analysed using TOP-Flash luciferase reporter assay. Cell were stimulated for 24h with Wnt3 CM or control CM (A), SB216367 or vehicle (B) and TOP/FOP activity was analysed 48h after the transfection with reporter plasmids. HEK293T cell line was used as a control. Tests were done in triplicates. Statistical significance was determined by two-tailed, unpaired Student's t-test (p<0.01; ***p<0.001); CM – conditioned medium.**

3.1.4. Fz7 activates canonical Wnt signalling pathway in SKBr3 cells

In the previous section, SKBr3 epithelial breast cancer cell line was identified as a suitable model to establish stable cell lines for signalling studies. To verify whether Fz7 is able to induce activation of canonical Wnt signalling in SKBr3 cells, when stimulated with Wnt3a, activity of TOPFlash reporter was assessed in cells transiently expressing FLAG-Fz7. SKBr3 cells were transfected with TOP-Flash reporter plasmids, and with vector expressing FLAG-Fz7 or mock transfected (pcDNA™3.1). Subsequently cells were incubated with Wnt3a conditioned medium or with control conditioned medium. Activation of Wnt signalling upon stimulation with Wnt3a was examined using the TOP-Flash luciferase assay. Cellular lysates obtained in the assay were also analysed by western blotting. The canonical Wnt pathway was significantly stronger activated in SKBr3 cells expressing Fz7 cells, as evidence by more than a six fold increase in signal (Figure 3.5.A). Accordingly, stabilization of β-catenin was observed in western blot experiments (Figure 3.5.B). Here, control SKBr3 cells (not expressing FLAG-Fz7) exhibit low pathway activation (four fold increase of TOPFlash activity over the base level). It can be explained by the fact that in this experiment more sensitive TOPFlash reporter construct was used. Specifically, the reporter construct contained eight binding sites for TCF/β-catenin, as compared to three sites in the construct used for the results shown in Figure 3.4. The 8xTOPFlash reporter plasmid was used in all following experiments.. Taken together, these experiments demonstrated the functionality of the ectopically expressed Flag-Fz7 construct in SKBr3 cell line.

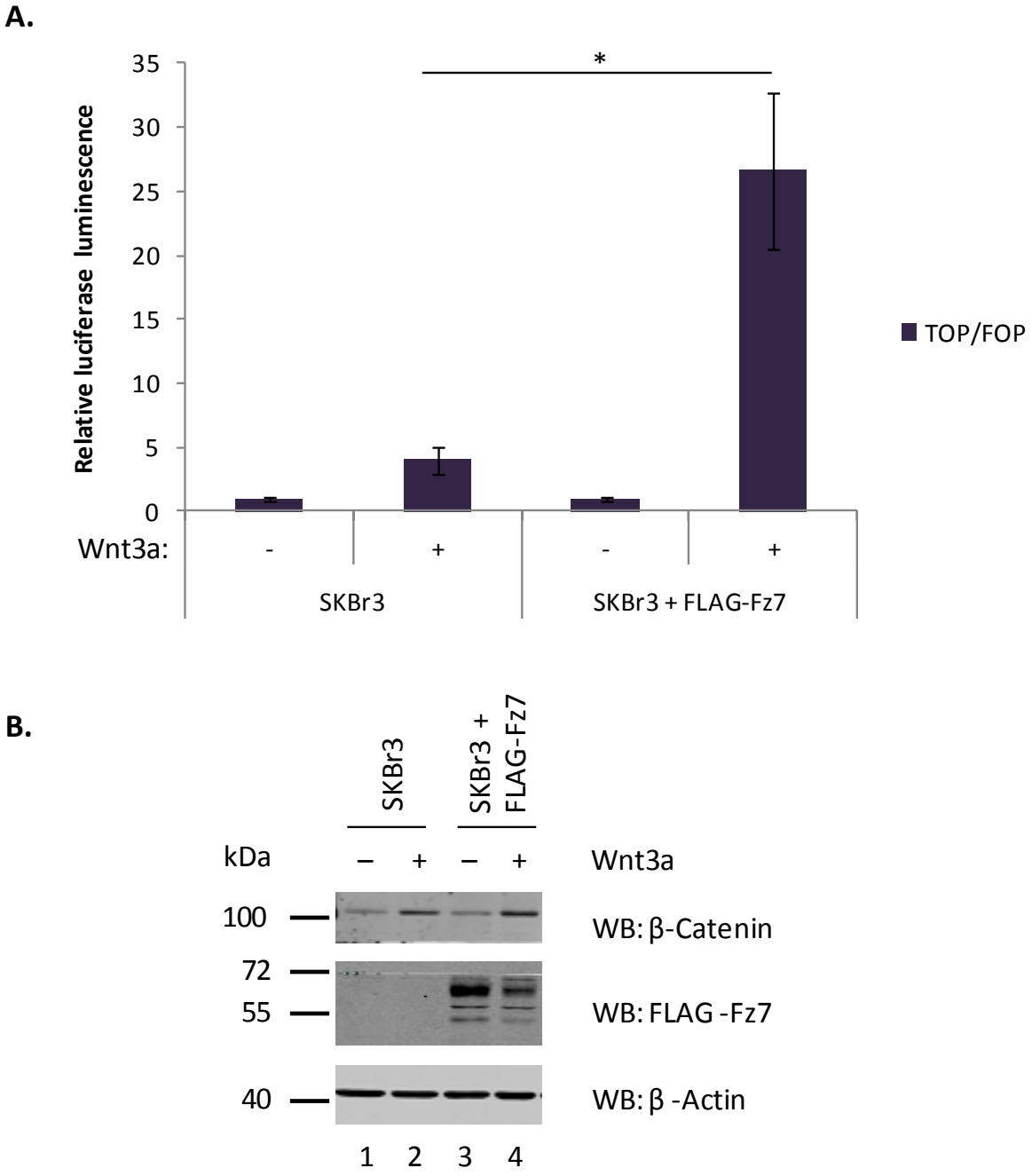

Figure 3. 5. Fz7 activates the canonical Wnt pathway in SKBr3 cells.

(A) Wnt-induced signalling was analysed using TOP-Flash luciferase assay. SKBr3 cells were transiently transfected with plasmid encoding FLAG-Fz7 or mock transfected. Cells were stimulated for 24h with Wnt3a conditioned medium and TOP/FOP activity was analysed 48h after transfection with reporter plasmids. Tests were done in triplicates and three independent experiments were performed. Statistical significance was determined by two-tailed, unpaired Student's t-test (* p<0.05). (B) Western blot analysis of Frizzzled-7 expression level in transiently transfected SKBr3 cells. β-actin served as a loading control. Image shown is a representative of three independent experiments.

3.1.5. Generation and characterization of SKBr3 cell lines stably expressing wild type and mutant of Fz7.

The SKBr3 cell line expresses endogenous Frizzled receptors at relatively low levels and canonical Wnt signalling in these cells can only be weakly induced by Wnt ligands. Nonetheless, introduction of Fz7 into SKBr3 cells leads to strong activation of the pathway in response to Wnt3a stimulation (sections 3.1.3. and 3.1.4.). These properties made SKBr3 cell line a suitable model to study Fz7-mediated signalling. SKBr3 cells were stably transfected with FLAG-Fz7 expression vector as described in section 2.2.7 of Materials and Methods. Fluorescence-activated Cell Sorting (FACS) using an anti-FLAG mAb was subsequently performed in order to select and separate FLAG-Fz7 expressing cells from non-expressing cells, as described in section 2.6.1 of Materials and Methods. FACS-based enrichment was performed twice to obtain a homogenous population of SKBr3 cells expressing Fz7 on the cell surface. This cell line will be hereafter referred to as SKBr3-FLAG-Fz7.

A similar approach was used to generate SKBr3 cell line expressing FLAG-Fz7 V574G mutant of Fz7. In this mutant, the hydrophobic valine at position 574 (Val574, V) was replaced with neutral amino acid glycine (Gly, G) (Figure 3.5.A). We predicted that such mutation would prevent binding of PDZ domain containing proteins to Fz7. This cell line will be referred to as SKBr3-FLAG-Fz7 V574G in the study.

3.1.5.1. Assessing cell surface expression, overall expression and cell localization of Fz7 in SKBr3 cells.

After generating the SKBr3-FLAG-Fz7 and SKBr3-FLAG-Fz7 V574G cell lines, expression of the wild type and V574G mutant Fz7 receptor was verified by WB, flow cytometry and immunofluorescence staining.

Figure 3.6.B. shows the results western blot experiments: comparable expression levels were observed for both Fz7 WT (lane 2) and Fz7 V574G (lane 3). However, we have observed differences in the appearance of antibody-reactive bands in cells expressing Fz7 WT and Fz7 V574G. Specifically, the relative abundance of the 60 kDa protein species was higher in cells expressing Fz7 V574G mutant, when compared with Fz7 WT. Flow cytometry analysis also revealed comparable cell surface levels of Fz7 in both cell lines (Figure 3.6.C). In order to determine localization of Fz7 in SKBr3 cells, an immunofluorescence staining analysis was carried out. Figure 3.6.D. shows that both, Fz7 WT and Fz7 V574G, were mainly detected on the plasma membrane. Interestingly, Fz7 V574G expressing cells formed small Fz7 positive membrane protrusions, which have not been observed in cells expressing wild type Fz7.

Taken together, WB analysis, flow cytometry, and immunofluorescence staining demonstrated that Fz7 is expressed in SKBr3-FLAG-Fz7 and SKBr3-FLAG-Fz7 V574G cells and that it is mainly localized on the cell surface.

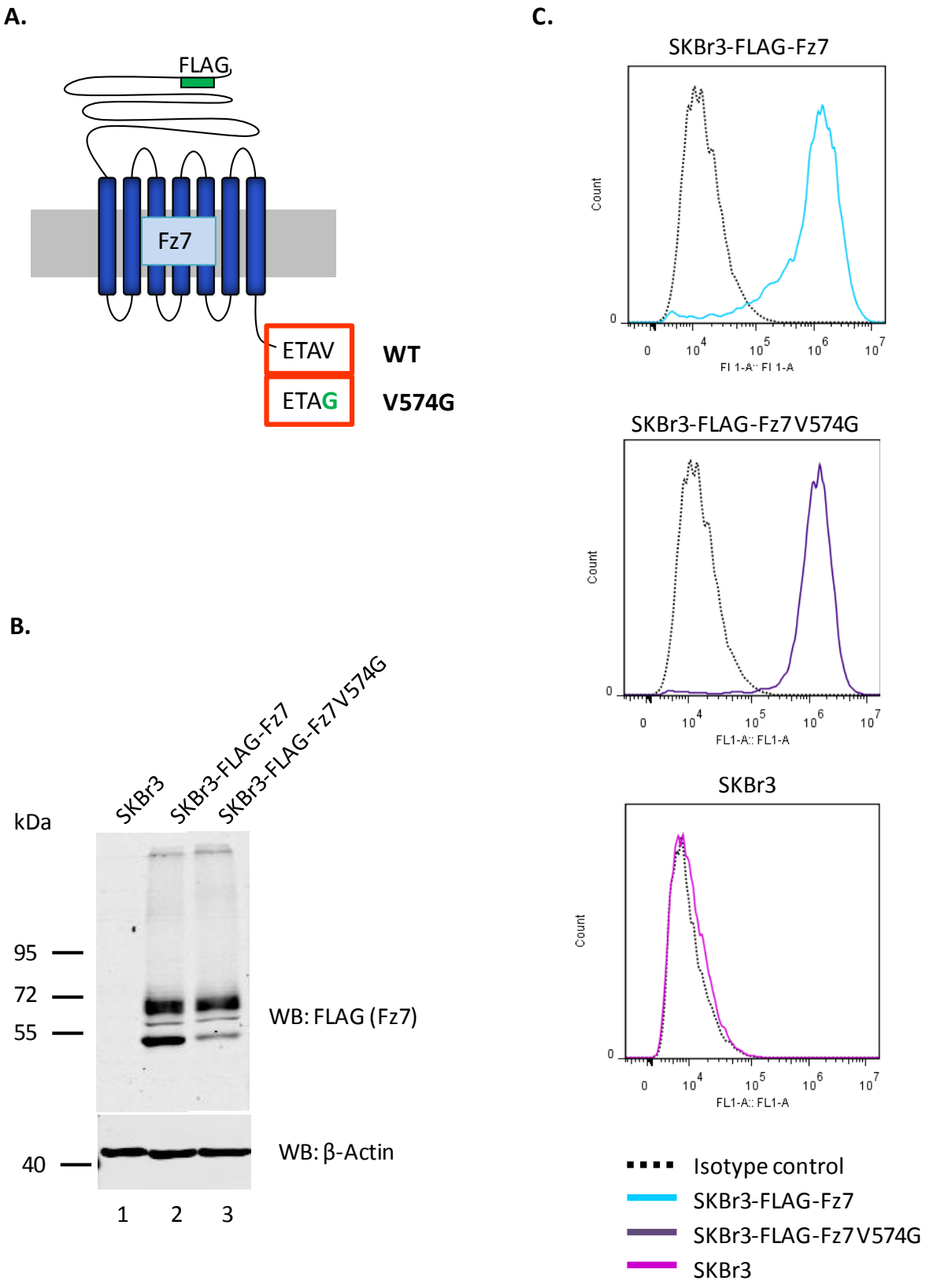
A.
FLAG
Fz7
ETAV
WT
ETAG
V574G
B.
kDa
SKBr3
SKBr3-FLAG-Fz7
SKBr3-FLAG-Fz7V574G
95
72
55
40
WB: FLAG (Fz7)
WB: β-Actin
1
2
3
C.
SKBr3-FLAG-Fz7
Count
FL1-A:: FL1-A
SKBr3-FLAG-Fz7V574G
Count
FL1-A:: FL1-A
SKBr3
Count
FL1-A:: FL1-A
Isotype control
SKBr3-FLAG-Fz7
SKBr3-FLAG-Fz7V574G
SKBr3

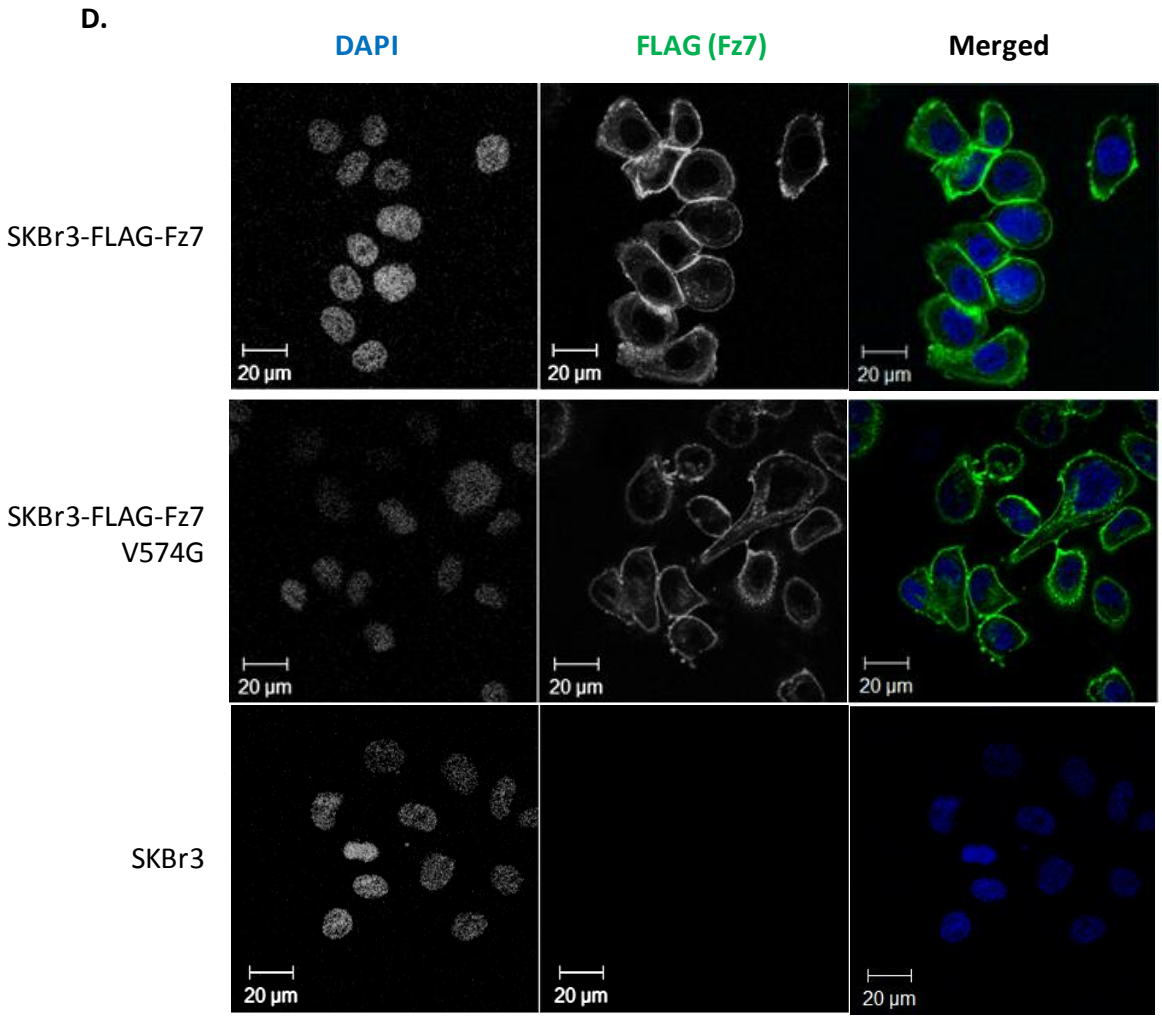

Figure 3. 6. Characterization of SKBr3 cells stably expressing Fz7 proteins (WT and V574G mutant).

(A) Schematic representation of Fz7 structure with PDZ binding motif (PDZ-BM) at the C-terminus. Mutation V574G was introduced in the PDZ-BM. (B) Equal amounts of protein lysates were resolved by SDS-PAGE, followed by western blotting and detection with rabbit anti-FLAG antibodies. β-actin served as a loading control. (C) Cells were incubated with either mouse anti-FLAG (M2) mAb or 4C5G, an isotype control mAb. Cell surface staining of FLAG-Fz7 (WT or V574G) were detected by flow cytometry following incubation with anti-mouse FITC-conjugated secondary antibodies. Data analysis was carried out using FlowJo analysis software. (D) Fz7 WT and V574G cell distribution was analysed by confocal imaging. Cells were fixed and stained with mouse anti-FLAG (M2) mAb and Alexa Fluor 488-conjugated goat-anti mouse ab (green). DAPI was used to visualize nuclei.

3.1.5.2. Mutation in the C-terminal PDZ binding motif of Fz7 attenuates canonical Wnt signalling in SKBr3 cells

Having established and characterized SKBr3 cell lines stably expressing FLAG-Fz7 wild type and FLAG-Fz7 V574G, activation of canonical Wnt signalling was compared in these two cell lines. SKBr3 parental, SKBr3-FLAG-Fz7 and SKBr3-FLAG-Fz7 V574G cells were transfected with reporter plasmids and incubated with Wnt3a conditioned medium for 24h. 48h after transfection, the activation of β-catenin-dependent signalling in the cell lines was assessed by TOP-Flash luciferase reporter assay. Lysates obtained in the assay were further analysed by WB to confirm Fz7 expression between cell lines and to monitor β-catenin stabilization within cells after Wnt3a stimulation. As demonstrated in the Figure 3.7. both, Fz7 WT and Fz7 V574G, activate Wnt signalling pathway over the background level of parental SKBr3 cell line. This was evident by the increase of TOPFlash reporter signal (Figure 3.7.A) and β-catenin stabilization detected in western blot analysis (Figure 3.7.B). The comparison of canonical Wnt pathway activation in cell lines expressing Fz7 WT or Fz7 V574G reveals that Fz7 wild type is more potent signalling receptor when compared with the Fz7 V574G mutant. In cells expressing Fz7 WT the signal TOPFlash reporter was five times stronger, when compared to the parental cell line. By comparison, cells expressing Fz7 V574G exhibited only a three fold signal increase. A histogram in the Figure 3.7.A represents one of three independent experiments. The compilation of the results obtain in three independent experiments is presented in the Supplementary Figure S.3. In some of the experiments we also noticed that the level of 60 kDa monomer in the Fz7 WT sample decreased after stimulation with Wnt3a ligand. However, these changes were not observed

in all the experiments and, therefore, require further investigation. Our results clearly demonstrate that the introduction of mutation V574G in the C-terminal PDZ-BM attenuates activation of the Wnt pathway. These findings provide an evidence for the importance of Fz7 binding to PDZ domain containing proteins in the regulation of the canonical Wnt signalling.

A.

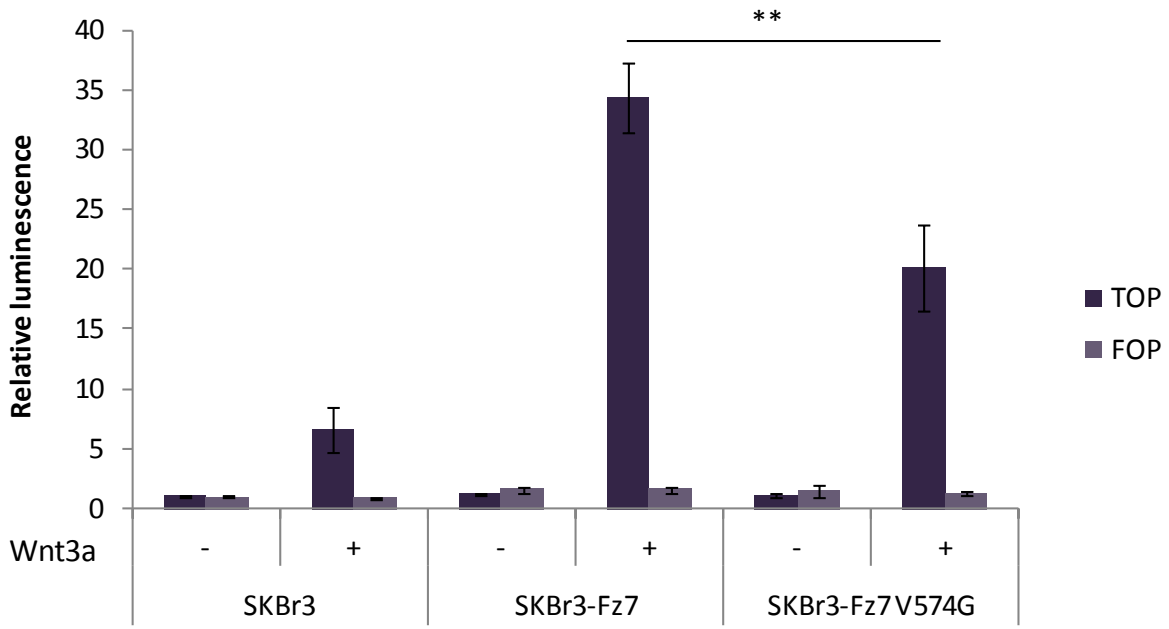
**
40
35
30
25
20
15
10
5
0
Relative luminescence
TOP
FOP
Wnt3a
-
+
-
+
-
+
SKBr3
SKBr3-Fz7
SKBr3-Fz7V574G

B.

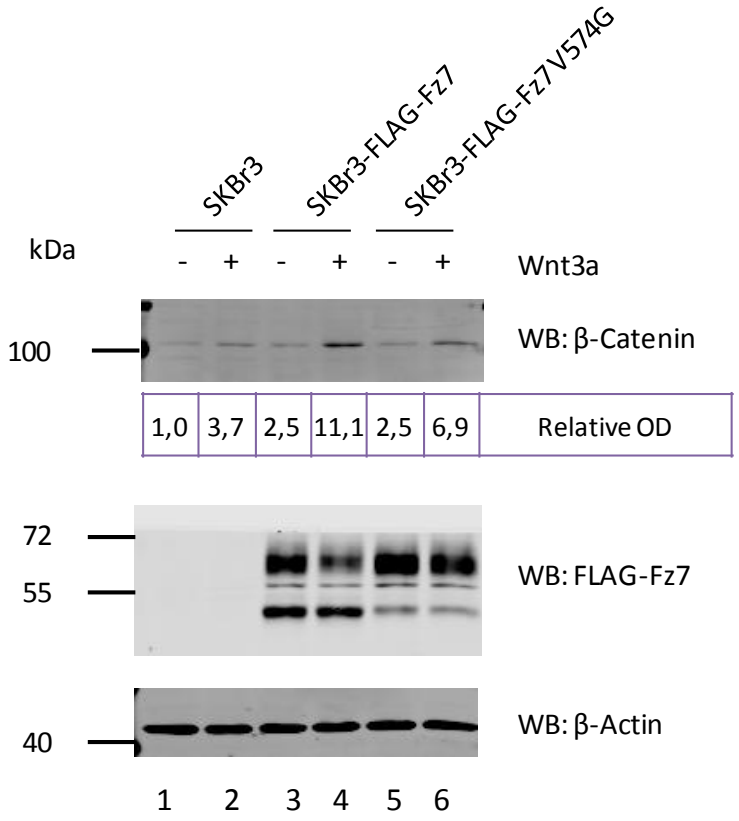
SKBr3
SKBr3-FLAG-Fz7
SKBr3-FLAG-Fz7V574G
kDa
- + - + - +
Wnt3a
100
WB: β-Catenin
1,0 3,7 2,5 11,1 2,5 6,9
Relative OD
72
55
WB: FLAG-Fz7
40
WB: β-Actin
1 2 3 4 5 6

Figure 3. 7. Mutation in the C-terminal PDZ-binding motif of Fz7 attenuates the canonical Wnt signalling in SKBr3 cells.

(A) Wnt-induced signalling was analysed using TOP-FLASH luciferase assay. SKBr3 cells were stimulated for 24h with Wnt3a conditioned medium and TOP/FOP activities were analysed 48 hours after the transfection with reporter plasmids. Tests were done in triplicates. Statistical significance was determined by two-tailed, unpaired Student's t-test (p<0.01). (B) Western blot analysis of Fz7 expression in SKBr3 cells using anti-FLAG pAb. β-catenin expression level was monitored using anti-β-catenin mAb. Densitometry values for β-catenin were standardized to the β-actin values of the same sample. β-actin served a loading control. Image shown is a representative of three independent experiments.**

3.1.6. Discussion

The ability to monitor the expression level of Fz7 receptor throughout the experiments was essential. Due to lack of reagents detecting the endogenous receptor in cells, it was necessary to generate constructs to express tagged forms of the Fz7 receptor.

Protein expression, subcellular localization and the luciferase-based TOP-Flash assays demonstrated that the insertion of the tag sequences did not affect the functionality of Fz7. Interestingly, we detected different forms of Fz7 in cells, including two monomers (50 kDa and 60 kDa) characterized by different degree of *N*-glycosylation, dimers (around 130 kDa) and higher oligomers with sized exceeding 200 kDa. Similar forms of Fz7 have been reported by Struewing and colleagues, who analysed expression of the protein in bovine aortic endothelial cells (BAEC) (Struewing et al. 2007). They showed that both monomers of Fz7 (54 kDa and 64 kDa) were sensitive to tunicamycin treatment, an inhibitor of N-glycosylation. Furthermore, the lower molecular weight species were also sensitive to endoglycosidase H treatment that specifically removes N-linked oligomannose, but not complex oligosaccharides. Oligomannose chains are adjoined to the receptor during the initial steps of glycosylation in the ER, whereas more complex oligosaccharides are added in the Golgi. Hence it was concluded that the 64 kDa monomer is a fully mature receptor, while the 54 kDa monomer is an immature receptor retained in the ER (Struewing et al. 2007). Protein glycosylation has been shown in the past to be crucial in Wnt signalling. Specifically, porcupine (Por)/Mom-1 has been shown to be involved in N-glycosylation of Wnt ligands in the ER (Kadowaki et al. 1996;Tanaka et al. 2002), whereas Boca/Mesd has been implicated to act as a chaperone for LRP5/6 (Culi et al. 2003). However glycosylation of Frizzled receptors

haven't been extensively studied. Yamamoto and colleagues found that Frizzled glycosylation is regulated by the protein Shisa, which mediates Fz7 retention in the ER during maturation (Yamamoto et al. 2005). In another study glycosylation was suggested to facilitate binding of Wnt ligands to mature receptors (Schulte et al. 2007).

We have observed that in HEK293T cells FLAG-tagged Fz7 formed dimers and high order oligomers. Similarly, the ability of Frizzled receptors to form dimers and oligomers has been reported previously (Kaykas et al. 2004). These authors have shown that different Frizzled receptors (Fz1, 2, 4, 7 and 9) form specific homo- and hetero-oligomers. The heptahelical transmembrane domain of receptors is sufficient for the oligomerization, which occurs independently of the CRD domain C-terminal tail and associated scaffolding proteins, and is not influenced by Wnt ligands. Frizzled oligomerization has been also shown to occur in the ER during or after translation. It was suggested that the process may modulate Wnt signalling, as different combinations hetero-oligomers may signal in a distinct fashion than homo-oligomers (Kaykas et al. 2004).

To assess the functionality of the generated tagged-Fz7 constructs we relied on the luciferase-based reporter assay (called TOP-Flash). It is a widely used test, enabling to quantify activation level of canonical Wnt pathway in cells, first described in (Korinek et al. 1997). We found that all generated constructs are functional, thus demonstrating the tag insertion on the N-terminal site did not influence ability of the receptor to transduce signals. On the other hand, C-terminally tagged Fz7-V5-His was not able to efficiently activate the canonical Wnt pathway (Figure 3.3.), indicating the importance of the C-terminus in signal transduction. Importantly, the critical role of the C-terminal PDZ-BM was further confirmed in experiments involving the Fz7 V574G mutant: ligand-induced activation of the canonical

Wnt pathway in cells expressing the mutant receptor was ~30% lower when compared to that observed in the Fz7 wild type expressing cells. To our knowledge this is the first demonstration of the involvement of the C-terminal PDZ-BM of a Frizzled receptor in the canonical Wnt pathway. Several studies also shown that the PDZ-BM of a protein is important for regulation of its signalling. For example, Delta1, a ligand for the Notch receptor, contains a PDZ-BM within its C-terminus. Mutation of its C-terminal valine leads to activation of Notch signalling (Estrach et al. 2007). PDZ proteins also affect GPCR signalling. For example, $GABA_B$ receptors interaction with PDZ protein MUPP1 (multi PDZ protein 1) enhances receptor signalling by affecting G-protein coupling or association of the receptor with other proteins (Balasubramanian et al. 2007).

Fz7 is the only member of Frizzled family reported to be overexpressed in breast cancer, especially in basal-like, triple-negative breast cancer (Yang et al. 2011). While searching for a suitable model breast cancer cell line to study the involvement of the Fz7 C-terminal PDZ-BM in the canonical Wnt pathway, we confirmed its functionality in MDA-MB-231 cells, a model triple negative breast cancer cell line (Yang et al. 2011). On the other hand, we found that the β-catenin-dependent pathway is not functional in T47D and MCF7 cells In this regard, it has been shown that high expression level of NHERF1, protein which interacts with Fz2, Fz4 and Fz7, attenuates canonical Wnt pathway in MCF7 cells by preventing Dishevelled recruitment to the receptor. Accordingly, NHERF1 depletion enabled activation of Wnt signalling in MCF7 cells (Wheeler et al. 2011). In a more recent study Simmons and colleagues have shown that T47D cell line expresses a set of different Frizzled receptors, including Fz7, and that activation of Wnt/β-catenin pathway in these cells can be stimulated by Wnt1 (Simmons, Jr. et al. 2014). One possible explanation for the observed

discrepancies is differences in ligands (i.e. Wnt1 vs. Wnt3a) and their concentrations. Also, the outcome of used test depends greatly on the transfection efficiency wherein low transfection efficiency might explain lack of signal increase after stimulation with Wnt ligand or GSK3 inhibitor.

Although, mutation of the C-terminal PDZ-BM did not seem to have an apparent effect on cellular distribution of Fz7, we observed differences in the relative abundance of two Fz7 molecular species: high- (60kDa) and low-glycosylated (50kDa). The immunoreactivity for the low-glycosylated form of Fz7 V574G in the western blot was weaker when compared with corresponding band of the Fz7 WT. These results suggest that the mutation in the PDZ-BM influences the Fz7 maturation process. Although we have not explored it further, previous reports have identified a role for PDZ domain proteins in biosynthetic trafficking of the associated transmembrane receptors. It was shown for example for cystic fibrosis transmembrane conductance regulator, CTFR, reviewed in (Pranke et al. 2014).

Immunofluorescence analysis of SKBr3-FLAG-Fz7 and SKBr3-FLAG-Fz7 V574G cell lines revealed that both Fz7 and Fz7 V574G, localize mainly to the plasma membrane. Nonetheless, Fz7 V574G expressing cells formed small Fz7 positive membrane protrusions, which have not been observed in cells expressing wild type Fz7 (Figure 3.6). This indicates that one or more of PDZ proteins interacting with Fz7 may be involved in regulation of the trafficking of the receptor. Indeed, many PDZ domain containing proteins have been implicated in the regulation of receptor trafficking. As an example may serve PDZ proteins interacting with G protein coupled receptors (GPCRs), another group of heptahelical membrane receptors structurally similar to Frizzled proteins, e.g. NHERF/EBP50 interacting

with β_2AR, NHERF1 with type I parathyroid hormone receptor (PTHR1R) or Golgi associated CAL (cystic fibrosis transmembrane conductance regulator-associated ligand) interacting with somatostatin receptor subtype 5 (SSTR5), all reviewed in (Magalhaes et al. 2012). On the other hand, observed differences may occur due to aberrant signalling on the actin cytoskeleton, and Fz7 is present in the protrusions simply because the protein is localised on the plasma membrane.

In summary, work discussed in this chapter included generation of expression vectors for tagged Fz7 and subsequent characterization of SKBr3-FLAG-Fz7 and SKBr3-FLAG-Fz7 V574G stable cell lines, as well assessing activation of the canonical Wnt signalling in those cell lines. We have demonstrated that mutation introduced in the membrane distal PDZ-BM of Fz7 attenuates activation of the canonical Wnt signalling pathway in epithelial breast cancer cell line SKBr3. We have established, for the first time, that canonical Wnt signalling is regulated by Fz7 interactions with PDZ domain containing proteins through the C-terminal PDZ binding motif of the receptor.

3.2. Investigating the role of the Fz7 interaction with syntenin-1

In the previous chapter it was shown that the mutation introduced in a membrane distal PDZ-BM of Fz7 attenuates activation of the canonical Wnt signalling pathway in the epithelial breast cancer cell line SKBR3. This finding implies that Fz7 interaction with a protein or proteins through its C-terminal PDZ binding motif is important for the regulation of the canonical Wnt pathway. To examine this further, we decided to focus initially on Fz7 interaction with syntenin-1. Syntenin-1 is a protein containing two PDZ domains, which functions as a scaffolding partner for a number of transmembrane receptors (Beekman et al. 2008), Importantly, it was reported to interact with Fz7 and regulate non-canonical Wnt signalling (Luyten et al. 2008). The aim of the work described in this chapter was to investigate whether expression, cell localization and signalling function of Fz7 are regulated by syntenin-1.

3.2.1. Examination of Fz7 binding to syntenin-1

3.2.1.1. Fz7 interaction with syntenin-1 involves PDZ domains

To examine the Fz7–syntenin-1 interaction, a co-immunoprecipitation assay was performed. In these experiments we used wild type and Fz7 V574G expressing cells. We have also included a Fz7 V574E mutant in which the last C-terminal amino acid Val574 was replaced with glutamic acid (Glu, E). We predicted that the replacement of hydrophobic valine with glutamic acid, an amino acid containing negatively charged side chain would have a more dramatic affect on binding of Fz7 to PDZ proteins. HEK293T cells were co-transfected with FLAG-syntenin-1 and Myc-Fz7 (WT, or with mutation V574G or V574E). Cells were lysed and incubated with anti-FLAG agarose beads to pull down syntenin-1 together with associated proteins. Proteins retained by the beads were resolved by SDS-PAGE and analysed by western blotting. Membranes were incubated with anti-FLAG pAb to detect syntenin-1 and anti-Myc pAb to detect Fz7. Immunoprecipitation samples were prepared under non-reduced conditions to facilitate Fz7 detection. WB analysis revealed that syntenin-1 interacts with the wild type Fz7 (lane 2, Figure 3.8.A). In these experiments we also observed the association with both mutants of Fz7 V574G and V574E (lanes 4 and 6, respectively). Densitometry analysis was performed on data obtained in three independent experiments and presented as a histogram, plotted as a percentage of syntenin-1 binding to Fz7 mutants relative to the interaction of syntenin-1 with the wild type Fz7 (taken as 100%) (Figure 3.8.B). Optical density (OD) was measured for both, Fz7 and syntenin-1, and the ratios between the two proteins were calculated for each sample. This allowed us to compare

samples with each other. Analysis revealed that syntenin-1 binding to Fz7 V574G was ~40% lower, and to Fz7 V574E was 60% lower, when compared to the interaction of syntenin-1 with wild type Fz7. Thus, V574E mutation had more substantial impact on the syntenin-1 – Fz7 interaction.

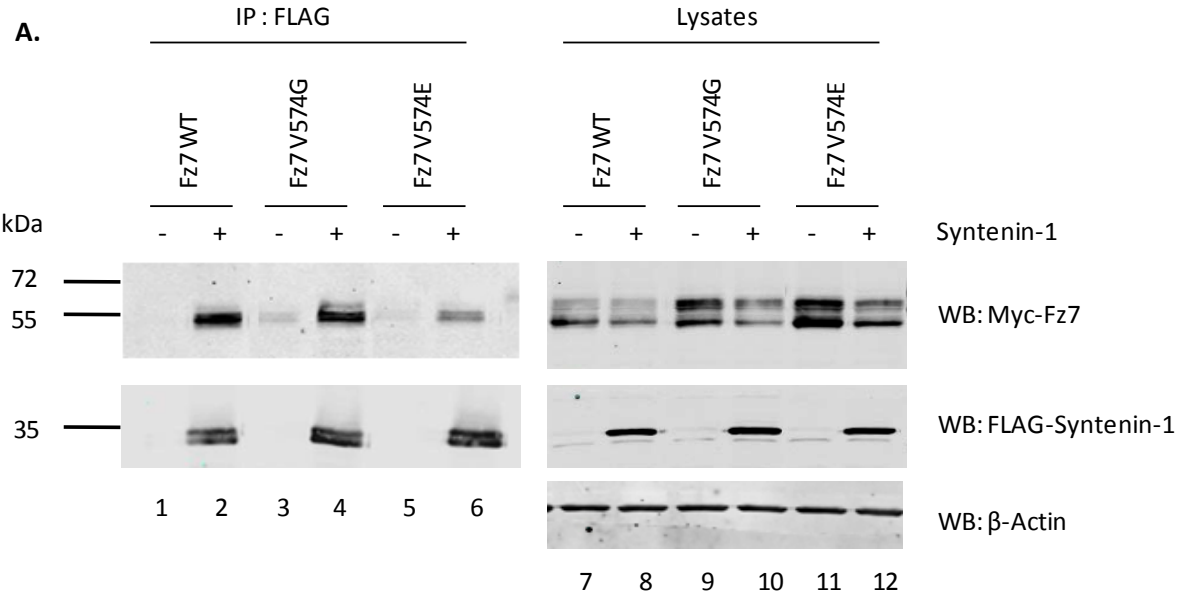

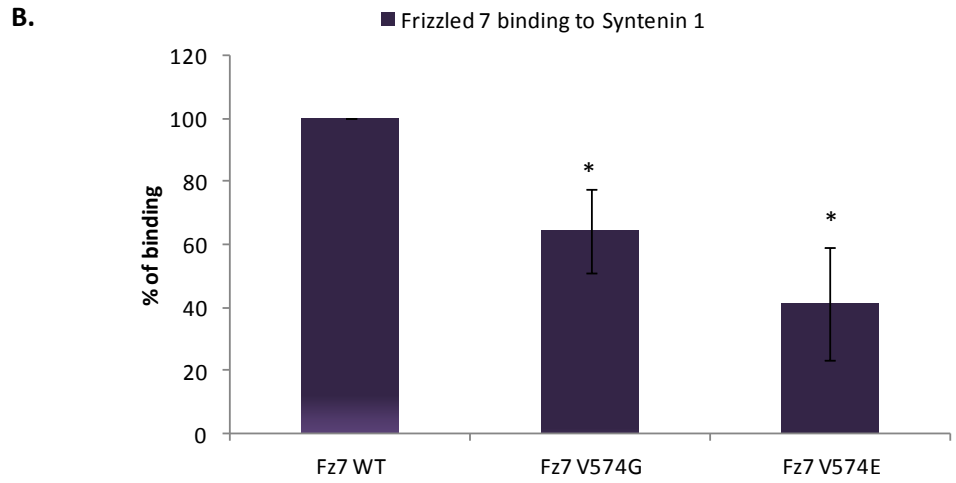

Figure 3. 8. Fz7 interaction with syntenin-1 involves PDZ domains.

(A) HEK293T cells were co-transfected with Myc-Fz7 (WT, V574G or V574E) and FLAG-syntenin-1. 24h after transfection cells were lysed in 0.5% Brij98-0.5% Triton X-100 and lysates were incubated with Anti-FLAG®M2 Agarose Beads. After immunoprecipitation, the retained proteins were resolved by SDS-PAGE, followed by western blotting and protein detection using rabbit anti-Myc pAb and rabbit anti-FLAG pAb. Images depict a representative of three independent experiments. (B) Densitometry analysis performed on data obtained in three independent experiments and demonstrated on a histogram, plotted as percentage of Syntenin-1 binding to Fz7 mutants relative to the interaction of syntenin-1 with the wild type Fz7 (taken as 100%). The statistical significance was determined by a two-tailed, unpaired Student's t-test (*p<0.05).

Reciprocal co-immunoprecipitation experiments were also performed. HEK293T cells were transiently transfected to express FLAG-Fz7, FLAG-Fz7 V574G or FLAG-Fz7 V574E and the interaction with the endogenous syntenin-1 was examined after immunoprecipitation with anti-Flag mAb (Figure.3.9.A). Syntenin-1 was found to interact with Fz7 WT (lane 2), and also with Fz7 V574G (lane 3) and Fz7 V574E (lane 4), albeit the interaction with the two mutants was dramatically diminished. Densitometry analysis (performed as above) showed that syntenin-1 binding to Fz7 V574G was five fold lower, and to Fz7 V574E was more than ten fold lower, when compared with binding to the wild type Fz7. These experiments clearly demonstrated that mutations in the PDZ-BM of Fz7 significantly decreases interactions of the protein with syntenin-1. These results also suggested that the interaction with Fz7 involves at least one of the PDZ domains of syntenin-1.

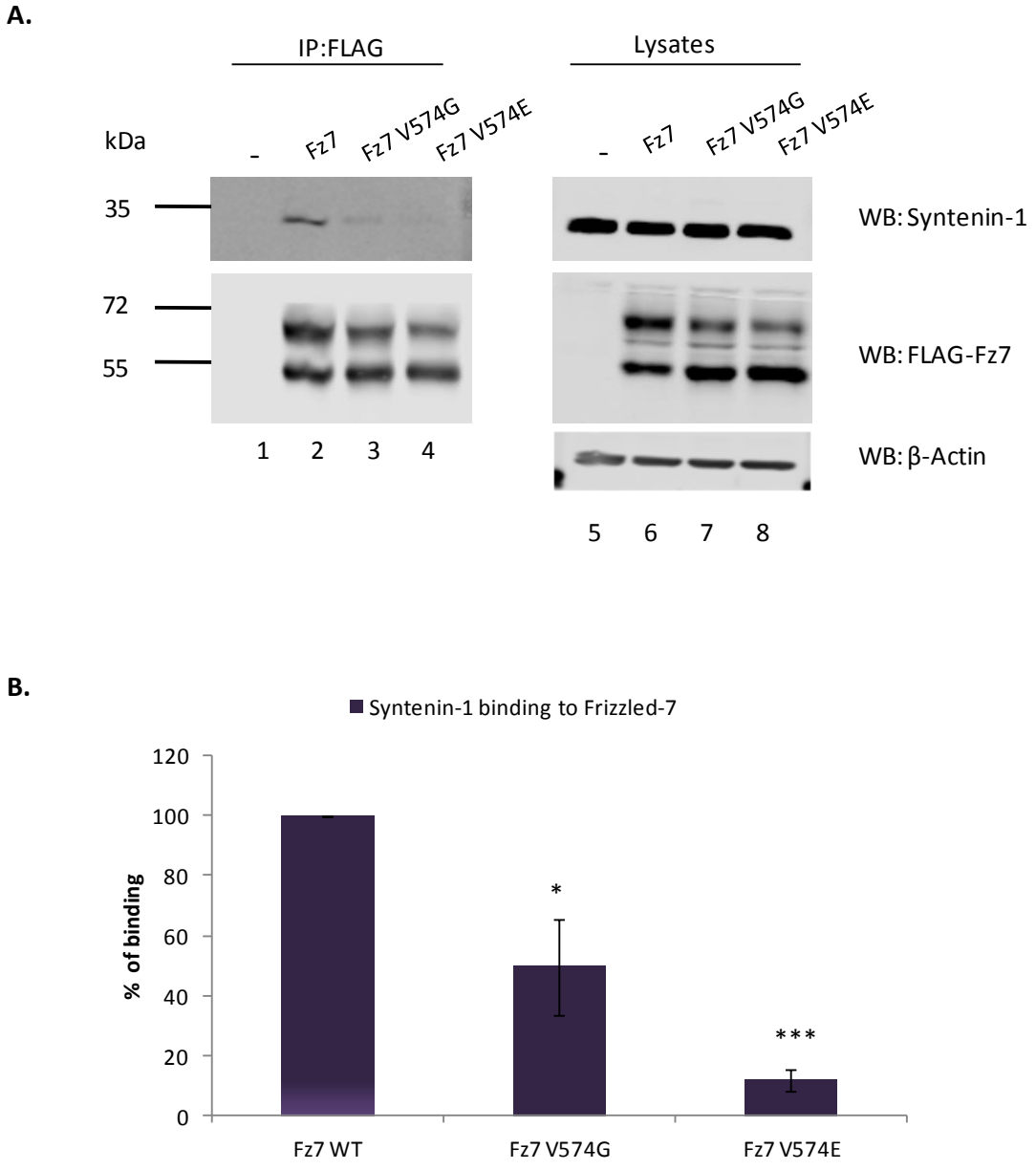

Figure 3. 9. Fz7 interacts with endogenous syntenin-1.

HEK293T cells were co-transfected with FLAG-Fz7 (WT, V574G or V574E). 24h after transfection cells were lysed in 1% Triton X-100 and lysates were incubated with Anti-FLAG® M2 magnetic beads. Immunoprecipitated proteins were resolved by SDS-PAGE, followed by western blotting and protein detection using rabbit anti-FLAG pAb and rabbit anti-syntenin-1 mAb. Images depict representatives of at least three independent experiments. (A) Densitometry analysis performed on data obtained in three independent experiments and presented as a histogram, plotted as percentage of syntenin-1 binding to Fz7 mutants relative to the interaction of syntenin-1 with the wild type Fz7 (taken as 100%). The statistical significance was determined by a two-tailed, unpaired Student's t-test (*p<0.05; ***p<0.001).

3.2.1.2. Mapping of syntenin-1 domain that interacts with Fz7

The nature of the syntenin-1 - Fz7 interaction was analysed further using the following synteinin-1 – encoding constructs: HA-syntenin-1-PDZ1* (G126D), PDZ2* (G210E) or PDZ1*PDZ2* (G126D, G210E) with introduced mutations in the interacting loops that prevented binding through the PDZ1, PDZ2 or both, respectively (Latysheva et al. 2006). In the control experiments we used a construct encoding HA-tagged syntenin-1 (wild type). HEK293T were co-transfected with FLAG-Fz7 and one of the syntenin-1 – encoding plasmids and the interaction between the proteins was analysed by immunoprecipitation. These experiments revealed that both PDZ domains of syntenin-1 are required for its interaction with Fz7 (Fig.3.10.A). This was evident by a significant decrease in the amount of syntenin-1 mutants detected in Fz7 immunoprecipitates: compare signals in lane 4 (PDZ1*), lane 6 (PDZ2*) and lane 8 (PDZ1*2*) with lane 2 (syntenin-1 WT). Densitometry analysis showed that both PDZ domains of syntenin-1 contribute to the interaction with Fz7, as syntenin-1 PDZ1* binding to Fz7 was ten fold lower, whereas syntenin-1 PDZ2* and syntenin-1 PDZ1*PDZ2* binding was 20 times lower when compared with the interaction of wild type syntenin-1 to Fz7 (Figure 3.10.B)

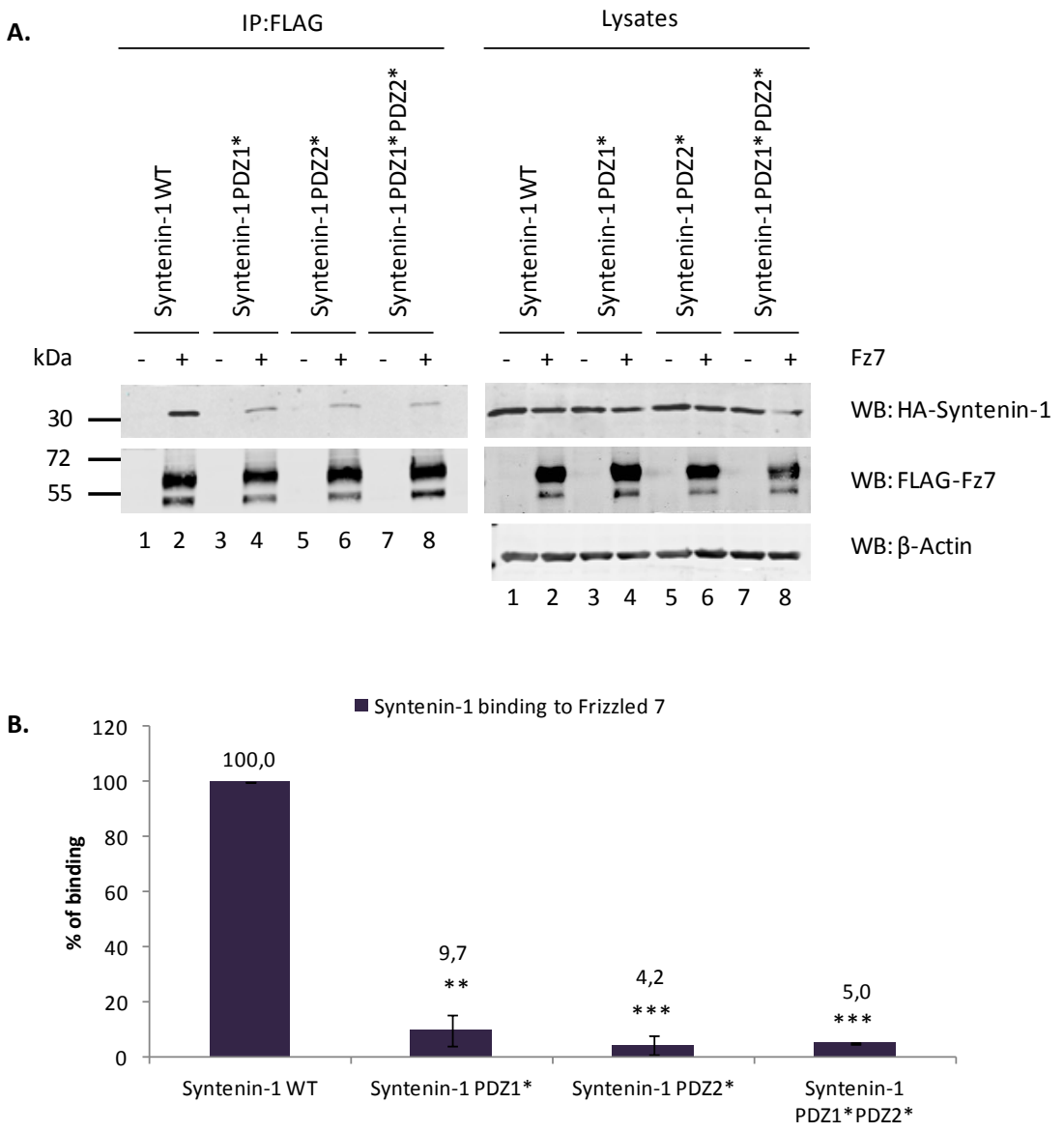

Figure 3. 10. Interaction with Fz7 involves both PDZ domains of syntenin-1.

(A)HEK293T cells were co-transfected with FLAG-Fz7 and HA-syntenin (WT or with introduced mutation in PDZ1*, PDZ2* or both PDZ1*PDZ2*). Immunoprecipitation assay was carried out in 0.8% Brij98-0.2% Triton X-100 buffer. Lysates were incubated with Anti-FLAG®M2 Agarose Beads. After immunoprecipitation, beads were washed and resuspended in 2x SDS sample-loading buffer. Retained proteins were resolved by SDS-PAGE, followed by western blotting and protein detection using rabbit anti-FLAG pAb and rabbit anti-HA pAb. Images depict a representative of two independent experiments. (B) Densitometry analysis was performed on data obtained in two independent experiments and demonstrated on a histogram, plotted as percentage of syntenin-1 binding to Fz7 mutants relative to the interaction of syntenin-1 with the wild type Fz7, taken as 100%. The statistical significance was determined by a two-tailed, unpaired Student's t-test (p<0.01; ***p<0.001).**

To investigate the interaction between Fz7 and syntenin-1 in more detail nuclear magnetic resonance (NMR) analysis was used in collaboration with Dr Sundaresan Rajesh. NMR titration analysis of ^{15}N-labeled syntenin-1-PDZ1-2 domains with unlabeled Fz7 peptide, corresponding to the last 8 amino acid of cytoplasmic tail of the receptor, was carried out. The method was previously described in (Latysheva et al. 2006;Rajesh et al. 2011) where detailed structural information on the role of syntenin-1's individual amino acids is provided. The decrease in signal intensity (chemical shift) for each amino acid of syntenin-1 upon interaction with Fz7 peptide at various concentrations (50 μM – 800 μM) was calculated and later mapped onto the crystal structure of the syntenin-1-PDZ1-2 monomer, PDB:1N99 (Kang et al. 2003). The colour code was used to highlight the calculated values: green represents a decrease in signal intensity of 25-40%; yellow represents a decrease of 40-60%, orange represents a decrease of 60-80%; and red a decrease of more than 80% (Figure 3.11). The decrease of NMR signal intensity correlates with the proximity of the relevant amino acid with the interacting peptide. Analysis revealed that syntenin-1-PDZ2 domain is predominantly involved in the Fz7 peptide binding, although the involvement of PDZ1 was also observed. When the Fz7 peptide was used at 50 μM (1:0.25 ration toward syntenin-1 monomer concentration) a chemical shift was observed for Ile125 (PDZ1) and Thr219 (PDZ2), suggesting that the initial step of Fz7 binding involves both PDZ domains (Figure 3.11.A). However, when the concentration of Fz7 peptide was increased to 100 μM (1:0.5 ratio) a chemical shift of Gly210 was observed in the carboxylate binding loop of PDZ2, as well as of several residues in the vicinity of this site Phe211, Phe213, Gly216, and Thr219. In contrast, chemical shift perturbations in PDZ1 were limited to Ile125 and Gly126 in the carboxylate binding loop of PDZ1, and to Arg191 (Figure 3.11.B). The chemical shift perturbations,

obtained when peptide was added in four fold excess (800 μM) (Figure 3.11.C), were used to map binding sites and revealed a contact surface present predominantly in the syntenin-PDZ2 domain binding pocket, and to a lesser extent in the PDZ1 (Figure 3.11.D). Namely residues 199-201, 203-204, 207-211, 213-216, 220, 223-226, 229-235, 239, 242, 246, 255-256, 258-259 and 265-270 in PDZ2, and 120, 125-127, 130, 141, 147, 179, 186 and 190-191 in PDZ1 were involved in Fz7 peptide binding. This structural data support our co-immunoprecipitation assay observations presented in the previous paragraph.

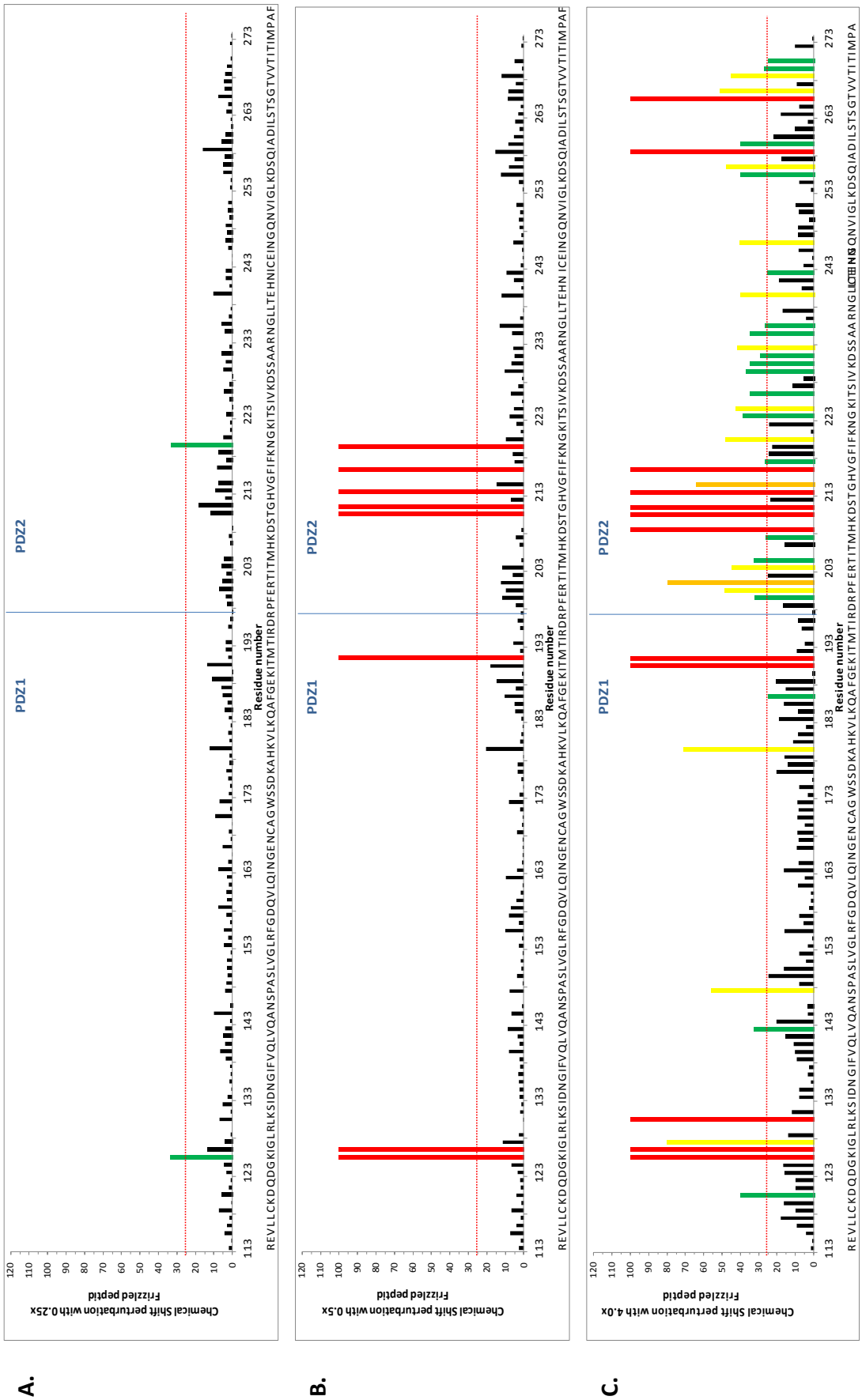
A.
B.
C.
PDZ1
PDZ2
Chemical Shift perturbation with 0.25x
Chemical Shift perturbation with 0.5x
Chemical Shift perturbation with 4.0x
Frizzled peptid
Residue number
REVLLCKDQDGKIGLRLKSIDNGIFVQLVQANSPASLVGLRFGDQVLQINGENCAGWSSDKAHKVLKQAFGEKITMTIRDRPFERTITMHKDSTGHVGFIFKNGKITSIVKDSSAARNGLLTEHNICEINGQNVIGLKDSQIADILSTSGTVVTITIMPAF

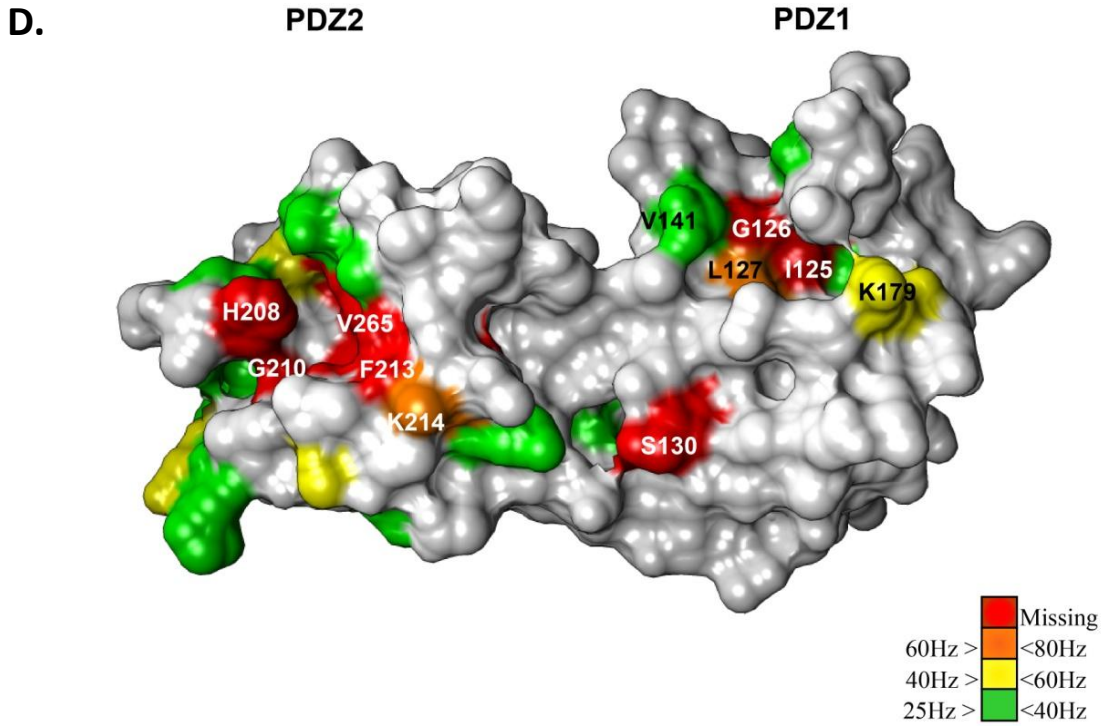

Figure 3.11. Interaction with Fz7 is predominantly mediated by PDZ2 domain of syntenin-1.

Graphs present perturbation of syntenin-1 PDZ1-2 NMR signals upon interaction with Fz7 peptide: (A) equal concentration of the peptide and syntenin-1 monomer; (B) four fold excess of the peptide . The residues displaying combined chemical shift changes greater than the mean value plus one (25 Hz) are colour coded as indicated below and (C) mapped onto the surface of crystal structure of the syntenin-1 PDZ1-2 (PDB:1N99) monomer resolved by (Kang et al. 2003). The decrease in signal intensity (chemical shift changes) for every amino acid of syntenin-1 PDZ1-2 monomer upon interaction with the peptide was calculated and represented using the following colour code: green represents a decrease in signal intensity of 25-40%; yellow represents a decrease of 40-60%, orange represents a decrease of 60-80%; and red a decrease of more than 80%. The degree of decrease in signal indicates the proximity between the relevant amino acid of syntenin-1 with the target peptide.

3.2.2. Syntenin-1 modulates canonical Wnt signalling pathway

3.2.2.1. Syntenin-1 knockdown attenuates canonical Wnt pathway signalling in the SKBr3 cell line

The role of syntenin-1 in canonical Wnt signalling was examined in the SKBr3 epithelial breast cancer cell line stably expressing FLAG-Fz7 wild type or FLAG-Fz7 V574G mutant, after syntenin-1 depletion. For this purpose SKBr3 cells were transfected with the siRNA targeting syntenin-1, or with a control siRNA (siNeg) and with reporter plasmids. On the following day, cells were stimulated with Wnt3a. 24h after later β-catenin reporter activity was compared to cells with and without syntenin-1 knock-down (Figure 3.15.A). Cellular lysates obtained in the experiment were analysed by SDS-PAGE and WB to quantify the level of syntenin-1 knockdown (Figure 3.15.B). WB analysis confirmed the syntenin-1 knockdown (lanes 3, 4, 7 and 8). The protein expression levels were reduced by 90%, compared with the control samples. These experiments showed that syntenin-1 depletion attenuates activation of Wnt signalling in cells expressing wild type Fz7. Reporter activity in SKBr3-FLAG-Fz7 cells with syntenin-1 knockdown was reduced by 40%, when compared with control cells. On the other hand, syntenin-1 depletion didn't alter Wnt signalling in SKBr3 cells expressing the Fz7 V574G mutant. Taken together, syntenin-1 depletion attenuates canonical Wnt signalling in SKBr3 cells expressing wild type Fz7, but not the Fz7 V574G mutant.

A.

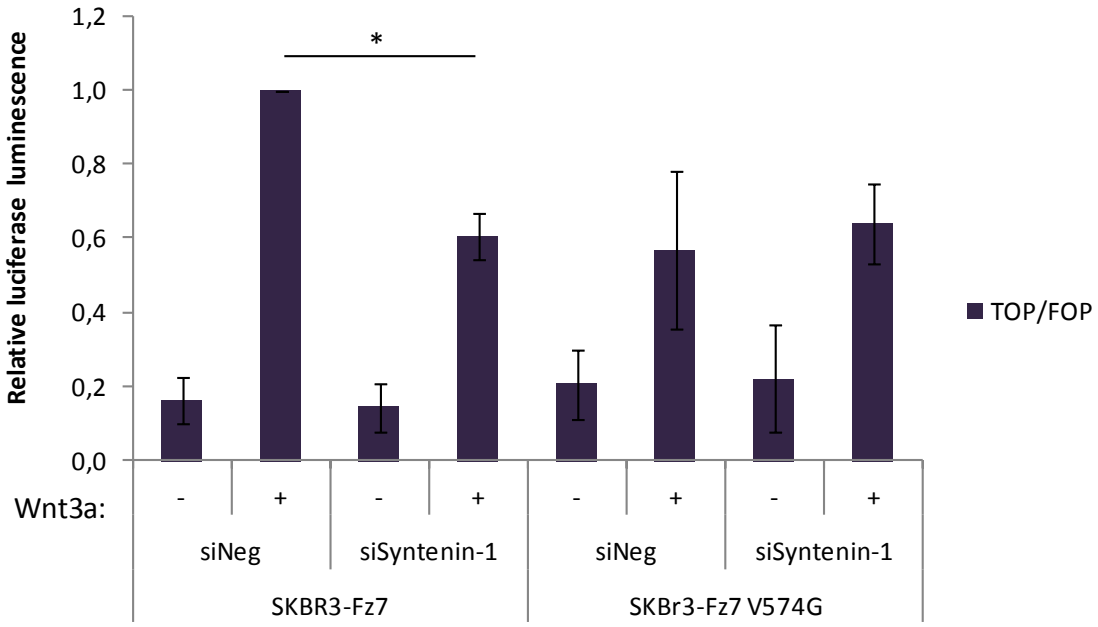
Relative luciferase luminescence
1,2
1,0
0,8
0,6
0,4
0,2
0,0
*
Wnt3a:
- + - + - + - +
siNeg
siSyntenin-1
siNeg
siSyntenin-1
SKBR3-Fz7
SKBr3-Fz7 V574G
TOP/FOP

B.

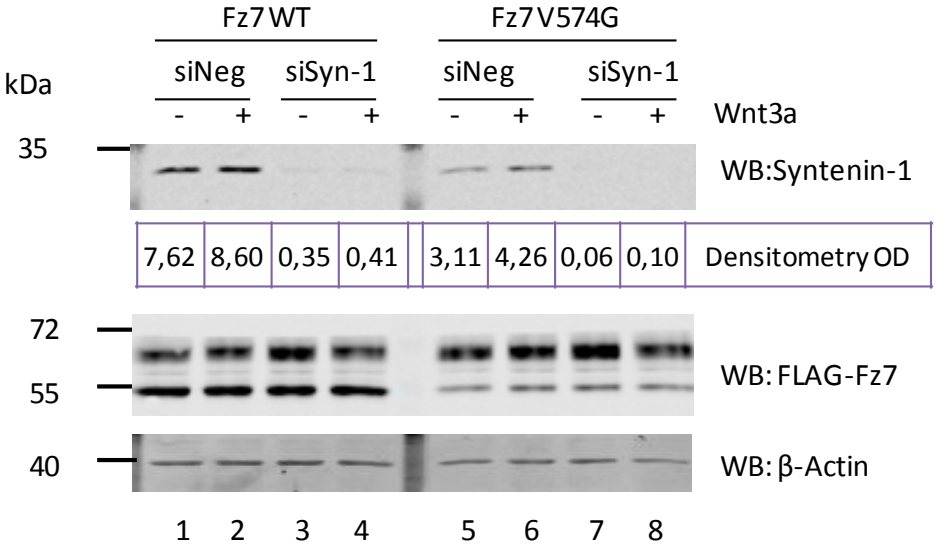
Fz7 WT
Fz7 V574G
kDa
siNeg
siSyn-1
siNeg
siSyn-1
- + - + - + - +
Wnt3a
35
WB:Syntenin-1
7,62 8,60 0,35 0,41 3,11 4,26 0,06 0,10
Densitometry OD
72
55
WB: FLAG-Fz7
40
WB: β-Actin
1 2 3 4 5 6 7 8

Figure 3. 12. Syntenin-1 depletion attenuates canonical Wnt signalling in SKBr3 cells expressing Fz7 WT.

(A) Wnt3a-induced signalling was analysed using the TOP-Flash luciferase reporter assay. SKBr3-FLAG-Fz7 and SKBr3-FLAG-Fz7 V574G cells were transfected with siRNA against Syntenin-1 or control siNegative. Cells were stimulated for 24h with Wnt3a conditioned medium and TOP/FOP activity was analysed 48h after transfection with reporter plasmids. Assays were performed in triplicate and three independent experiments were performed. Statistical significance was determined by two-tailed, unpaired Student's t-test (* p<0.05). (B) Cellular lysates obtained in the assay were examined in SDS-PAGE and WB, with anti-syntenin-1 mAb and anti-FLAG pAb. Image presents a representative of three independent experiments. Densitometry analysis was performed on syntenin-1 immunoreactive bands. Optical densities (OD), standardized to β-actin, are shown for each lane.

3.2.2.2. Syntenin-1 regulates canonical Wnt signalling through its interaction with Fz7

Our results indicate that syntenin-1 regulates canonical Wnt signalling due to its direct interaction with Fz7. However, one can't exclude the possibility that syntenin-1 also interferes with canonical Wnt signalling downstream of the Fz7 receptor, or indirectly by affecting the activity of alternative pathways (see Introduction). To address this issue, we compared activation of the canonical Wnt pathway in syntenin-1-depleted cells either stimulated with Wnt3a, or treated with the GSK3 inhibitor (SB216763), which activates the β–catenin – dependent pathway downstream of the receptor. In control experiments, cells were treated with control siRNA. SKBr3-FLAG-Fz7 cells were transfected with siSyntenin-1 or siNeg and incubated with Wnt3a conditioned medium or control medium. In parallel, cells transfected with siRNA were treated with 10 μM GSK3i or equivalent amounts of DMSO. Wnt activation was quantified by TOP-Flash reporter assay 24h later; data is presented in Figure 3.16.A. Analysis of the reporter assay showed that syntenin-1 depletion only downregulates Wnt pathway when cells are stimulated with Wnt3a ligand and not with GSK3i. The level of syntenin-1 knock-down was assessed by analysing cell lysates obtained the assay by SDS-PAGE and WB with anti-syntenin-1 pAb (Figure 3.16.B), which confirmed that the protein expression level was more than 90% lower when compared with control samples. These results provide an additional evidence for syntenin-1 affecting canonical Wnt signalling upstream of GSK3.

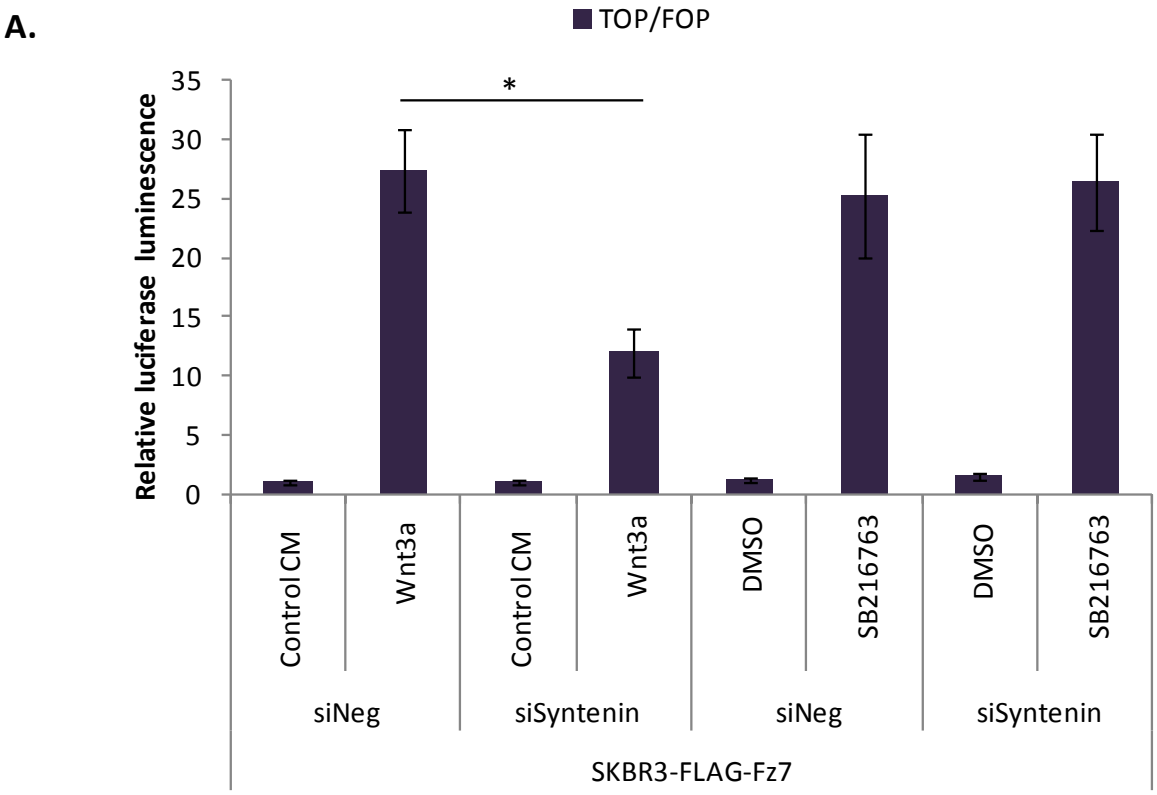
A.
TOP/FOP
Relative luciferase luminescence
35
30
25
20
15
10
5
0
*
Control CM
Wnt3a
Control CM
Wnt3a
DMSO
SB216763
DMSO
SB216763
siNeg
siSyntenin
siNeg
siSyntenin
SKBR3-FLAG-Fz7

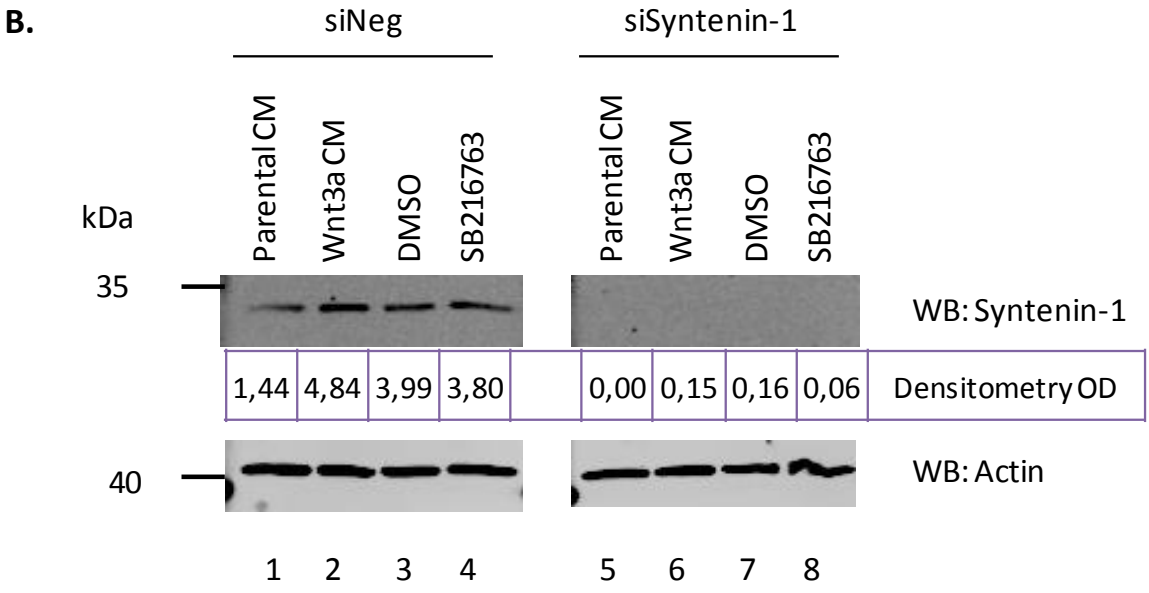
B.
siNeg
siSyntenin-1
Parental CM
Wnt3a CM
DMSO
SB216763
Parental CM
Wnt3a CM
DMSO
SB216763
kDa
35
WB: Syntenin-1
1,44
4,84
3,99
3,80
0,00
0,15
0,16
0,06
Densitometry OD
40
WB: Actin
1
2
3
4
5
6
7
8

Figure 3. 13. Syntenin-1 regulates canonical Wnt signalling due to its interaction with Fz7.

A) Wnt3a-induced signalling was analysed using TOP-Flash luciferase reporter assay. SKBr3-FLAG-Fz7 cells were transfected with siRNA against Syntenin-1 or control siNegative. Cells were stimulated for 24h with Wnt3a conditioned medium or with 10 μM GSK-3i (SB216763) and TOP/FOP activity was analysed 48h after transfection with reporter plasmids. Assays were performed in triplicate and three independent experiments were performed. Statistical significance was determined by two-tailed, unpaired Student's t-test (*p<0.05). (B) Cellular lysates obtained in the assay were examined in SDS-PAGE and WB, with anti-syntenin-1 mAb and anti-β-actin mAb. Image presents a representative of three independent experiments. Densitometry analysis was performed on syntenin-1 immunoreactive bands. Optical densities (OD), standardized to β-actin, are shown for each lane.

3.2.3. Syntenin-1 regulates Fz7 distribution in SKBr3 cells

SKBr3 cell lines stably expressing FLAG-Fz7 or FLAG-Fz7 V574G were used to determine whether syntenin-1 co-localizes with Fz7. Due to the lack of a suitable antibody to detect endogenous syntenin-1 by immunofluorescence staining, Myc-syntenin-1 was used for the co-localization studies. SKBr3, SKBr3-FLAG-Fz7 and SKBr3-FLAG-Fz7 V574G cells were transfected with Myc-syntenin-1 and, 48h later, fixed and stained with rabbit anti-FLAG and mouse anti-Myc antibodies. DAPI was used to visualize nuclei. Immunoreactivity for both proteins was analysed by confocal microscopy and presented in the Figure 3.12. Syntenin-1 has been found to be abundantly present in the cytoplasm of parental SKBr3 cells. Using a transient transfection approach in which only ~25% cells were transfected with a syntenin-1 – encoding plasmid allowed us to examine the effect of syntenin-1 overexpression on localization of Fz7. These experiments revealed that syntenin-1 overexpression changes Fz7 cell distribution. In both cell lines, SKBr3-FLAG-Fz7 and SKBr3-FLAG-Fz7 V574G, immunoreactivity for Fz7 was not observed in plasma membrane, in cells overexpressing syntenin-1. On the other hand, Fz7 immunoreactivity was detected in small puncta (presumably intracellular vesicles) in the cytoplasm. As expected, no reactivity with anti-Flag Ab was detected in SKBr3 control cells.

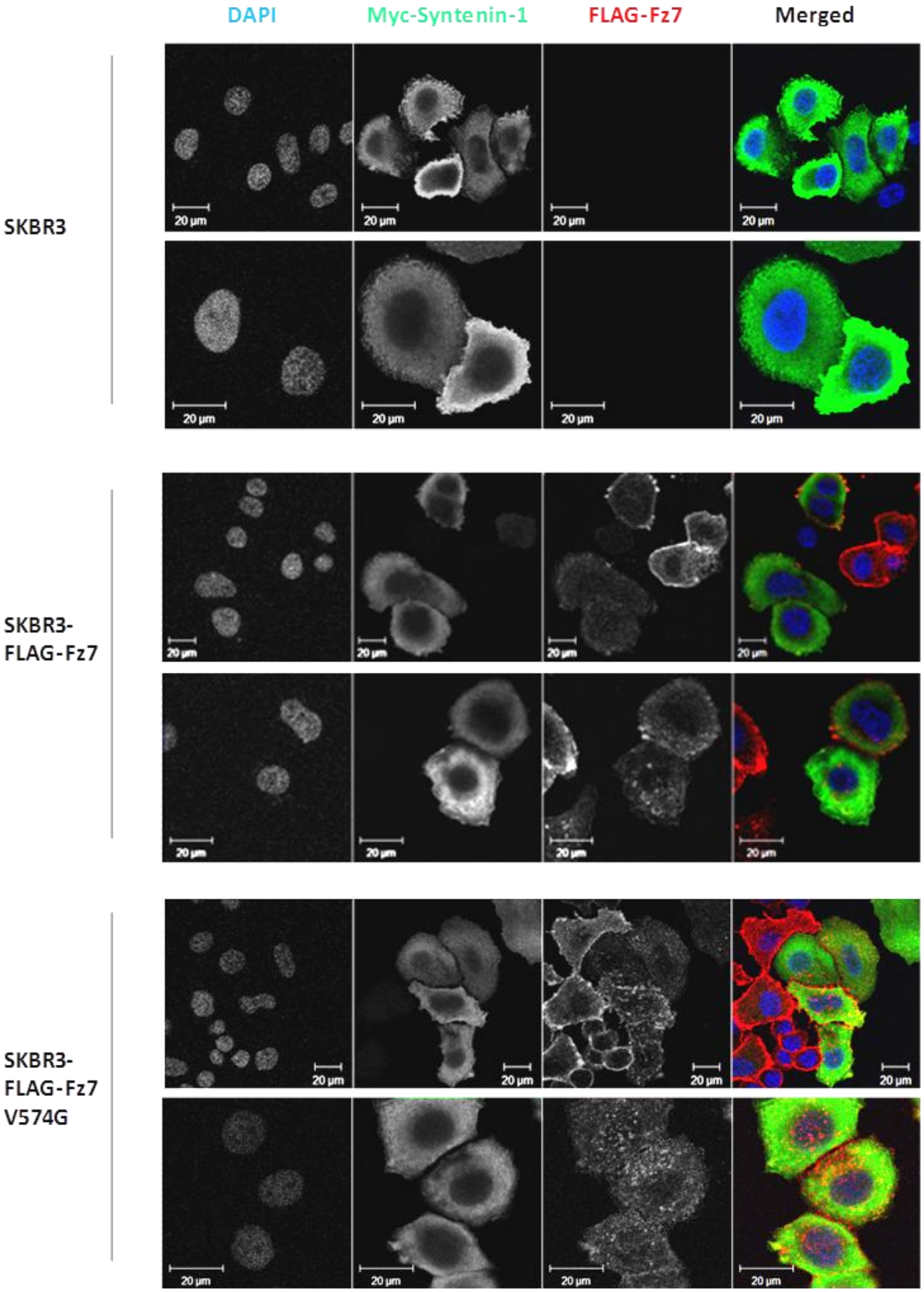
DAPI
Myc-Syntenin-1
FLAG-Fz7
Merged
SKBR3
SKBR3-
FLAG-Fz7
SKBR3-
FLAG-Fz7
V574G
20 μm

Figure 3. 14. Overexpression of syntenin-1 alters Fz7 cell distribution.

SKBr3, SKBr3-FLAG-Fz7 WT and SKBr3-FLAG-Fz7 V574G cells were transfected with Myc-Syntenin-1 and proteins distribution was analysed by confocal imaging. Cells were fixed 48h after transfection and stained with rabbit anti-FLAG pAb and with mouse anti-Myc mAb. DAPI was used to visualize nuclei. Overexpression of syntenin-1 resulted in redistribution of both, Fz7 WT and Fz7 V574G from plasma membrane to cytoplasmic vesicles.

Considering the fact that mutations introduced in PDZ domains of syntenin-1 attenuate its interaction with Fz7 (as shown the previous section), we wished to investigate whether the activity of syntenin-1 towards Fz7 is dependent on its PDZ domains. For this purpose SKBr3-FLAG-Fz7 cells were transfected with different HA-tagged syntenin-1 constructs. 48h after the transfection, SKBR3-FLAG-Fz7 cells were fixed and stained with mouse anti-HA mAb to detect syntenin-1 and rabbit anti-FLAG pAb to detect Fz7. Immunoreactivities for both proteins were analysed by confocal microscopy and representative images are presented in Figure 3.13. When HA-syntenin-1 WT was overexpressed, Fz7 staining was not observed in the plasma membrane, but in vesicles in a cytoplasm, similarly as previously observed in cells transfected with Myc-Syntenin-1. However, when cells were transfected with HA-syntenin-1 PDZ1*, HA-syntenin-1 PDZ2* or HA-syntenin-1 PDZ1*PDZ2*, Fz7 receptor remained in the plasma membrane, where it co-localized with the mutants of syntenin-1.

Taken together, overexpression of wild type syntenin-1 leads to relocalisation of Fz7 from plasma membrane in SKbr3 cells and this activity of syntenin is dependent on PDZ domains of the protein.

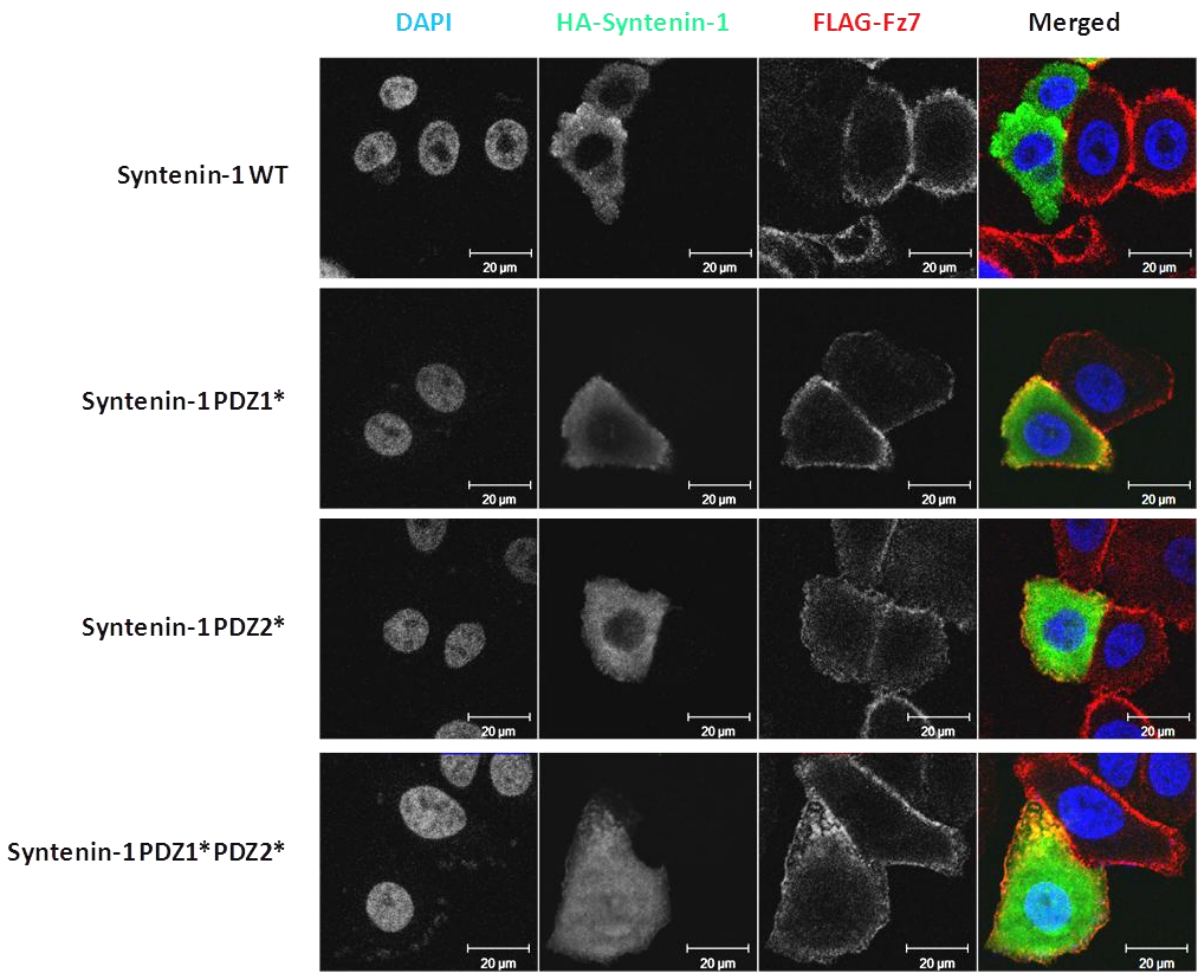

Figure 3.15. Fz7 co-localizes with syntenin-1 with mutations introduced in PDZ domains .

SKBr3, SKBr3-FLAG-Fz7 WT and SKBr3-FLAG-Fz7 V574G cells were co-transfected with FLAG-Fz7 and HA-syntenin-1 (WT or with introduced mutation in PDZ1*, PDZ2* or both PDZ1*PDZ2*) and proteins distribution was analysed by confocal imaging. Cells were fixed 48h after transfection and stained with rabbit anti-FLAG pAb and with mouse anti-HA mAb. DAPI was used to visualize nuclei. Overexpression of wild type syntenin-1 led to removal of Fz7 from plasma membrane. All three syntenin-1 PDZ mutants co-localize with Fz7.

3.2.4. Syntenin-1 is not involved in the regulation of Fz7 expression

Syntenin-1 overexpression induces changes in Fz7 distribution in SKBr3 cells (Section 3.2.2.). In the reverse experiments we analysed whether depletion of syntenin-1 would also influence the cellular distribution of Fz7. SKBr3-FLAG-Fz7 and SKBr3-FLAG-Fz7 V574G cells were transfected with siRNA targeting syntenin-1 (or with control siRNA) and 24h later cells were stimulated with Wnt3a conditioned medium or with control conditioned medium. Cells were collected after further 24h and expression levels and distribution were analysed by WB, flow cytometry and immunofluorescence. Densitometry analysis confirmed syntenin-1 expression level was 90% lower in cells transfected with siSyntenin-1, than in the control cells. The analysis of Fz7 expression in whole cell lysates (using anti-FLAG pAb), revealed no significant changes in total expression level of both, Fz7 WT and Fz7 V574G (Figure 3.14.A). In parallel, flow cytometry analysis was conducted to assess the surface expression of Fz7 in collected cells, using anti-FLAG mAb. Fz7 wild type or Fz7 V574G mutant cell surface expression was not altered in cells with syntenin-1 knock-down (Figure 3.14.B). Finally, cell localization of Fz7 was examined by immunofluorescence. We noticed that syntenin-1 depletion changed morphology of SKBr3 cells, as they became more flattened. Nonetheless, no obvious alterations were observed in the receptor distribution in cells with syntenin-1 knock-down.

Taken together, the analysis of total and membrane expression of Fz7 and cell distribution by western blot, flow cytometry and immunofluorescence didn't provide evidence that syntenin-1 knock-down influences Fz7 expression in SKBr3 cells.

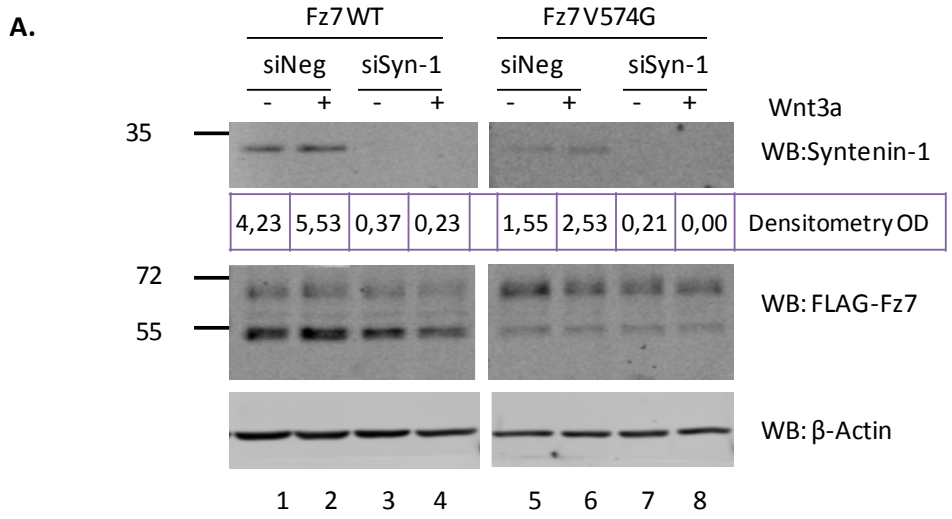
A.
Fz7 WT
Fz7 V574G
siNeg
siSyn-1
siNeg
siSyn-1
- + - + - + - +
Wnt3a
35
WB:Syntenin-1
4,23 5,53 0,37 0,23 1,55 2,53 0,21 0,00 Densitometry OD
72
55
WB: FLAG-Fz7
WB: β-Actin
1 2 3 4 5 6 7 8

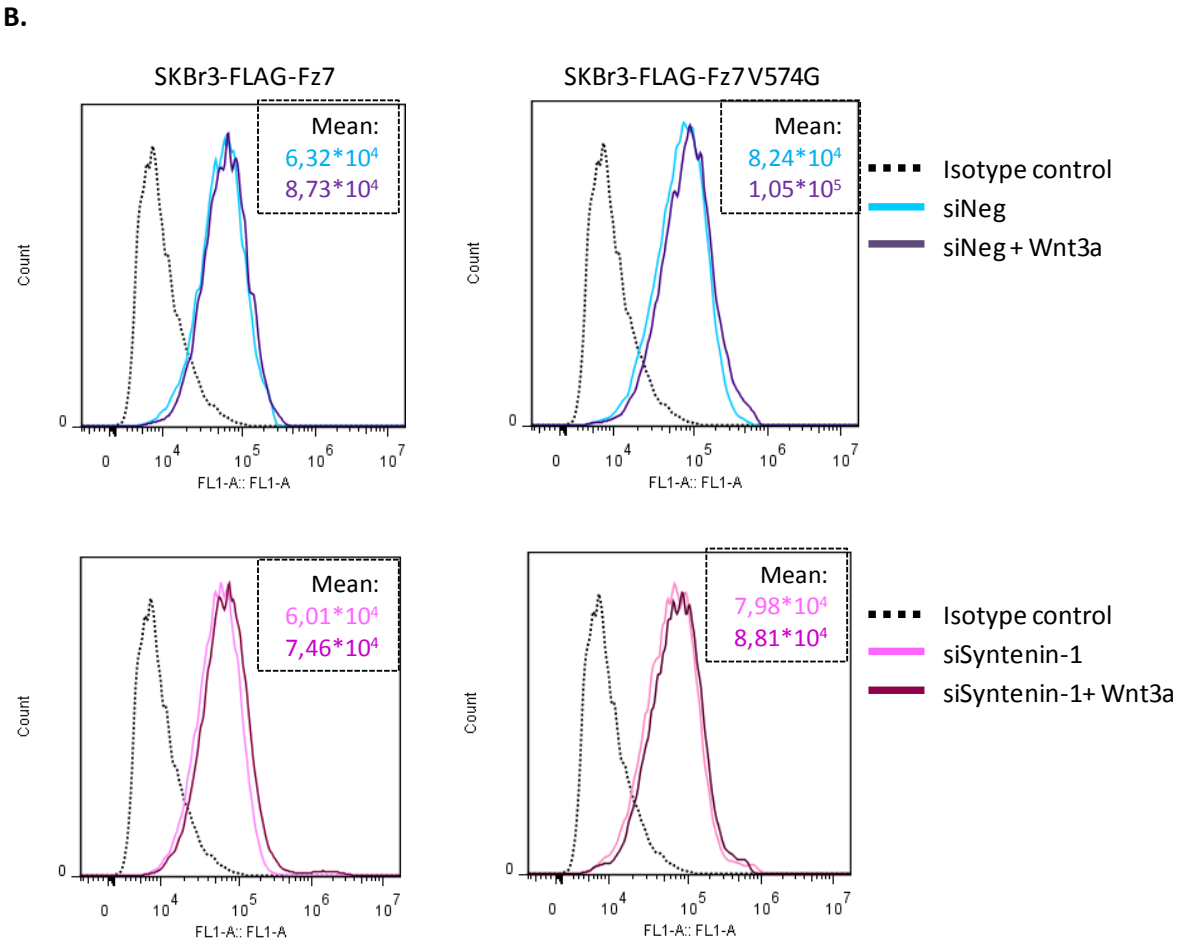
B.
SKBr3-FLAG-Fz7
SKBr3-FLAG-Fz7 V574G
Mean:
6,32*10⁴
8,73*10⁴
Mean:
8,24*10⁴
1,05*10⁵
Isotype control
siNeg
siNeg + Wnt3a
Mean:
6,01*10⁴
7,46*10⁴
Mean:
7,98*10⁴
8,81*10⁴
Isotype control
siSyntenin-1
siSyntenin-1+ Wnt3a
Count
FL1-A:: FL1-A

C.

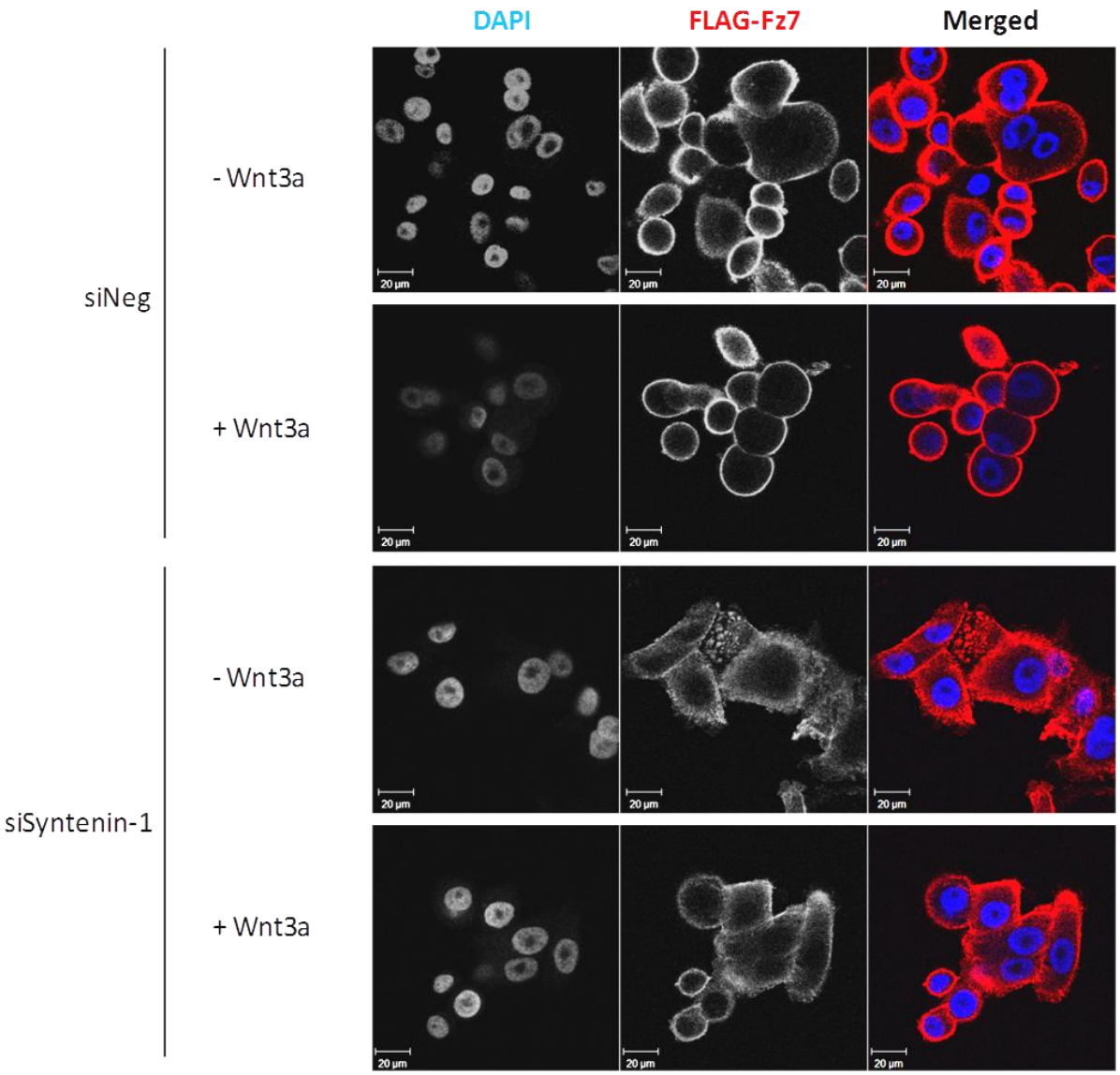
DAPI
FLAG-Fz7
Merged
siNeg
- Wnt3a
+ Wnt3a
siSyntenin-1
- Wnt3a
+ Wnt3a
20 µm

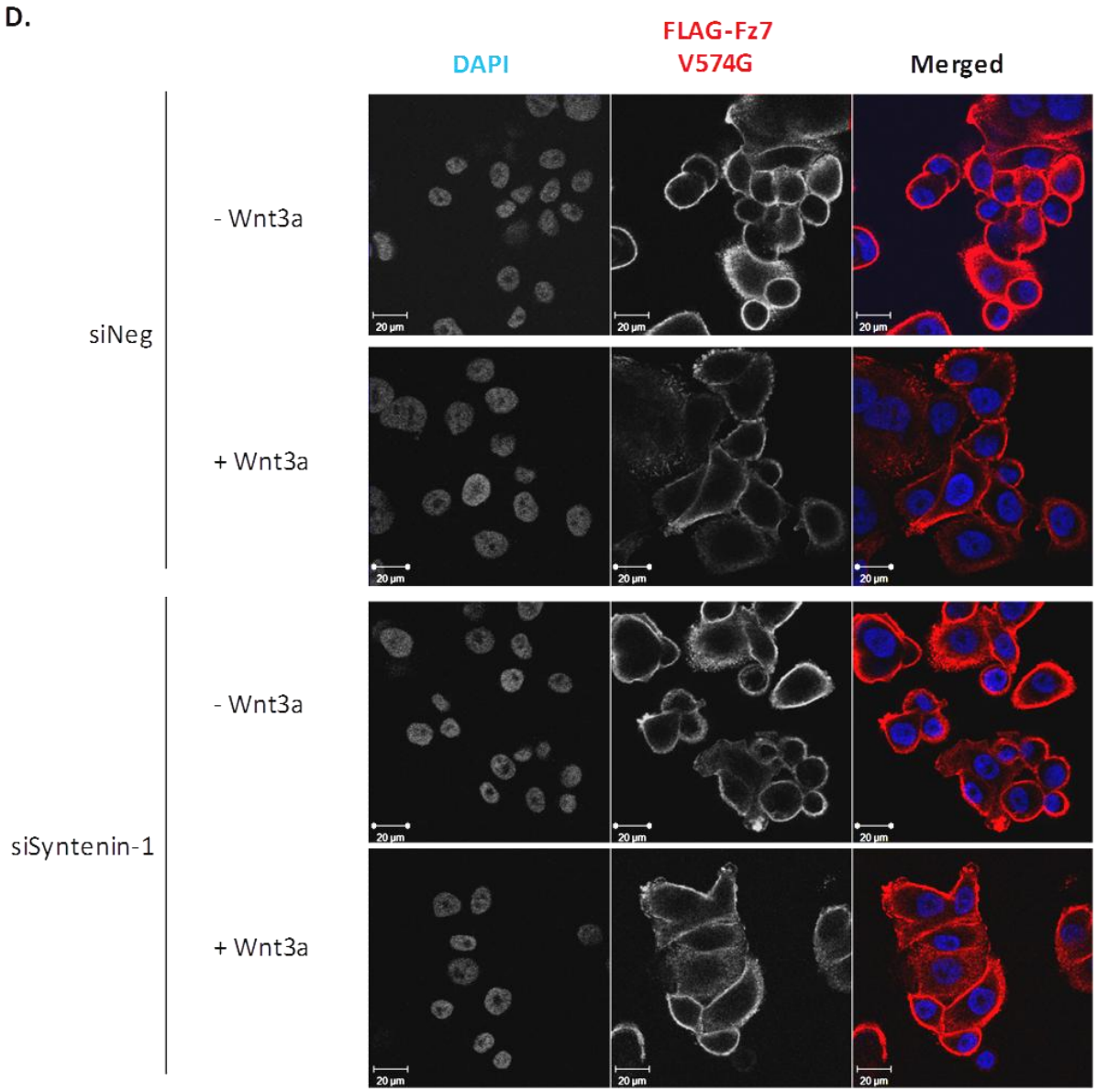
D.
DAPI
FLAG-Fz7
V574G
Merged
siNeg
- Wnt3a
+ Wnt3a
siSyntenin-1
- Wnt3a
+ Wnt3a
20 µm

Figure 3. 16. Syntenin-1 depletion does not change Fz7 membrane expression or cell distribution.

SKBr3-FLAG-Fz7 and SKBr3-FLAG-Fz7 V574G cells were transfected with siRNA against Syntenin-1 or with control siNeg. 24h later cells were stimulated with Wnt3a conditioned medium or with control conditioned medium. 48h after the transfection cell lysates were collected and analysed by SDS-PAGE and WB, flow cytometry and immunofluorescence. (A) Lysates of equal protein concentration were resolved by SDS-PAGE, followed by western blotting with Anti-FLAG pAb to examined Fz7 expression level, anti-Syntenin-1 mAb to monitor LNX2 knock-down level. β-actin served as a loading control. (B) Flow cytometry with anti-FLAG mAb was used to examine membrane expression of Fz7. Cells were incubated on ice for 1h with mouse anti-FLAG (M2) mAb. 4C5G monoclonal antibody against phosphatidylinositol 4-kinase was used as an isotype control. Cell surface staining of FLAG-Fz7 (WT or V574G) was detected by flow cytometry following incubation for 1h on ice with anti-mouse FITC-conjugated secondary antibodies. Data analysis was carried out using FlowJo analysis software. The values of calculated mean fluorescence are presented in top-right corner of the plots. (C-D) Fz7 WT (C) and V574G (D) cell distribution was analysed by confocal imaging. Cells were fixed and stained with mouse anti-FLAG (M2) mAb and Alexa Fluor 488-conjugated goat-anti mouse ab (green). DAPI was used to visualize nuclei.

3.2.5. Discussion

We have found in the proceeding chapter that the canonical Wnt signalling is regulated by Fz7 interactions through its C-terminal PDZ-BM. Additionally, Fz7 expression and cell distribution also seem to be dependent on the receptor associations with PDZ proteins. To examine this issue further, we have initially decided to focus on the interaction between Fz7 and syntenin-1. Syntenin-1 is a scaffold protein with a tandem of PDZ domains, previously shown to bind Fz7 (Luyten et al. 2008). The protein was reported to regulate trafficking of several membrane receptors, such as syndecans, syndecan associated receptors e.g. FGF, or tetraspanin CD63 (Beekman et al. 2008) (see Introduction). For these reasons, we have decided to determine whether syntenin-1 regulates Fz7 functions, as well as canonical Wnt signalling in breast cancer cells.

Our experiments confirmed that syntenin-1 binds to Fz7 in our breast cancer model. Furthermore, as expected, mutations in both PDZ-BM of Fz7 and PDZ domains in syntenin-1, significantly decreased the interaction between the two proteins. These results clearly demonstrate the importance of PDZ domains in Fz7 – syntenin-1 interactions. However, the fact that none of the mutations analysed completely abolish the association might indicate a possible contribution of the other part(s) of Fz7 (and syntenin-1) in stabilization of the complex. If proved in future experiments this would be reminiscent of a model of Frizzled-Dishevelled interactions, which was recently presented by Tauriello and colleagues. Specifically, it was demonstrated that this interaction involves a three-segmented discontinuous binding surface, comprising of the internal PDZ-BM and two additional motifs in intracellular loops of the Frizzled receptor (Tauriello et al. 2012). Alternatively, one

can not exclude a possibility that a small proportion of syntenin-1 is recruited to the Fz7 complex indirectly via a network of PDZ-independent interactions.

Our results demonstrated that PDZ2 plays a predominant role in recruiting syntenin-1 to Fz7. Nevertheless, we have shown that the mutation in PDZ1 also decreased the interaction of syntenin-1 with Fz7. Luyten and colleagues (2008) reported that syntenin-1 interaction with Fz7 relies on PDZ1. In their study recombinant GST-PDZ domains of syntenin-1 were used in different type of test (overlay assay), which might explain differences between our findings and (Luyten et al. 2008). The authors showed single GST-PDZ1, but not GST-PDZ2, was sufficient to bind to Fz7 peptide. Interestingly, tandem GST-PDZ2-PDZ2 displayed strong interaction with Fz7. Most protein ligands of syntenin-1 show preference for PDZ2 (for example syndecans and ephrinB), whereas PDZ1 binds with higher affinity to IL-5Rα (interleukin-5 receptor α), neurexin, merlin and CD63 (Beekman et al. 2008). Previous reports have also shown that despite preference for one of the PDZ domain, both of them are required for the interaction of syntenin-1 with different transmembrane proteins (Sarkar et al. 2004).

Syntenin-1 was reported to be involved in the regulation of non-canonical Wnt signalling by controlling activation of the PKC/CDC42 pathway (Luyten et al. 2008). This study also suggested that syntenin-1 does not contribute to the canonical Wnt pathway. By contrast, our results clearly indicate that depletion of syntenin-1 in breast cancer cells attenuated β-catenin – dependent signalling as tested in the TOPFlash reporter assay. We based our conclusion on two lines of evidence. Firstly, observed decrease of TOP-Flash signal following syntenin-1 depletion occurs only in SKBr3 cells expressing Fz7 WT, and not in cells expressing the Fz7 mutant with reduced capability to bind to syntenin-1 (Figure 3.12).

Secondly, analysis of the canonical Wnt pathway activation after treatment with an inhibitor of GSK3 (Figure 3.13) leads to a conclusion that syntenin-1 regulates Wnt signalling upstream of GSK3 kinase, presumably on Wnt receptor level. One possible explanation for the discrepancy between our results and conclusions from the previous study is that different cell models were used. Conclusions by Luyten and colleagues were based on the experiments performed using MCF7 cells, wherein overexpression of syntenin-1 didn't have any significant effects on β-catenin – dependent signalling (TOP-Flash experiments). However, we and others (Wheeler et al. 2011) have shown that canonical Wnt pathway is not functional in this cell line, due to inhibitory effect of NHERF overexpression.

Further research is required to elucidated the exact mechanism in which syntenin-1 regulates canonical Wnt signalling. However, syntenin-1 was shown to bind syndecans, ubiquitous transmembrane heparan sulphate proteoglycans. The heparan sulphate chains of their extracellular domain allow syndecans to act as co-receptors, as they bind and concentrate growth factors, including Wnts, at the cell surface and facilitate their interactions with receptors (Bishop et al. 2007;Couchman 2003). It was proposed previously in (Luyten et al. 2008) that syntenin-1 serves as a scaffold for Fz7-syndecan-4 complex and therefore regulate noncanonical Wnt signalling, due to the ability of syndecan-4 to bind and activate PKCα. In this regard, syndecan-1 was recently described as a regulator of β-catenin dependent Wnt signalling in triple negative subtype of breast cancer. The authors showed that syndecan-1 depletion correlates with downregulation of LRP6 and reduced responsiveness to Wnt signalling (Ibrahim et al. 2013). Another possible mechanism may involve syntenin-1 interaction with another binding partner, such as merlin (neurofibromatosis 2, NF2). Merlin acts a membrane stabilizing protein and was shown to

bind and colocalize with syntenin-1 at the plasma membrane (Jannatipour et al. 2001). Merlin was found to interact with proteins forming adherens junctions (AJs): cadherins and catenins (Lallemand et al. 2003), with which syntenin-1 was also reported to colocalize (Zimmermann et al. 2001). Recently, it was shown merlin knockout leads to increased canonical Wnt signalling in mouse embryonic fibroblasts (Zhou et al. 2011). Thus, interaction between these two proteins might also be important for regulation of Wnt signalling.

Our results indicate that syntenin-1 may be involved in regulation of receptor trafficking. Specifically. syntenin-1 overexpression in both SKBr3-FLAG-Fz7 and SKBr3-FLAG-Fz7 V574G resulted in redistribution of the receptor from the plasma membrane to small puncta, supposedly cytoplasmic vesicles (Figure 3.14.). Importantly, all three PDZ mutants of syntenin-1 (PDZ1*, PDZ2* and PDZ1*PDZ2*) were deficient towards Fz7. These results seem to indicate that syntenin-1 interaction through PDZ domains regulates subcellular localization of Fz7. Surprisingly, we found that Fz7 V574G mutant was also redistributed from plasma membrane upon overexpression of the wild type syntenin-1. It seems that the effect of syntenin-1 on Fz7 distribution is likely to be indirect and involves another protein (or proteins) whose interaction with syntenin-1 requires PDZ domain. Syntenin-1 is known to regulate trafficking of a number transmembrane receptors (Beekman et al. 2008). It has been also reported that complex syndecan-syntenin-1-ALIX is able to recruit syndecan associated proteins to the intraluminal vesicles of multivesicular endosomes and exosomes (Baietti et al. 2012). Since syndecan-1 was also implicated in Wnt signalling (Ibrahim et al. 2013), it is possible that syndecan-1-syntenin-1-ALIX complex recognize Fz7 as a cargo and traps it in the intraluminal vesicles.

Finally, we have examined whether syntenin-1 depletion alters Fz7 expression. SKBr3-FLAG-Fz7 WT and SKBr3-FLAG-Fz7 V574G cells were transfected with siRNA against syntenin-1 and stimulated with Wnt3a. Subsequently total and membrane expression, as well as cellular localization of Fz7 was assessed. Analysis by western blot, flow cytometry and immunofluorescence did not provide evidence that syntenin-1 knock-down affects Fz7 WT or Fz7 V574G expression (Figure 3.16).

Taken together, syntenin-1 is a scaffold protein binding Fz7 in PDZ dependent manner. For the first time, we have determined that the interaction between the two proteins plays a role in regulation of the canonical Wnt signalling in breast cancer cells. We have also shown that syntenin-1 regulates trafficking and cell localization of Fz7 receptor.

3.3. Fz7 interacts with PDZ domain containing proteins

Cytoplasmic tails of all Frizzled receptors contain Postsynaptic density-95, Disc large, ZO-1 (PDZ) binding motifs (PDZ-BMs). The C-terminal PDZ-BM (x-S/T-x-φ, where φ represents a hydrophobic residue) was reported to bind different PDZ proteins including GOPC, MAGI-3, Syntenin-1, Kermit, PSD-95 (Wawrzak et al. 2009) (discussed in the Introduction). Whilst some of these proteins were implicated in noncanonical Wnt pathways, their roles in transduction of canonical Wnt signalling haven't been widely addressed in the past. The aim of work described in this chapter was to identify PDZ proteins that interact with Fz7 in breast cancer cells, and thus to help elucidate the mechanism by which the C-terminal PDZ-BM of Fz7 works.

3.3.1. Pull-down of Fz7 binding partners and their identification by Mass-Spectrometry

In order to find binding partners of Fz7 that interact with WT but not with V574G, a pull-down assay was performed, described in details in section 2.4.6. of Materials and Methods. Schematic representation of designed experiments is presented in the Figure 3.17.A. Cellular lysates of epithelial breast cancer cell line MCF7 were incubated either with biotin-conjugated Fz7 WT or with Fz7 V574G peptide immobilized on agarose resins (Figure 3.17.B). For the control sample, NeutrAvidin agarose resins without peptide were used. Retained proteins were resolved on SDS-PAGE gel and stained with InstantBlue. Marked

differences were observed, when "WT" and "V574G" pull-down samples were compared (Figure 3.17.B), indicating that the C-terminal PDZ binding motif of Fz7 is essential for interactions with a number of cellular proteins. Proteins specifically pulled down by WT peptide (marked by red arrows in the Figure 3.17.B) were digested with trypsin and analyzed by mass spectrometry. Details of samples preparation are described in section 2.4.7. Protein sequencing was performed by Dr Douglas Ward using liquid chromatography and mass spectrometry (LS-MS) at the Proteomics Facility of University of Birmingham. Analysis revealed several PDZ domain-containing proteins that could be Fz7 binding partners. Identified proteins are listed in the Table 3.1. Among the identified candidates were proteins involved in receptor trafficking (DLG1, SNX27, LNX1, LNX2, MAGI3, Scribble) and establishment of cell polarity and tight junction formation (MPP5, MPP7, ZO-2, MAGI3, INADL, Scribble).

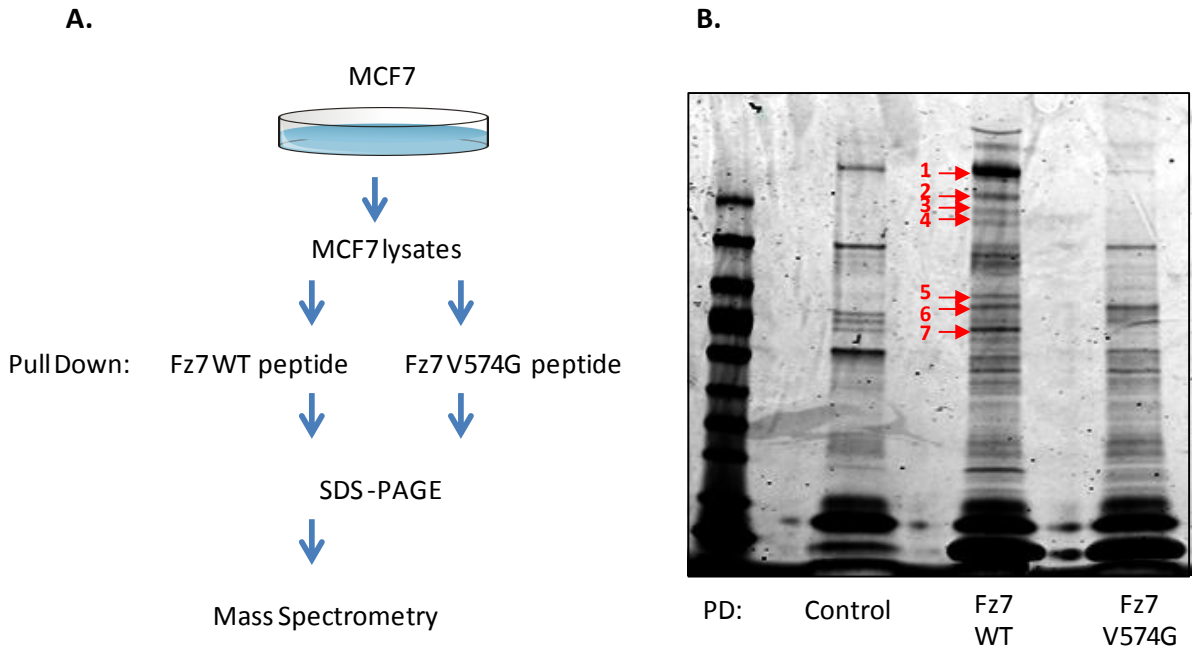

Figure 3. 17. Pull down of PDZ domain containing binding partners of Fz7.

(A) MCF7 cells were lysed in 1% Triton X-100. The lysates were firstly precleared with NeutrAvidin agarose resins and then incubated with NeutrAvidin agarose resins with immobilized biotinylated peptides: Fz7 WT or V574G. For the control sample, NeutrAvidin agarose resin without peptide was used. After the pull-downs the beads were washed and resuspended in 2x SDS sample-loading buffer. (B) Samples were subjected to SDS-PAGE and stained with the Coomassie dye. The protein bands that were visible in Fz7 WT pull-down lanes, but not in Fz7 V574G pull-down lane or beads alone pull-down control lane, (marked by red arrows) were excised, processed and analysed by mass spectrometry

Table 3. 1. Mass spectrometry results showing potential Fz7-binding proteins.

The table indicates the gene symbol, name, molecular weight and number of detected peptides obtained from the digested gel fragments (samples) labelled in the Fig. 3.17.

Accession	Protein	MW (kDa)	Peptides	Sample
	PDZ PROTEINS:			
SCRIB	Protein scribble homolog	174.8	62	1,2,3,4,5,6,7
INADL	InaD-like protein	196.2	37	1,2,3
MPP5	MAGUK p55 subfamily member 5	77.2	36	5,6,7
MAGI3	Membrane-associated guanylate kinase, WW and PDZ domain-containing protein 3	165.5	35	2,3,4
MPP7	MAGUK p55 subfamily member 7	65.5	27	5,6,7
MAGI1	Membrane-associated guanylate kinase, WW and PDZ domain-containing protein 1	164.5	27	2,3,4
DLG1	Disks large homolog 1	100.4	11	5,6,7
SNX27	Sorting nexin-27	61.2	11	5,6,7
ZO-2	Tight junction protein ZO-2	133.9	7	4
LNX2	Ligand of Numb protein X 2	76.0	6	5,6
MPDZ	Multiple PDZ domain protein	218.5	6	2
LNX1	E3 ubiquitin-protein ligase LNX	80.6	5	5
CSKP	Peripheral plasma membrane protein CASK	105.1	4	5,6,7
ZO-1	Tight junction protein ZO-1	193.3	1	1
	OTHER MISCALLENOUS HITS:			
PLOD3	Procollagen-lysine,2-oxoglutarate 5-dioxygenase 3	84.7	22	5,6
PLOD1	Procollagen-lysine,2-oxoglutarate 5-dioxygenase 1	83.5	18	5,6,7
MYH9	Myosin-9	226.4	18	1,2,3,4,5,6,7
MCCA	Methylcrotonoyl-CoA carboxylase subunit alpha, mitochondrial	80.4	11	6
DDX5	Probable ATP-dependent RNA helicase DDX5	69.1	10	7
TP4A3	Protein tyrosine phosphatase type IVA 3	19.5	9	1,2,3,4,5,6,7
DTNB	Dystrobrevin beta	71.3	6	7
KU70	ATP-dependent DNA helicase 2 subunit 1	69.8	6	7
DDX17	Probable ATP-dependent RNA helicase DDX17	72.3	5	7
HNRPQ	Heterogeneous nuclear ribonucleoprotein Q	69.6	5	7
DTNA	Dystrobrevin alpha OS=Homo sapiens	83.8	4	6
PYC	Pyruvate carboxylase, mitochondrial	129.6	4	5,7
KU86	ATP-dependent DNA helicase 2 subunit 2	82.7	4	5

3.3.2. Mutation in the C-terminal PDZ binding motif of Fz7 affects binding of PDZ domain containing proteins

In order to verify data obtained in mass spectrometry and check whether replacement of C-terminal valine (Val574) with glycine can disrupt Fz7 binding to identified proteins, a series of pull-down experiments was conducted. MCF7 cells were transiently transfected with plasmids encoding PDZ domain containing proteins identified in the section 3.2.1. (Scribble, INADL, MAGI3, MAGI1, DLG1, LNX2, MPP7, SNX27 and MPP5). In additional experiments we also examined the interaction of Fz7 peptides with PDZ proteins that have been previously reported to bind Fz7 (syntenin-1, GIPC1, NHERF, GOBC, and PSD95) (Wawrzak et al. 2009). The interaction with syntenin-1 was examined using endogenous protein. Lysates of MCF7 cells expressing PDZ domain-containing proteins were incubated with NeutrAvidin beads conjugated with biotinylated Fz7 peptides (Fz7 WT or Fz7 V574G). As a control for unspecific binding of proteins to the beads lysates were incubated with NeutrAvidin beads without conjugated peptide.

Pull-down assays showed that all of the tested proteins can be pulled down with Fz7 WT peptide (lane 7) and that most of them did not bind to Fz7 V574G peptide (lane 8) (Figure 3.18.A). However five of the PDZ proteins (syntenin-1, SNX27, MPP5, GOPC and PSD95) partially retained the ability to bind Fz7 V574G peptide (lane 8), albeit their binding capacities were markedly diminished (lane 7, Figure 3.18.B).

Taken together, these results revealed that the Val to Gly mutation at the C-terminus of Fz7 (V574G) affects the ability of the receptor for PDZ-mediated binding to all identified

PDZ domain-containing partners. Nonetheless, it should be noted that several proteins posses the ability to bind to Fz7 V574G, however with lower capacity than to Fz7 WT. In the next chapters, interactions between Fz7 and selected proteins of both types will be further investigated.

A.

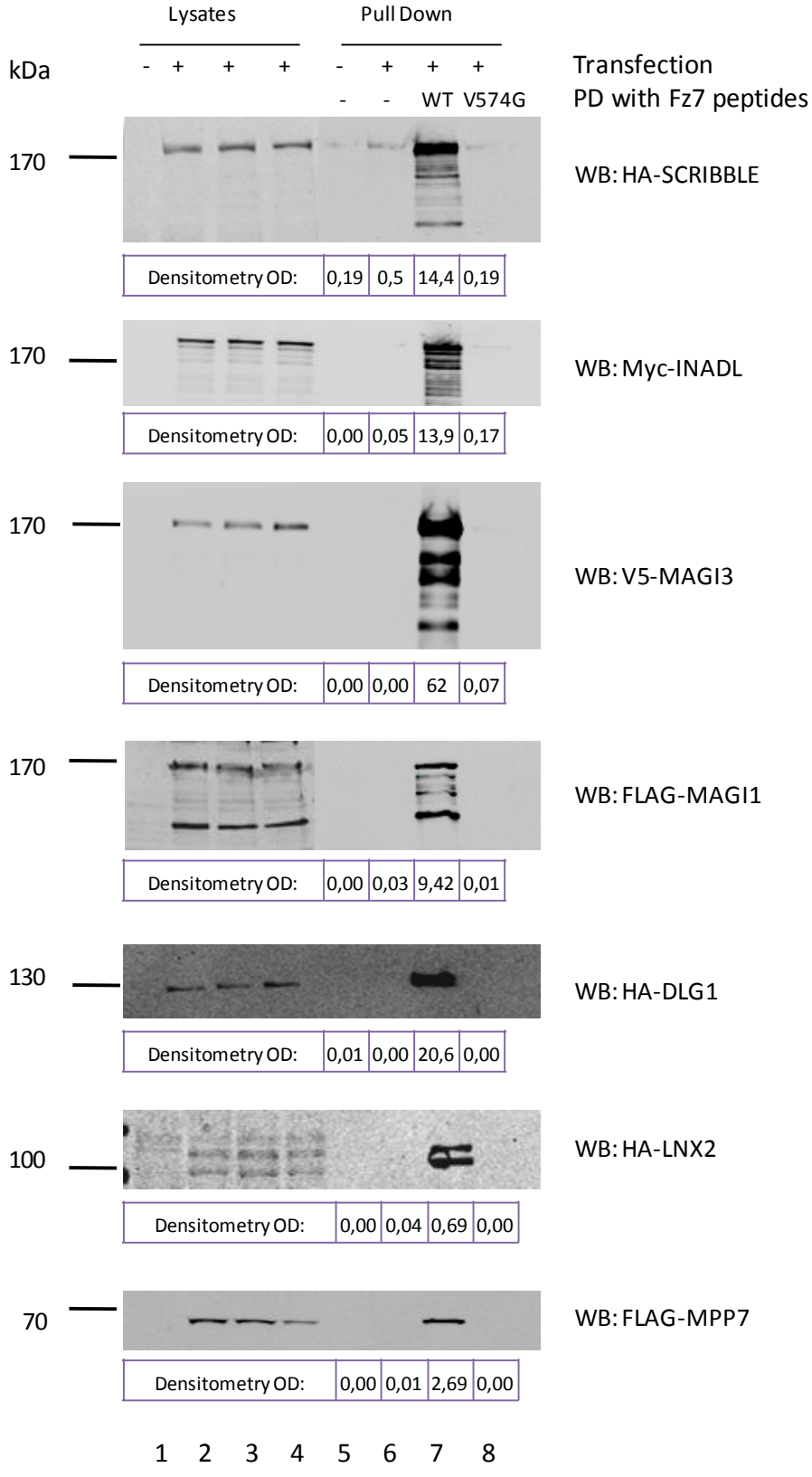
Lysates
Pull Down
kDa
- + + + - + + +
- - WT V574G
Transfection
PD with Fz7 peptides
170
WB: HA-SCRIBBLE
Densitometry OD: 0,19 0,5 14,4 0,19
170
WB: Myc-INADL
Densitometry OD: 0,00 0,05 13,9 0,17
170
WB: V5-MAGI3
Densitometry OD: 0,00 0,00 62 0,07
170
WB: FLAG-MAGI1
Densitometry OD: 0,00 0,03 9,42 0,01
130
WB: HA-DLG1
Densitometry OD: 0,01 0,00 20,6 0,00
100
WB: HA-LNX2
Densitometry OD: 0,00 0,04 0,69 0,00
70
WB: FLAG-MPP7
Densitometry OD: 0,00 0,01 2,69 0,00
1 2 3 4 5 6 7 8

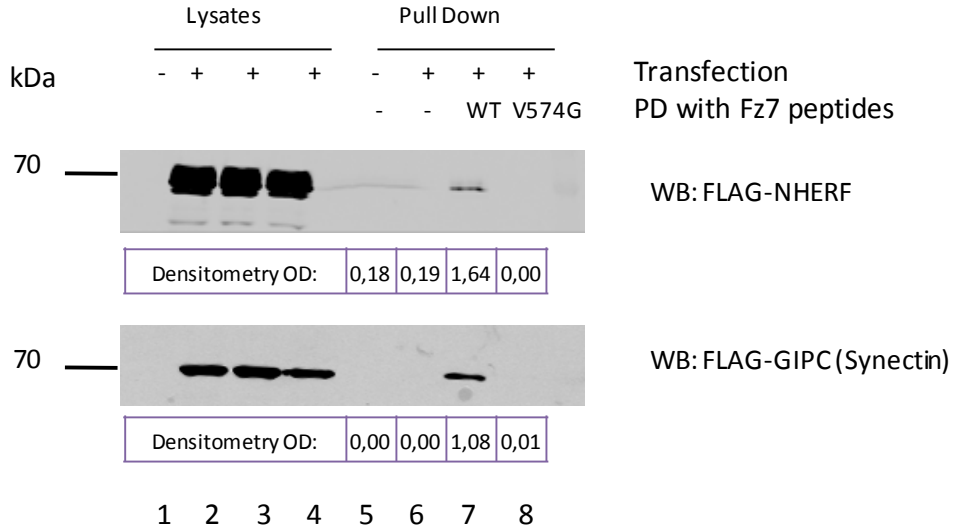
Lysates
Pull Down
kDa
- + + + - + + +
- - WT V574G
Transfection
PD with Fz7 peptides
70
WB: FLAG-NHERF
Densitometry OD: 0,18 0,19 1,64 0,00
70
WB: FLAG-GIPC (Synectin)
Densitometry OD: 0,00 0,00 1,08 0,01
1 2 3 4 5 6 7 8

B.

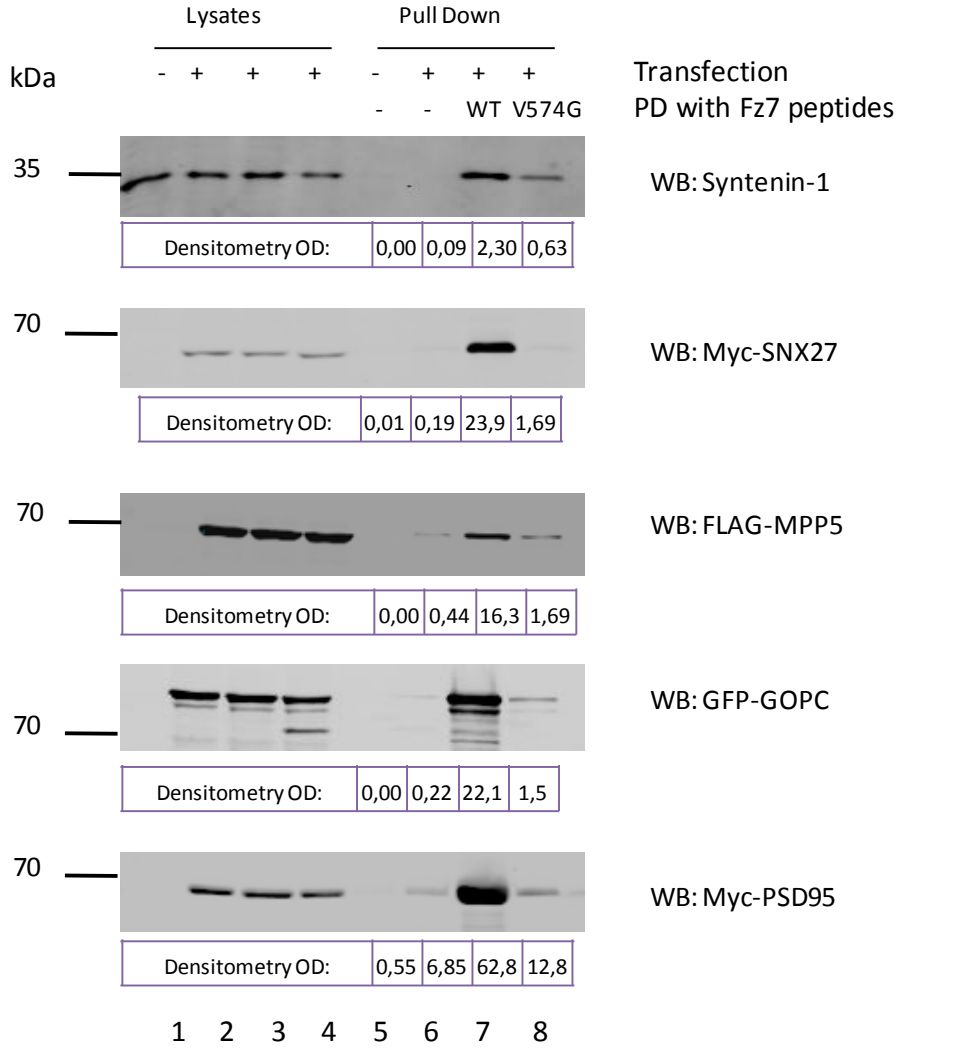
Lysates
Pull Down
kDa
- + + + - + + +
- - WT V574G
Transfection
PD with Fz7 peptides
35
WB: Syntenin-1
Densitometry OD: 0,00 0,09 2,30 0,63
70
WB: Myc-SNX27
Densitometry OD: 0,01 0,19 23,9 1,69
70
WB: FLAG-MPP5
Densitometry OD: 0,00 0,44 16,3 1,69
70
WB: GFP-GOPC
Densitometry OD: 0,00 0,22 22,1 1,5
70
WB: Myc-PSD95
Densitometry OD: 0,55 6,85 62,8 12,8
1 2 3 4 5 6 7 8

Figure 3. 18. Western blot confirming pull down of PDZ domain-containing proteins with Fz7 WT or V574G peptide.

Interaction of Fz7 PDZ domain containing partners with Fz7 WT and Fz7 V574G peptides was assessed by pull down assay. The interaction with Scribble, INADL, MAGI3, MAGI1, DLG1, LNX2, MPP7, NHERF, GIBC1, SNX27, GOPC, MPP5 and PSD95 was analysed using cells transfected to express epitope-tagged proteins. The interaction with syntenin-1 was examined using antibodies recognizing an endogenous protein. MCF7 cells were lysed with 1% Triton X-100 48h after transfection. Lysates were precleared and incubated with NeutrAvidin agarose resins with immobilized biotinylated peptides. For the control sample, NeutrAvidin agarose resin without peptide was used. After the pull-downs retained proteins were resolved by SDS-PAGE, followed by western blotting. Proteins were detected with epitope-specific antibodies (rabbit anti-HA pAb; rabbit anti-Myc pAb; rabbit anti-V5 pAb; rabbit anti-FLAG pAb; rabbit anti-GFP pAb) and with rabbit anti-Syntenin-1 mAb. Densitometry analysis was performed on pull down blots and optical densities (OD) are shown for each lane. (A) Scribble, INADL, MAGI3, MAGI1, DLG1, LNX2, MPP7, NHERF and GIPC1 interact with the wild type, but not mutant Fz7 peptide. (B) Syntenin-1, SNX27, GOPC, MPP5 and PSD95 interact with Fz7 WT peptide and are able to retain partial binding to Fz7 V574G peptide.

GOPC – Golgi-associated PDZ and coiled-coil motif-containing protein; GIPC1 - PDZ domain-containing protein GIPC1 ; NHERF – Na(+)/H(+) exchange regulatory cofactor; PSD95– Postsynaptic density protein 95;

3.3.3. Further investigation of Fz7 interaction with LNX1 and LNX2 proteins

3.3.3.1. Fz7 interaction with proteins from LNX family involves PDZ domains

In the mass spectroscopy analysis two members of the LNX family were identified: LNX1 and LNX2, as potential binding partners of Fz7. These two proteins share an identical domain structure (RING domain and four PDZ domains), but LNX1 has two isoforms, full length p80 and p70, which lacks the RING domain (Wolting et al. 2011). To verify whether different isoforms of LNX can bind to Fz7, a pull-down assay with Fz7 WT and Fz7 V574G peptides was employed. HEK293T cells were transfected with GFP-LNX1 p80, GFP-LNX1 p70 and GFP-LNX2. Non-transfected cells were used to examine binding of endogenous LNX2 to peptides. Due to lack of suitable antibody to detect endogenous LNX1 by western blot, the analysis of this protein was limited to GFP-tagged LNX1 isoforms. Collected cell lysates were incubated with NeutrAvidin beads with immobilized biotinylated peptides, Fz7 WT and Fz7 V574G, but also with Fz3 and Fz8 peptides. Sequences of the two latter peptides represented the last 25 C-terminal amino acids of Frizzled-3 or Frizzled-8, respectively, two Frizzled receptors which may share some of the PDZ partners with Fz7 (Luyten et al. 2008). In theses experiments we compared the binding specificities of LNX proteins with that of syntenin-1. Proteins retained by beads were resolved in SDS-PAGE and detected using anti-GFP, anti-LNX2 or anti-syntenin-1 antibodies. Results presented in the Figure 3.19. show that both isoforms of LNX1, p80 and p70, bind strongly to the Fz7 WT peptide, and weaker to the

Fz7 V574G peptide. Specifically, binding capacity of LNX1 p80 to Fz7 V574G peptide is more than three times lower than to Fz7 WT peptide, whereas of LNX1 p70 is 18 times lower. Neither isoform binds to Fz3 or Fz8 peptides. LNX2 binds to Fz7 WT peptide, but not to Fz7 V574G peptide. LNX2 also binds to Fz8 with a similar capacity as to Fz7, but not to Fz3 peptide. Finally, we observed that syntenin-1 binds to Fz7 WT, and, to certain extent, to Fz7 V574G (with 10 times lower capacity), as already reported in previous section. Syntenin-1 was also found to bind to Fz3, but not to Fz8 peptide. It's binding to Fz3 peptide was, however, twofold lower when compared with Fz7 peptide. Taken together, LNX1, LNX2 and syntenin-1 have different binding capacities towards tested Frizzled peptides.

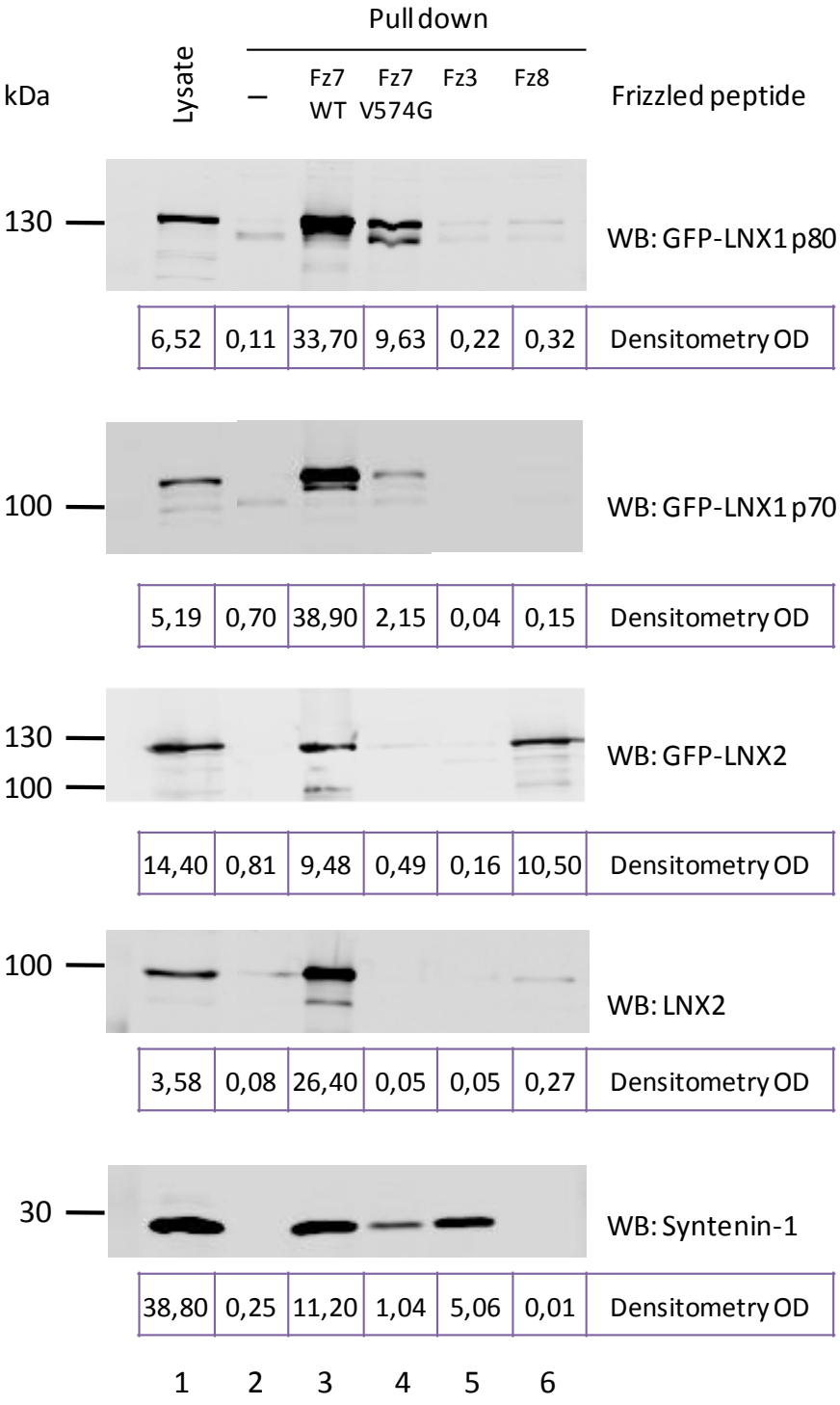
Pull down
kDa
Lysate
–
Fz7 WT
Fz7 V574G
Fz3
Fz8
Frizzled peptide
130
WB: GFP-LNX1 p80
6,52 0,11 33,70 9,63 0,22 0,32 Densitometry OD
100
WB: GFP-LNX1 p70
5,19 0,70 38,90 2,15 0,04 0,15 Densitometry OD
130
100
WB: GFP-LNX2
14,40 0,81 9,48 0,49 0,16 10,50 Densitometry OD
100
WB: LNX2
3,58 0,08 26,40 0,05 0,05 0,27 Densitometry OD
30
WB: Syntenin-1
38,80 0,25 11,20 1,04 5,06 0,01 Densitometry OD
1 2 3 4 5 6

Figure 3. 19. Pull down assays demonstrating interactions of LNX1, LNX2 and syntenin-1 proteins with Fz7, Fz3, and Fz8 peptides.

The interaction of LNX1, LNX2, syntenin-1 and Fz7, Fz3 and Fz8 was assessed by pull-down assay. HEK293T cells were lysed 24h after transfection with DNA plasmid encoding LNX proteins (GFP-LNX1 p80; GFP-LNX1 p70 and GFP-LNX2). Interaction with endogenous LNX2 and syntenin-1 was also examined. Lysates were precleared and incubated with NeutrAvidin agarose resins with immobilized biotinylated peptides (Fz7 WT; Fz7 V574G; Fz3; Fz8). Peptide sequences correspond to the last 25 amino acids of the C-terminal cytoplasmic regions of Frizzled receptors. As a control sample, NeutrAvidin agarose resin without peptide was used. After the pull-downs retained proteins were resolved by SDS-PAGE, followed by western blotting and protein detection using rabbit anti-GFP pAb. rabbit anti-LNX2 pAb or rabbit anti-Syntenin-1 mAb. Densitometry analysis was performed on pull down blots and optical densities (OD) are shown for each lane.

The interaction between Fz7 and LNX proteins was also verified by co-immunoprecipation using full length FLAG-Fz7 and FLAG-Fz7 V574G mutant. While very useful, pull-down assays, where only short peptides are used, do not always reflect the binding dynamics of proteins in cells. The reason for that might be the tertiary structure of the proteins, their complexes with other binding partners or different compartmentalization within the cell. In these experiments we also used the FLAG-Fz7 V574E mutant.

HEK293T cells were co-transfected with GFP-LNX1 p80, GFP-LNX1 p70 or GFP-LNX2 and FLAG-Fz7 WT, FLAG-Fz7 V574G or FLAG-Fz7 V574E. FLAG-Fz7 (WT, V574G and V574E) complexes were pulled down by the beads and proteins immunoprecipitated together with Fz7 were analysed by SDS-PAGE and WB. Lysates from cells transfected with GFP-LNX proteins, but not with Fz7, were used as control samples to visualise possible unspecific binding of LNX to the beads. To compare binding capacities of LNX proteins to Fz7 wild type and mutants, densitometry analysis was performed. Optical density (OD) was measured for both, LNX and Fz7, and the ratio between the two proteins was calculated for each sample. This allowed us to compare different samples with each other, as the amount of precipitated proteins may vary between them.

GFP-LNX1 p80 isoform was not immunoprecipitated together with Fz7 (Figure 3.20.A). It is contrary with findings from pull-down experiments. On the other hand, GFP-LNX1 p70 isoform has been found to interact with Fz7 WT (Figure 3.20.B, lane 2). The signal was also detected in the immunoprecipitated prepared from cells expressing V574G (lane 3) and V574E mutants (lane 4), as presented in the Figure 3.20.B. Densitometry analysis revealed that LNX1 p70 binding to Fz7 V574G was threefold lower, and to Fz7 V574E was

five fold lower, when compared with binding to the wild type Fz7. Thus, as predicted, the V574E mutation inhibited the interaction more drastically than V574G.

Similar analysis was performed for the LNX2 interaction with Fz7. As illustrated in Figure 3.20.D, LNX2 has been found to interact with Fz7 WT (lane 2), with Fz7 V574G (lane 3) and V574E (lane 4). Densitometry analysis was performed on data obtained in three independent experiments and presented as a histogram: plotted are percentages of LNX2 binding to Fz7 mutants relative to the interaction of LNX2 with the wild type Fz7 (taken as 100%) (Figure 3.20.E). Analysis revealed that LNX2 binding to Fz7 V574G was four fold lower, and to Fz7 V574E was more than 16 fold lower, when compared with binding to the wild type Fz7. Thus, as in the case of LNX1 p70, the V574E mutation inhibited the interaction more drastically than V574G.

Additionally, the interaction between Fz7 and LNX2 was verified using GFP-Trap system. HEK293T cells were transfected with Myc-LNX2 and GFP or GFP-Fz7 (WT, V574G or V574E). Lysates from these cells were incubated with GFP-Trap beads to pull down GFP-tagged proteins. Retained proteins were resolved by the SDS-PAGE and detected by western blotting using anti-Myc and anti-GFP antibody (Supplementary Figure S.4.A). LNX2 has been found to interact with Fz7 WT (lane 2), but also with Fz7 V574G (lane 3) and V574E (lane 4). Densitometry analysis was performed on data obtained in three independent experiments and presented as a histogram: plotted are percentages of LNX2 binding to Fz7 mutants relative to the interaction of LNX2 with the wild type Fz7 (taken as 100%) (Supplementary Figure S.4.B). Analysis of this experiment confirmed that LNX2 binding to Fz7 V574G was four fold lower, and to Fz7 V574E was more than ten fold lower, when compared with binding to the wild type Fz7.

Taken together, pull down experiments and immunoprecipitation assays, demonstrated that Fz7 interacts with proteins from LNX family and that this interaction is mediated by PDZ domains of LNX and C-terminal PDZ binding motif of Fz7. To start investigating functional consequences of Fz7-LNX interactions, we decided to focus on LNX2.

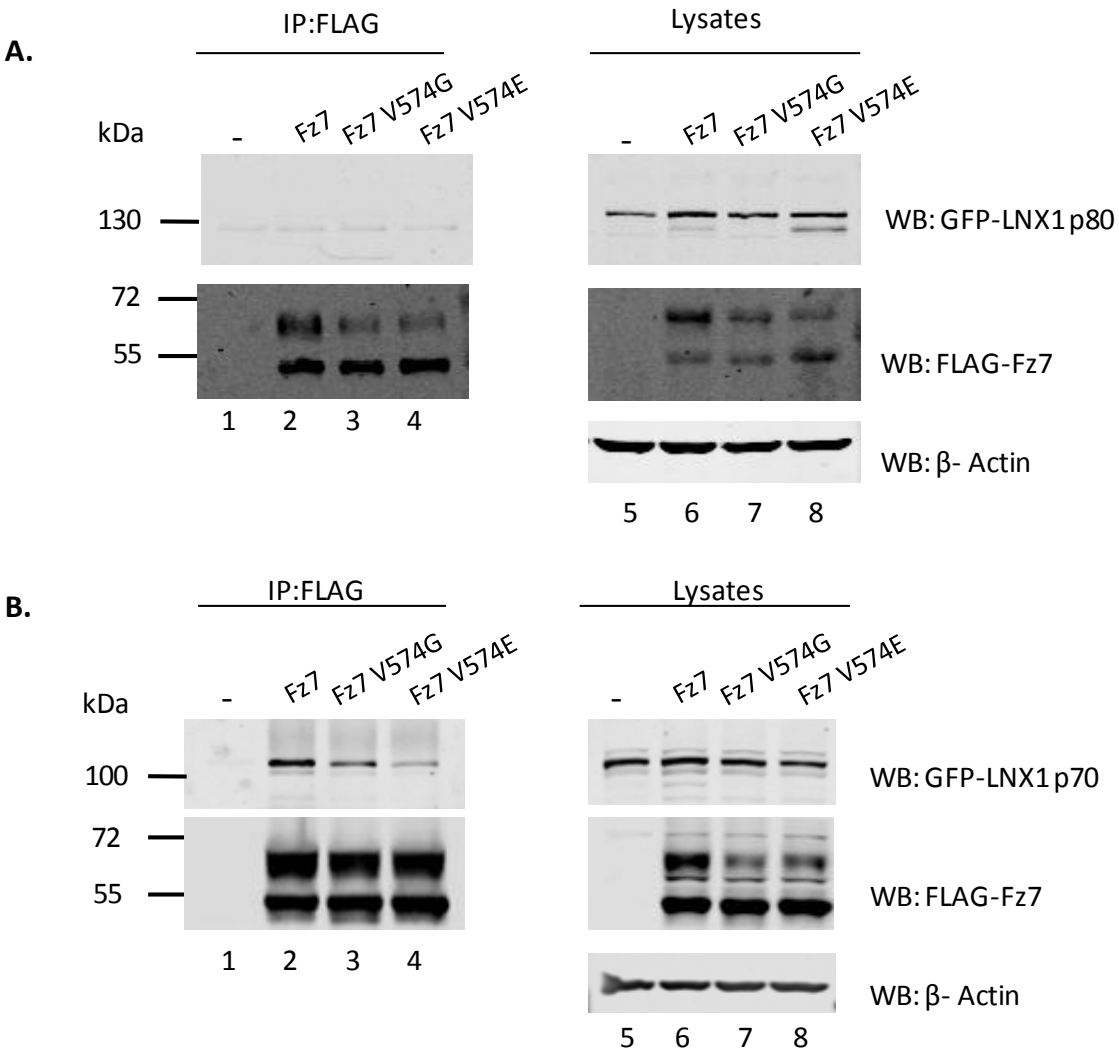
A.
IP:FLAG
Lysates
kDa
-
Fz7
Fz7 V574G
Fz7 V574E
130
72
55
WB: GFP-LNX1 p80
WB: FLAG-Fz7
WB: β- Actin
1 2 3 4
5 6 7 8
B.
IP:FLAG
Lysates
kDa
100
72
55
WB: GFP-LNX1 p70
WB: FLAG-Fz7
WB: β- Actin
1 2 3 4
5 6 7 8
C.
LNX1 p70 binding
% of binding
120
100
80
60
40
20
0
*
***
Frizzled 7
Frizzled 7 V574G
Frizzled 7 V574E

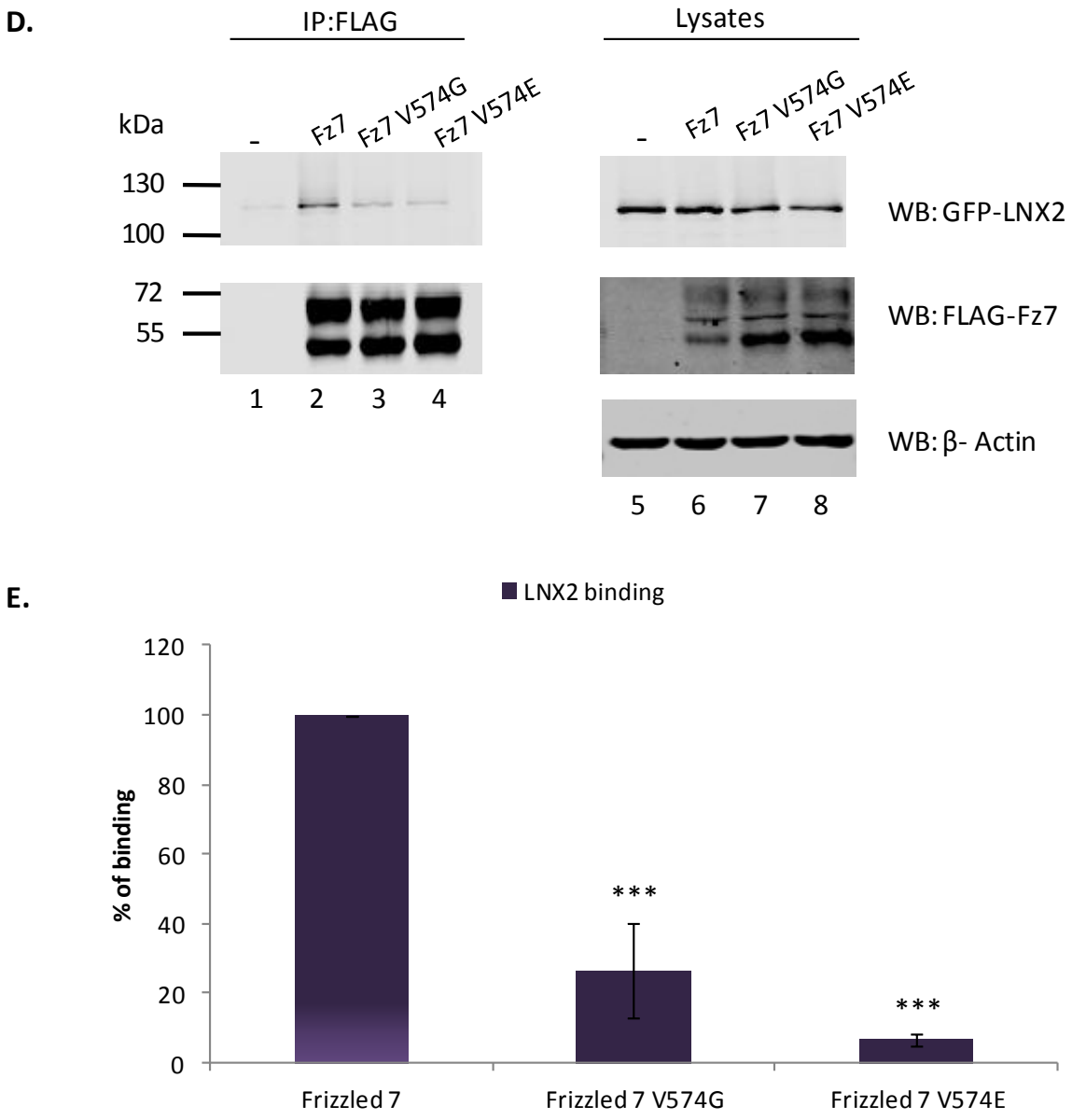

Figure 3. 20. Fz7 interaction with LNX1 p70 and LNX2 involves PDZ domains.

HEK293T cells were co-transfected with FLAG-Fz7 (WT, V574G or V574E) and GFP-LNX1 p80 (A), GFP-LNX1 p70 (B) or GFP-LNX2 (D). 24h after transfection cells were lysed in 1% Triton X-100 and lysates were incubated with Anti-FLAG ® M2 Magnetic Beads. Immunoprecipitated proteins were resolved by SDS-PAGE, followed by western blotting and protein detection using rabbit anti-GFP pAb. Shown images represent one of at least three independent experiments. (C and E) Densitometry analysis was performed on data obtained in three independent experiments and presented as a histogram: plotted are percentages of LNX2 binding to Fz7 mutants relative to the interaction of LNX2 with the wild type Fz7 (taken as 100%). The statistical significance was determined by a two-tailed, unpaired Student's t test (*p<0.05; *** p<0.001).

3.3.3.2. Mapping of LNX2 domain that interacts with Fz7

LNX2 contains four PDZ domains. Pull-down assays were performed to determine whether the interaction with Fz7 is mediated by one or more PDZ domains. HEK293T cells were transfected with constructs to express HA-tagged LNX2 wild type, and truncation mutants of LNX2, containing only the four PDZ domains (PDZ1-4), the first two domains (PDZ1-2) or the last two domains (PDZ3-4) of the protein. Lysates from the transfected cells were incubated with NeutrAvidin beads conjugated with biotinylated Fz7 peptide. Pulled down proteins were resolved using SDS-PAGE and detected by western blotting with anti-HA antibody (Figure 3.21.A). Densitometry analysis was performed on the data obtained in two independent experiments and presented as a histogram, showing percentage of binding to Fz7 peptide relative to the total levels of the proteins in corresponding lysates (Figure 3.21.B). These experiments showed that LNX2 PDZ1-4 binding to Fz7 peptide was 4 fold lower, LNX2 PDZ1-2 was 500 fold lower and LNX2 PDZ3-4 was 100 fold lower, when compared with wild type LNX2. Thus, more than one PDZ domains of LNX2 is involved in the interaction, as the binding affinity of the LNX2 truncation mutants to Fz7 peptide is significantly lower when compared to the full length protein.

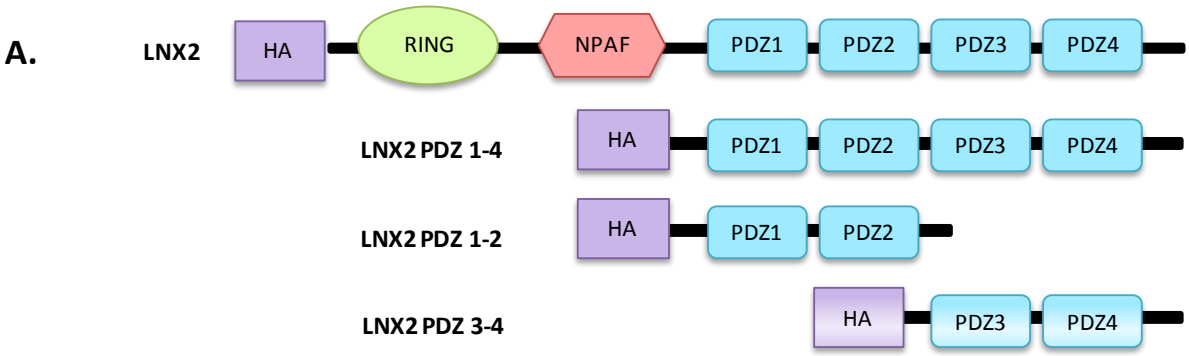
A.
LNX2
HA
RING
NPAF
PDZ1
PDZ2
PDZ3
PDZ4
LNX2 PDZ 1-4
LNX2 PDZ 1-2
LNX2 PDZ 3-4

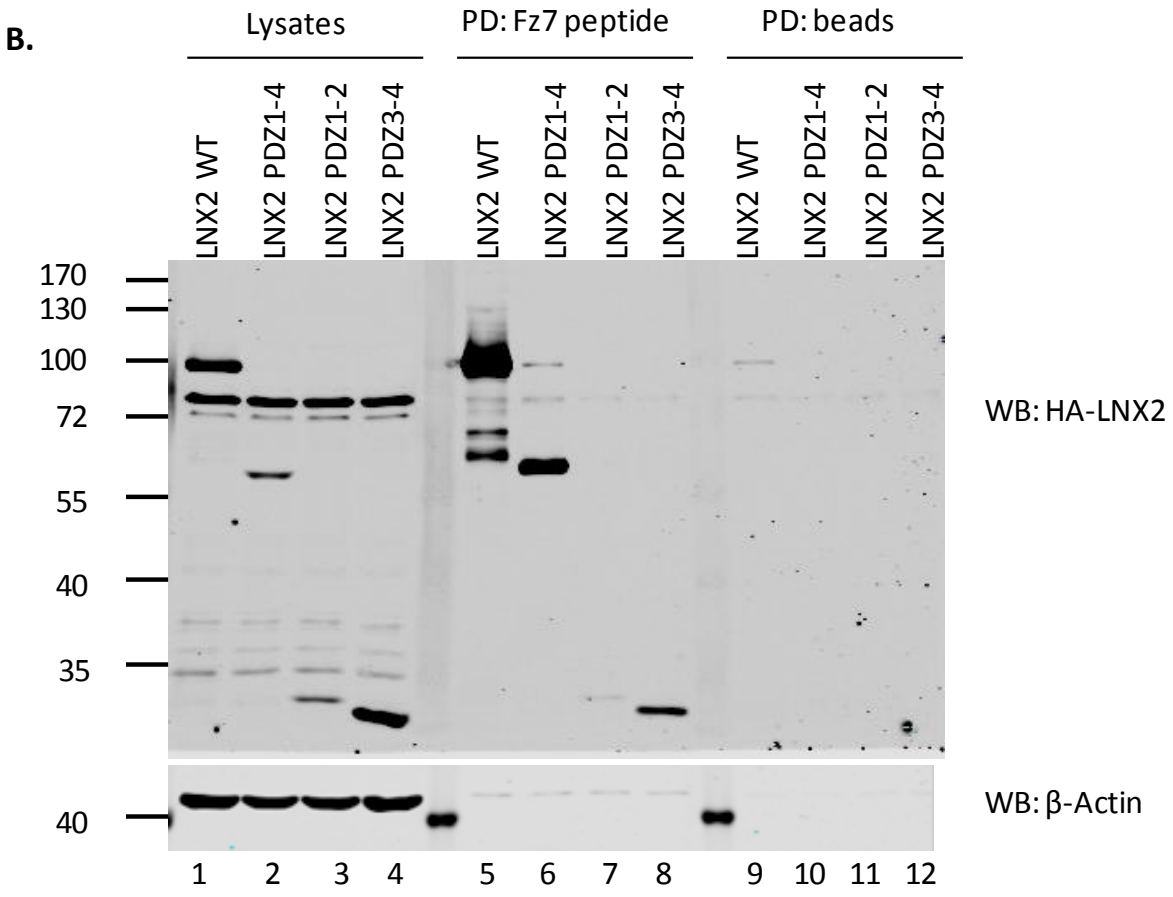
B.
Lysates
PD: Fz7 peptide
PD: beads
LNX2 WT
LNX2 PDZ1-4
LNX2 PDZ1-2
LNX2 PDZ3-4
170
130
100
72
55
40
35
40
WB: HA-LNX2
WB: β-Actin
1 2 3 4 5 6 7 8 9 10 11 12

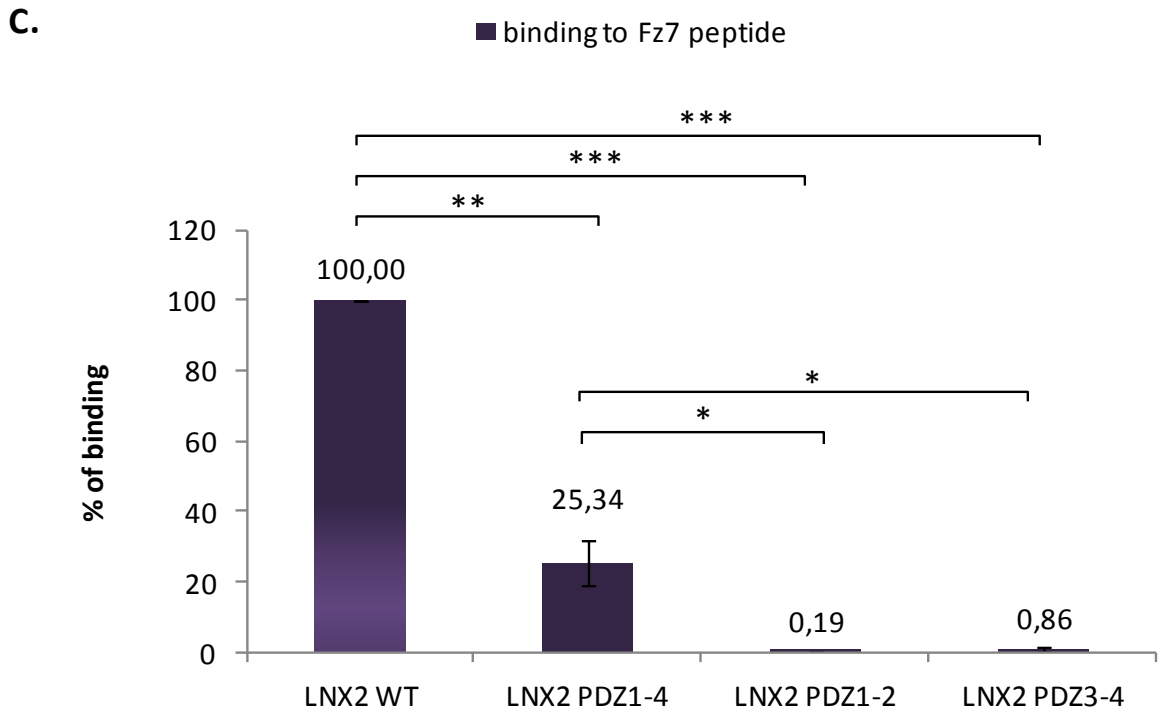

Figure 3. 21. Interaction with Fz7 involves more than one PDZ domain of LNX2.

(A) Schematic representation of HA-tagged LNX2 constructs. (B) HEK293T cells were transfected with plasmids encoding HA-tagged LNX2 WT, LNX2 PDZ1-4, LNX2 PDZ 1-2 or LNX2 PDZ 3-4. Lysates were precleared and incubated with NeutrAvidin agarose resins with immobilized biotinylated Fz7 WT peptide. For the control samples, NeutrAvidin agarose resins without peptide were used. After the pull-downs the beads were washed and resuspended in 2x SDS sample-loading buffer. Retained proteins were resolved by SDS-PAGE, followed by western blotting and protein detection using rabbit anti-HA pAb. (C) Densitometry analysis of the blots, plotted as percentage of LNX2 WT binding to the Fz7 peptide. Data shown is an average of at least two independent experiments. The statistical significance was determined by a two-tailed, unpaired Student's t-test (*p<0.05; **p<0.01; ***p<0.001).

3.3.3.3. Testing co-localization of Fz7 and LNX2 in SKBr3 cells

If LNX2 interacts with Fz7, these two proteins should be present in the same cellular compartments. To verify whether they co-localize we performed immunofluorescence experiments on SKBr3 cell lines stably expressing FLAG-Fz7 WT and FLAG-Fz7 V574G. Due to lack of a suitable antibody to detect endogenous LNX2 by immunofluorescence, Myc-LNX2 was used for the co-localization study. SKBr3, SKBr3-FLAG-Fz7 and SKBr3-FLAG-Fz7 V574G cells were transfected with Myc-LNX2 and co-distribution of the proteins was analysed 48h later using rabbit anti-FLAG and mouse anti-Myc antibodies. DAPI was used to visualize nuclei.

LNX2 was predominantly found in the cytoplasm but was also detected close to the plasma membrane in parental SKBr3 cells. In both cell lines, SKBr3-FLAG-Fz7 and FLAG-Fz7 V574G, clear co-localization with LNX2 was observed in plasma membrane proximity (Figure 3.22.). These results provided a supporting evidence for the interaction between LNX2 and Fz7 *in vivo*.

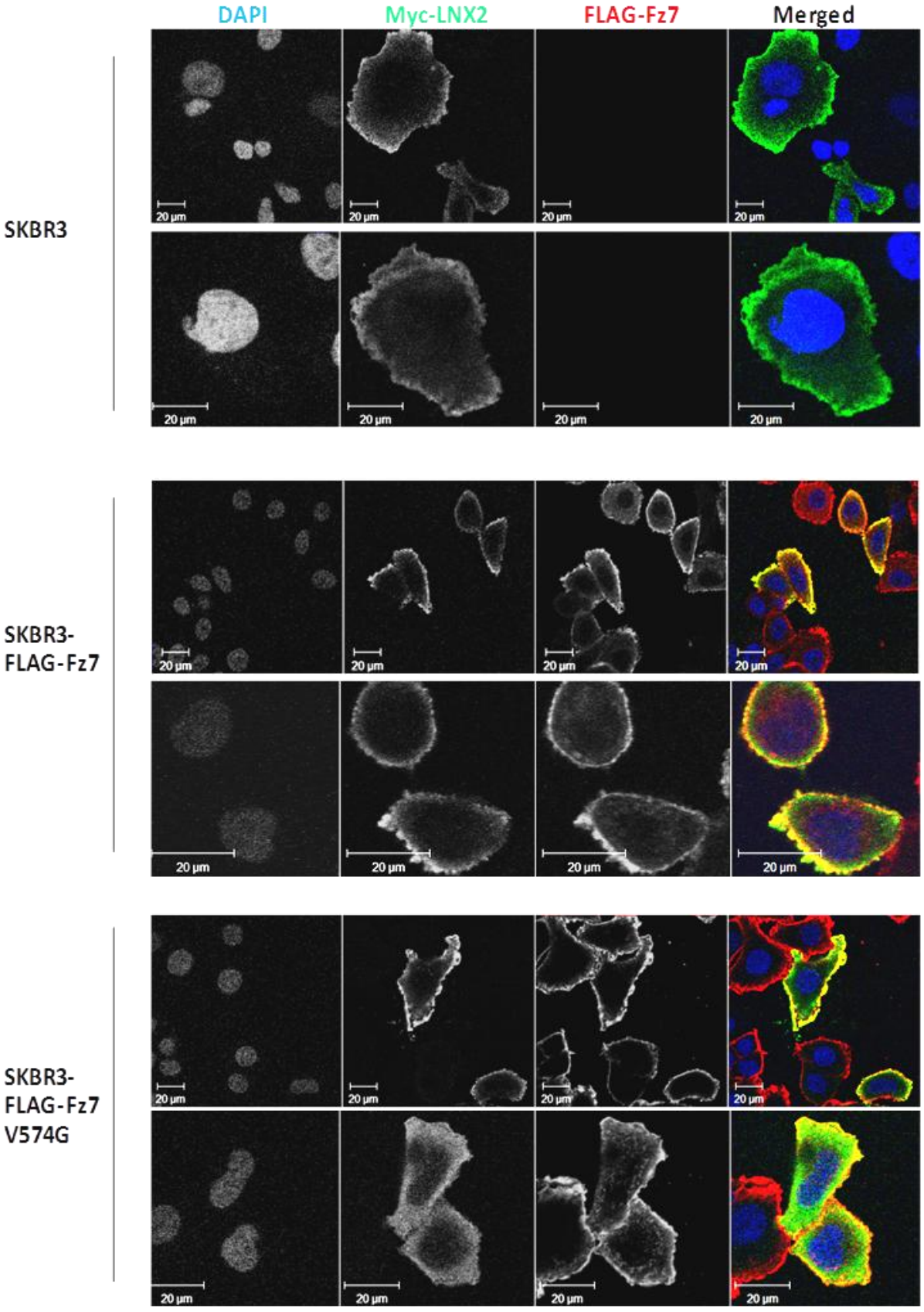
DAPI
Myc-LNX2
FLAG-Fz7
Merged
SKBR3
SKBR3-
FLAG-Fz7
SKBR3-
FLAG-Fz7
V574G
20 µm

Figure 3. 22. LNX2 co-localizes with Fz7 in SKBr3 cells.

SKBr3, SKBr3-FLAG-Fz7 WT and SKBr3-FLAG-Fz7 V574G cells were transfected with Myc-LNX2 and co-distribution was analysed by confocal imaging. Cells were fixed 48h after transfection and stained with rabbit anti-FLAG pAb and with mouse anti-Myc mAb. DAPI was used to visualize nuclei. Both, Fz7 WT and Fz7 V574G co-localize with LNX2.

3.3.4. Discussion

We have found in the proceeding chapters that introduction of a mutation in the C-terminal PDZ binding motif of Frizzled-7 receptor affects canonical Wnt signalling in breast cancer cell lines. Subsequently, we have provided evidence that Fz7 interaction with PDZ protein syntenin-1 regulates functions of the receptor. Nonetheless, one could not exclude the possibility that other PDZ domain containing proteins are also involved in modulating Fz7 signalling. To identify cellular proteins that might be responsible for PDZ-BM – dependent regulation of the canonical Wnt pathway we were searching for novel Fz7 binding partners. We have employed a standard pull-down assay using biotinylated peptides and found striking differences in an amount of proteins pulled down by Fz7 WT peptide and Fz7 V574G peptide (Figure 3.17). Proteins pulled down by Fz7 WT peptide, but not Fz7 V574G peptide, are known to be involved in receptor trafficking, as well as in establishment of cell polarity and tight junction formation (INADL/PATJ, MPDZ, Scribble, DLG1, ZO-1, ZO-2, PALS1/MPP5, MPP7, MAGI1, MAGI3, SNX27, LNX1, LNX2; Table 3.1). Among the identified proteins only MAGI3 and INADL/PATJ were previously reported to interact with Frizzled receptors. MAGI3 was shown to bind Fz4 and support non-canonical Wnt/JNK signalling (Yao et al. 2004), whereas INADL/PATJ interacts with dFz1 and inhibits Wnt/PCP signalling (Djiane et al. 2005).

The remaining proteins are potentially novel binding partners of Fz7. The interactions with a number of "polarity proteins" suggest a link between Fz7 and basoapical tissue polarity. Basoapical polarity in the normal epithelium relies on polarity protein complexes and cell junction components asymmetrically localized between the apex and the base of the

cell (Bazzoun et al. 2013). Three conserved complexes of protein have been determined: Crumbs (Crumbs/PALS/PATJ) and Par (Par3/Par6/aPKC/Cdc42) which are apical, and Scribble (Scribble/Dlg/Lgl) which is basolateral. Polarity proteins control the establishment of cell junction complexes that consist of transmembrane proteins (occludin, claudin and JAM for tight junctions; cadherins for adherens junctions; connexins for gap junctions) associated with cytoplasmic proteins (ZO proteins, catenins and others). Par complex ensures the localization of tight junctions at the apical domain of cells. The Crumbs complex also regulates tight junction maintenance through its reciprocal interactions with Par proteins. The basolateral side of cells is characterized by the presence of both adherence and gap junctions. Scribble complex associates with adherence junctions to assure their segregation from tight junctions and to stabilize the coupling of E-cadherins with catenins, but it's not certain how Scribble regulates gap junctions (Bazzoun et al. 2013).

One needs to remember that all of the pulled-down proteins contain PDZ domains and some of them form complexes with each other (see below). Hence at this stage we cannot be certain which of the proteins is a primary binding partner of Fz7. Among the identified potential binding partners of Fz7 are PALS1/MPP5 and PATJ/INADL (present in the Crumbs complex), Scribble and DLG1 (Scribble complex), ZO-1 and ZO-2 (tight and gap junctions), as well as MPP7 (interacting with DLG1) and MAGI1, protein regulating cell junctions. PALS1 was reported as an adaptor protein facilitating interaction between Crumbs and PATJ, which is a scaffolding protein that regulates protein targeting and integrity of tight junctions (Roh et al. 2002). MPDZ (MUPP1), also identified in our proteomic screen, is a protein homological to PATJ, and it was shown to bind identical proteins (Assemat et al. 2008). Scribble is a large (175 kDa) cytoplasmic multi-domain scaffold, playing various roles

in cells. It physically interacts with DLG proteins (Mathew et al. 2002) and with ZO-2 (Metais et al. 2005). As already mentioned, Scribble co-localizes with adherens junctions, thus interaction with ZO-2 probably takes place before ZO-2 is segregated to the tight junctions. Additionally, ZO-2 has been shown to bind to ZO-1, among other components of tight junction (Itoh et al. 1999). Scribble has been shown to regulate Ras/MAPK and JNK signalling pathways (Subbaiah et al. 2011), and reported to play an important role in the recycling and signalling of transmembrane receptor TSHR (thyroid stimulating hormone receptor) (Lahuna et al. 2005). Similarly to Frizzled receptors, TSHR belongs to GPCR superfamily of proteins. Thus it is possible that Scribble may be also be involved in Fz7 recycling. The function of DLG1 protein is not clear, but it associates with APC protein (Matsumine et al. 1996) and it has been shown to regulate its correct subcellular localization, in a PDZ domain dependent fashion; however, the functional significance of this interaction remained unknown (Etienne-Manneville et al. 2005). It also interacts with MPP2, MPP3, MPP7 and Lin7 (Assemat et al. 2008). The interaction between DLG1 and MPP7 regulates formation of tight junction, whereas Lin7 stabilizes DLG1 and its distribution (Bohl et al. 2007;Stucke et al. 2007). MAGI1 was also implicated in regulation of tight and adherens junction (Subbaiah et al. 2011). Furthermore it was shown to bind β-catenin (Dobrosotskaya et al. 2000) and to regulate the tumour suppressor, PTEN (Glaunsinger et al. 2000). Potentially it forms a trimeric β-catenin-MAGI-PTEN complex (Kotelevets et al. 2005). Further research would be required to explore which of the identified proteins directly interacts with Fz7 receptor, whether they affect distribution of Fz7 and whether interaction with any of these proteins affect the canonical Wnt pathway.

Fz7 has been reported to be involved in regulation of planar tissue polarity, as it acts as a receptor in planar cell polarity (PCP) pathway, one of the non-canonical Wnt signalling pathways (Dijksterhuis et al. 2014). The link between basoapical and planar cell polarity remains poorly understood. Djiane and colleagues reported apical localization of dFz1 (a PCP receptor) in *Drosophila* epithelial cells and its direct interaction with dPatj, a component of the Crumbs complex. The authors proposed that dFz1-dPatj interaction leads to aPKC recruitment and subsequent phosphorylation and inhibition of Fz1/PCP signalling (Djiane et al. 2005). Since Fz7 is also involved in PCP signal transduction, there is possibility that one the polarity proteins regulates its basoapical localization in cells. Additionally, Scribble has been implicated in PCP establishment in the *Drosophila* eye and wing, by interaction with Stbm/Vang complex (Courbard et al. 2009). Interestingly, Frizzled receptors have also been implicated to interact with Stbm/Vang during PCP signalling (Wu et al. 2008).

Loss of basoapical cell polarity is a hallmark of the epithelial-to-mesenchymal transition (EMT), a process in which cells become more spindle-shaped, mobile and acquire stemlike characteristics. Interestingly, the role of Wnt signalling in promotion of EMT has been established in various human cancers, e.g. HCC, prostate and breast cancer (Talbot et al. 2012). Indeed, Scribble was reported to regulate EMT through modulation of the MAPK-ERK signalling (Elsum et al. 2013). Thus a potential Scribble-Fz7 interaction might play role in the process.

Another protein identified in the proteomics screen was SNX27 (sorting nexin-27). It functions as an endosome-associated cargo adaptor. It interacts with transmembrane proteins containing NPxY motif through its C-terminal FERM-like domain, or PDZ-BM (S/T-x-φ) through the PDZ domain (Lauffer et al. 2010). SNX27 forms a complex with retromer, a

heterotrimer composed of VPS26, VPS29 and VPS35, and regulates recycling of cargo-proteins from endosomes to plasma membrane (Temkin et al. 2011). Interestingly, VPS26A binding to SNX27 increases the affinity of the PDZ domain of the protein to the ligands, implying cooperativity in cargo selection (Gallon et al. 2014). SNX27-retromer complex in involved in regulation of trafficking of β2-adrenergic receptor, ionotrophic glutamate receptors (NMDA and AMPA receptors) (Loo et al. 2014), potassium channels (Balana et al. 2011), somatostatin receptor (Bauch et al. 2014) and the glucose transporter (Steinberg et al. 2013). Recent proteomics analysis also identified Fz1 and Fz2 among more than 80 transmembrane proteins that can bind to SNX27 (Steinberg et al. 2013). Taking it all into account, it is possible that SNX27-retromer regulates Fz7 recycling from endosomes to plasma membrane. Further research is necessary to explore the nature of Fz7-SNX27 interaction.

Finally, we have also identified two proteins from the LNX family. Ligand of Numb Protein X (LNX) family contains proteins described as E3 ubiquitin ligases, characterized by the presence a RING domain (see Introduction for more details). Our proteomics analysis revealed that two members of the LNX family: LNX1 and LNX2, are potential binding partners of Fz7. These two proteins share an identical domain structure (RING domain and four PDZ domains), with LNX1 having two isoforms, a full length p80 and p70 which lacks the RING domain (Wolting et al. 2011). Interestingly, phylogenetic analysis revealed that LNX1/2 share a common ancestor with two other proteins, also identified in the proteomic screen: MPDZ/MUPP1 and INADL/PATJ. LNX1/2 have been also shown to associate with tight junction proteins JAM4, claudin-1 and CAR, and the later two also interact with MUPP1 (Flynn et al. 2011). Recently, several reports have suggested the role of LNX proteins

in regulation of Wnt signalling. LNX1 was shown to bind to Wnt signalling regulators Naked2 (Nkd2) and Dishevelled-3 (Dvl3) (Wolting et al. 2011). LNX2b (an LNX zebrafish ortholog) has been shown to bind and ubiquitylate the Wnt inhibitor Bozozok and in consequence upregulate the β-catenin Wnt signalling (Ro et al. 2009). Finally, siRNA-mediated silencing of LNX2 reduces Wnt signalling in colorectal cancer cells through downregulation of TCF7L2 (Camps et al. 2013). For that reason we have decided to further explore the nature of the interaction between Fz7 and LNX.

To verify whether different isoforms of LNX can bind to Fz7, a pull-down assay with Fz7 peptides was employed (Figure 3.19). Both isoforms of LNX1, p80 and p70, bind strongly to the Fz7 WT peptide but not to the peptides corresponding to the C-terminal cytoplasmic tails of Fz3 or Fz8. On the other hand LNX2 binds to both Fz7 WT and Fz8 peptides (but not to Fz3 peptide). The observed binding specificity of LNX1 and LNX2 supports distinct binding properties of LNX PDZ domains (Guo et al. 2012) and suggests non-redundant functions of these enzymes in Frizzled-dependent pathways. In other experiments we found that syntenin-1 binds to Fz7 and Fz3, but not to Fz8 peptide. While our observation on syntenin-1 binding to Fz7 and Fz3 is in agreement with the report by Luyten and colleagues (2008), were unable to confirm their finding on the syntenin-1 – Fz8 interaction. Although the reasons behind these differences remain unknown, one the possible explanation may be difference in the experimental protocols used by us (peptide-based pull down from cellular lysates) and these authors (interaction between recombinant syntenin-1 and the peptide) (Luyten et al. 2008).

Pull-down assays with peptides do not always reflect the binding dynamics of proteins in living cells. Accordingly, we have used co-immunoprecipitation assay to further

verify the interactions. We have established that LNX1 p70 and LNX2 bind to the full length Fz7, however p80 isoform of LNX1 does not. It might be due to the tertiary structure of the proteins, their complexes with another binding partners or different compartmentalization within the cell. Importantly, in the immunoprecipitation experiments we confirmed that LNX-Fz7 interactions are mediated through PDZ domain interactions. Furthermore, our results indicate that more than one PDZ domains of LNX2 is involved in these interactions (Figure 3.21). In this regard, several other proteins has also been shown to bind two PDZ domain of LNX ligases, e.g. PLEKH5 (PDZ1 and PDZ3), or PAK6 and PKC-α1 (PDZ2 and PDZ4) (Wolting et al. 2011).

Taken together, work presented in this chapter included identification of novel binding partners of Fz7 by mass spectrometry. To our knowledge, it's the first systematic proteomic screen in search of cytoplasmic proteins interacting with Fz7. Among identified interactors we have found a number of PDZ proteins forming polarity complexes, thus suggesting the involvement of Fz7 in establishment or disruption of basoapical cell polarity. We have also identified several proteins, previously reported to be involved in trafficking of membrane receptors, to associate with Fz7, such as SNX27, Scribble, DLG1, MAGI3. They might be novel regulators of Fz7 recycling. Finally, two proteins from LNX family, LNX1 and LNX2, were also recognized to associate with Fz7 in PDZ domain dependent fashion. Further analysis confirmed interaction between full length Fz7 and LNX2 in epithelial cells, as well their colocalization in plasma membrane proximity. The functional significance of this interaction will be explored in the next section.

3.4. Investigating the role of the Fz7 interaction with proteins from LNX family

We have established that Fz7 interacts with LNX1 and LNX2. Whilst previous studies have reported a functional connection between Wnt signalling and LNX proteins (Camps et al. 2013;Ro et al. 2009), to date, no investigation has identified a link between LNX and a specific Frizzled receptor or determined a mechanism explaining how LNX is involved in regulating Wnt signalling. The aim of the work described in this chapter was to assess whether Fz7 functions are regulated by LNX proteins.

3.4.1. LNX1 and LNX2 modulate Fz7 ubiquitylation.

3.4.1.1. LNX1 p80, LNX1 p70 and LNX2 overexpression decreases Fz7 ubiquitylation level

In order to verify whether Fz7 is an ubiquitylation substrate of LNX1 or LNX2, an *in vivo* ubiquitylation assay was performed, as described in Materials and Methods (section 2.5.2.). HEK293T cells were transfected with plasmids encoding GFP-LNX1 p80, GFP-LNX1 p70, GFP-LNX2 or GFP, together with FLAG-Fz7 and HA-ubiquitin. 24h post transfection, cells were lysed and Fz7 was immunoprecipitated using anti-FLAG magnetic beads. Protein ubiquitylation was analysed by SDS-PAGE and WB using anti-HA pAb (Figure 3.23). Fz7 ubiquitylation was detected as a smear in the anti-FLAG immunoprecipitate by anti-HA antibodies, indicating protein polyubiquitylation. Interestingly, the amounts of ubiquitylated

protein species in Fz-immunoprecipitates were consistently lower than in the control samples. Specifically, densitometry analysis revealed that the levels of ubiquitylated Fz7 were decreased by 50% when both isoforms of LNX1 or LNX2 proteins were overexpressed. Whilst these experiments involved incubation of samples at 60°C to ease Fz7 detection by western blotting, additional test with samples incubated at 100°C before SDS-PAGE analysis confirmed the decreased ubiquitylation level of Fz7 after LNX overexpression (data not shown).

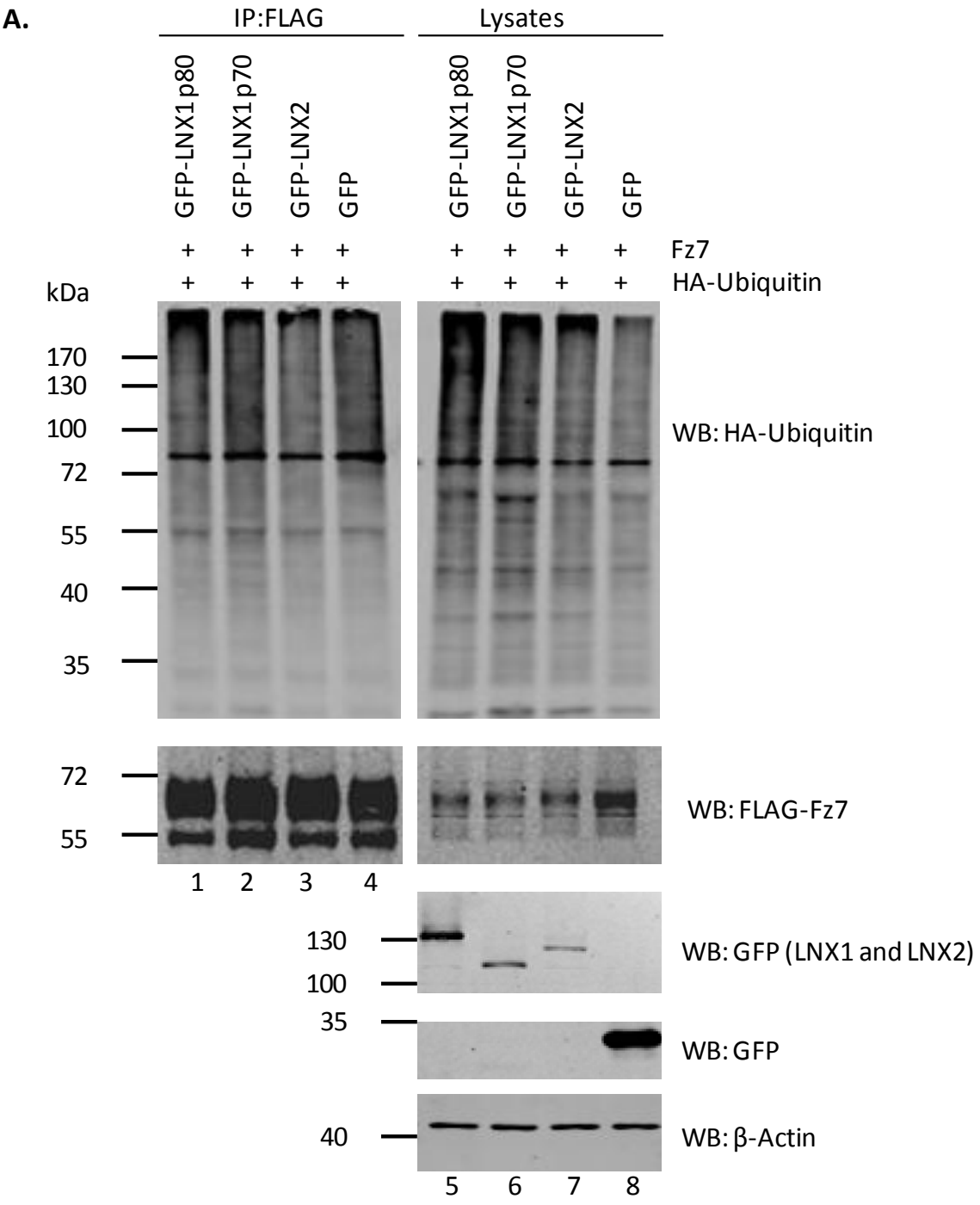
A.
IP:FLAG
Lysates
GFP-LNX1 p80
GFP-LNX1 p70
GFP-LNX2
GFP
Fz7
HA-Ubiquitin
kDa
170
130
100
72
55
40
35
WB: HA-Ubiquitin
72
55
WB: FLAG-Fz7
1 2 3 4
130
100
WB: GFP (LNX1 and LNX2)
35
WB: GFP
40
WB: β-Actin
5 6 7 8

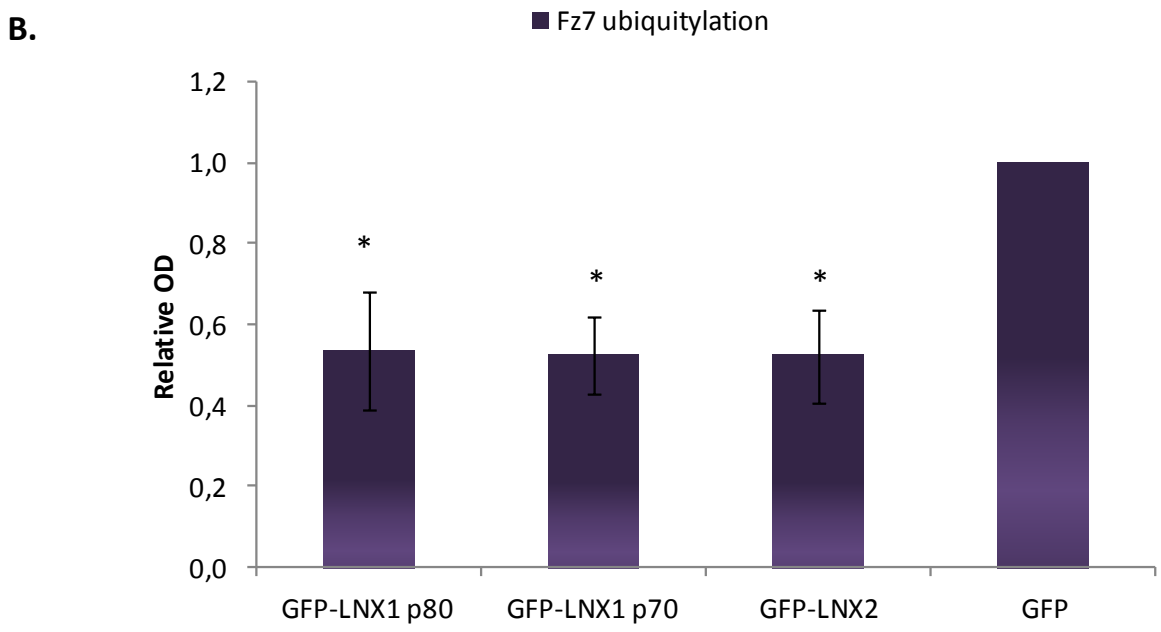

Figure 3. 23. LNX1 and LNX2 decrease the levels of Fz7 ubiquitylation.

(A) HEK293T cells were co-transfected with GFP-LNX1 p80, GFP-LNX1 p70, GFP-LNX2 or GFP, FLAG-Fz7 WT and HA-Ubiquitin. Subsequently cells were lysed in the lysis buffer containing 0.5% SDS, incubated at 60°C, diluted with 1% Triton X-100 and sonicated. Subsequently lysates were incubated with Anti-FLAG®M2 Magnetic Beads and to pull-down FLAG-Fz7. Ubiquitylated proteins were detected by immunoblotting with anti-HA antibody. Images depict representatives of at least three independent experiments. (B) Densitometry analysis of the blots. Data shown is an average of at least three independent experiments. Ratios between densitometry values (optical density, OD) of immunoprecipitated HA-ubiquitin and Fz7 were calculated for each sample and presented in the histogram. This allowed to compare different samples with each other, as the amount of precipitated proteins may vary between them. Ubiquitylation values of Fz7 were standardized to the value of the control sample (Fz7 co-transfected with GFP, lane 4). The statistical significance was determined by a two-tailed, unpaired Student's t-test (*p<0.05).

3.4.1.2. LNX2 modulation of Fz7 ubiquitination does not involve proteasomal degradation of the receptor

In the previous section, decreased levels of Fz7 ubiquitylation were observed in response to LNX1 and LNX2 overexpression. LNX proteins may regulate Fz7 ubiquitylation and expression levels through a mechanism involving proteasome dependent protein degradation. To address this question, we carried out *in vivo* ubiquitylation experiments in the presence of MG132, a widely used proteasome inhibitor. HEK293T were co-transfected with FLAG-Fz7, HA-ubiquitin and GFP-LNX2 or GFP. Cells were then treated with 10 μM MG132 or the vehicle (DMSO) for 24h. Subsequently, they were lysed, and Fz7 complexes were immunoprecipitated using anti-FLAG beads (as described in the section 2.5.2. of Materials and Methods). Protein ubiquitylation was analysed by WB using anti-HA pAb for detecting HA-ubiquitin (Figure 3.24).

As expected, MG132 treatment increased the overall levels of protein ubiquitylation in cells. Furthermore, the treatment with MG132 increased the levels of Fz7 ubiquitylation by 70% in control cells. LNX2 expression led to a reduction inFz7 ubiquitylation in the absence (lane 1) and in the presence (lane 3) of the proteasome inhibitor MG132. Densitometry analysis revealed that ubiquitylation of Fz7 cells expressing LNX2 was two fold lower (treated with the vehicle) or three fold lower (treated with MG132), when compared to the control samples. These findings suggest that the level of Fz7 ubiquitylation is decreased in cells overexpressing LNX2. However, a decrease in the overall levels of ubiquitylation of cellular proteins was also observed in cells overexpressing LNX2. The mechanism of observed alterations do not seem to involve proteasome-dependent degradation. Finally, we

have also noticed that the total level of LNX2 is increased in MG132-treated cells, suggesting that LNX2 expression level is controlled by proteasomal degradation.

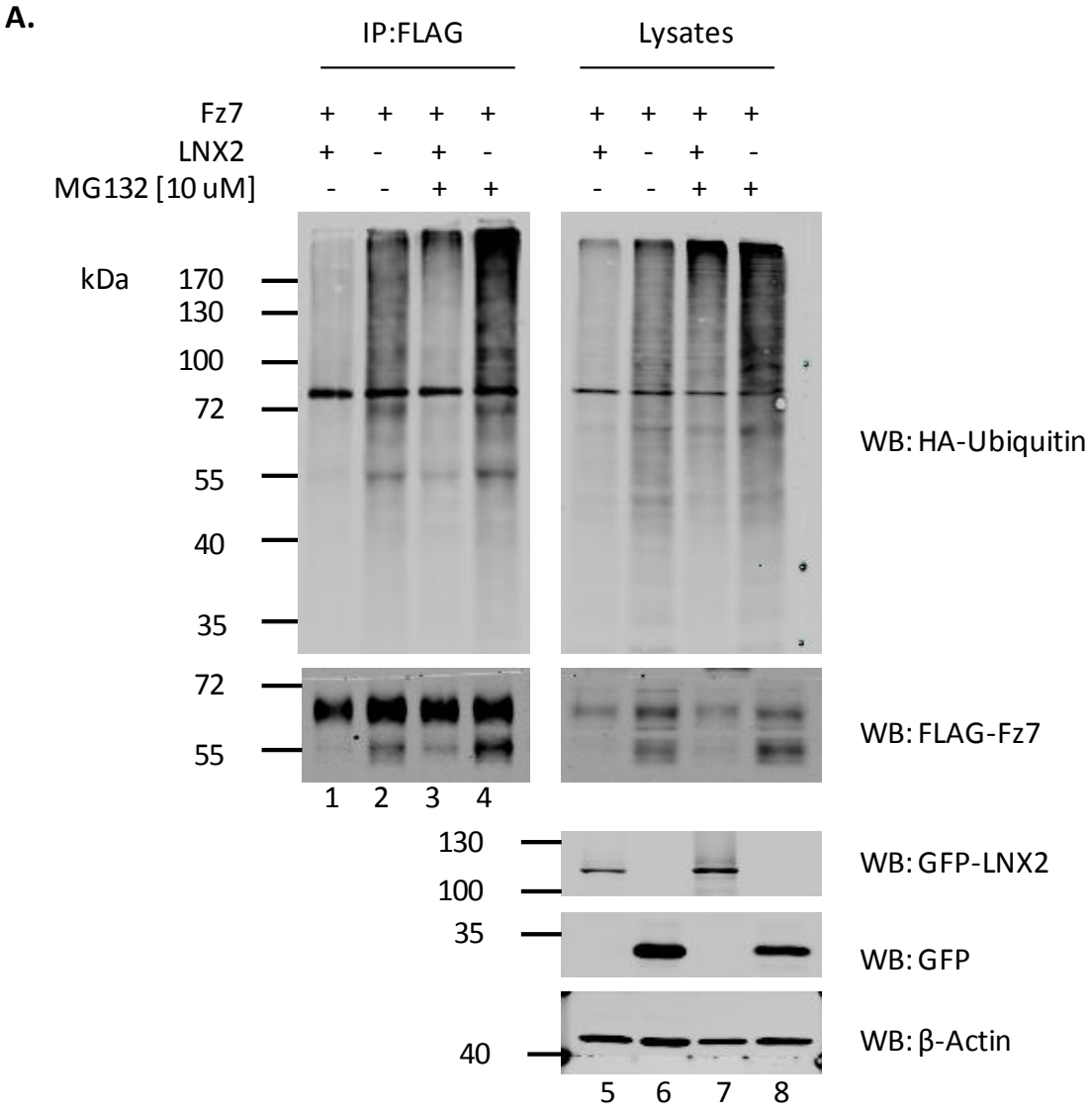
A.
IP:FLAG
Lysates
Fz7 + + + + + + + +
LNX2 + - + - + - + -
MG132 [10 uM] - - + + - - + +
kDa
170
130
100
72
55
40
35
WB: HA-Ubiquitin
72
55
WB: FLAG-Fz7
1 2 3 4
130
100
WB: GFP-LNX2
35
WB: GFP
40
WB: β-Actin
5 6 7 8

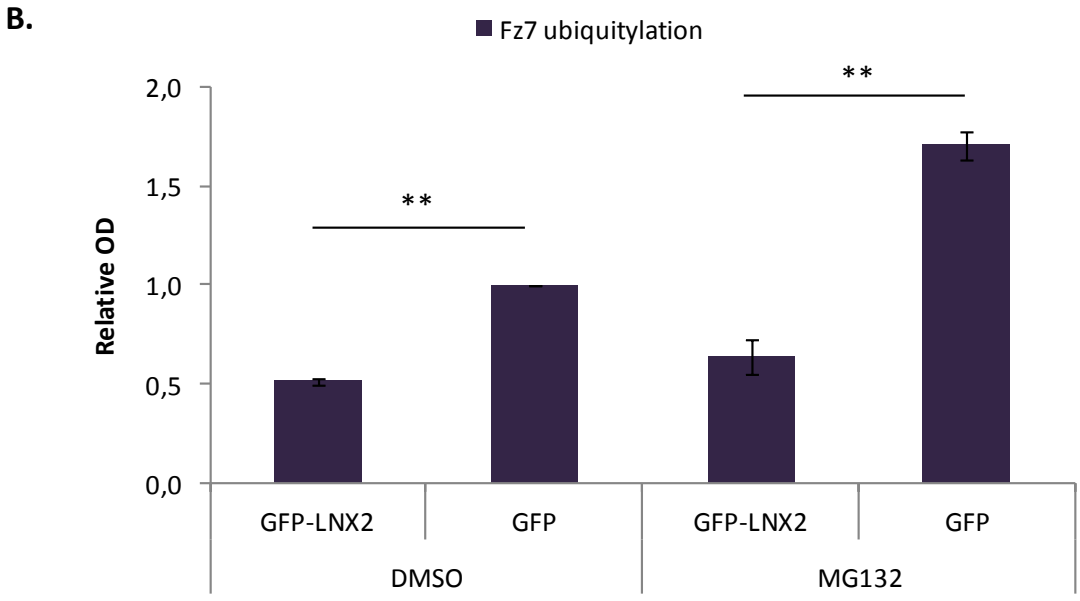
B.
Fz7 ubiquitylation
Relative OD
2,0
1,5
1,0
0,5
0,0
**
**
GFP-LNX2
GFP
GFP-LNX2
GFP
DMSO
MG132

Figure 3.24. LNX2 decrease the level of Fz7 ubiquitylation in the presence of the proteasome inhibitor MG132.

HEK293T cells were co-transfected with GFP-LNX2 (or GFP), FLAG-Fz7 WT and HA-Ubiquitin. Cells were subsequently treated with the proteasome inhibitor MG132 (10 μM) or DMSO for 24h. Subsequently cells were lysed in 0.5% SDS lysis buffer, incubated at 60°C, diluted in 1% Triton X-100 and sonicated. Lysates were subsequently incubated with Anti-FLAG®M2 Magnetic Beads to pull-down FLAG-Fz7, followed by detection of ubiquitylation of Fz7 by immunoblotting with anti-HA antibody. Images depict a representative of three independent experiments. (B) Densitometry analysis of the blots. Optical density (OD) was measured for both, HA-ubiquitin and Fz7. Ratios between densitometry values of immunoprecipitated HA-Ubiquitin and Fz7 were calculated for each sample and presented in the histogram. Ubiquitylation values of Fz7 were standardized to the value of the control sample (Fz7 co-transfected with GFP and not treated with MG132, lane 2). Data shown is an average of at least three independent experiments. The statistical significance was determined by a two-tailed, unpaired Student's t-test (p<0.01).**

3.4.1.3. Mutations in PDZ-BM of Fz7 lead to increased ubiquitylation of the receptor

Given that the interaction of Fz7 with LNX2 involves PDZ domains of the latter and mutations in the C-terminal binding motif of Fz7 inhibit this interaction (section 3.2.3.1.), ubiquitylation of the Fz7 V574G mutant was also examined. The influence of LNX2 on the Fz7 mutant was tested by *in vivo* ubiquitylation assay as described above. These analyses revealed that the Fz7 V574G mutant is ubiquitylated to higher levels than Fz7 WT, compared to samples transfected with GFP only (Figure 3.25.). Ubiquitylation of Fz7 V574G (lane 4) mutant was more than two fold higher, than that of the Fz7 WT (lane 2). Introduction of LNX2 into the cells decreased ubiquitylation of both Fz7 WT and Fz7 V574G mutant. However, the LNX2-induced changes in ubiquitylation levels of Fz7 V574G were not as pronounced as they were in the case of Fz7 WT. The levels of ubiquitylation of Fz7 WT was reduced by 50%, and Fz7 V574G by 40% when transfected with LNX2, though there was higher experimental variation in case of the latter. The analysis of several experiments showed a trend, although the data did not reach statistical significance. These experiments suggest that modulation of Fz7 ubiquitylation by LNX2, might be partially dependent on a direct interaction between these two proteins.

A.

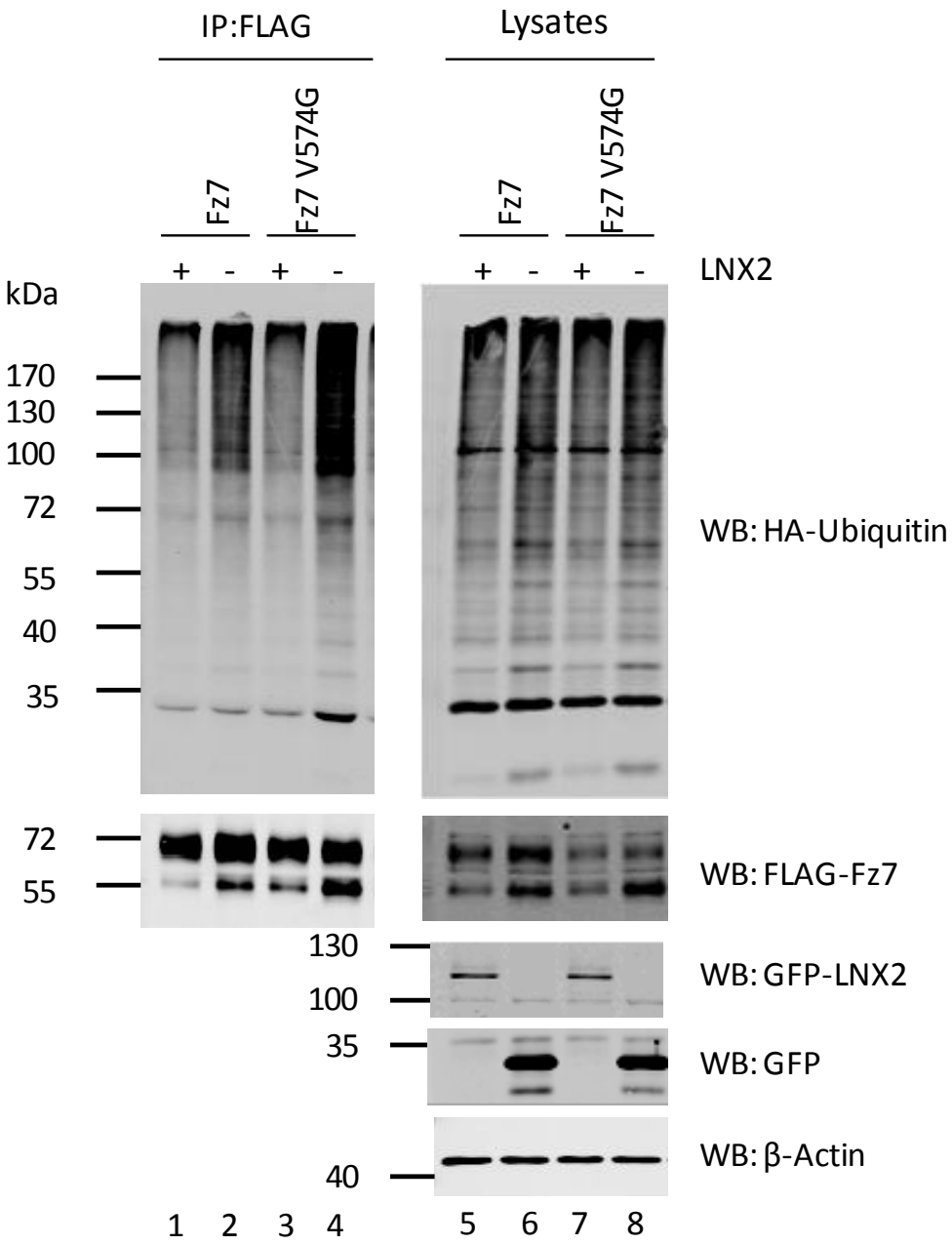
IP:FLAG
Lysates
Fz7
Fz7 V574G
Fz7
Fz7 V574G
+ - + -
+ - + -
LNX2
kDa
170
130
100
72
55
40
35
WB: HA-Ubiquitin
72
55
WB: FLAG-Fz7
130
100
WB: GFP-LNX2
35
WB: GFP
40
WB: β-Actin
1 2 3 4 5 6 7 8

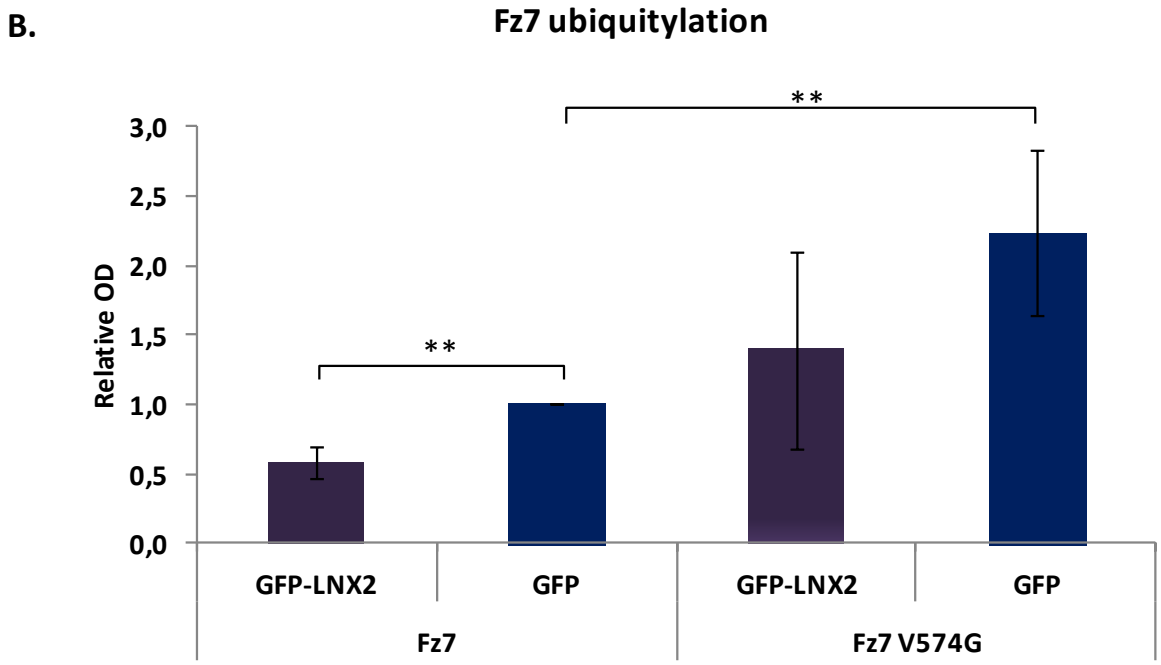

Figure 3.25. LNX2 decreases the levels of Fz7 ubiquitylation with mutation introduced in the PDZ binding motif.

(A) HEK293T cells were co-transfected with GFP-LNX2 or GFP, FLAG-Fz7 (WT or V574G) and HA-Ubiquitin. Subsequently cells were lysed in 0.5% SDS lysis buffer, incubated at 60°C, diluted with 1% Triton X-100 and sonicated. Lysates were incubated with Anti-FLAG®M2 Magnetic Beads, to pull-down FLAG-Fz7, followed by detection of ubiquitylation of Fz7 by immunoblotting with anti-HA antibody. Images depict a representative of three independent experiments. (B) Densitometry analysis of the blots. Optical density (OD) was measured for both, HA-ubiquitin and Fz7. Ratios between densitometry values of immunoprecipitated HA-ubiquitin and Fz7 were calculated for each sample and presented in the histogram. Ubiquitylation values of Fz7 were standardized to the value of the control sample (Fz7 WT co-transfected with GFP, lane 2). Data shown is an average of three independent experiments. The statistical significance was determined by a two-tailed, unpaired Student's t-test (p<0.01).**

3.4.2. LNX2 depletion does not alter Fz7 expression

Given the involvement of LNX2 in Fz7 ubiquitylation, it was important to assess whether knock-down of the enzyme would also influence the levels of expression and the intracellular distribution of the receptor. SKBr3-FLAG-Fz7 and SKBr3-FLAG-Fz7 V574G cells were transfected with siRNA against LNX2 or with control siNeg. 24h later cells were stimulated with Wnt3a conditioned medium or with control conditioned medium. Subsequent analyses were carried out 48h post transfection. The efficiency of LNX2 knock-down was shown to be ~90% in cells transfected with siLNX2compared to control cells. The analysis of Fz7 expression in whole cell lysates (using anti-FLAG pAb), showed an increase in the total expression level of Fz7 WT in non-stimulated LNX2-depleted cells; the expression level was decreased in these cells after stimulation with Wnt3a. By contrast, no changes were observed in Fz7 V574G expression (Figure 3.26.A). In parallel flow cytometry experiments, we found that depletion of LNX2 did not affect surface expression of surface expression of either Fz7 WT or Fz7 V574G proteins as assessed by staining with anti-FLAG mAb (Figure 3.26.B). Finally, no apparent alterations in the receptor localization were observed in cells with transfected with siRNA that target LNX2.

Taken together, apart from the observation that under basal conditions Fz7 WT expression is increased in LNX2-depleted cells, the analysis of total and membrane of Fz7, WT and V574G, as well as examination of receptor cell localization by immunofluorescence didn't indicate that LNX2 knock-down influence major changes in Fz7 expression in SKBr3 cells.

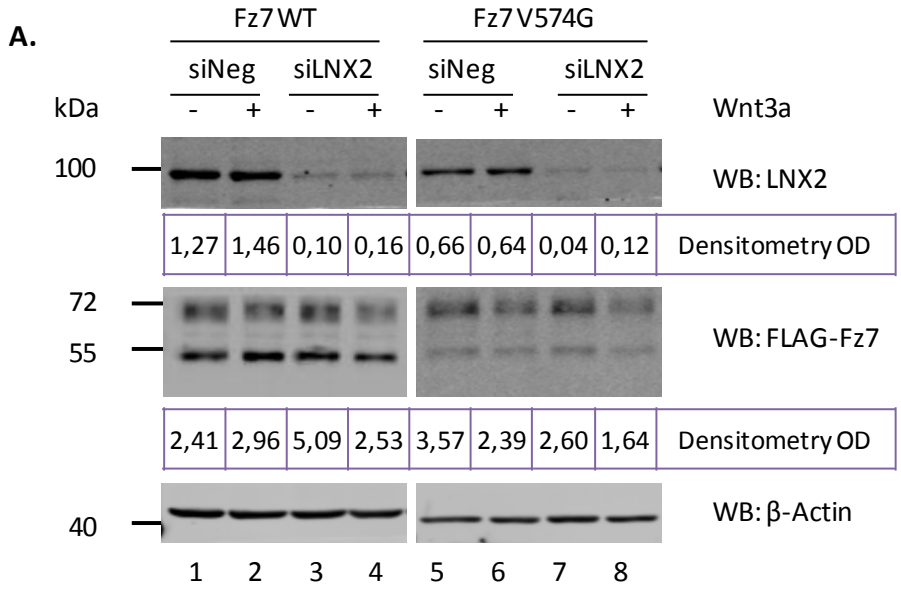
A.
Fz7 WT
Fz7 V574G
siNeg
siLNX2
siNeg
siLNX2
kDa
- + - + - + - + Wnt3a
100
WB: LNX2
1,27 1,46 0,10 0,16 0,66 0,64 0,04 0,12 Densitometry OD
72
55
WB: FLAG-Fz7
2,41 2,96 5,09 2,53 3,57 2,39 2,60 1,64 Densitometry OD
40
WB: β-Actin
1 2 3 4 5 6 7 8

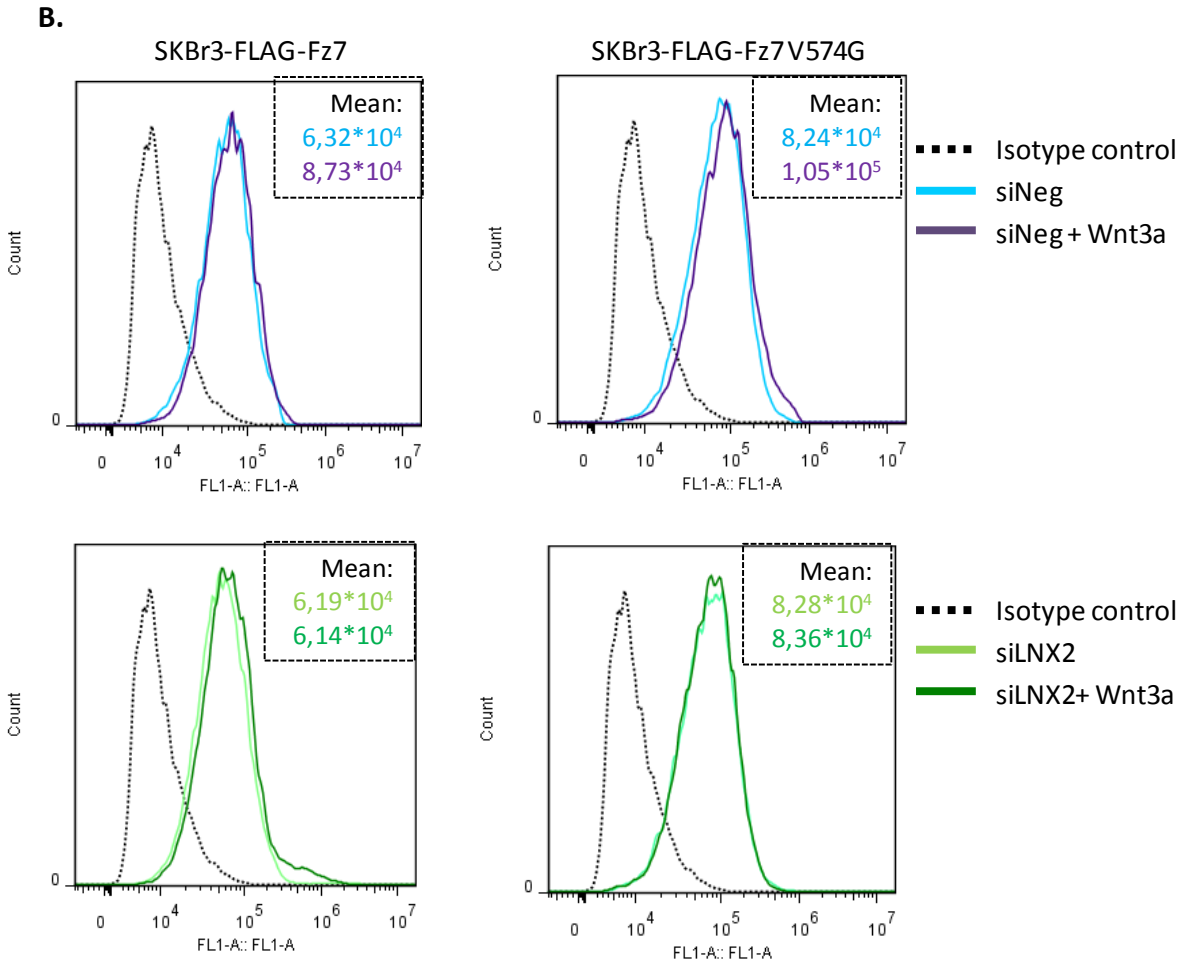
B.
SKBr3-FLAG-Fz7
SKBr3-FLAG-Fz7 V574G
Mean:
6,32*10⁴
8,73*10⁴
Mean:
8,24*10⁴
1,05*10⁵
Isotype control
siNeg
siNeg + Wnt3a
Count
FL1-A:: FL1-A
Mean:
6,19*10⁴
6,14*10⁴
Mean:
8,28*10⁴
8,36*10⁴
Isotype control
siLNX2
siLNX2+ Wnt3a

C.

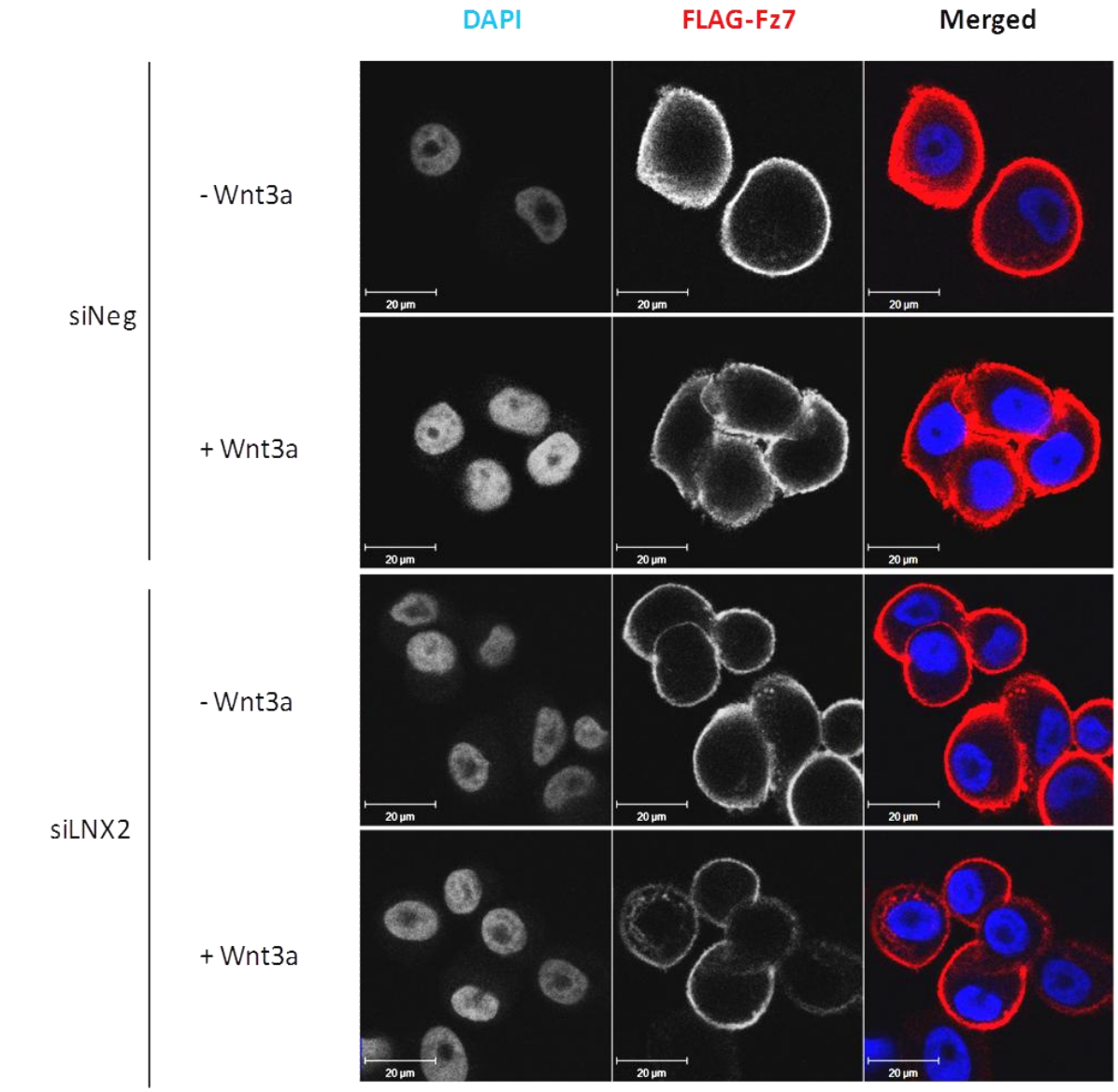
DAPI
FLAG-Fz7
Merged
siNeg
- Wnt3a
+ Wnt3a
siLNX2
- Wnt3a
+ Wnt3a
20 µm

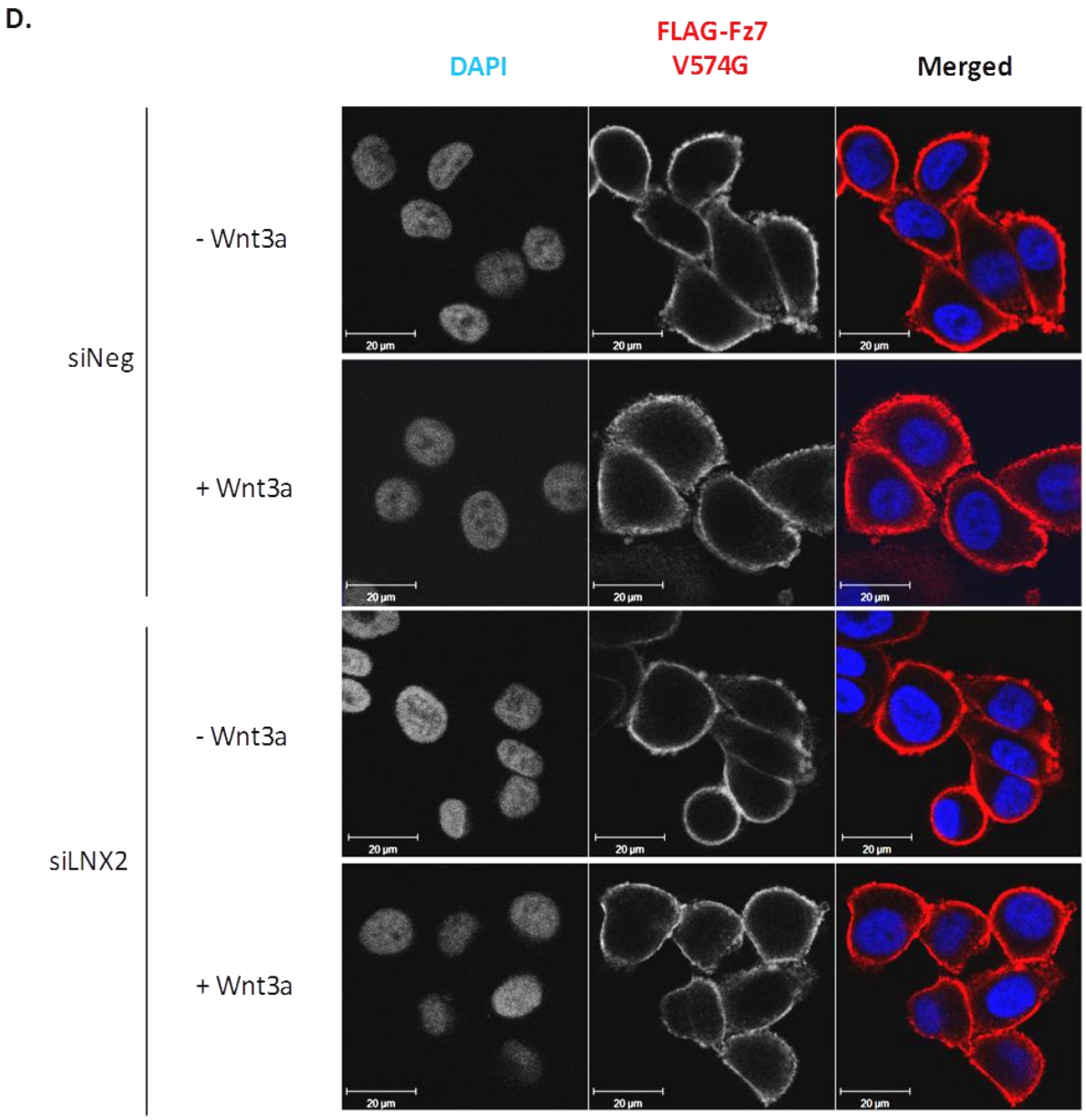
D.
DAPI
FLAG-Fz7
V574G
Merged
siNeg
- Wnt3a
+ Wnt3a
siLNX2
- Wnt3a
+ Wnt3a
20 µm

Figure 3.26. LNX2 depletion does not change Fz7 membrane expression or cell distribution.

SKBr3-FLAG-Fz7 and SKBr3-FLAG-Fz7 V574G cells were transfected with siRNA against LNX2 or with control siNeg. 24h later cells were stimulated with Wnt3a conditioned medium or with control conditioned medium. 48h after the transfection cell lysates were collected and analysed by SDS-PAGE and WB, flow cytometry and immunofluorescence. (A) Lysates of equal protein concentrations (2 μg/μl) were resolved on SDS-PAGE, followed by western blotting with Anti-FLAG pAb to examined Fz7 expression level, anti-LNX2 pAb to monitor LNX2 knock-down level. β-actin served as a loading control. (B) Flow cytometry with anti-FLAG mAb was used to examine membrane expression of Fz7. Cells were incubated on ice for 1h with mouse anti-FLAG (M2) mAb. 4C5G monoclonal antibody against phosphatidylinositol 4-kinase was used as an isotype control. Cell surface staining of FLAG-Fz7 (WT or V574G) was revealed by flow cytometry following incubation for 1h on ice with anti-mouse FITC-conjugated secondary antibodies. Data analysis was carried out using FlowJo analysis software. The values of calculated mean fluorescence are presented in top-right corner of the plots. (C-D) Fz7 WT (C) and V574G (D) cell distribution was analysed by confocal imaging. Cells were fixed and stained with mouse anti-FLAG (M2) mAb and Alexa Fluor 488-conjugated goat-anti mouse Ab (green). DAPI was used to visualize nuclei.

3.4.3. LNX2 is involved in regulation of canonical Wnt signalling pathway in epithelial breast cancer cells

3.4.3.1. LNX2 depletion attenuates canonical Wnt pathway in SKBr3 cell line

Fz7 is a membrane receptor involved in Wnt signalling. LNX2 has been shown to interact with Fz7 in a PDZ dependent manner (section 3.2.3). Given that Fz7 signalling is regulated by interactions via its C-terminal PDZ-BM (section 3.1.5.2.), the role of LNX2 in canonical Wnt pathway signalling was examined. Activation of the pathway was assessed in SKBr3 epithelial breast cancer cell line stably expressing FLAG-Fz7 wild type or FLAG-Fz7 V574G mutant, after LNX2 depletion, using the TOP-Flash reporter assay. SKBr3 cells were transfected with the siRNA targeting LNX2, or with a control siNegative. On the following day, cells were stimulated with Fz7 ligand, Wnt3a, and 24h later, TOPFlash activity was assessed, as described in section 2.5.1 of Materials and Methods. The β-catenin reporter activity was compared in cells with and without LNX2 knock-down (Figure 3.27.). Western blot analysis confirmed the efficiency of LNX2 knockdown (lanes 3, 4, 7 and 8), as the protein expression level was more than 90% lower, when compared with the control samples (lanes 1, 2, 5 and 6). These experiments showed that LNX2 depletion attenuates activation of Wnt signalling in cells expressing wild type Fz7. Cells with LNX2 knockdown were characterized by 50% lower reporter activity, when compared with control cells. On the other hand, LNX2 depletion did not alter Wnt signalling in SKBr3 cells expressing the Fz7 V574G mutant.

Examination of the levels of total β-catenin by western blotting showed that the degree of the protein stabilization in cells corresponds to the TOP-Flash results.

Taken together, LNX2 depletion attenuates canonical Wnt signalling in SKBr3 cells expressing wild type Fz7, but not Fz7 V574G mutant.

A.

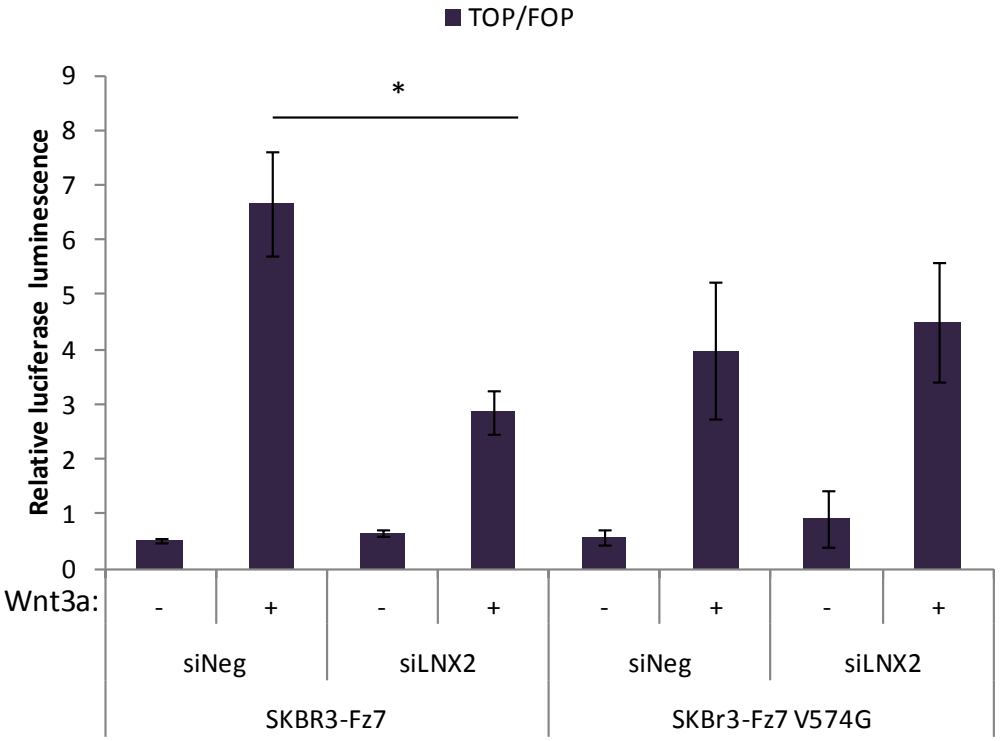
TOP/FOP
Relative luciferase luminescence
9
8
7
6
5
4
3
2
1
0
*
Wnt3a:
-
+
-
+
-
+
-
+
siNeg
siLNX2
siNeg
siLNX2
SKBR3-Fz7
SKBr3-Fz7 V574G

B.

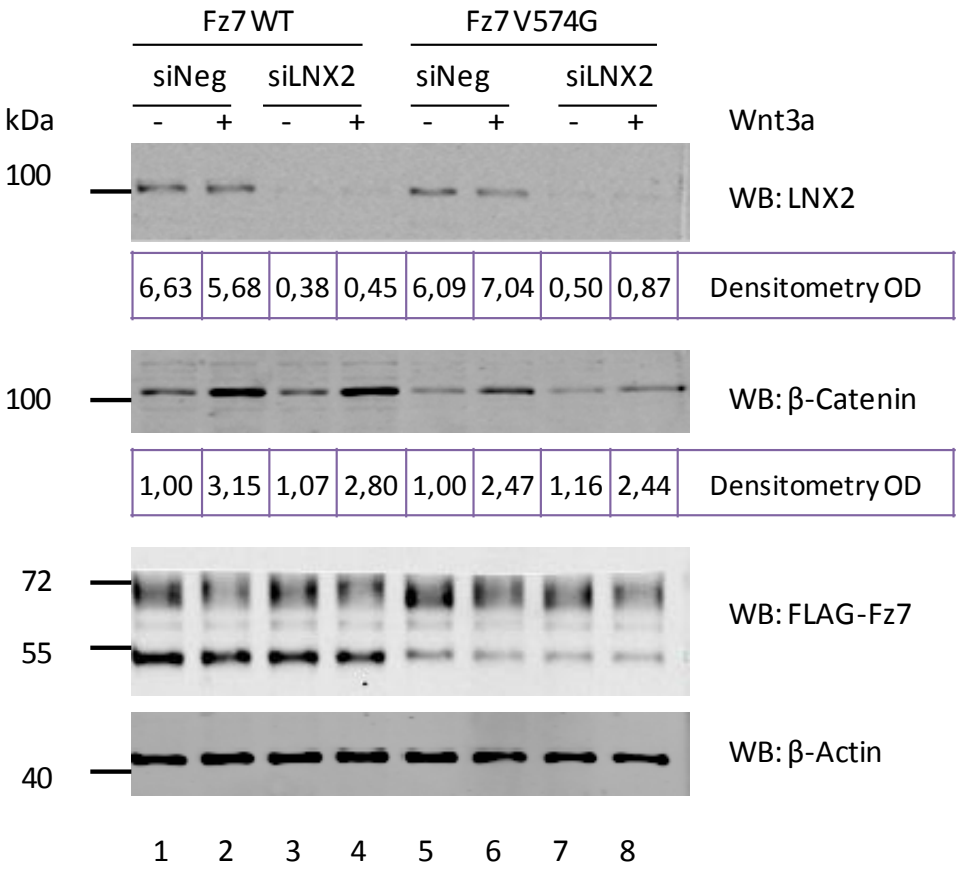
Fz7 WT
Fz7 V574G
siNeg
siLNX2
siNeg
siLNX2
kDa
- + - + - + - +
Wnt3a
100
WB: LNX2
6,63 5,68 0,38 0,45 6,09 7,04 0,50 0,87
Densitometry OD
100
WB: β-Catenin
1,00 3,15 1,07 2,80 1,00 2,47 1,16 2,44
Densitometry OD
72
55
WB: FLAG-Fz7
40
WB: β-Actin
1 2 3 4 5 6 7 8

Figure 3.27. LNX2 depletion attenuates canonical Wnt signalling in SKBr3 cells expressing Fz7 WT.

(A) Wnt-induced signalling was analysed using TOP-Flash luciferase assay. SKBr3-FLAG-Fz7 and SKBr3-FLAG-Fz7 V574G cells were transfected with siRNA against LNX2 or control siNeg. Cells were stimulated for 24h with Wnt3a conditioned medium and TOP/FOP activity was analysed 48h after transfection with reporter plasmids. Tests were done in triplicates and three independent experiments were performed. Statistical significance was determined by two-tailed, unpaired Student's t-test (*p<0.05). (B) Cellular lysates obtained in the assay were examined in SDS-PAGE and WB, with anti-LNX2 pAb, anti-β-catenin mAb, anti-FLAG pAb and anti-β-actin mAb. Image present a representative of three independent experiments. Densitometry analysis was performed on LNX2 and β-catenin immunoreactive bands. Optical densities (OD), standardized to β-actin, are shown for each lane.

3.4.3.2. LNX2 regulates canonical Wnt signalling through its interaction with Fz7

Our results suggest that the direct interaction of LNX2 with Fz7 may regulate canonical Wnt signalling. However, one can't exclude a possibility that LNX2 also interferes with Wnt pathway downstream of Fz7 receptor, or affects alternative pathways which impinge on the canonical Wnt pathway (see Introduction). To address this issue, we compared activation of the canonical Wnt pathway in LNX2-depleted cells either stimulated with Wnt3a, or treated with the GSK3 inhibitor (SB216763), which induced Wnt signalling downstream of the receptor. SKBr3-FLAG-Fz7 cells were transfected with siLNX2 or siNeg and incubated with Wnt3a conditioned medium or control medium. In parallel, cells transfected with siRNA were treated with 10 μM GSK3i or DMSO. Wnt activation was quantified by the TOP-Flash reporter assay 24h later and presented in the Figure 3.28.A. Analysis of the reporter assay showed that LNX2 depletion only downregulates Wnt pathway when cells are stimulated with Wnt3a ligand and not with GSK3i. That result provides an additional evidence for LNX2-mediated regulation of canonical Wnt signalling pathway occurs upstream of GSK3.

A.

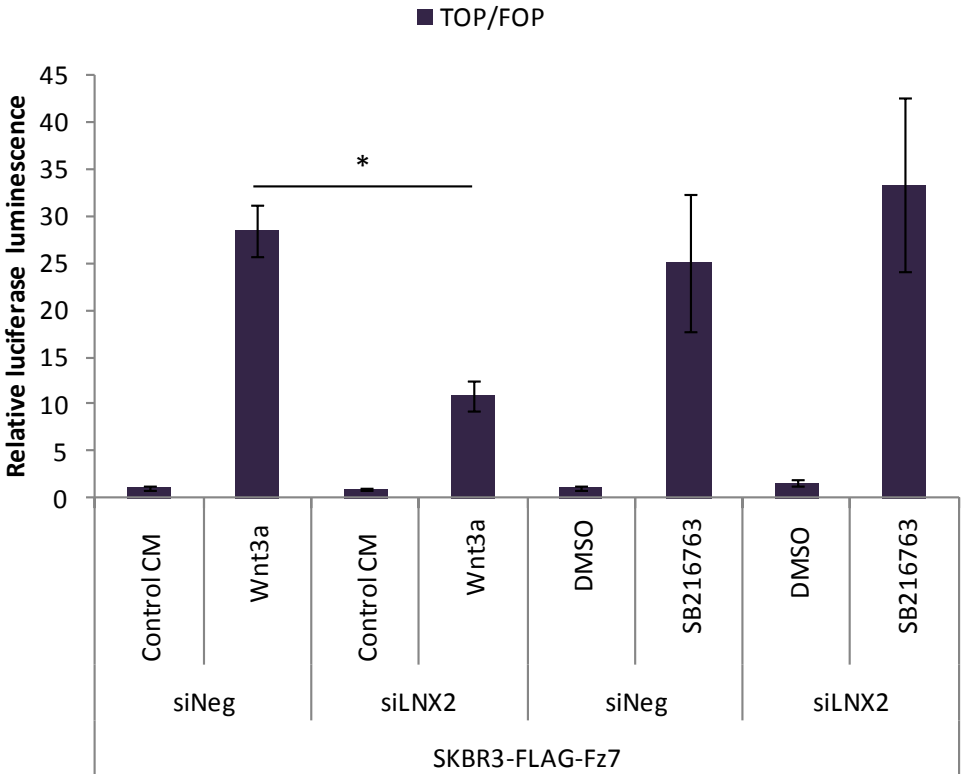
TOP/FOP
Relative luciferase luminescence
45
40
35
30
25
20
15
10
5
0
*
Control CM
Wnt3a
Control CM
Wnt3a
DMSO
SB216763
DMSO
SB216763
siNeg
siLNX2
siNeg
siLNX2
SKBR3-FLAG-Fz7

B.

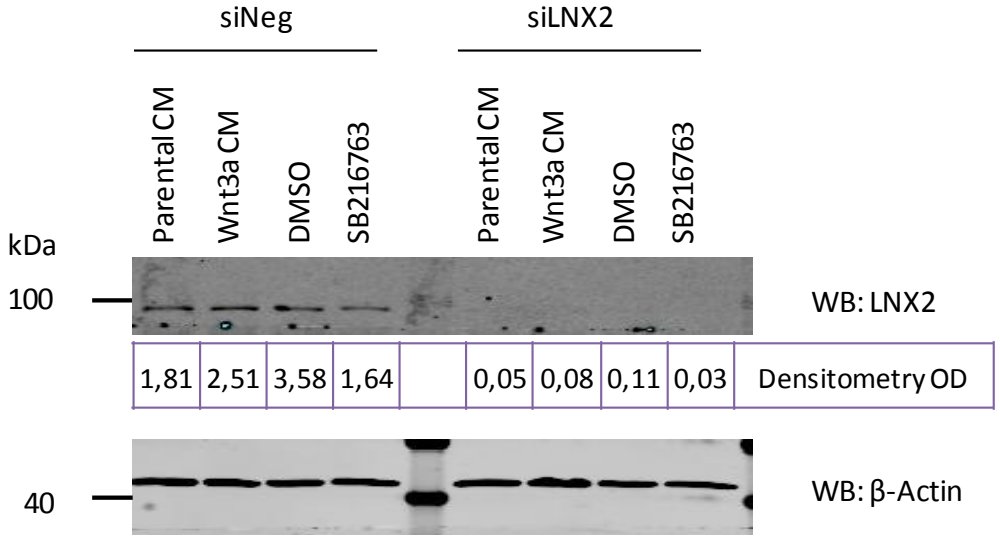
siNeg
siLNX2
Parental CM
Wnt3a CM
DMSO
SB216763
Parental CM
Wnt3a CM
DMSO
SB216763
kDa
100
WB: LNX2
1,81
2,51
3,58
1,64
0,05
0,08
0,11
0,03
Densitometry OD
40
WB: β-Actin

Figure 3. 28. LNX2 regulates canonical Wnt signalling upstream of GSK3.

(A) Wnt-induced signalling was analysed using TOP-Flash luciferase assay. SKBr3-FLAG-Fz7 cells were transfected with siRNA against LNX2 or control siNegative. Cell were stimulated for 24h with Wnt3a conditioned medium or with 10 μM GSK3i (SB216763) and TOP/FOP activity was analysed 48h after transfection with reporter plasmids. Test was done in triplicates and three independent experiments were performed. Statistical significance was determined by two-tailed, unpaired Student's t-test (*p<0.05). (B) Cellular lysates obtained in the assay were examined in SDS-PAGE and WB, with anti-LNX2 pAb and anti-β-actin mAb. Image presents a representative of three independent experiments. Densitometry analysis was performed on LNX2 and immunoreactive bands. Optical densities (OD), standardized to β-actin, are shown for each lane.

3.4.4. Discussion

The work described in the proceeding chapter demonstrate that the E3 ubiquitin ligases: LNX1 and LNX2 are novel binding partners of Fz7. Surprisingly, *in vivo* ubiquitylation experiments demonstrated that overexpression of LNX proteins (LNX1p80, LNX1p70 and LNX2), led to an overall decrease in the levels of ubiquitylatied cellular proteins (i.e. in total protein lysates), as well asa decrease in the levels of Fz7 ubiquitylation compared to control samples. It is important to consider that due to the conditions used in the protocol (incubation of samples for 10 minutes at 60°C before loading on SDS-PAGE gel), it is possible that the anti-HA signals (HA-ubiquitin) observed in the anti-FLAG immunoprecipitate may constitute HA-ubiquitin tagged proteins found in a complex with Fz7. Given that the interaction of Fz7 with LNX2 involves the PDZ domains of the latter, the ubiquitylation of the Fz7 V574G mutant was also investigated (Figure 3.25*).* Basal ubiquitylation of Fz7 V574G was found to be higher than that of Fz7 WT, which identifies a contribution of the Fz7 PDZ-BM in receptor ubiquitylation. Thus, our data seem to indicate that Fz7 is not directly ubiquitylated by LNX proteins, which, in fact, function as negative regulators of ubiquitylation. Although the molecular mechanism(s) underlying this phenomenon remains to be explored, there are several possibilities which may be considered. Firstly, LNX proteins might sterically impede interactions of Fz7 with other ubiquitin ligases. So far, the only identified E3 ubiquitin ligases of Frizzled receptors are two transmembrane proteins ZNRF3 (zinc and ring finger 3) and RNF43 (ring finger 43), detected in LGR5 crypt stem cells and colon cancer (Hao et al. 2012;Koo et al. 2012). Both have been reported to regulate the stability and cell-surface expression of Frizzled receptors (Fz5 and

Fz8) via multiubiquitylation and subsequent targeting for lysosomal degradation. Whether Fz7 is also targeted by ZNRF3 and RNF43 and the structural requirements for specific targeting of Fz receptors by these E3 ligases remain unknown. Another possibility is that different, as yet unidentified, E3 ubiquitin ligase(s) of Fz7 bind to the receptor indirectly via another PDZ partner. In this scenario, overexpressed LNX would out compete the alternative PDZ partners in cells, leading to decreased ubiquitylation of Fz7. Thirdly, one might hypothesise that LNX itself interacts and regulates the activity of an E3 ubiquitin ligase targeting Fz7. To elucidate the mechanism of LNX2 dependent regulation of protein ubiquitylation further experiments are required. Since it is possible that LNX proteins may target other regulators of the ubiquitylation process in cells, it should be assessed whether the E3 ligase activity of LNX2 contributes to the observed decrease of protein ubiquitylation. Introduction of LNX2 with an inactivating mutation in the RING domain in cells expressing Fz7 might be used for this purpose. Employing the novel CRISPR/Cas9 technology would allow to replace endogenous LNX2 with the mutant and should be followed by testing the ubiquitylation of proteins *in vivo*. Fz7 ubiquitylation should also be assessed in cells with LNX1 and LNX2 depletion. Additionally mutations can be introduced in PDZ domains of LNX2 to verify whether such disruption of binding to Fz7 would affect ubiquitylation of the receptor.

Our data appear to indicate that LNX2 modulates Fz7 expression. We have consistently observed that in LNX2-overexpressing cells, the total levels of Fz7 is lower than in control cells. Furthermore, expression of Fz7 V574G mutant, which displays a reduced capacity to bind to PDZ proteins, seems to be less susceptible to the effects of LNX2. In agreement with this observation, LNX2 depletion increases the total expression of Fz7 WT,

but not Fz7 V574G, under basal conditions. At the same time, Fz7 cell surface expression and subcellular localization remains unchanged. It might be possible that LNX2 regulates stability of the receptor by affecting its endocytic trafficking. Recently, Sewduth and colleagues have shown that LNX3/PDZRN3 in endothelial cells ubiquitylates Dvl3 to promote endocytosis of the Fz4/Dvl3 complex, for activation of PCP signalling pathway (Sewduth et al. 2014). However, the proposed mechanisms are unlikely to be similar to the LNX2-dependent regulation of Fz7. The study reports that it is the interaction between LNX3 and PDZ domain of Dvl that is required for recruitment of LNX3 to the Fz4 complex. Interestingly, Dvl3 has been also identified as a binding partner of LNX1 in a proteomic screen presented in (Wolting et al. 2011). Performing biotinalytion assay on Fz7 expressing cells, when LNX2 is overexpressed or depleted, would provide further evidence whether this protein is (or is not) involved in regulation of Fz7 cell surface expression. Futhermore, assessing Fz7 expression and trafficking using bafilomycin A1, would allow LNX2 plays role in lysosome-dependent degradation of the receptor.

Finally, LNX2 role in regulation of the canonical Wnt signalling was examined. We have established that LNX2 is a novel regulator of Fz7 signalling in breast cancer cells. Importantly, the contribution of LNX2 to β–catenin signalling was not observed in cells expressing Fz7 V574G thus further emphasising the importance of the C-terminal PDZ-BM in the canonical Wnt pathway. It was previously reported that siRNA-mediated silencing of LNX2 downregulates Wnt signalling in colorectal cancer cells (Camps et al. 2013). Our data obtained in breast cancer are in agreement with this report. Whilst, Camps and colleagues have not determined what is the mechanism of Wnt signalling regulation by LNX2, our results strongly indicate that the direct interaction of LNX2 with Fz7 receptor is an important

factor. It is also possible that LNX2 interacts with other proteins that form complex with Fz7, for example Dishevelled. As already mention, one of the Dishevelled isoforms, Dvl3, has been found to interact with LNX1 and LNX3 (Sewduth et al. 2014;Wolting et al. 2011). Although the authors haven't reported a role of those proteins in canonical Wnt signalling.

In summary, in this chapter we have reported LNX2 as a novel regulator of Fz7-dependent canonical Wnt signalling in breast cancer cells. We have found out that LNX2 plays role in regulation of Fz7 ubiquitylation and expression level, which might be responsible for the modulation of the receptor signalling. It was proposed previously that the expression level of Frizzled receptor correlates with Wnt responsiveness, is controlled by the interplay between E3 ubiquitin ligase and an deubiquitylating enzyme (Mukai et al. 2010). However further study is required to elucidated the exact mechanisms underlying the role of LNX2 in Fz7 functions.

4. GENERAL DISCUSSION AND FUTURE WORK

Activation of Wnt signalling, as evidenced by nuclear localisation of β−catenin, has been previously observed in human breast cancer (Lin at al. 2000; Lopez-Knowles et al. 2010). However, unlike colorectal cancer, this is not a consequence of mutations in APC or β−catenin (Candidus et al. 1996;Sorlie et al. 1998), but instead deregulation frequently occurs through epigenetic modulation of key target genes (Klarmann et al. 2008;Suzuki et al. 2008). Frizzled-7 seems to be one of the most important Wnt receptors involved in breast cancer. Its expression is characteristic for triple-negative breast cancer (TNBC) and TNBC-derived cell lines, where it activates the β-catenin/Wnt pathway and plays a crucial role in regulation of cell proliferation (Yang et al. 2011). PDZ domain-containing proteins are often involved in regulation of cell signalling. Indeed, several of them have been implicated in Wnt signalling. The aim of our study was to determine the role of PDZ domain-containing proteins in modulating Frizzled-7 signalling and its trafficking pathways, in the context of epithelial breast cancer cells. Obtained data demonstrate the importance of the C-terminal PDZ-BM of Frizzled receptors in canonical Wnt signalling. Focusing on syntenin-1 and LNX2, we reported them as novel regulators of Frizzled-7 and Wnt signalling. Finally, we have also laid out a strong platform for future investigations by identifying novel binding partners of Frizzled-7.

Firstly, we have demonstrated, for the first time, the importance of the C-terminal PDZ-BM of Frizzled-7 for the correct functioning of the receptor. Our findings illustrate that Frizzled-7 interactions mediated by the C-terminal PDZ binding motif are crucial for regulation of trafficking and signalling of the receptor. Investigation of these processes in more detail and, particularly, the contribution of the newly identified Fz7 partners will certainly be merited in the future. Our data seem to suggest that mutation introduced in C-terminal PDZ binding site alters Fz7 maturation process, demonstrated by changes in ratio between expression levels of two monomers with different degree of glycosylation. The detailed mechanism of the receptor maturation and the role of Fz7 glycosylation in signalling have not been addressed widely in the past. Thus it would be important to further explore the involvement of PDZ proteins in the process. So far, the only known regulator of Fz7 glycosylation is Shisa, protein localized in the ER (Yamamoto et al. 2005). However, since it does not contain a PDZ domain, its interaction with Frizzled-7 does not explain observed changes occurring after introduction of mutations into PDZ-BM of the receptor. Thus, it is likely that other mechanisms are involved.

Secondly, our findings clearly indicate the involvement of syntenin-1 in the modulation of Fz7 signalling in the canonical Wnt pathway and in the trafficking of the receptor. Syntenin-1 was reported as an adaptor for a number of transmembrane proteins (Beekman et al. 2008), thus it may act as a platform for bringing other proteins into the complex with Fz7. Among those proteins syndecans and tetraspanins are of a particular interest, given their well-established role as modulators of signalling and trafficking. Furthermore, syntenin-1, in complex with syndecans and ALIX, was shown to recruit syndecan-associated proteins to multivesicular endosomes and exosomes (Baietti et al. 2012).

This might explain Fz7 redistribution from plasma membrane in cells overexpressing syntenin-1. However syndecans, similarly like Fz7, were shown to bind preferentially to PDZ2 of syntenin-1, even though both PDZ domains seem to be essential for the association (Grootjans et al. 2000). Therefore, they might compete with Fz7 for binding to syntenin-1. On the other hand, tetraspanin CD63 binds syntenin-1 via PDZ1 (Latysheva et al. 2006). CD63 is a transmembrane protein present in plasma membrane, but also in lysosomes and late endosomes. It is enriched on the intraluminal vesicles, which are secreted as exosomes. Additionally CD63 is implicated to function as a regulator of a transport of its interacting partners (Pols et al. 2009). Thus it may contribute to the receptor trafficking by forming a tripartite complex with Fz7 and syntenin-1. Another possibility may involve syntenin-1 ability to link transmembrane proteins to ubiquitylated proteins. Ubiquitin binding seems to be an important factor controlling syntenin-1 relocalization to late endocytic compartments (Rajesh et al. 2011). To verify whether Fz7 redistribution depends on syntenin-1 interaction with ubiquitin, one may analyze receptor localization in syntenin-depleted cells and reconstituted with various syntenin-1 mutants, unable to bind ubiquitin. Interestingly, ubiquitin binding involves a specific motif in the N-terminal domain of syntenin-1 and is controlled by Ulk-1 dependent phosphorylation (Rajesh et al. 2011). Ulk-1 is a Ser/Thr kinase involved in regulation of different trafficking pathways, but also plays a crucial role in autophagy. Since autophagy was recently reported to attenuate canonical Wnt signalling in colon cancer, there is possibility for syntenin-1-Ulk-1 involvement in the process (Gao et al. 2010a;Zhang et al. 2011). Considering all possible scenarios, it is important to determine the fate of Fz7 in cells expressing syntenin-1.

Thirdly, our data demonstrate, for the first time, that direct interaction of Frizzled-7 with LNX proteins modulates canonical Wnt signalling mediated by the receptor in epithelial breast cancer cells. Our findings have identified several avenues in need of further investigation in order to fully understand the contribution of these proteins in regulation of Frizzled functionality. Proteins from LNX family of molecular scaffolds were reported to act as E3 ubiquitin ligases (D'Agostino et al. 2011;Nie et al. 2002). However, our data clearly demonstrate that Fz7 is not a substrate for ubiquitylation by LNX1 or LNX2, two proteins identified in proteomics analysis. Interestingly, overexpression of these proteins leads to a significant decrease of Fz7 ubiquitylation level. These findings indicate that after all LNX proteins are involved in regulation of Fz7 ubiquitylation, nonetheless via an unknown mechanism. Our results point towards previously unsuspected function of LNX as an adaptor protein or a competitive inhibitor of ubiquitylation. Therefore, it would be essential to do more research into a structural aspect of the Fz7-LNX interaction. In this regard our observation concerning the differential association of Fz7 with LNX1 isoforms is particularly intriguing. Overexpression of both LNX1 isoforms decreases Fz7 ubiquitylation, even though LNX1p80 did not bind to Fz7, as shown in the immunoprecipation assay. On the other hand, LNX1p70, lacking the RING domain, forms a complex with Fz7 and affects the receptor in a similar way as LNX2. One also needs to identify a relevant Fz7 ubiquitin ligase and understand the relationship between LNX and this enzyme. A starting point here might involve establishing a possible link between LNX proteins and ZNRF3 or RNF43, ubiquitin ligases that were shown to target other Fz receptors (Hao et al. 2012;Koo et al. 2012).

Finally, we have identified a number of novel putative binding partners of Fz7; namely INADL/PATJ, MPDZ, Scribble, DLG1, ZO-1, ZO-2, PALS1/MPP5, MPP7, MAGI1,

MAGI3, SNX27, LNX1, LNX2. These PDZ proteins have been previously shown to be involved in regulation of trafficking of other membrane receptors, as well as in establishment of cell polarity. One of them is SNX27, sorting nexin-27, an endosome-associated adaptor controlling recycling of proteins to plasma membrane (Temkin et al. 2011). It is highly probable that SNX27 regulates Fz7 trafficking between endosomes and plasma membrane. Thus it would be very interesting to investigate the interaction between these two proteins and its functional implications. Interestingly, recycling activity of SNX27 requires both, PDZ domain–dependent binding of the cytoplasmic tail of the ligand and Phox homology (PX) domain–dependent interaction with the phosphoinositides in endosome membrane (Lauffer et al. 2010). Hence, one speculate about possible link between SNX27 and syntenin-1 through phosphoinositides, as the latter also interacts with PtdIns, but via PDZ1 domain (Zimmermann 2006). Furthermore, SNX27 was shown recently to cooperate with two other PDZ proteins (GOPC/PIST and NHERF1/3) in regulation of the subcellular localization and plasma membrane availability of a GPCR protein, somatostatin receptor subtype 5 (SSTR5) (Bauch et al. 2014). It was reported that those PDZ proteins act sequentially on the transmembrane ligand during the subcellular trafficking. Accordingly, it is possible that a similar mechanism regulates Frizzled receptor trafficking. Last but not least, a very interesting link emerges between Fz7 and basoapical cell polarity, as several of the identified proteins are components of polarity complexes. Fz7 has been implicated in regulation of planar cell polarity (Dijksterhuis et al. 2014), yet it wasn't associated with basoapical polarity. Basoapical polarity in epithelial cells relies on three conserved complexes, two apical: Crumbs (Crumbs/PALS/PATJ) and Par (Par3/Par6/aPKC/Cdc42) and one basolateral: Scribble (Scribble/Dlg/Lgl) (Bazzoun et al. 2013). In the proteomic screen we have identified

PALS and PATJ (Crumbs complex), as well as Scribble and DLG1 (Scribble complex). The Crumbs complex regulates tight junction maintenance, whereas the Scribble complex associates with adherence junctions and controls their segregation from tight junctions. We have also identified ZO-1 and ZO-2 (elements of tight junctions) and MPP7, protein interacting with DLG1, as potential interactors of Fz7. Due to the fact that many of the proteins mentioned above associate with each other, it is crucial to find among them a primary binding partner (or partners) of Fz7. Subsequently the function and relevance of this interaction should be assessed. Importantly, the involvement of the polarity proteins in the distribution of Fz7 needs to be examined. Furthermore, the possible involvement of these interactions in the EMT (epithelial-to-mesenchymal transition) should be also considered. Basoapical polarity is tightly regulated in epithelial cells and its loss correlates with gaining migratory and invasive properties by cells (Talbot et al. 2012). Since activation of Wnt signalling promotes EMT in cancer cells, it would be beneficial to establish whether interaction between Fz7 and polarity proteins plays role in the process.

In summary, the data presented in this study demonstrate the importance of Frizzled-7 interactions through its C-terminal PDZ binding motif. Our findings provide an insight into the role of PDZ domain containing proteins, focusing on LNX2 and syntenin-1, in regulation of Fz7 functions in breast cancer cells. The mechanisms in which the two proteins regulate Fz7 functions seem to be distinct, as evidenced by different effects on the receptor function when introduced into the model system. Nonetheless, both of them modulate canonical Wnt signalling in epithelial breast cancer cells due to their binding to Fz7

.

5. APPENDIX: SUPPLEMENTARY FIGURES

A.

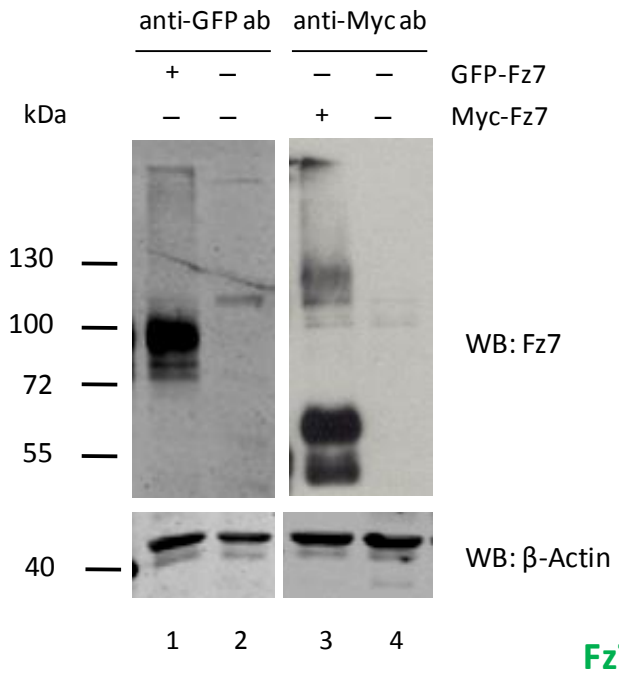

B.

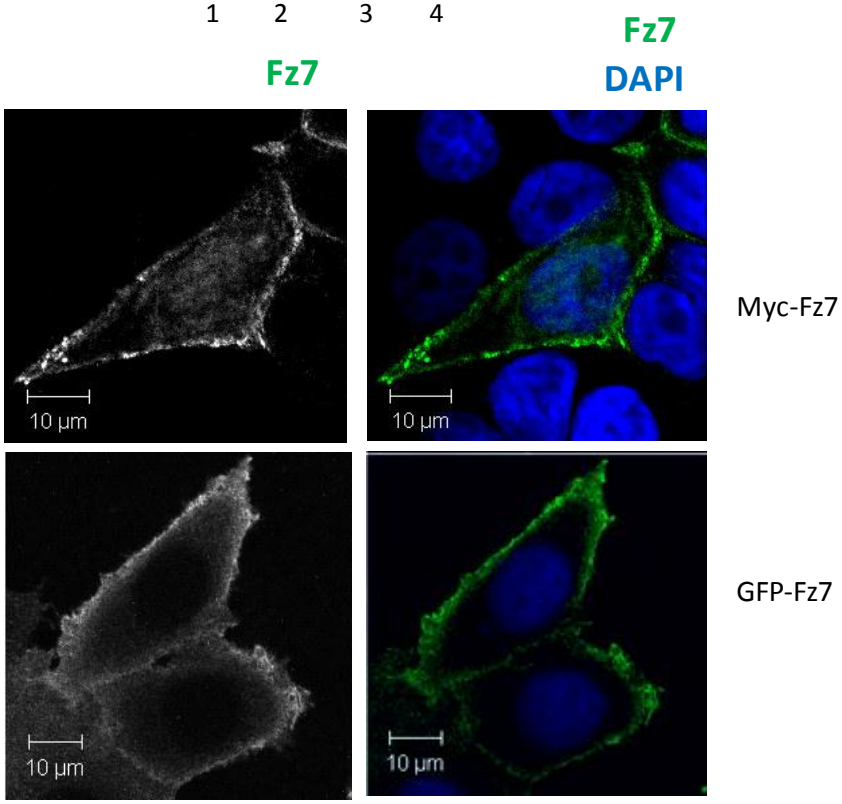

Figure S. 1. Characterization of Myc-Fz7 and GFP-Fz7 expression constructs.

(A) Western blot analysis of whole cell lysates of HEK293T cells transiently transfected with GFP-Fz7 (lane 1) or Myc-Fz7 (lane 3) expression vectors. Cells were lysed in 1% Triton X-100 and lysates of equal protein concentration were resolved by SDS-PAGE under non-reduced conditions, followed by detection with rabbit anti-GFP or rabbit anti-Myc antibodies. β-actin served as a loading control. (B) MCF7 cells transiently transfected with Myc-Fz7 or GFP-Fz7 expression vector display membrane immunoreactivity. 48h after transfection cells were fixed and stained with mouse anti-Myc mAb and Alexa Fluor 488-conjugated goat-anti mouse ab (green). Autofluorescence of GFP was examined. DAPI was used to visualize nuclei.

A.

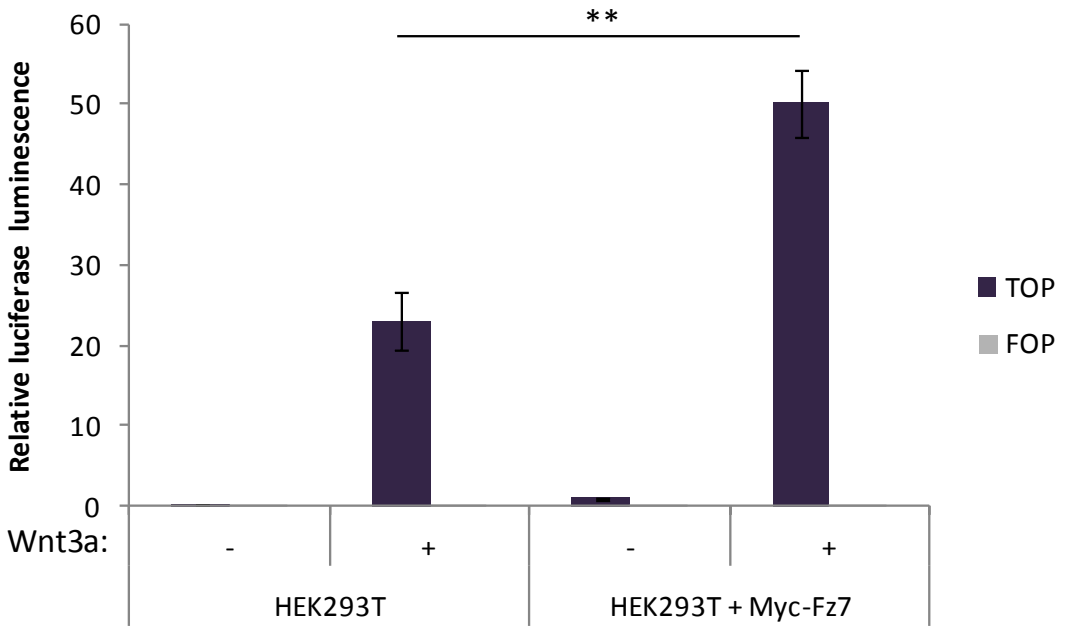
**
Relative luciferase luminescence
60
50
40
30
20
10
0
Wnt3a:
-
+
-
+
HEK293T
HEK293T + Myc-Fz7
TOP
FOP

B.

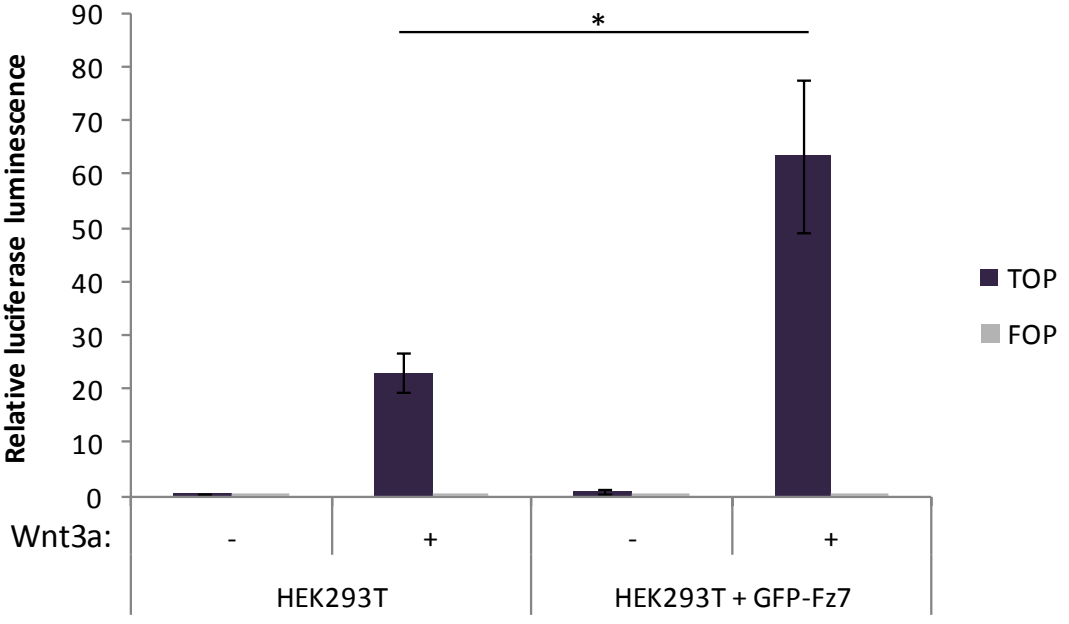
*
Relative luciferase luminescence
90
80
70
60
50
40
30
20
10
0
Wnt3a:
-
+
-
+
HEK293T
HEK293T + GFP-Fz7
TOP
FOP

Figure S. 2. Verification of Myc-Fz7 and GFP-Fz7 constructs functionality.

Wnt3a-induced signalling was analysed using TOP-Flash luciferase assay. HEK293T cells were transfected with reporter plasmids and with plasmid encoding Myc-Fz7 (A), GFP-Fz7 (B) or mock transfected. Cells were stimulated for 24h with Wnt3a conditioned medium and TOP/FOP activity was analysed 48h after the transfection. Test was done in triplicates and three independent experiments were performed. Statistical significance was determined by two-tailed, unpaired Student's t-test (* $p<0.05$; ** $p<0.01$)

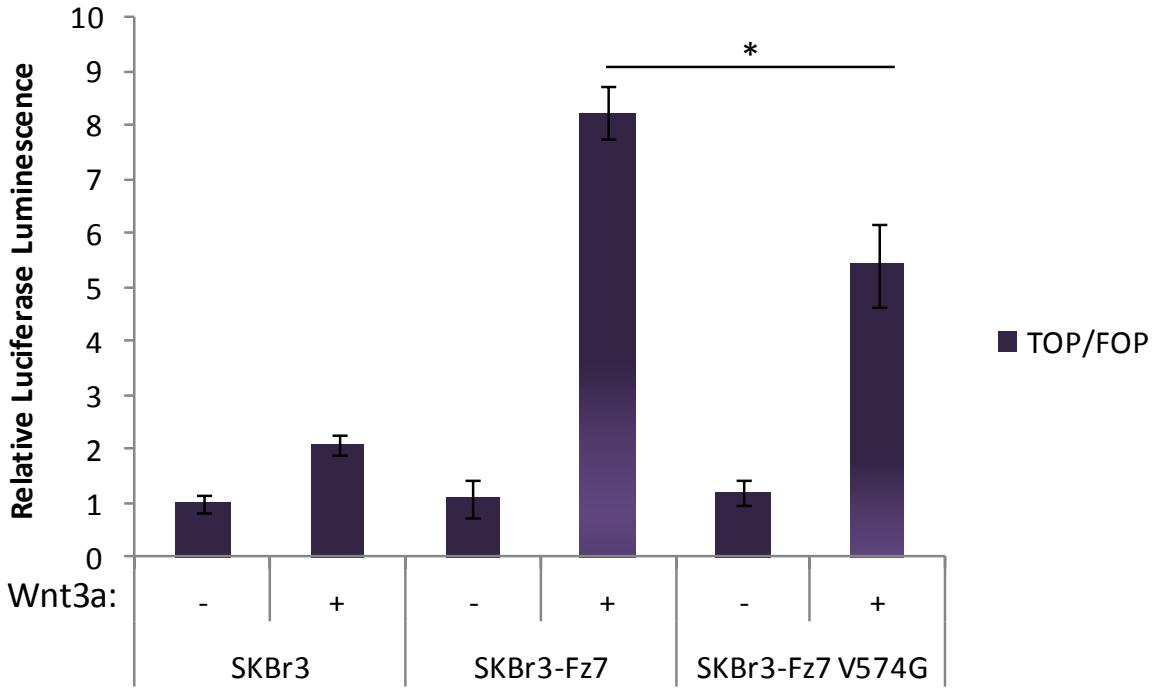

Figure S. 3. Mutation in C-terminal PDZ-binding motif of Fz7 attenuates canonical Wnt signalling pathway in SKBr3 cells.

Wnt-induced signalling was analysed using TOP-FLASH luciferase assay. SKBr3 breast cancer cells were stably transfected with Fz7 (WT or V574G). Cells were stimulated for 24h with Wnt3a conditioned medium and TOP/FOP activity was analysed 48 hours after the transfection with reporter plasmids. Test was done in triplicates and three independent experiments were performed. Statistical significance was determined by two-tailed, unpaired Student's t-test (*p<0.05).

A.

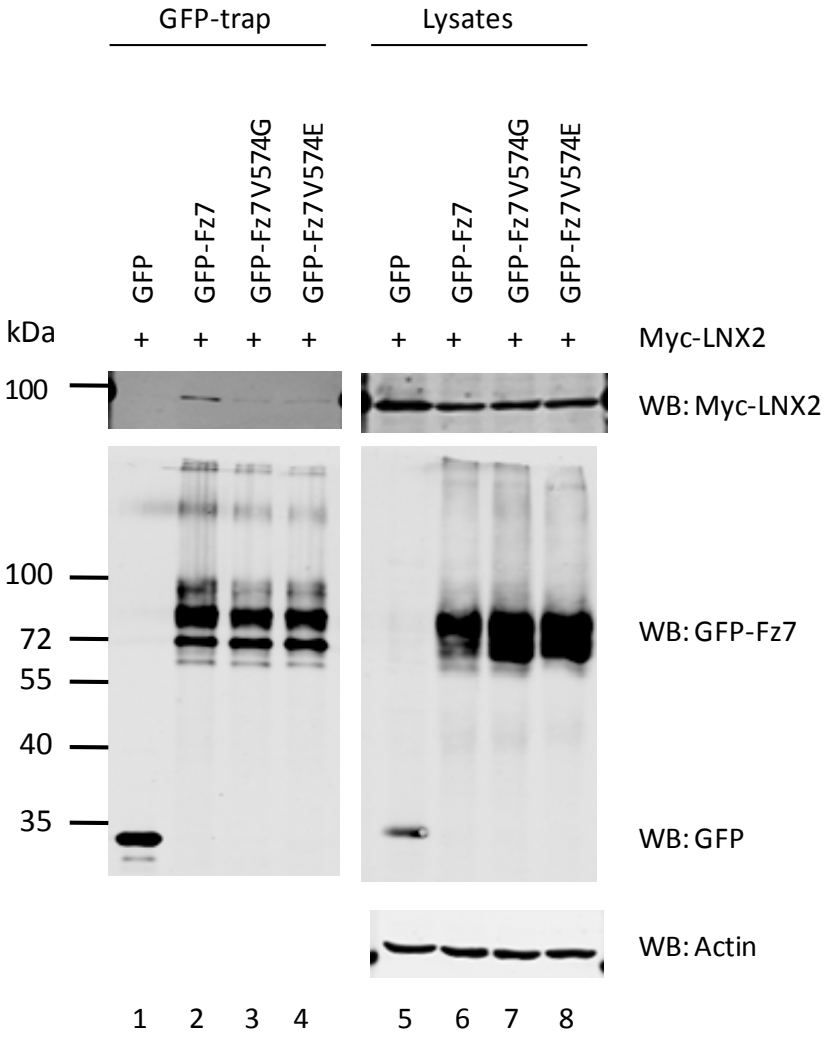
GFP-trap
Lysates
GFP
GFP-Fz7
GFP-Fz7V574G
GFP-Fz7V574E
kDa
Myc-LNX2
100
WB: Myc-LNX2
100
72
55
40
35
WB: GFP-Fz7
WB: GFP
WB: Actin
1 2 3 4 5 6 7 8

B.

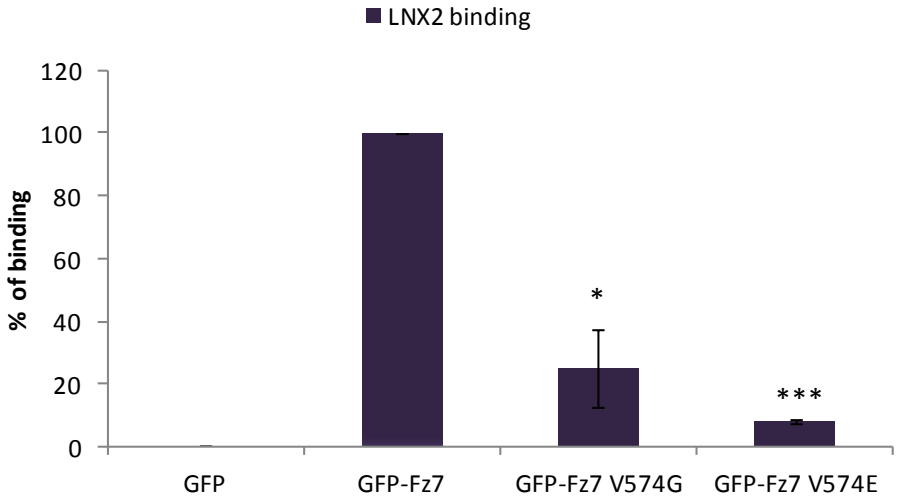
LNX2 binding
% of binding
120
100
80
60
40
20
0
*
***
GFP
GFP-Fz7
GFP-Fz7 V574G
GFP-Fz7 V574E

Figure S. 4. Fz7 interaction with LNX2 involves PDZ domains (GFP-trap).

(A) HEK293T cells were co-transfected with GFP, GFP-Fz7 (WT, V574G or V574E) and Myc-LNX2. 24h after transfection cells were lysed in 1% Triton X-100 and lysates were incubated with GFP-Trap beads. After immunoprecipitation, retained proteins were resolved by SDS-PAGE, followed by western blotting and protein detection using mouse anti-Myc mAb and rabbit anti-GFP pAb. Images depict representatives of two independent experiments. (B) Densitometry analysis performed on data obtained in two independent experiments and demonstrated on a histogram, plotted as percentage of LNX2 binding to Fz7 mutants relative to the interaction of LNX2 with the wild type Fz7 (taken as 100%). The statistical significance was determined by a two-tailed, unpaired Student's t-test (*p<0.05; *** p<0.001).

6. LIST OF REFERENCES

Acconcia, F., Sigismund, S., & Polo, S. 2009, "Ubiquitin in trafficking: the network at work", *Exp.Cell Res.*, vol. 315, no. 9, pp. 1610-1618.

Ai, L., Tao, Q., Zhong, S., Fields, C. R., Kim, W. J., Lee, M. W., Cui, Y., Brown, K. D., & Robertson, K. D. 2006, "Inactivation of Wnt inhibitory factor-1 (WIF1) expression by epigenetic silencing is a common event in breast cancer", *Carcinogenesis*, vol. 27, no. 7, pp. 1341-1348.

Akiri, G., Cherian, M. M., Vijayakumar, S., Liu, G., Bafico, A., & Aaronson, S. A. 2009, "Wnt pathway aberrations including autocrine Wnt activation occur at high frequency in human non-small-cell lung carcinoma", *Oncogene*, vol. 28, no. 21, pp. 2163-2172.

Amit, S., Hatzubai, A., Birman, Y., Andersen, J. S., Ben-Shushan, E., Mann, M., Ben-Neriah, Y., & Alkalay, I. 2002, "Axin-mediated CKI phosphorylation of beta-catenin at Ser 45: a molecular switch for the Wnt pathway", *Genes Dev.*, vol. 16, no. 9, pp. 1066-1076.

Anastas, J. N. & Moon, R. T. 2013, "WNT signalling pathways as therapeutic targets in cancer", *Nat.Rev.Cancer*, vol. 13, no. 1, pp. 11-26.

Angers, S., Thorpe, C. J., Biechele, T. L., Goldenberg, S. J., Zheng, N., MacCoss, M. J., & Moon, R. T. 2006, "The KLHL12-Cullin-3 ubiquitin ligase negatively regulates the Wnt-beta-catenin pathway by targeting Dishevelled for degradation", *Nat.Cell Biol.*, vol. 8, no. 4, pp. 348-357.

Armbruester, V., Sauter, M., Roemer, K., Best, B., Hahn, S., Nty, A., Schmid, A., Philipp, S., Mueller, A., & Mueller-Lantzsch, N. 2004, "Np9 protein of human endogenous retrovirus K interacts with ligand of numb protein X", *J.Virol.*, vol. 78, no. 19, pp. 10310-10319.

Assemat, E., Bazellieres, E., Pallesi-Pocachard, E., Le, B. A., & Massey-Harroche, D. 2008, "Polarity complex proteins", *Biochim.Biophys.Acta*, vol. 1778, no. 3, pp. 614-630.

Ataman, B., Ashley, J., Gorczyca, D., Gorczyca, M., Mathew, D., Wichmann, C., Sigrist, S. J., & Budnik, V. 2006, "Nuclear trafficking of Drosophila Frizzled-2 during synapse development requires the PDZ protein dGRIP", *Proc.Natl.Acad.Sci.U.S.A*, vol. 103, no. 20, pp. 7841-7846.

Ayyanan, A., Civenni, G., Ciarloni, L., Morel, C., Mueller, N., Lefort, K., Mandinova, A., Raffoul, W., Fiche, M., Dotto, G. P., & Brisken, C. 2006, "Increased Wnt signaling triggers oncogenic conversion of human breast epithelial cells by a Notch-dependent mechanism", *Proc.Natl.Acad.Sci.U.S.A*, vol. 103, no. 10, pp. 3799-3804.

Bafico, A., Liu, G., Goldin, L., Harris, V., & Aaronson, S. A. 2004, "An autocrine mechanism for constitutive Wnt pathway activation in human cancer cells", *Cancer Cell*, vol. 6, no. 5, pp. 497-506.

Baietti, M. F., Zhang, Z., Mortier, E., Melchior, A., Degeest, G., Geeraerts, A., Ivarsson, Y., Depoortere, F., Coomans, C., Vermeiren, E., Zimmermann, P., & David, G. 2012, "Syndecan-syntenin-ALIX regulates the biogenesis of exosomes", *Nat.Cell Biol.*, vol. 14, no. 7, pp. 677-685.

Balana, B., Maslennikov, I., Kwiatkowski, W., Stern, K. M., Bahima, L., Choe, S., & Slesinger, P. A. 2011, "Mechanism underlying selective regulation of G protein-gated inwardly rectifying potassium channels by the psychostimulant-sensitive sorting nexin 27", *Proc.Natl.Acad.Sci.U.S.A*, vol. 108, no. 14, pp. 5831-5836.

Balasubramanian, S., Fam, S. R., & Hall, R. A. 2007, "GABAB receptor association with the PDZ scaffold Mupp1 alters receptor stability and function", *J.Biol.Chem.*, vol. 282, no. 6, pp. 4162-4171.

Bauch, C., Koliwer, J., Buck, F., Honck, H. H., & Kreienkamp, H. J. 2014, "Subcellular sorting of the G-protein coupled mouse somatostatin receptor 5 by a network of PDZ-domain containing proteins", *PLoS.One.*, vol. 9, no. 2, p. e88529.

Bazzoun, D., Lelievre, S., & Talhouk, R. 2013, "Polarity proteins as regulators of cell junction complexes: implications for breast cancer", *Pharmacol.Ther.*, vol. 138, no. 3, pp. 418-427.

Beekman, J. M. & Coffer, P. J. 2008, "The ins and outs of syntenin, a multifunctional intracellular adaptor protein", *J.Cell Sci.*, vol. 121, no. Pt 9, pp. 1349-1355.

Behrens, J., von Kries, J. P., Kuhl, M., Bruhn, L., Wedlich, D., Grosschedl, R., & Birchmeier, W. 1996, "Functional interaction of beta-catenin with the transcription factor LEF-1", *Nature*, vol. 382, no. 6592, pp. 638-642.

Bengochea, A., de Souza, M. M., Lefrancois, L., Le, R. E., Galy, O., Chemin, I., Kim, M., Wands, J. R., Trepo, C., Hainaut, P., Scoazec, J. Y., Vitvitski, L., & Merle, P. 2008, "Common dysregulation of Wnt/Frizzled receptor elements in human hepatocellular carcinoma", *Br.J.Cancer*, vol. 99, no. 1, pp. 143-150.

Bentzinger, C. F., von, M. J., Dumont, N. A., Stark, D. A., Wang, Y. X., Nhan, K., Frenette, J., Cornelison, D. D., & Rudnicki, M. A. 2014, "Wnt7a stimulates myogenic stem cell motility and engraftment resulting in improved muscle strength", *J.Cell Biol.*, vol. 205, no. 1, pp. 97-111.

Bhanot, P., Brink, M., Samos, C. H., Hsieh, J. C., Wang, Y., Macke, J. P., Andrew, D., Nathans, J., & Nusse, R. 1996, "A new member of the frizzled family from Drosophila functions as a Wingless receptor", *Nature*, vol. 382, no. 6588, pp. 225-230.

Bilic, J., Huang, Y. L., Davidson, G., Zimmermann, T., Cruciat, C. M., Bienz, M., & Niehrs, C. 2007, "Wnt induces LRP6 signalosomes and promotes Dishevelled-dependent LRP6 phosphorylation", *Science*, vol. 316, no. 5831, pp. 1619-1622.

Bishop, J. R., Schuksz, M., & Esko, J. D. 2007, "Heparan sulphate proteoglycans fine-tune mammalian physiology", *Nature*, vol. 446, no. 7139, pp. 1030-1037.

Blanc, E., Roux, G. L., Benard, J., & Raguenez, G. 2004, "Low expression of Wnt-5a gene is associated with high-risk neuroblastoma", *Oncogene*, vol. 24, no. 7, pp. 1277-1283.

Blitzer, J. T. & Nusse, R. 2006, "A critical role for endocytosis in Wnt signaling", *BMC.Cell Biol.*, vol. 7, p. 28.

Blom, T., Roselli, A., Tanner, M., & Nupponen, N. N. 2008, "Mutation and copy number analysis of LNX1 and Numbl in nervous system tumors", *Cancer Genet.Cytogenet.*, vol. 186, no. 2, pp. 103-109.

Bohl, J., Brimer, N., Lyons, C., & Vande Pol, S. B. 2007, "The stardust family protein MPP7 forms a tripartite complex with LIN7 and DLG1 that regulates the stability and localization of DLG1 to cell junctions", *J.Biol.Chem.*, vol. 282, no. 13, pp. 9392-9400.

Boland, G. M., Perkins, G., Hall, D. J., & Tuan, R. S. 2004, "Wnt 3a promotes proliferation and suppresses osteogenic differentiation of adult human mesenchymal stem cells", *J.Cell Biochem.*, vol. 93, no. 6, pp. 1210-1230.

Boukerche, H., Aissaoui, H., Prevost, C., Hirbec, H., Das, S. K., Su, Z. Z., Sarkar, D., & Fisher, P. B. 2010, "Src kinase activation is mandatory for MDA-9/syntenin-mediated activation of nuclear factor-kappaB", *Oncogene*, vol. 29, no. 21, pp. 3054-3066.

Boukerche, H., Su, Z. Z., Emdad, L., Baril, P., Balme, B., Thomas, L., Randolph, A., Valerie, K., Sarkar, D., & Fisher, P. B. 2005, "mda-9/Syntenin: a positive regulator of melanoma metastasis", *Cancer Res.*, vol. 65, no. 23, pp. 10901-10911.

Boukerche, H., Su, Z. Z., Emdad, L., Sarkar, D., & Fisher, P. B. 2007, "mda-9/Syntenin regulates the metastatic phenotype in human melanoma cells by activating nuclear factor-kappaB", *Cancer Res.*, vol. 67, no. 4, pp. 1812-1822.

Bryja, V., Cajanek, L., Grahn, A., & Schulte, G. 2007, "Inhibition of endocytosis blocks Wnt signalling to beta-catenin by promoting Dishevelled degradation", *Acta Physiol (Oxf)*, vol. 190, no. 1, pp. 55-61.

Budhidarmo, R., Nakatani, Y., & Day, C. L. 2012, "RINGs hold the key to ubiquitin transfer", *Trends Biochem.Sci.*, vol. 37, no. 2, pp. 58-65.

Burgner, D., Davila, S., Breunis, W. B., Ng, S. B., Li, Y., Bonnard, C., Ling, L., Wright, V. J., Thalamuthu, A., Odam, M., Shimizu, C., Burns, J. C., Levin, M., Kuijpers, T. W., & Hibberd, M. L. 2009, "A genome-wide association study identifies novel and functionally related susceptibility Loci for Kawasaki disease", *PLoS.Genet.*, vol. 5, no. 1, p. e1000319.

Cadigan, K. M. 2010, "Receptor endocytosis: Frizzled joins the ubiquitin club", *EMBO J.*, vol. 29, no. 13, pp. 2099-2100.

Caldwell, G. M., Jones, C. E., Taniere, P., Warrack, R., Soon, Y., Matthews, G. M., & Morton, D. G. 2006, "The Wnt antagonist sFRP1 is downregulated in premalignant large bowel adenomas", *Br.J.Cancer*, vol. 94, no. 6, pp. 922-927.

Camilli, T. C. & Weeraratna, A. T. 2010, "Striking the target in Wnt-y conditions: intervening in Wnt signaling during cancer progression", *Biochem.Pharmacol.*, vol. 80, no. 5, pp. 702-711.

Camps, J., Pitt, J. J., Emons, G., Hummon, A. B., Case, C. M., Grade, M., Jones, T. L., Nguyen, Q. T., Ghadimi, B. M., Beissbarth, T., Difilippantonio, M. J., Caplen, N. J., & Ried, T. 2013, "Genetic amplification of the NOTCH modulator LNX2 upregulates the WNT/beta-catenin pathway in colorectal cancer", *Cancer Res.*, vol. 73, no. 6, pp. 2003-2013.

Canalis, E. 2013, "Wnt signalling in osteoporosis: mechanisms and novel therapeutic approaches", *Nat.Rev.Endocrinol.*, vol. 9, no. 10, pp. 575-583.

Candidus, S., Bischoff, P., Becker, K. F., & Hofler, H. 1996, "No evidence for mutations in the alpha- and beta-catenin genes in human gastric and breast carcinomas", *Cancer Res.*, vol. 56, no. 1, pp. 49-52.

Capurro, M., Martin, T., Shi, W., & Filmus, J. 2014, "Glypican-3 binds to Frizzled and plays a direct role in the stimulation of canonical Wnt signaling", *J.Cell Sci.*, vol. 127, no. Pt 7, pp. 1565-1575.

Carey, L., Winer, E., Viale, G., Cameron, D., & Gianni, L. 2010, "Triple-negative breast cancer: disease entity or title of convenience?", *Nat.Rev.Clin.Oncol.*, vol. 7, no. 12, pp. 683-692.

Chen, J., Xu, J., Zhao, W., Hu, G., Cheng, H., Kang, Y., Xie, Y., & Lu, Y. 2005, "Characterization of human LNX, a novel ligand of Numb protein X that is downregulated in human gliomas", *Int.J.Biochem.Cell Biol.*, vol. 37, no. 11, pp. 2273-2283.

Chen, W., Hu, L. A., Semenov, M. V., Yanagawa, S., Kikuchi, A., Lefkowitz, R. J., & Miller, W. E. 2001, "beta-Arrestin1 modulates lymphoid enhancer factor transcriptional activity through interaction with phosphorylated Dishevelled proteins", *Proc.Natl.Acad.Sci.U.S.A*, vol. 98, no. 26, pp. 14889-14894.

Chen, W., ten, B. D., Brown, J., Ahn, S., Hu, L. A., Miller, W. E., Caron, M. G., Barak, L. S., Nusse, R., & Lefkowitz, R. J. 2003, "Dishevelled 2 recruits beta-arrestin 2 to mediate Wnt5A-stimulated endocytosis of Frizzled 4", *Science*, vol. 301, no. 5638, pp. 1391-1394.

Cheng, C. W., Yeh, J. C., Fan, T. P., Smith, S. K., & Charnock-Jones, D. S. 2008, "Wnt5a-mediated non-canonical Wnt signalling regulates human endothelial cell proliferation and migration", *Biochem.Biophys.Res.Commun.*, vol. 365, no. 2, pp. 285-290.

Cheng, J., Wang, H., & Guggino, W. B. 2005, "Regulation of cystic fibrosis transmembrane regulator trafficking and protein expression by a Rho family small GTPase TC10", *J.Biol.Chem.*, vol. 280, no. 5, pp. 3731-3739.

Chitalia, V. C., Foy, R. L., Bachschmid, M. M., Zeng, L., Panchenko, M. V., Zhou, M. I., Bharti, A., Seldin, D. C., Lecker, S. H., Dominguez, I., & Cohen, H. T. 2008, "Jade-1 inhibits Wnt signalling by ubiquitylating beta-catenin and mediates Wnt pathway inhibition by pVHL", *Nat.Cell Biol.*, vol. 10, no. 10, pp. 1208-1216.

Cierpicki, T., Bushweller, J. H., & Derewenda, Z. S. 2005, "Probing the supramodular architecture of a multidomain protein: the structure of syntenin in solution", *Structure.*, vol. 13, no. 2, pp. 319-327.

Cirone, P., Lin, S., Griesbach, H., Zhang, Y., Slusarski, D., & Crews, C. 2008, "A role for planar cell polarity signaling in angiogenesis", *Angiogenesis*, vol. 11, no. 4, pp. 347-360.

Civenni, G., Holbro, T., & Hynes, N. E. 2003, "Wnt1 and Wnt5a induce cyclin D1 expression through ErbB1 transactivation in HC11 mammary epithelial cells", *EMBO Rep.*, vol. 4, no. 2, pp. 166-171.

Clague, M. J. & Urbe, S. 2006, "Endocytosis: the DUB version", *Trends Cell Biol.*, vol. 16, no. 11, pp. 551-559.

Couchman, J. R. 2003, "Syndecans: proteoglycan regulators of cell-surface microdomains?", *Nat.Rev.Mol.Cell Biol.*, vol. 4, no. 12, pp. 926-937.

Courbard, J. R., Djiane, A., Wu, J., & Mlodzik, M. 2009, "The apical/basal-polarity determinant Scribble cooperates with the PCP core factor Stbm/Vang and functions as one of its effectors", *Dev.Biol.*, vol. 333, no. 1, pp. 67-77.

Culi, J. & Mann, R. S. 2003, "Boca, an endoplasmic reticulum protein required for wingless signaling and trafficking of LDL receptor family members in Drosophila", *Cell*, vol. 112, no. 3, pp. 343-354.

D'Agostino, M., Tornillo, G., Caporaso, M. G., Barone, M. V., Ghigo, E., Bonatti, S., & Mottola, G. 2011, "Ligand of Numb proteins LNX1p80 and LNX2 interact with the human glycoprotein CD8alpha and promote its ubiquitylation and endocytosis", *J.Cell Sci.*, vol. 124, no. Pt 21, pp. 3545-3556.

Dann, C. E., Hsieh, J. C., Rattner, A., Sharma, D., Nathans, J., & Leahy, D. J. 2001, "Insights into Wnt binding and signalling from the structures of two Frizzled cysteine-rich domains", *Nature*, vol. 412, no. 6842, pp. 86-90.

Das, S. K., Bhutia, S. K., Sokhi, U. K., Azab, B., Su, Z. Z., Boukerche, H., Anwar, T., Moen, E. L., Chatterjee, D., Pellecchia, M., Sarkar, D., & Fisher, P. B. 2012, "Raf kinase inhibitor RKIP inhibits MDA-9/syntenin-mediated metastasis in melanoma", *Cancer Res.*, vol. 72, no. 23, pp. 6217-6226.

Dasgupta, S., Menezes, M. E., Das, S. K., Emdad, L., Janjic, A., Bhatia, S., Mukhopadhyay, N. D., Shao, C., Sarkar, D., & Fisher, P. B. 2013, "Novel role of MDA-9/syntenin in regulating urothelial cell proliferation by modulating EGFR signaling", *Clin.Cancer Res.*, vol. 19, no. 17, pp. 4621-4633.

De Calisto, J., Araya, C., Marchant, L., Riaz, C. F., & Mayor, R. 2005, "Essential role of non-canonical Wnt signalling in neural crest migration", *Development*, vol. 132, no. 11, pp. 2587-2597.

de Lau, W., Peng, W. C., Gros, P., & Clevers, H. 2014, "The R-spondin/Lgr5/Rnf43 module: regulator of Wnt signal strength", *Genes Dev.*, vol. 28, no. 4, pp. 305-316.

Dejmek, J., Dejmek, A., Safholm, A., Sjolander, A., & Andersson, T. 2005a, "Wnt-5a protein expression in primary dukes B colon cancers identifies a subgroup of patients with good prognosis", *Cancer Res.*, vol. 65, no. 20, pp. 9142-9146.

Dejmek, J., Leandersson, K., Manjer, J., Bjartell, A., Emdin, S. O., Vogel, W. F., Landberg, G., & Andersson, T. 2005b, "Expression and signaling activity of Wnt-5a/discoidin domain receptor-1 and Syk plays distinct but decisive roles in breast cancer patient survival", *Clin.Cancer Res.*, vol. 11, no. 2 Pt 1, pp. 520-528.

Demir, K., Kirsch, N., Beretta, C. A., Erdmann, G., Ingelfinger, D., Moro, E., Argenton, F., Carl, M., Niehrs, C., & Boutros, M. 2013, "RAB8B is required for activity and caveolar endocytosis of LRP6", *Cell Rep.*, vol. 4, no. 6, pp. 1224-1234.

Deshaies, R. J. & Joazeiro, C. A. 2009, "RING domain E3 ubiquitin ligases", *Annu.Rev.Biochem.*, vol. 78, pp. 399-434.

Dey, N., Barwick, B. G., Moreno, C. S., Ordanic-Kodani, M., Chen, Z., Oprea-Ilies, G., Tang, W., Catzavelos, C., Kerstann, K. F., Sledge, G. W., Jr., Abramovitz, M., Bouzyk, M., De, P., & Leyland-Jones, B. R. 2013, "Wnt signaling in triple negative breast cancer is associated with metastasis", *BMC.Cancer*, vol. 13, p. 537.

Dho, S. E., French, M. B., Woods, S. A., & McGlade, C. J. 1999, "Characterization of four mammalian numb protein isoforms. Identification of cytoplasmic and membrane-associated variants of the phosphotyrosine binding domain", *J.Biol.Chem.*, vol. 274, no. 46, pp. 33097-33104.

Dho, S. E., Jacob, S., Wolting, C. D., French, M. B., Rohrschneider, L. R., & McGlade, C. J. 1998, "The mammalian numb phosphotyrosine-binding domain. Characterization of binding specificity and identification of a novel PDZ domain-containing numb binding protein, LNX", *J.Biol.Chem.*, vol. 273, no. 15, pp. 9179-9187.

Di Fiore, P. P., Polo, S., & Hofmann, K. 2003, "When ubiquitin meets ubiquitin receptors: a signalling connection", *Nat.Rev.Mol.Cell Biol.*, vol. 4, no. 6, pp. 491-497.

Dijksterhuis, J. P., Petersen, J., & Schulte, G. 2014, "WNT/Frizzled signalling: receptor-ligand selectivity with focus on FZD-G protein signalling and its physiological relevance: IUPHAR Review 3", *Br.J.Pharmacol.*, vol. 171, no. 5, pp. 1195-1209.

Dimitrova, Y. N., Li, J., Lee, Y. T., Rios-Esteves, J., Friedman, D. B., Choi, H. J., Weis, W. I., Wang, C. Y., & Chazin, W. J. 2010, "Direct ubiquitination of beta-catenin by Siah-1 and regulation by the exchange factor TBL1", *J.Biol.Chem.*, vol. 285, no. 18, pp. 13507-13516.

Djiane, A., Riou, J., Umbhauer, M., Boucaut, J., & Shi, D. 2000, "Role of frizzled 7 in the regulation of convergent extension movements during gastrulation in Xenopus laevis", *Development*, vol. 127, no. 14, pp. 3091-3100.

Djiane, A., Yogev, S., & Mlodzik, M. 2005, "The apical determinants aPKC and dPatj regulate Frizzled-dependent planar cell polarity in the Drosophila eye", *Cell*, vol. 121, no. 4, pp. 621-631.

Dobrosotskaya, I. Y. & James, G. L. 2000, "MAGI-1 interacts with beta-catenin and is associated with cell-cell adhesion structures", *Biochem.Biophys.Res.Commun.*, vol. 270, no. 3, pp. 903-909.

Doherty, G. J. & McMahon, H. T. 2009, "Mechanisms of endocytosis", *Annu.Rev.Biochem.*, vol. 78, pp. 857-902.

Dormeyer, W., Van, H. D., Braam, S. R., Heck, A. J., Mummery, C. L., & Krijgsveld, J. 2008, "Plasma membrane proteomics of human embryonic stem cells and human embryonal carcinoma cells", *J.Proteome.Res.*, vol. 7, no. 7, pp. 2936-2951.

Doyle, D. A., Lee, A., Lewis, J., Kim, E., Sheng, M., & MacKinnon, R. 1996, "Crystal structures of a complexed and peptide-free membrane protein-binding domain: molecular basis of peptide recognition by PDZ", *Cell*, vol. 85, no. 7, pp. 1067-1076.

Doyle, J. M., Gao, J., Wang, J., Yang, M., & Potts, P. R. 2010, "MAGE-RING protein complexes comprise a family of E3 ubiquitin ligases", *Mol.Cell*, vol. 39, no. 6, pp. 963-974.

Duan, S., Cermak, L., Pagan, J. K., Rossi, M., Martinengo, C., di Celle, P. F., Chapuy, B., Shipp, M., Chiarle, R., & Pagano, M. 2012, "FBXO11 targets BCL6 for degradation and is inactivated in diffuse large B-cell lymphomas", *Nature*, vol. 481, no. 7379, pp. 90-93.

Elsum, I. A., Martin, C., & Humbert, P. O. 2013, "Scribble regulates an EMT polarity pathway through modulation of MAPK-ERK signaling to mediate junction formation", *J.Cell Sci.*, vol. 126, no. Pt 17, pp. 3990-3999.

Endo, K., Ueda, T., Ueyama, J., Ohta, T., & Terada, T. 2000, "Immunoreactive E-cadherin, alpha-catenin, beta-catenin, and gamma-catenin proteins in hepatocellular carcinoma: relationships with

tumor grade, clinicopathologic parameters, and patients' survival", *Hum.Pathol.*, vol. 31, no. 5, pp. 558-565.

Endo, Y., Wolf, V., Muraiso, K., Kamijo, K., Soon, L., Uren, A., Barshishat-Kupper, M., & Rubin, J. S. 2005, "Wnt-3a-dependent cell motility involves RhoA activation and is specifically regulated by Dishevelled-2", *J.Biol.Chem.*, vol. 280, no. 1, pp. 777-786.

Estrach, S., Legg, J., & Watt, F. M. 2007, "Syntenin mediates Delta1-induced cohesiveness of epidermal stem cells in culture", *J.Cell Sci.*, vol. 120, no. Pt 16, pp. 2944-2952.

Etienne-Manneville, S., Manneville, J. B., Nicholls, S., Ferenczi, M. A., & Hall, A. 2005, "Cdc42 and Par6-PKCzeta regulate the spatially localized association of Dlg1 and APC to control cell polarization", *J.Cell Biol.*, vol. 170, no. 6, pp. 895-901.

Fatima, S., Lee, N. P., & Luk, J. M. 2011, "Dickkopfs and Wnt/beta-catenin signalling in liver cancer", *World J.Clin.Oncol.*, vol. 2, no. 8, pp. 311-325.

Fearon, E. R. & Spence, J. R. 2012, "Cancer biology: a new RING to Wnt signaling", *Curr.Biol.*, vol. 22, no. 19, p. R849-R851.

Fernandez-Larrea, J., Merlos-Suarez, A., Urena, J. M., Baselga, J., & Arribas, J. 1999, "A role for a PDZ protein in the early secretory pathway for the targeting of proTGF-alpha to the cell surface", *Mol.Cell*, vol. 3, no. 4, pp. 423-433.

Finn, R. D., Mistry, J., Schuster-Bockler, B., Griffiths-Jones, S., Hollich, V., Lassmann, T., Moxon, S., Marshall, M., Khanna, A., Durbin, R., Eddy, S. R., Sonnhammer, E. L., & Bateman, A. 2006, "Pfam: clans, web tools and services", *Nucleic Acids Res.*, vol. 34, no. Database issue, p. D247-D251.

Flynn, M., Saha, O., & Young, P. 2011, "Molecular evolution of the LNX gene family", *BMC.Evol.Biol.*, vol. 11, p. 235.

Foord, S. M., Bonner, T. I., Neubig, R. R., Rosser, E. M., Pin, J. P., Davenport, A. P., Spedding, M., & Harmar, A. J. 2005, "International Union of Pharmacology. XLVI. G protein-coupled receptor list", *Pharmacol.Rev.*, vol. 57, no. 2, pp. 279-288.

Fre, S., Pallavi, S. K., Huyghe, M., Lae, M., Janssen, K. P., Robine, S., Artavanis-Tsakonas, S., & Louvard, D. 2009, "Notch and Wnt signals cooperatively control cell proliferation and tumorigenesis in the intestine", *Proc.Natl.Acad.Sci.U.S.A*, vol. 106, no. 15, pp. 6309-6314.

Fredriksson, R., Lagerstrom, M. C., Lundin, L. G., & Schioth, H. B. 2003, "The G-protein-coupled receptors in the human genome form five main families. Phylogenetic analysis, paralogon groups, and fingerprints", *Mol.Pharmacol.*, vol. 63, no. 6, pp. 1256-1272.

Fuerer, C., Nusse, R., & ten, B. D. 2008, "Wnt signalling in development and disease. Max Delbruck Center for Molecular Medicine meeting on Wnt signaling in Development and Disease", *EMBO Rep.*, vol. 9, no. 2, pp. 134-138.

Gagliardi, M., Piddini, E., & Vincent, J. P. 2008, "Endocytosis: a positive or a negative influence on Wnt signalling?", *Traffic.*, vol. 9, no. 1, pp. 1-9.

Gallardo, R., Ivarsson, Y., Schymkowitz, J., Rousseau, F., & Zimmermann, P. 2010, "Structural diversity of PDZ-lipid interactions", *Chembiochem.*, vol. 11, no. 4, pp. 456-467.

Gallon, M., Clairfeuille, T., Steinberg, F., Mas, C., Ghai, R., Sessions, R. B., Teasdale, R. D., Collins, B. M., & Cullen, P. J. 2014, "A unique PDZ domain and arrestin-like fold interaction reveals mechanistic details of endocytic recycling by SNX27-retromer", *Proc.Natl.Acad.Sci.U.S.A*, vol. 111, no. 35, p. E3604-E3613.

Gao, C., Cao, W., Bao, L., Zuo, W., Xie, G., Cai, T., Fu, W., Zhang, J., Wu, W., Zhang, X., & Chen, Y. G. 2010a, "Autophagy negatively regulates Wnt signalling by promoting Dishevelled degradation", *Nat.Cell Biol.*, vol. 12, no. 8, pp. 781-790.

Gao, C. & Chen, Y. G. 2010b, "Dishevelled: The hub of Wnt signaling", *Cell Signal.*, vol. 22, no. 5, pp. 717-727.

Geijsen, N., Uings, I. J., Pals, C., Armstrong, J., McKinnon, M., Raaijmakers, J. A., Lammers, J. W., Koenderman, L., & Coffer, P. J. 2001, "Cytokine-specific transcriptional regulation through an IL-5Ralpha interacting protein", *Science*, vol. 293, no. 5532, pp. 1136-1138.

Geyer, F. C., Lacroix-Triki, M., Savage, K., Arnedos, M., Lambros, M. B., Mackay, A., Natrajan, R., & Reis-Filho, J. S. 2011, "beta-Catenin pathway activation in breast cancer is associated with triple-negative phenotype but not with CTNNB1 mutation", *Mod.Pathol.*, vol. 24, no. 2, pp. 209-231.

Glaunsinger, B. A., Lee, S. S., Thomas, M., Banks, L., & Javier, R. 2000, "Interactions of the PDZ-protein MAGI-1 with adenovirus E4-ORF1 and high-risk papillomavirus E6 oncoproteins", *Oncogene*, vol. 19, no. 46, pp. 5270-5280.

Gregorieff, A., Pinto, D., Begthel, H., Destree, O., Kielman, M., & Clevers, H. 2005, "Expression pattern of Wnt signaling components in the adult intestine", *Gastroenterology*, vol. 129, no. 2, pp. 626-638.

Grembecka, J., Cierpicki, T., Devedjiev, Y., Derewenda, U., Kang, B. S., Bushweller, J. H., & Derewenda, Z. S. 2006, "The binding of the PDZ tandem of syntenin to target proteins", *Biochemistry*, vol. 45, no. 11, pp. 3674-3683.

Grootjans, J. J., Reekmans, G., Ceulemans, H., & David, G. 2000, "Syntenin-syndecan binding requires syndecan-synteny and the co-operation of both PDZ domains of syntenin", *J.Biol.Chem.*, vol. 275, no. 26, pp. 19933-19941.

Grootjans, J. J., Zimmermann, P., Reekmans, G., Smets, A., Degeest, G., Durr, J., & David, G. 1997, "Syntenin, a PDZ protein that binds syndecan cytoplasmic domains", *Proc.Natl.Acad.Sci.U.S.A*, vol. 94, no. 25, pp. 13683-13688.

Guo, Z., Song, E., Ma, S., Wang, X., Gao, S., Shao, C., Hu, S., Jia, L., Tian, R., Xu, T., & Gao, Y. 2012, "Proteomics strategy to identify substrates of LNX, a PDZ domain-containing E3 ubiquitin ligase", *J.Proteome.Res.*, vol. 11, no. 10, pp. 4847-4862.

Gusterson, B. 2009, "Do 'basal-like' breast cancers really exist?", *Nat.Rev.Cancer*, vol. 9, no. 2, pp. 128-134.

Hagemann, A. I., Kurz, J., Kauffeld, S., Chen, Q., Reeves, P. M., Weber, S., Schindler, S., Davidson, G., Kirchhausen, T., & Scholpp, S. 2014, "In-vivo analysis of formation and endocytosis of the Wnt/beta-Catenin signaling complex in zebrafish embryos", *J.Cell Sci.*

Haglund, K., Di Fiore, P. P., & Dikic, I. 2003, "Distinct monoubiquitin signals in receptor endocytosis", *Trends Biochem.Sci.*, vol. 28, no. 11, pp. 598-603.

Haglund, K. & Dikic, I. 2005, "Ubiquitylation and cell signaling", *EMBO J.*, vol. 24, no. 19, pp. 3353-3359.

Hao, H. X., Xie, Y., Zhang, Y., Charlat, O., Oster, E., Avello, M., Lei, H., Mickanin, C., Liu, D., Ruffner, H., Mao, X., Ma, Q., Zamponi, R., Bouwmeester, T., Finan, P. M., Kirschner, M. W., Porter, J. A., Serluca, F. C., & Cong, F. 2012, "ZNRF3 promotes Wnt receptor turnover in an R-spondin-sensitive manner", *Nature*, vol. 485, no. 7397, pp. 195-200.

Harris, B. Z., Hillier, B. J., & Lim, W. A. 2001, "Energetic determinants of internal motif recognition by PDZ domains", *Biochemistry*, vol. 40, no. 20, pp. 5921-5930.

He, J., Bellini, M., Xu, J., Castleberry, A. M., & Hall, R. A. 2004, "Interaction with cystic fibrosis transmembrane conductance regulator-associated ligand (CAL) inhibits beta1-adrenergic receptor surface expression", *J.Biol.Chem.*, vol. 279, no. 48, pp. 50190-50196.

Helmke, B. M., Polychronidis, M., Benner, A., Thome, M., Arribas, J., & Deichmann, M. 2004, "Melanoma metastasis is associated with enhanced expression of the syntenin gene", *Oncol.Rep.*, vol. 12, no. 2, pp. 221-228.

Hering, H. & Sheng, M. 2002, "Direct interaction of Frizzled-1, -2, -4, and -7 with PDZ domains of PSD-95", *FEBS Lett.*, vol. 521, no. 1-3, pp. 185-189.

Herr, P., Hausmann, G., & Basler, K. 2012, "WNT secretion and signalling in human disease", *Trends Mol.Med.*, vol. 18, no. 8, pp. 483-493.

Higa, S., Tokoro, T., Inoue, E., Kitajima, I., & Ohtsuka, T. 2007, "The active zone protein CAST directly associates with Ligand-of-Numb protein X", *Biochem.Biophys.Res.Commun.*, vol. 354, no. 3, pp. 686-692.

Honda, T., Yamamoto, H., Ishii, A., & Inui, M. 2010, "PDZRN3 negatively regulates BMP-2-induced osteoblast differentiation through inhibition of Wnt signaling", *Mol.Biol.Cell*, vol. 21, no. 18, pp. 3269-3277.

Huang, C. L., Liu, D., Nakano, J., Ishikawa, S., Kontani, K., Yokomise, H., & Ueno, M. 2005, "Wnt5a expression is associated with the tumor proliferation and the stromal vascular endothelial growth factor--an expression in non-small-cell lung cancer", *J.Clin.Oncol.*, vol. 23, no. 34, pp. 8765-8773.

Hui, S., Xing, X., & Bader, G. D. 2013, "Predicting PDZ domain mediated protein interactions from structure", *BMC.Bioinformatics.*, vol. 14, p. 27.

Ibrahim, S. A., Hassan, H., Vilardo, L., Kumar, S. K., Kumar, A. V., Kelsch, R., Schneider, C., Kiesel, L., Eich, H. T., Zucchi, I., Reinbold, R., Greve, B., & Gotte, M. 2013, "Syndecan-1 (CD138) modulates triple-negative breast cancer stem cell properties via regulation of LRP-6 and IL-6-mediated STAT3 signaling", *PLoS.One.*, vol. 8, no. 12, p. e85737.

Ikeda, F. & Dikic, I. 2008, "Atypical ubiquitin chains: new molecular signals. 'Protein Modifications: Beyond the Usual Suspects' review series", *EMBO Rep.*, vol. 9, no. 6, pp. 536-542.

Itoh, K., Lisovsky, M., Hikasa, H., & Sokol, S. Y. 2005, "Reorganization of actin cytoskeleton by FRIED, a Frizzled-8 associated protein tyrosine phosphatase", *Dev.Dyn.*, vol. 234, no. 1, pp. 90-101.

Itoh, M., Furuse, M., Morita, K., Kubota, K., Saitou, M., & Tsukita, S. 1999, "Direct binding of three tight junction-associated MAGUKs, ZO-1, ZO-2, and ZO-3, with the COOH termini of claudins", *J.Cell Biol.*, vol. 147, no. 6, pp. 1351-1363.

Jamieson, C., Sharma, M., & Henderson, B. R. 2014, "Targeting the beta-catenin nuclear transport pathway in cancer", *Semin.Cancer Biol.*

Janda, C. Y., Waghray, D., Levin, A. M., Thomas, C., & Garcia, K. C. 2012, "Structural basis of Wnt recognition by Frizzled", *Science*, vol. 337, no. 6090, pp. 59-64.

Jannatipour, M., Dion, P., Khan, S., Jindal, H., Fan, X., Laganiere, J., Chishti, A. H., & Rouleau, G. A. 2001, "Schwannomin isoform-1 interacts with syntenin via PDZ domains", *J.Biol.Chem.*, vol. 276, no. 35, pp. 33093-33100.

Jelen, F., Oleksy, A., Smietana, K., & Otlewski, J. 2003, "PDZ domains - common players in the cell signaling", *Acta Biochim.Pol.*, vol. 50, no. 4, pp. 985-1017.

Jemth, P. & Gianni, S. 2007, "PDZ domains: folding and binding", *Biochemistry*, vol. 46, no. 30, pp. 8701-8708.

Jeon, H. Y., Das, S. K., Dasgupta, S., Emdad, L., Sarkar, D., Kim, S. H., Lee, S. G., & Fisher, P. B. 2013, "Expression patterns of MDA-9/syntenin during development of the mouse embryo", *J.Mol.Histol.*, vol. 44, no. 2, pp. 159-166.

Jiang, Y., He, X., & Howe, P. H. 2012, "Disabled-2 (Dab2) inhibits Wnt/beta-catenin signalling by binding LRP6 and promoting its internalization through clathrin", *EMBO J.*, vol. 31, no. 10, pp. 2336-2349.

Jin, Z., Tamura, G., Tsuchiya, T., Sakata, K., Kashiwaba, M., Osakabe, M., & Motoyama, T. 2001, "Adenomatous polyposis coli (APC) gene promoter hypermethylation in primary breast cancers", *Br.J.Cancer*, vol. 85, no. 1, pp. 69-73.

Jost, E., Gezer, D., Wilop, S., Suzuki, H., Herman, J. G., Osieka, R., & Galm, O. 2009, "Epigenetic dysregulation of secreted Frizzled-related proteins in multiple myeloma", *Cancer Lett.*, vol. 281, no. 1, pp. 24-31.

Jung, H., Kim, B. G., Han, W. H., Lee, J. H., Cho, J. Y., Park, W. S., Maurice, M. M., Han, J. K., Lee, M. J., Finley, D., & Jho, E. H. 2013, "Deubiquitination of Dishevelled by Usp14 is required for Wnt signaling", *Oncogenesis.*, vol. 2, p. e64.

Kadowaki, T., Wilder, E., Klingensmith, J., Zachary, K., & Perrimon, N. 1996, "The segment polarity gene porcupine encodes a putative multitransmembrane protein involved in Wingless processing", *Genes Dev.*, vol. 10, no. 24, pp. 3116-3128.

Kang, B. S., Cooper, D. R., Jelen, F., Devedjiev, Y., Derewenda, U., Dauter, Z., Otlewski, J., & Derewenda, Z. S. 2003, "PDZ tandem of human syntenin: crystal structure and functional properties", *Structure.*, vol. 11, no. 4, pp. 459-468.

Kansaku, A., Hirabayashi, S., Mori, H., Fujiwara, N., Kawata, A., Ikeda, M., Rokukawa, C., Kurihara, H., & Hata, Y. 2006, "Ligand-of-Numb protein X is an endocytic scaffold for junctional adhesion molecule 4", *Oncogene*, vol. 25, no. 37, pp. 5071-5084.

Katoh, M. & Katoh, M. 2007, "Comparative integromics on FZD7 orthologs: conserved binding sites for PU.1, SP1, CCAAT-box and TCF/LEF/SOX transcription factors within 5'-promoter region of mammalian FZD7 orthologs", *Int.J.Mol.Med.*, vol. 19, no. 3, pp. 529-533.

Katoh, M., Kirikoshi, H., Terasaki, H., & Shiokawa, K. 2001, "WNT2B2 mRNA, up-regulated in primary gastric cancer, is a positive regulator of the WNT- beta-catenin-TCF signaling pathway", *Biochem.Biophys.Res.Commun.*, vol. 289, no. 5, pp. 1093-1098.

Katoh, Y. & Katoh, M. 2005, "Comparative genomics on Shisa orthologs", *Int.J.Mol.Med.*, vol. 16, no. 1, pp. 181-185.

Kaucka, M., Plevova, K., Pavlova, S., Janovska, P., Mishra, A., Verner, J., Prochazkova, J., Krejci, P., Kotaskova, J., Ovesna, P., Tichy, B., Brychtova, Y., Doubek, M., Kozubik, A., Mayer, J., Pospisilova, S., & Bryja, V. 2013, "The planar cell polarity pathway drives pathogenesis of chronic lymphocytic leukemia by the regulation of B-lymphocyte migration", *Cancer Res.*, vol. 73, no. 5, pp. 1491-1501.

Kaykas, A., Yang-Snyder, J., Heroux, M., Shah, K. V., Bouvier, M., & Moon, R. T. 2004, "Mutant Frizzled 4 associated with vitreoretinopathy traps wild-type Frizzled in the endoplasmic reticulum by oligomerization", *Nat.Cell Biol.*, vol. 6, no. 1, pp. 52-58.

Kemp, C. R., Willems, E., Wawrzak, D., Hendrickx, M., Agbor, A. T., & Leyns, L. 2007, "Expression of Frizzled5, Frizzled7, and Frizzled10 during early mouse development and interactions with canonical Wnt signaling", *Dev.Dyn.*, vol. 236, no. 7, pp. 2011-2019.

Khan, N. I., Bradstock, K. F., & Bendall, L. J. 2007, "Activation of Wnt/beta-catenin pathway mediates growth and survival in B-cell progenitor acute lymphoblastic leukaemia", *Br.J.Haematol.*, vol. 138, no. 3, pp. 338-348.

Khramtsov, A. I., Khramtsova, G. F., Tretiakova, M., Huo, D., Olopade, O. I., & Goss, K. H. 2010, "Wnt/beta-catenin pathway activation is enriched in basal-like breast cancers and predicts poor outcome", *Am.J.Pathol.*, vol. 176, no. 6, pp. 2911-2920.

Kikuchi, A., Yamamoto, H., & Kishida, S. 2007, "Multiplicity of the interactions of Wnt proteins and their receptors", *Cell Signal.*, vol. 19, no. 4, pp. 659-671.

Kikuchi, A., Yamamoto, H., & Sato, A. 2009, "Selective activation mechanisms of Wnt signaling pathways", *Trends Cell Biol.*, vol. 19, no. 3, pp. 119-129.

Kim, G. H. & Han, J. K. 2007, "Essential role for beta-arrestin 2 in the regulation of Xenopus convergent extension movements", *EMBO J.*, vol. 26, no. 10, pp. 2513-2526.

Kim, G. H., Her, J. H., & Han, J. K. 2008a, "Ryk cooperates with Frizzled 7 to promote Wnt11-mediated endocytosis and is essential for Xenopus laevis convergent extension movements", *J.Cell Biol.*, vol. 182, no. 6, pp. 1073-1082.

Kim, M., Lee, H. C., Tsedensodnom, O., Hartley, R., Lim, Y. S., Yu, E., Merle, P., & Wands, J. R. 2008b, "Functional interaction between Wnt3 and Frizzled-7 leads to activation of the Wnt/beta-catenin signaling pathway in hepatocellular carcinoma cells", *J.Hepatol.*, vol. 48, no. 5, pp. 780-791.

King, T. D., Suto, M. J., & Li, Y. 2012a, "The Wnt/beta-catenin signaling pathway: a potential therapeutic target in the treatment of triple negative breast cancer", *J.Cell Biochem.*, vol. 113, no. 1, pp. 13-18.

King, T. D., Zhang, W., Suto, M. J., & Li, Y. 2012b, "Frizzled7 as an emerging target for cancer therapy", *Cell Signal.*, vol. 24, no. 4, pp. 846-851.

Kinoshita, N., Iioka, H., Miyakoshi, A., & Ueno, N. 2003, "PKC delta is essential for Dishevelled function in a noncanonical Wnt pathway that regulates Xenopus convergent extension movements", *Genes Dev.*, vol. 17, no. 13, pp. 1663-1676.

Kinzler, K. W. & Vogelstein, B. 1996, "Lessons from hereditary colorectal cancer", *Cell*, vol. 87, no. 2, pp. 159-170.

Kirikoshi, H., Sekihara, H., & Katoh, M. 2001, "Up-regulation of Frizzled-7 (FZD7) in human gastric cancer", *Int.J.Oncol.*, vol. 19, no. 1, pp. 111-115.

Kitada, T., Asakawa, S., Hattori, N., Matsumine, H., Yamamura, Y., Minoshima, S., Yokochi, M., Mizuno, Y., & Shimizu, N. 1998, "Mutations in the parkin gene cause autosomal recessive juvenile parkinsonism", *Nature*, vol. 392, no. 6676, pp. 605-608.

Klarmann, G. J., Decker, A., & Farrar, W. L. 2008, "Epigenetic gene silencing in the Wnt pathway in breast cancer", *Epigenetics.*, vol. 3, no. 2, pp. 59-63.

Klaus, A. & Birchmeier, W. 2008, "Wnt signalling and its impact on development and cancer", *Nat.Rev.Cancer*, vol. 8, no. 5, pp. 387-398.

Knowlton, M. N. & Kelly, G. M. 2004, "Zebrafish Mir antagonizes Frizzled 7-induced gastrulation defects", *Zebrafish.*, vol. 1, no. 2, pp. 133-144.

Ko, J. A., Kimura, Y., Matsuura, K., Yamamoto, H., Gondo, T., & Inui, M. 2006, "PDZRN3 (LNX3, SEMCAP3) is required for the differentiation of C2C12 myoblasts into myotubes", *J.Cell Sci.*, vol. 119, no. Pt 24, pp. 5106-5113.

Kohn, A. D. & Moon, R. T. 2005, "Wnt and calcium signaling: beta-catenin-independent pathways", *Cell Calcium*, vol. 38, no. 3-4, pp. 439-446.

Komander, D. & Rape, M. 2012, "The ubiquitin code", *Annu.Rev.Biochem.*, vol. 81, pp. 203-229.

Koo, B. K., Spit, M., Jordens, I., Low, T. Y., Stange, D. E., van de Wetering, M., van Es, J. H., Mohammed, S., Heck, A. J., Maurice, M. M., & Clevers, H. 2012, "Tumour suppressor RNF43 is a stem-cell E3 ligase that induces endocytosis of Wnt receptors", *Nature*, vol. 488, no. 7413, pp. 665-669.

Koo, T. H., Lee, J. J., Kim, E. M., Kim, K. W., Kim, H. D., & Lee, J. H. 2002, "Syntenin is overexpressed and promotes cell migration in metastatic human breast and gastric cancer cell lines", *Oncogene*, vol. 21, no. 26, pp. 4080-4088.

Korinek, V., Barker, N., Morin, P. J., van, W. D., de, W. R., Kinzler, K. W., Vogelstein, B., & Clevers, H. 1997, "Constitutive transcriptional activation by a beta-catenin-Tcf complex in APC-/- colon carcinoma", *Science*, vol. 275, no. 5307, pp. 1784-1787.

Koroll, M., Rathjen, F. G., & Volkmer, H. 2001, "The neural cell recognition molecule neurofascin interacts with syntenin-1 but not with syntenin-2, both of which reveal self-associating activity", *J.Biol.Chem.*, vol. 276, no. 14, pp. 10646-10654.

Kotelevets, L., van, H. J., Bruyneel, E., Mareel, M., van, R. F., & Chastre, E. 2005, "Implication of the MAGI-1b/PTEN signalosome in stabilization of adherens junctions and suppression of invasiveness", *FASEB J.*, vol. 19, no. 1, pp. 115-117.

Kuhl, M., Sheldahl, L. C., Park, M., Miller, J. R., & Moon, R. T. 2000, "The Wnt/Ca2+ pathway: a new vertebrate Wnt signaling pathway takes shape", *Trends Genet.*, vol. 16, no. 7, pp. 279-283.

Kurayoshi, M., Oue, N., Yamamoto, H., Kishida, M., Inoue, A., Asahara, T., Yasui, W., & Kikuchi, A. 2006, "Expression of Wnt-5a is correlated with aggressiveness of gastric cancer by stimulating cell migration and invasion", *Cancer Res.*, vol. 66, no. 21, pp. 10439-10448.

Kwon, C., Cheng, P., King, I. N., Andersen, P., Shenje, L., Nigam, V., & Srivastava, D. 2011, "Notch post-translationally regulates beta-catenin protein in stem and progenitor cells", *Nat.Cell Biol.*, vol. 13, no. 10, pp. 1244-1251.

Lagerstrom, M. C. & Schioth, H. B. 2008, "Structural diversity of G protein-coupled receptors and significance for drug discovery", *Nat.Rev.Drug Discov.*, vol. 7, no. 4, pp. 339-357.

Lahuna, O., Quellari, M., Achard, C., Nola, S., Meduri, G., Navarro, C., Vitale, N., Borg, J. P., & Misrahi, M. 2005, "Thyrotropin receptor trafficking relies on the hScrib-betaPIX-GIT1-ARF6 pathway", *EMBO J.*, vol. 24, no. 7, pp. 1364-1374.

Lallemand, D., Curto, M., Saotome, I., Giovannini, M., & McClatchey, A. I. 2003, "NF2 deficiency promotes tumorigenesis and metastasis by destabilizing adherens junctions", *Genes Dev.*, vol. 17, no. 9, pp. 1090-1100.

Latysheva, N., Muratov, G., Rajesh, S., Padgett, M., Hotchin, N. A., Overduin, M., & Berditchevski, F. 2006, "Syntenin-1 is a new component of tetraspanin-enriched microdomains: mechanisms and consequences of the interaction of syntenin-1 with CD63", *Mol.Cell Biol.*, vol. 26, no. 20, pp. 7707-7718.

Lauffer, B. E., Melero, C., Temkin, P., Lei, C., Hong, W., Kortemme, T., & von, Z. M. 2010, "SNX27 mediates PDZ-directed sorting from endosomes to the plasma membrane", *J.Cell Biol.*, vol. 190, no. 4, pp. 565-574.

Le Grand, F., Jones, A. E., Seale, V., Scime, A., & Rudnicki, M. A. 2009, "Wnt7a activates the planar cell polarity pathway to drive the symmetric expansion of satellite stem cells", *Cell Stem Cell*, vol. 4, no. 6, pp. 535-547.

Lehmann, B. D., Bauer, J. A., Chen, X., Sanders, M. E., Chakravarthy, A. B., Shyr, Y., & Pietenpol, J. A. 2011, "Identification of human triple-negative breast cancer subtypes and preclinical models for selection of targeted therapies", *J.Clin.Invest*, vol. 121, no. 7, pp. 2750-2767.

Li, J., Ying, J., Fan, Y., Wu, L., Ying, Y., Chan, A. T., Srivastava, G., & Tao, Q. 2010, "WNT5A antagonizes WNT/beta-catenin signaling and is frequently silenced by promoter CpG methylation in esophageal squamous cell carcinoma", *Cancer Biol.Ther.*, vol. 10, no. 6, pp. 617-624.

Li, Y. & Dudley, A. T. 2009, "Noncanonical frizzled signaling regulates cell polarity of growth plate chondrocytes", *Development*, vol. 136, no. 7, pp. 1083-1092.

Lin, J. J., Jiang, H., & Fisher, P. B. 1998, "Melanoma differentiation associated gene-9, mda-9, is a human gamma interferon responsive gene", *Gene*, vol. 207, no. 2, pp. 105-110.

Lin, S. Y., Xia, W., Wang, J. C., Kwong, K. Y., Spohn, B., Wen, Y., Pestell, R. G., & Hung, M. C. 2000, "Beta-catenin, a novel prognostic marker for breast cancer: its roles in cyclin D1 expression and cancer progression", *Proc.Natl.Acad.Sci.U.S.A*, vol. 97, no. 8, pp. 4262-4266.

Linker, C., Lesbros, C., Gros, J., Burrus, L. W., Rawls, A., & Marcelle, C. 2005, "beta-Catenin-dependent Wnt signalling controls the epithelial organisation of somites through the activation of paraxis", *Development*, vol. 132, no. 17, pp. 3895-3905.

Lipkowitz, S. & Weissman, A. M. 2011, "RINGs of good and evil: RING finger ubiquitin ligases at the crossroads of tumour suppression and oncogenesis", *Nat.Rev.Cancer*, vol. 11, no. 9, pp. 629-643.

Liu, C., Li, Y., Semenov, M., Han, C., Baeg, G. H., Tan, Y., Zhang, Z., Lin, X., & He, X. 2002, "Control of beta-catenin phosphorylation/degradation by a dual-kinase mechanism", *Cell*, vol. 108, no. 6, pp. 837-847.

Liu, C. C., Prior, J., Piwnica-Worms, D., & Bu, G. 2010, "LRP6 overexpression defines a class of breast cancer subtype and is a target for therapy", *Proc.Natl.Acad.Sci.U.S.A*, vol. 107, no. 11, pp. 5136-5141.

Loh, Y. N., Hedditch, E. L., Baker, L. A., Jary, E., Ward, R. L., & Ford, C. E. 2013, "The Wnt signalling pathway is upregulated in an in vitro model of acquired tamoxifen resistant breast cancer", *BMC.Cancer*, vol. 13, p. 174.

Loo, L. S., Tang, N., Al-Haddawi, M., Dawe, G. S., & Hong, W. 2014, "A role for sorting nexin 27 in AMPA receptor trafficking", *Nat.Commun.*, vol. 5, p. 3176.

Lopez-Knowles, E., Zardawi, S. J., McNeil, C. M., Millar, E. K., Crea, P., Musgrove, E. A., Sutherland, R. L., & O'Toole, S. A. 2010, "Cytoplasmic localization of beta-catenin is a marker of poor outcome in breast cancer patients", *Cancer Epidemiol.Biomarkers Prev.*, vol. 19, no. 1, pp. 301-309.

Lu, Z., Je, H. S., Young, P., Gross, J., Lu, B., & Feng, G. 2007, "Regulation of synaptic growth and maturation by a synapse-associated E3 ubiquitin ligase at the neuromuscular junction", *J.Cell Biol.*, vol. 177, no. 6, pp. 1077-1089.

Luga, V., Zhang, L., Viloria-Petit, A. M., Ogunjimi, A. A., Inanlou, M. R., Chiu, E., Buchanan, M., Hosein, A. N., Basik, M., & Wrana, J. L. 2012, "Exosomes mediate stromal mobilization of autocrine Wnt-PCP signaling in breast cancer cell migration", *Cell*, vol. 151, no. 7, pp. 1542-1556.

Luyten, A., Mortier, E., Van, C. C., Taelman, V., Degeest, G., Wuytens, G., Lambaerts, K., David, G., Bellefroid, E. J., & Zimmermann, P. 2008, "The postsynaptic density 95/disc-large/zona occludens protein syntenin directly interacts with frizzled 7 and supports noncanonical Wnt signaling", *Mol.Biol.Cell*, vol. 19, no. 4, pp. 1594-1604.

MacDonald, B. T. & He, X. 2012, "Frizzled and LRP5/6 receptors for Wnt/beta-catenin signaling", *Cold Spring Harb.Perspect.Biol.*, vol. 4, no. 12.

Magalhaes, A. C., Dunn, H., & Ferguson, S. S. 2012, "Regulation of GPCR activity, trafficking and localization by GPCR-interacting proteins", *Br.J.Pharmacol.*, vol. 165, no. 6, pp. 1717-1736.

Major, M. B., Roberts, B. S., Berndt, J. D., Marine, S., Anastas, J., Chung, N., Ferrer, M., Yi, X., Stoick-Cooper, C. L., von Haller, P. D., Kategaya, L., Chien, A., Angers, S., MacCoss, M., Cleary, M. A., Arthur, W. T., & Moon, R. T. 2008, "New regulators of Wnt/beta-catenin signaling revealed by integrative molecular screening", *Sci.Signal.*, vol. 1, no. 45, p. ra12.

Marikawa, Y. & Elinson, R. P. 1998, "beta-TrCP is a negative regulator of Wnt/beta-catenin signaling pathway and dorsal axis formation in Xenopus embryos", *Mech.Dev.*, vol. 77, no. 1, pp. 75-80.

Masckauchan, T. N. & Kitajewski, J. 2006, "Wnt/Frizzled signaling in the vasculature: new angiogenic factors in sight", *Physiology.(Bethesda.)*, vol. 21, pp. 181-188.

Mathew, D., Gramates, L. S., Packard, M., Thomas, U., Bilder, D., Perrimon, N., Gorczyca, M., & Budnik, V. 2002, "Recruitment of scribble to the synaptic scaffolding complex requires GUK-holder, a novel DLG binding protein", *Curr.Biol.*, vol. 12, no. 7, pp. 531-539.

Matsumine, A., Ogai, A., Senda, T., Okumura, N., Satoh, K., Baeg, G. H., Kawahara, T., Kobayashi, S., Okada, M., Toyoshima, K., & Akiyama, T. 1996, "Binding of APC to the human homolog of the Drosophila discs large tumor suppressor protein", *Science*, vol. 272, no. 5264, pp. 1020-1023.

McClelland, A. C., Sheffler-Collins, S. I., Kayser, M. S., & Dalva, M. B. 2009, "Ephrin-B1 and ephrin-B2 mediate EphB-dependent presynaptic development via syntenin-1", *Proc.Natl.Acad.Sci.U.S.A*, vol. 106, no. 48, pp. 20487-20492.

McCrea, P. D., Turck, C. W., & Gumbiner, B. 1991, "A homolog of the armadillo protein in Drosophila (plakoglobin) associated with E-cadherin", *Science*, vol. 254, no. 5036, pp. 1359-1361.

Medina, A., Reintsch, W., & Steinbeisser, H. 2000, "Xenopus frizzled 7 can act in canonical and non-canonical Wnt signaling pathways: implications on early patterning and morphogenesis", *Mech.Dev.*, vol. 92, no. 2, pp. 227-237.

Mehraj, V., Boucherit, N., Ben, A. A., Capo, C., Bonatti, S., Mege, J. L., Mottola, G., & Ghigo, E. 2012, "The ligands of Numb proteins X1 and X2 are specific markers for chronic Q fever", *FEMS Immunol.Med.Microbiol.*, vol. 64, no. 1, pp. 98-100.

Merle, P., de la Monte, S., Kim, M., Herrmann, M., Tanaka, S., Von Dem, B. A., Kew, M. C., Trepo, C., & Wands, J. R. 2004, "Functional consequences of frizzled-7 receptor overexpression in human hepatocellular carcinoma", *Gastroenterology*, vol. 127, no. 4, pp. 1110-1122.

Merle, P., Kim, M., Herrmann, M., Gupte, A., Lefrancois, L., Califano, S., Trepo, C., Tanaka, S., Vitvitski, L., de la Monte, S., & Wands, J. R. 2005, "Oncogenic role of the frizzled-7/beta-catenin pathway in hepatocellular carcinoma", *J.Hepatol.*, vol. 43, no. 5, pp. 854-862.

Metais, J. Y., Navarro, C., Santoni, M. J., Audebert, S., & Borg, J. P. 2005, "hScrib interacts with ZO-2 at the cell-cell junctions of epithelial cells", *FEBS Lett.*, vol. 579, no. 17, pp. 3725-3730.

Metzger, M. B., Pruneda, J. N., Klevit, R. E., & Weissman, A. M. 2014, "RING-type E3 ligases: master manipulators of E2 ubiquitin-conjugating enzymes and ubiquitination", *Biochim.Biophys.Acta*, vol. 1843, no. 1, pp. 47-60.

Miller, J. R. 2002, "The Wnts", *Genome Biol.*, vol. 3, no. 1, p. REVIEWS3001.

Miyazaki, K., Fujita, T., Ozaki, T., Kato, C., Kurose, Y., Sakamoto, M., Kato, S., Goto, T., Itoyama, Y., Aoki, M., & Nakagawara, A. 2004, "NEDL1, a novel ubiquitin-protein isopeptide ligase for Dishevelled-1, targets mutant superoxide dismutase-1", *J.Biol.Chem.*, vol. 279, no. 12, pp. 11327-11335.

Moffat, L. L., Robinson, R. E., Bakoulis, A., & Clark, S. G. 2014, "The conserved transmembrane RING finger protein PLR-1 downregulates Wnt signaling by reducing Frizzled, Ror and Ryk cell-surface levels in C. elegans", *Development*, vol. 141, no. 3, pp. 617-628.

Moldovan, G. L. & D'Andrea, A. D. 2009, "How the fanconi anemia pathway guards the genome", *Annu.Rev.Genet.*, vol. 43, pp. 223-249.

Mosimann, C., Hausmann, G., & Basler, K. 2009, "Beta-catenin hits chromatin: regulation of Wnt target gene activation", *Nat.Rev.Mol.Cell Biol.*, vol. 10, no. 4, pp. 276-286.

Mu, Y., Cai, P., Hu, S., Ma, S., & Gao, Y. 2014, "Characterization of diverse internal binding specificities of PDZ domains by yeast two-hybrid screening of a special peptide library", *PLoS.One.*, vol. 9, no. 2, p. e88286.

Mukai, A., Yamamoto-Hino, M., Awano, W., Watanabe, W., Komada, M., & Goto, S. 2010, "Balanced ubiquitylation and deubiquitylation of Frizzled regulate cellular responsiveness to Wg/Wnt", *EMBO J.*, vol. 29, no. 13, pp. 2114-2125.

Mukhopadhyay, D. & Riezman, H. 2007, "Proteasome-independent functions of ubiquitin in endocytosis and signaling", *Science*, vol. 315, no. 5809, pp. 201-205.

Munoz, R., Moreno, M., Oliva, C., Orbenes, C., & Larrain, J. 2006, "Syndecan-4 regulates non-canonical Wnt signalling and is essential for convergent and extension movements in Xenopus embryos", *Nat.Cell Biol.*, vol. 8, no. 5, pp. 492-500.

Nambotin, S. B., Lefrancois, L., Sainsily, X., Berthillon, P., Kim, M., Wands, J. R., Chevallier, M., Jalinot, P., Scoazec, J. Y., Trepo, C., Zoulim, F., & Merle, P. 2011, "Pharmacological inhibition of Frizzled-7 displays anti-tumor properties in hepatocellular carcinoma", *J.Hepatol.*, vol. 54, no. 2, pp. 288-299.

Nie, J., Li, S. S., & McGlade, C. J. 2004, "A novel PTB-PDZ domain interaction mediates isoform-specific ubiquitylation of mammalian Numb", *J.Biol.Chem.*, vol. 279, no. 20, pp. 20807-20815.

Nie, J., McGill, M. A., Dermer, M., Dho, S. E., Wolting, C. D., & McGlade, C. J. 2002, "LNX functions as a RING type E3 ubiquitin ligase that targets the cell fate determinant Numb for ubiquitin-dependent degradation", *EMBO J.*, vol. 21, no. 1-2, pp. 93-102.

Niehrs, C. 2012, "The complex world of WNT receptor signalling", *Nat.Rev.Mol.Cell Biol.*, vol. 13, no. 12, pp. 767-779.

Nishioka, M., Ueno, K., Hazama, S., Okada, T., Sakai, K., Suehiro, Y., Okayama, N., Hirata, H., Oka, M., Imai, K., Dahiya, R., & Hinoda, Y. 2013, "Possible involvement of Wnt11 in colorectal cancer progression", *Mol.Carcinog.*, vol. 52, no. 3, pp. 207-217.

Nojima, M., Suzuki, H., Toyota, M., Watanabe, Y., Maruyama, R., Sasaki, S., Sasaki, Y., Mita, H., Nishikawa, N., Yamaguchi, K., Hirata, K., Itoh, F., Tokino, T., Mori, M., Imai, K., & Shinomura, Y. 2007, "Frequent epigenetic inactivation of SFRP genes and constitutive activation of Wnt signaling in gastric cancer", *Oncogene*, vol. 26, no. 32, pp. 4699-4713.

Okino, K., Nagai, H., Hatta, M., Nagahata, T., Yoneyama, K., Ohta, Y., Jin, E., Kawanami, O., Araki, T., & Emi, M. 2003, "Up-regulation and overproduction of DVL-1, the human counterpart of the Drosophila Dishevelled gene, in cervical squamous cell carcinoma", *Oncol.Rep.*, vol. 10, no. 5, pp. 1219-1223.

Onishi, K., Shafer, B., Lo, C., Tissir, F., Goffinet, A. M., & Zou, Y. 2013, "Antagonistic functions of Dishevelleds regulate Frizzled3 endocytosis via filopodia tips in Wnt-mediated growth cone guidance", *J.Neurosci.*, vol. 33, no. 49, pp. 19071-19085.

Penzo-Mendez, A., Umbhauer, M., Djiane, A., Boucaut, J. C., & Riou, J. F. 2003, "Activation of Gbetagamma signaling downstream of Wnt-11/Xfz7 regulates Cdc42 activity during Xenopus gastrulation", *Dev.Biol.*, vol. 257, no. 2, pp. 302-314.

Pickart, C. M. 2001, "Mechanisms underlying ubiquitination", *Annu.Rev.Biochem.*, vol. 70, pp. 503-533.

Polakis, P. 2000, "Wnt signaling and cancer", *Genes Dev.*, vol. 14, no. 15, pp. 1837-1851.

Polakis, P. 2007, "The many ways of Wnt in cancer", *Curr.Opin.Genet.Dev.*, vol. 17, no. 1, pp. 45-51.

Polakis, P. 2012, "Wnt signaling in cancer", *Cold Spring Harb.Perspect.Biol.*, vol. 4, no. 5.

Pols, M. S. & Klumperman, J. 2009, "Trafficking and function of the tetraspanin CD63", *Exp.Cell Res.*, vol. 315, no. 9, pp. 1584-1592.

Pranke, I. M. & Sermet-Gaudelus, I. 2014, "Biosynthesis of cystic fibrosis transmembrane conductance regulator", *Int.J.Biochem.Cell Biol.*, vol. 52, pp. 26-38.

Pukrop, T., Klemm, F., Hagemann, T., Gradl, D., Schulz, M., Siemes, S., Trumper, L., & Binder, C. 2006, "Wnt 5a signaling is critical for macrophage-induced invasion of breast cancer cell lines", *Proc.Natl.Acad.Sci.U.S.A*, vol. 103, no. 14, pp. 5454-5459.

Rajesh, S., Bago, R., Odintsova, E., Muratov, G., Baldwin, G., Sridhar, P., Rajesh, S., Overduin, M., & Berditchevski, F. 2011, "Binding to syntenin-1 protein defines a new mode of ubiquitin-based interactions regulated by phosphorylation", *J.Biol.Chem.*, vol. 286, no. 45, pp. 39606-39614.

Rao, T. P. & Kuhl, M. 2010, "An updated overview on Wnt signaling pathways: a prelude for more", *Circ.Res.*, vol. 106, no. 12, pp. 1798-1806.

Rice, D. S., Northcutt, G. M., & Kurschner, C. 2001, "The Lnx family proteins function as molecular scaffolds for Numb family proteins", *Mol.Cell Neurosci.*, vol. 18, no. 5, pp. 525-540.

Ripka, S., Konig, A., Buchholz, M., Wagner, M., Sipos, B., Kloppel, G., Downward, J., Gress, T., & Michl, P. 2007, "WNT5A--target of CUTL1 and potent modulator of tumor cell migration and invasion in pancreatic cancer", *Carcinogenesis*, vol. 28, no. 6, pp. 1178-1187.

Ro, H. & Dawid, I. B. 2009, "Organizer restriction through modulation of Bozozok stability by the E3 ubiquitin ligase Lnx-like", *Nat.Cell Biol.*, vol. 11, no. 9, pp. 1121-1127.

Roh, M. H., Makarova, O., Liu, C. J., Shin, K., Lee, S., Laurinec, S., Goyal, M., Wiggins, R., & Margolis, B. 2002, "The Maguk protein, Pals1, functions as an adapter, linking mammalian homologues of Crumbs and Discs Lost", *J.Cell Biol.*, vol. 157, no. 1, pp. 161-172.

Rual, J. F., Venkatesan, K., Hao, T., Hirozane-Kishikawa, T., Dricot, A., Li, N., Berriz, G. F., Gibbons, F. D., Dreze, M., Ayivi-Guedehoussou, N., Klitgord, N., Simon, C., Boxem, M., Milstein, S., Rosenberg, J., Goldberg, D. S., Zhang, L. V., Wong, S. L., Franklin, G., Li, S., Albala, J. S., Lim, J., Fraughton, C., Llamosas, E., Cevik, S., Bex, C., Lamesch, P., Sikorski, R. S., Vandenhaute, J., Zoghbi, H. Y., Smolyar, A., Bosak, S., Sequerra, R., Doucette-Stamm, L., Cusick, M. E., Hill, D. E., Roth, F. P., & Vidal, M. 2005, "Towards a proteome-scale map of the human protein-protein interaction network", *Nature*, vol. 437, no. 7062, pp. 1173-1178.

Sagara, N., Toda, G., Hirai, M., Terada, M., & Katoh, M. 1998, "Molecular cloning, differential expression, and chromosomal localization of human frizzled-1, frizzled-2, and frizzled-7", *Biochem.Biophys.Res.Commun.*, vol. 252, no. 1, pp. 117-122.

Saitoh, T., Mine, T., & Katoh, M. 2002, "Up-regulation of Frizzled-10 (FZD10) by beta-estradiol in MCF-7 cells and by retinoic acid in NT2 cells", *Int.J.Oncol.*, vol. 20, no. 1, pp. 117-120.

Sala-Valdes, M., Gordon-Alonso, M., Tejera, E., Ibanez, A., Cabrero, J. R., Ursa, A., Mittelbrunn, M., Lozano, F., Sanchez-Madrid, F., & Yanez-Mo, M. 2012, "Association of syntenin-1 with M-RIP polarizes Rac-1 activation during chemotaxis and immune interactions", *J.Cell Sci.*, vol. 125, no. Pt 5, pp. 1235-1246.

Sarkar, D., Boukerche, H., Su, Z. Z., & Fisher, P. B. 2004, "mda-9/syntenin: recent insights into a novel cell signaling and metastasis-associated gene", *Pharmacol.Ther.*, vol. 104, no. 2, pp. 101-115.

Sarkar, D., Boukerche, H., Su, Z. Z., & Fisher, P. B. 2008, "mda-9/Syntenin: more than just a simple adapter protein when it comes to cancer metastasis", *Cancer Res.*, vol. 68, no. 9, pp. 3087-3093.

Satija, Y. K., Bhardwaj, A., & Das, S. 2013, "A portrayal of E3 ubiquitin ligases and deubiquitylases in cancer", *Int.J.Cancer*, vol. 133, no. 12, pp. 2759-2768.

Sato, H., Suzuki, H., Toyota, M., Nojima, M., Maruyama, R., Sasaki, S., Takagi, H., Sogabe, Y., Sasaki, Y., Idogawa, M., Sonoda, T., Mori, M., Imai, K., Tokino, T., & Shinomura, Y. 2007, "Frequent epigenetic inactivation of DICKKOPF family genes in human gastrointestinal tumors", *Carcinogenesis*, vol. 28, no. 12, pp. 2459-2466.

Schioth, H. B. & Fredriksson, R. 2005, "The GRAFS classification system of G-protein coupled receptors in comparative perspective", *Gen.Comp Endocrinol.*, vol. 142, no. 1-2, pp. 94-101.

Schlange, T., Matsuda, Y., Lienhard, S., Huber, A., & Hynes, N. E. 2007, "Autocrine WNT signaling contributes to breast cancer cell proliferation via the canonical WNT pathway and EGFR transactivation", *Breast Cancer Res.*, vol. 9, no. 5, p. R63.

Schmuck, R., Warneke, V., Behrens, H. M., Simon, E., Weichert, W., & Rocken, C. 2011, "Genotypic and phenotypic characterization of side population of gastric cancer cell lines", *Am.J.Pathol.*, vol. 178, no. 4, pp. 1792-1804.

Schroeder, J. A., Adriance, M. C., McConnell, E. J., Thompson, M. C., Pockaj, B., & Gendler, S. J. 2002, "ErbB-beta-catenin complexes are associated with human infiltrating ductal breast and murine mammary tumor virus (MMTV)-Wnt-1 and MMTV-c-Neu transgenic carcinomas", *J.Biol.Chem.*, vol. 277, no. 25, pp. 22692-22698.

Schroeder, J. A., Troyer, K. L., & Lee, D. C. 2000, "Cooperative induction of mammary tumorigenesis by TGFalpha and Wnts", *Oncogene*, vol. 19, no. 28, pp. 3193-3199.

Schulte, G. 2010, "International Union of Basic and Clinical Pharmacology. LXXX. The class Frizzled receptors", *Pharmacol.Rev.*, vol. 62, no. 4, pp. 632-667.

Schulte, G. & Bryja, V. 2007, "The Frizzled family of unconventional G-protein-coupled receptors", *Trends Pharmacol.Sci.*, vol. 28, no. 10, pp. 518-525.

Schwarz-Romond, T., Fiedler, M., Shibata, N., Butler, P. J., Kikuchi, A., Higuchi, Y., & Bienz, M. 2007, "The DIX domain of Dishevelled confers Wnt signaling by dynamic polymerization", *Nat.Struct.Mol.Biol.*, vol. 14, no. 6, pp. 484-492.

Scott, C. C., Vacca, F., & Gruenberg, J. 2014, "Endosome maturation, transport and functions", *Semin.Cell Dev.Biol.*, vol. 31, pp. 2-10.

Semenov, M. V., Habas, R., Macdonald, B. T., & He, X. 2007, "SnapShot: Noncanonical Wnt Signaling Pathways", *Cell*, vol. 131, no. 7, p. 1378.

Sewduth, R. N., Jaspard-Vinassa, B., Peghaire, C., Guillabert, A., Franzl, N., Larrieu-Lahargue, F., Moreau, C., Fruttiger, M., Dufourcq, P., Couffinhal, T., & Duplaa, C. 2014, "The ubiquitin ligase PDZRN3 is required for vascular morphogenesis through Wnt/planar cell polarity signalling", *Nat.Commun.*, vol. 5, p. 4832.

Sheldahl, L. C., Slusarski, D. C., Pandur, P., Miller, J. R., Kuhl, M., & Moon, R. T. 2003, "Dishevelled activates Ca2+ flux, PKC, and CamKII in vertebrate embryos", *J.Cell Biol.*, vol. 161, no. 4, pp. 769-777.

Shulewitz, M., Soloviev, I., Wu, T., Koeppen, H., Polakis, P., & Sakanaka, C. 2006, "Repressor roles for TCF-4 and Sfrp1 in Wnt signaling in breast cancer", *Oncogene*, vol. 25, no. 31, pp. 4361-4369.

Simmons, G. E., Jr., Pandey, S., Nedeljkovic-Kurepa, A., Saxena, M., Wang, A., & Pruitt, K. 2014, "Frizzled 7 expression is positively regulated by SIRT1 and beta-catenin in breast cancer cells", *PLoS.One.*, vol. 9, no. 6, p. e98861.

Simons, M., Gloy, J., Ganner, A., Bullerkotte, A., Bashkurov, M., Kronig, C., Schermer, B., Benzing, T., Cabello, O. A., Jenny, A., Mlodzik, M., Polok, B., Driever, W., Obara, T., & Walz, G. 2005, "Inversin, the gene product mutated in nephronophthisis type II, functions as a molecular switch between Wnt signaling pathways", *Nat.Genet.*, vol. 37, no. 5, pp. 537-543.

Sollerbrant, K., Raschperger, E., Mirza, M., Engstrom, U., Philipson, L., Ljungdahl, P. O., & Pettersson, R. F. 2003, "The Coxsackievirus and adenovirus receptor (CAR) forms a complex with the PDZ domain-containing protein ligand-of-numb protein-X (LNX)", *J.Biol.Chem.*, vol. 278, no. 9, pp. 7439-7444.

Song, E., Gao, S., Tian, R., Ma, S., Huang, H., Guo, J., Li, Y., Zhang, L., & Gao, Y. 2006, "A high efficiency strategy for binding property characterization of peptide-binding domains", *Mol.Cell Proteomics.*, vol. 5, no. 8, pp. 1368-1381.

Sorlie, T., Bukholm, I., & Borresen-Dale, A. L. 1998, "Truncating somatic mutation in exon 15 of the APC gene is a rare event in human breast carcinomas. Mutations in brief no. 179. Online", *Hum.Mutat.*, vol. 12, no. 3, p. 215.

Staal, F. J., Luis, T. C., & Tiemessen, M. M. 2008, "WNT signalling in the immune system: WNT is spreading its wings", *Nat.Rev.Immunol.*, vol. 8, no. 8, pp. 581-593.

Steinberg, F., Gallon, M., Winfield, M., Thomas, E. C., Bell, A. J., Heesom, K. J., Tavare, J. M., & Cullen, P. J. 2013, "A global analysis of SNX27-retromer assembly and cargo specificity reveals a function in glucose and metal ion transport", *Nat.Cell Biol.*, vol. 15, no. 5, pp. 461-471.

Struewing, I. T., Barnett, C. D., Zhang, W., Yadav, S., & Mao, C. D. 2007, "Frizzled-7 turnover at the plasma membrane is regulated by cell density and the Ca(2+) -dependent protease calpain-1", *Exp.Cell Res.*, vol. 313, no. 16, pp. 3526-3541.

Stucke, V. M., Timmerman, E., Vandekerckhove, J., Gevaert, K., & Hall, A. 2007, "The MAGUK protein MPP7 binds to the polarity protein hDlg1 and facilitates epithelial tight junction formation", *Mol.Biol.Cell*, vol. 18, no. 5, pp. 1744-1755.

Subbaiah, V. K., Kranjec, C., Thomas, M., & Banks, L. 2011, "PDZ domains: the building blocks regulating tumorigenesis", *Biochem.J.*, vol. 439, no. 2, pp. 195-205.

Suzuki, H., Toyota, M., Carraway, H., Gabrielson, E., Ohmura, T., Fujikane, T., Nishikawa, N., Sogabe, Y., Nojima, M., Sonoda, T., Mori, M., Hirata, K., Imai, K., Shinomura, Y., Baylin, S. B., & Tokino, T. 2008, "Frequent epigenetic inactivation of Wnt antagonist genes in breast cancer", *Br.J.Cancer*, vol. 98, no. 6, pp. 1147-1156.

Swain, R. K., Medina, A., & Steinbeisser, H. 2001, "Functional analysis of the Xenopus frizzled 7 protein domains using chimeric receptors", *Int.J.Dev.Biol.*, vol. 45, no. 1, pp. 259-264.

Takahashi, S., Iwamoto, N., Sasaki, H., Ohashi, M., Oda, Y., Tsukita, S., & Furuse, M. 2009, "The E3 ubiquitin ligase LNX1p80 promotes the removal of claudins from tight junctions in MDCK cells", *J.Cell Sci.*, vol. 122, no. Pt 7, pp. 985-994.

Takahashi-Yanaga, F. & Kahn, M. 2010, "Targeting Wnt signaling: can we safely eradicate cancer stem cells?", *Clin.Cancer Res.*, vol. 16, no. 12, pp. 3153-3162.

Talbot, L. J., Bhattacharya, S. D., & Kuo, P. C. 2012, "Epithelial-mesenchymal transition, the tumor microenvironment, and metastatic behavior of epithelial malignancies", *Int.J.Biochem.Mol.Biol.*, vol. 3, no. 2, pp. 117-136.

Tan, C., Deardorff, M. A., Saint-Jeannet, J. P., Yang, J., Arzoumanian, A., & Klein, P. S. 2001, "Kermit, a frizzled interacting protein, regulates frizzled 3 signaling in neural crest development", *Development*, vol. 128, no. 19, pp. 3665-3674.

Tanaka, K., Kitagawa, Y., & Kadowaki, T. 2002, "Drosophila segment polarity gene product porcupine stimulates the posttranslational N-glycosylation of wingless in the endoplasmic reticulum", *J.Biol.Chem.*, vol. 277, no. 15, pp. 12816-12823.

Tanaka, S., Akiyoshi, T., Mori, M., Wands, J. R., & Sugimachi, K. 1998, "A novel frizzled gene identified in human esophageal carcinoma mediates APC/beta-catenin signals", *Proc.Natl.Acad.Sci.U.S.A*, vol. 95, no. 17, pp. 10164-10169.

Tanegashima, K., Zhao, H., & Dawid, I. B. 2008, "WGEF activates Rho in the Wnt-PCP pathway and controls convergent extension in Xenopus gastrulation", *EMBO J.*, vol. 27, no. 4, pp. 606-617.

Tauriello, D. V., Haegebarth, A., Kuper, I., Edelmann, M. J., Henraat, M., Canninga-van Dijk, M. R., Kessler, B. M., Clevers, H., & Maurice, M. M. 2010a, "Loss of the tumor suppressor CYLD enhances Wnt/beta-catenin signaling through K63-linked ubiquitination of Dvl", *Mol.Cell*, vol. 37, no. 5, pp. 607-619.

Tauriello, D. V., Jordens, I., Kirchner, K., Slootstra, J. W., Kruitwagen, T., Bouwman, B. A., Noutsou, M., Rudiger, S. G., Schwamborn, K., Schambony, A., & Maurice, M. M. 2012, "Wnt/beta-catenin signaling requires interaction of the Dishevelled DEP domain and C terminus with a discontinuous motif in Frizzled", *Proc.Natl.Acad.Sci.U.S.A*, vol. 109, no. 14, p. E812-E820.

Tauriello, D. V. & Maurice, M. M. 2010b, "The various roles of ubiquitin in Wnt pathway regulation", *Cell Cycle*, vol. 9, no. 18, pp. 3700-3709.

Tekmal, R. R. & Keshava, N. 1997, "Role of MMTV integration locus cellular genes in breast cancer", *Front Biosci.*, vol. 2, p. d519-d526.

Temkin, P., Lauffer, B., Jager, S., Cimermancic, P., Krogan, N. J., & von, Z. M. 2011, "SNX27 mediates retromer tubule entry and endosome-to-plasma membrane trafficking of signalling receptors", *Nat.Cell Biol.*, vol. 13, no. 6, pp. 715-721.

Tomoda, T., Kim, J. H., Zhan, C., & Hatten, M. E. 2004, "Role of Unc51.1 and its binding partners in CNS axon outgrowth", *Genes Dev.*, vol. 18, no. 5, pp. 541-558.

Tonikian, R., Zhang, Y., Sazinsky, S. L., Currell, B., Yeh, J. H., Reva, B., Held, H. A., Appleton, B. A., Evangelista, M., Wu, Y., Xin, X., Chan, A. C., Seshagiri, S., Lasky, L. A., Sander, C., Boone, C., Bader, G. D., & Sidhu, S. S. 2008, "A specificity map for the PDZ domain family", *PLoS.Biol.*, vol. 6, no. 9, p. e239.

Tuttle, A. M., Hoffman, T. L., & Schilling, T. F. 2014, "Rabconnectin-3a regulates vesicle endocytosis and canonical Wnt signaling in zebrafish neural crest migration", *PLoS.Biol.*, vol. 12, no. 5, p. e1001852.

Ueno, K., Hazama, S., Mitomori, S., Nishioka, M., Suehiro, Y., Hirata, H., Oka, M., Imai, K., Dahiya, R., & Hinoda, Y. 2009, "Down-regulation of frizzled-7 expression decreases survival, invasion and metastatic capabilities of colon cancer cells", *Br.J.Cancer*, vol. 101, no. 8, pp. 1374-1381.

Ueno, K., Hiura, M., Suehiro, Y., Hazama, S., Hirata, H., Oka, M., Imai, K., Dahiya, R., & Hinoda, Y. 2008, "Frizzled-7 as a potential therapeutic target in colorectal cancer", *Neoplasia.*, vol. 10, no. 7, pp. 697-705.

Umbhauer, M., Djiane, A., Goisset, C., Penzo-Mendez, A., Riou, J. F., Boucaut, J. C., & Shi, D. L. 2000, "The C-terminal cytoplasmic Lys-thr-X-X-X-Trp motif in frizzled receptors mediates Wnt/beta-catenin signalling", *EMBO J.*, vol. 19, no. 18, pp. 4944-4954.

van 't Veer, L. J., van Kessel, A. G., van, H. H., van, O. A., & Nusse, R. 1984, "Molecular cloning and chromosomal assignment of the human homolog of int-1, a mouse gene implicated in mammary tumorigenesis", *Mol.Cell Biol.*, vol. 4, no. 11, pp. 2532-2534.

van Amerongen R. & Nusse, R. 2009, "Towards an integrated view of Wnt signaling in development", *Development*, vol. 136, no. 19, pp. 3205-3214.

Veeck, J., Niederacher, D., An, H., Klopocki, E., Wiesmann, F., Betz, B., Galm, O., Camara, O., Durst, M., Kristiansen, G., Huszka, C., Knuchel, R., & Dahl, E. 2006, "Aberrant methylation of the Wnt antagonist SFRP1 in breast cancer is associated with unfavourable prognosis", *Oncogene*, vol. 25, no. 24, pp. 3479-3488.

Veeman, M. T., Axelrod, J. D., & Moon, R. T. 2003a, "A second canon. Functions and mechanisms of beta-catenin-independent Wnt signaling", *Dev.Cell*, vol. 5, no. 3, pp. 367-377.

Veeman, M. T., Slusarski, D. C., Kaykas, A., Louie, S. H., & Moon, R. T. 2003b, "Zebrafish prickle, a modulator of noncanonical Wnt/Fz signaling, regulates gastrulation movements", *Curr.Biol.*, vol. 13, no. 8, pp. 680-685.

Vincan, E., Brabletz, T., Faux, M. C., & Ramsay, R. G. 2007a, "A human three-dimensional cell line model allows the study of dynamic and reversible epithelial-mesenchymal and mesenchymal-epithelial transition that underpins colorectal carcinogenesis", *Cells Tissues.Organs*, vol. 185, no. 1-3, pp. 20-28.

Vincan, E., Darcy, P. K., Farrelly, C. A., Faux, M. C., Brabletz, T., & Ramsay, R. G. 2007b, "Frizzled-7 dictates three-dimensional organization of colorectal cancer cell carcinoids", *Oncogene*, vol. 26, no. 16, pp. 2340-2352.

Vincan, E., Flanagan, D. J., Pouliot, N., Brabletz, T., & Spaderna, S. 2010, "Variable FZD7 expression in colorectal cancers indicates regulation by the tumour microenvironment", *Dev.Dyn.*, vol. 239, no. 1, pp. 311-317.

Wallingford, J. B. & Habas, R. 2005, "The developmental biology of Dishevelled: an enigmatic protein governing cell fate and cell polarity", *Development*, vol. 132, no. 20, pp. 4421-4436.

Wang, L. H., Kalb, R. G., & Strittmatter, S. M. 1999, "A PDZ protein regulates the distribution of the transmembrane semaphorin, M-SemF", *J.Biol.Chem.*, vol. 274, no. 20, pp. 14137-14146.

Wang, Q., Williamson, M., Bott, S., Brookman-Amissah, N., Freeman, A., Nariculam, J., Hubank, M. J., Ahmed, A., & Masters, J. R. 2007, "Hypomethylation of WNT5A, CRIP1 and S100P in prostate cancer", *Oncogene*, vol. 26, no. 45, pp. 6560-6565.

Wang, Y. 2009, "Wnt/Planar cell polarity signaling: a new paradigm for cancer therapy", *Mol.Cancer Ther.*, vol. 8, no. 8, pp. 2103-2109.

Wawrzak, D., Luyten, A., Lambaerts, K., & Zimmermann, P. 2009, "Frizzled-PDZ scaffold interactions in the control of Wnt signaling", *Adv.Enzyme Regul.*, vol. 49, no. 1, pp. 98-106.

Wawrzyniak, A. M., Vermeiren, E., Zimmermann, P., & Ivarsson, Y. 2012, "Extensions of PSD-95/discs large/ZO-1 (PDZ) domains influence lipid binding and membrane targeting of syntenin-1", *FEBS Lett.*, vol. 586, no. 10, pp. 1445-1451.

Weeraratna, A. T., Jiang, Y., Hostetter, G., Rosenblatt, K., Duray, P., Bittner, M., & Trent, J. M. 2002, "Wnt5a signaling directly affects cell motility and invasion of metastatic melanoma", *Cancer Cell*, vol. 1, no. 3, pp. 279-288.

Weiss, A., Baumgartner, M., Radziwill, G., Dennler, J., & Moelling, K. 2007, "c-Src is a PDZ interaction partner and substrate of the E3 ubiquitin ligase Ligand-of-Numb protein X1", *FEBS Lett.*, vol. 581, no. 26, pp. 5131-5136.

Welcsh, P. L. & King, M. C. 2001, "BRCA1 and BRCA2 and the genetics of breast and ovarian cancer", *Hum.Mol.Genet.*, vol. 10, no. 7, pp. 705-713.

Wente, W., Stroh, T., Beaudet, A., Richter, D., & Kreienkamp, H. J. 2005, "Interactions with PDZ domain proteins PIST/GOPC and PDZK1 regulate intracellular sorting of the somatostatin receptor subtype 5", *J.Biol.Chem.*, vol. 280, no. 37, pp. 32419-32425.

Wheeler, D. S., Barrick, S. R., Grubisha, M. J., Brufsky, A. M., Friedman, P. A., & Romero, G. 2011, "Direct interaction between NHERF1 and Frizzled regulates beta-catenin signaling", *Oncogene*, vol. 30, no. 1, pp. 32-42.

Whittaker, S., Marais, R., & Zhu, A. X. 2010, "The role of signaling pathways in the development and treatment of hepatocellular carcinoma", *Oncogene*, vol. 29, no. 36, pp. 4989-5005.

Willert, K., Brown, J. D., Danenberg, E., Duncan, A. W., Weissman, I. L., Reya, T., Yates, J. R., III, & Nusse, R. 2003, "Wnt proteins are lipid-modified and can act as stem cell growth factors", *Nature*, vol. 423, no. 6938, pp. 448-452.

Wissmann, C., Wild, P. J., Kaiser, S., Roepcke, S., Stoehr, R., Woenckhaus, M., Kristiansen, G., Hsieh, J. C., Hofstaedter, F., Hartmann, A., Knuechel, R., Rosenthal, A., & Pilarsky, C. 2003, "WIF1, a component of the Wnt pathway, is down-regulated in prostate, breast, lung, and bladder cancer", *J.Pathol.*, vol. 201, no. 2, pp. 204-212.

Wolting, C. D., Griffiths, E. K., Sarao, R., Prevost, B. C., Wybenga-Groot, L. E., & McGlade, C. J. 2011, "Biochemical and computational analysis of LNX1 interacting proteins", *PLoS.One.*, vol. 6, no. 11, p. e26248.

Wong, H. C., Bourdelas, A., Krauss, A., Lee, H. J., Shao, Y., Wu, D., Mlodzik, M., Shi, D. L., & Zheng, J. 2003, "Direct binding of the PDZ domain of Dishevelled to a conserved internal sequence in the C-terminal region of Frizzled", *Mol.Cell*, vol. 12, no. 5, pp. 1251-1260.

Wu, C. H. & Nusse, R. 2002, "Ligand receptor interactions in the Wnt signaling pathway in Drosophila", *J.Biol.Chem.*, vol. 277, no. 44, pp. 41762-41769.

Wu, J. & Mlodzik, M. 2008, "The frizzled extracellular domain is a ligand for Van Gogh/Stbm during nonautonomous planar cell polarity signaling", *Dev.Cell*, vol. 15, no. 3, pp. 462-469.

Wu, J. & Mlodzik, M. 2009, "A quest for the mechanism regulating global planar cell polarity of tissues", *Trends Cell Biol.*, vol. 19, no. 7, pp. 295-305.

Wu, Y., Ginther, C., Kim, J., Mosher, N., Chung, S., Slamon, D., & Vadgama, J. V. 2012, "Expression of Wnt3 activates Wnt/beta-catenin pathway and promotes EMT-like phenotype in trastuzumab-resistant HER2-overexpressing breast cancer cells", *Mol.Cancer Res.*, vol. 10, no. 12, pp. 1597-1606.

Xie, Y., Zhao, W., Wang, W., Zhao, S., Tang, R., Ying, K., Zhou, Z., & Mao, Y. 2001, "Identification of a human LNX protein containing multiple PDZ domains", *Biochem.Genet.*, vol. 39, no. 3-4, pp. 117-126.

Xu, W. & Kimelman, D. 2007, "Mechanistic insights from structural studies of beta-catenin and its binding partners", *J.Cell Sci.*, vol. 120, no. Pt 19, pp. 3337-3344.

Xu, Y. K. & Nusse, R. 1998, "The Frizzled CRD domain is conserved in diverse proteins including several receptor tyrosine kinases", *Curr.Biol.*, vol. 8, no. 12, p. R405-R406.

Xu, Z., Oshima, K., & Heller, S. 2010, "PIST regulates the intracellular trafficking and plasma membrane expression of cadherin 23", *BMC.Cell Biol.*, vol. 11, p. 80.

Yamamoto, A., Nagano, T., Takehara, S., Hibi, M., & Aizawa, S. 2005, "Shisa promotes head formation through the inhibition of receptor protein maturation for the caudalizing factors, Wnt and FGF", *Cell*, vol. 120, no. 2, pp. 223-235.

Yamamoto, H., Komekado, H., & Kikuchi, A. 2006, "Caveolin is necessary for Wnt-3a-dependent internalization of LRP6 and accumulation of beta-catenin", *Dev.Cell*, vol. 11, no. 2, pp. 213-223.

Yang, L., Wu, X., Wang, Y., Zhang, K., Wu, J., Yuan, Y. C., Deng, X., Chen, L., Kim, C. C., Lau, S., Somlo, G., & Yen, Y. 2011, "FZD7 has a critical role in cell proliferation in triple negative breast cancer", *Oncogene*, vol. 30, no. 43, pp. 4437-4446.

Yang, S. Z., Kohno, N., Yokoyama, A., Kondo, K., Hamada, H., & Hiwada, K. 2001, "Decreased E-cadherin augments beta-catenin nuclear localization: studies in breast cancer cell lines", *Int.J.Oncol.*, vol. 18, no. 3, pp. 541-548.

Yao, R., Maeda, T., Takada, S., & Noda, T. 2001, "Identification of a PDZ domain containing Golgi protein, GOPC, as an interaction partner of frizzled", *Biochem.Biophys.Res.Commun.*, vol. 286, no. 4, pp. 771-778.

Yao, R., Natsume, Y., & Noda, T. 2004, "MAGI-3 is involved in the regulation of the JNK signaling pathway as a scaffold protein for frizzled and Ltap", *Oncogene*, vol. 23, no. 36, pp. 6023-6030.

Ying, J., Li, H., Chen, Y. W., Srivastava, G., Gao, Z., & Tao, Q. 2007, "WNT5A is epigenetically silenced in hematologic malignancies and inhibits leukemia cell growth as a tumor suppressor", *Blood*, vol. 110, no. 12, pp. 4130-4132.

Ying, J., Li, H., Yu, J., Ng, K. M., Poon, F. F., Wong, S. C., Chan, A. T., Sung, J. J., & Tao, Q. 2008, "WNT5A exhibits tumor-suppressive activity through antagonizing the Wnt/beta-catenin signaling, and is frequently methylated in colorectal cancer", *Clin.Cancer Res.*, vol. 14, no. 1, pp. 55-61.

Young, P., Nie, J., Wang, X., McGlade, C. J., Rich, M. M., & Feng, G. 2005, "LNX1 is a perisynaptic Schwann cell specific E3 ubiquitin ligase that interacts with ErbB2", *Mol.Cell Neurosci.*, vol. 30, no. 2, pp. 238-248.

Yu, A., Rual, J. F., Tamai, K., Harada, Y., Vidal, M., He, X., & Kirchhausen, T. 2007, "Association of Dishevelled with the clathrin AP-2 adaptor is required for Frizzled endocytosis and planar cell polarity signaling", *Dev.Cell*, vol. 12, no. 1, pp. 129-141.

Yu, H., Ye, X., Guo, N., & Nathans, J. 2012, "Frizzled 2 and frizzled 7 function redundantly in convergent extension and closure of the ventricular septum and palate: evidence for a network of interacting genes", *Development*, vol. 139, no. 23, pp. 4383-4394.

Zeng, X., Tamai, K., Doble, B., Li, S., Huang, H., Habas, R., Okamura, H., Woodgett, J., & He, X. 2005, "A dual-kinase mechanism for Wnt co-receptor phosphorylation and activation", *Nature*, vol. 438, no. 7069, pp. 873-877.

Zeng, Z. Y., Zhou, Y. H., Zhang, W. L., Xiong, W., Fan, S. Q., Li, X. L., Luo, X. M., Wu, M. H., Yang, Y. X., Huang, C., Cao, L., Tang, K., Qian, J., Shen, S. R., & Li, G. Y. 2007, "Gene expression profiling of nasopharyngeal carcinoma reveals the abnormally regulated Wnt signaling pathway", *Hum.Pathol.*, vol. 38, no. 1, pp. 120-133.

Zhang, Y., Wang, F., Han, L., Wu, Y., Li, S., Yang, X., Wang, Y., Ren, F., Zhai, Y., Wang, D., Jia, B., Xia, Y., & Chang, Z. 2011, "GABARAPL1 negatively regulates Wnt/beta-catenin signaling by mediating Dvl2 degradation through the autophagy pathway", *Cell Physiol Biochem.*, vol. 27, no. 5, pp. 503-512.

Zhang, Y., Yeh, J. R., Mara, A., Ju, R., Hines, J. F., Cirone, P., Griesbach, H. L., Schneider, I., Slusarski, D. C., Holley, S. A., & Crews, C. M. 2006, "A chemical and genetic approach to the mode of action of fumagillin", *Chem.Biol.*, vol. 13, no. 9, pp. 1001-1009.

Zheng, D., Gu, S., Li, Y., Ji, C., Xie, Y., & Mao, Y. 2011, "A global genomic view on LNX siRNA-mediated cell cycle arrest", *Mol.Biol.Rep.*, vol. 38, no. 4, pp. 2771-2783.

Zheng, D., Sun, Y., Gu, S., Ji, C., Zhao, W., Xie, Y., & Mao, Y. 2010, "LNX (Ligand of Numb-protein X) interacts with RhoC, both of which regulate AP-1-mediated transcriptional activation", *Mol.Biol.Rep.*, vol. 37, no. 5, pp. 2431-2437.

Zhou, L., Ercolano, E., Ammoun, S., Schmid, M. C., Barczyk, M. A., & Hanemann, C. O. 2011, "Merlin-deficient human tumors show loss of contact inhibition and activation of Wnt/beta-catenin signaling linked to the PDGFR/Src and Rac/PAK pathways", *Neoplasia.*, vol. 13, no. 12, pp. 1101-1112.

Zimmermann, P. 2006, "The prevalence and significance of PDZ domain-phosphoinositide interactions", *Biochim.Biophys.Acta*, vol. 1761, no. 8, pp. 947-956.

Zimmermann, P., Meerschaert, K., Reekmans, G., Leenaerts, I., Small, J. V., Vandekerckhove, J., David, G., & Gettemans, J. 2002, "PIP(2)-PDZ domain binding controls the association of syntenin with the plasma membrane", *Mol.Cell*, vol. 9, no. 6, pp. 1215-1225.

Zimmermann, P., Tomatis, D., Rosas, M., Grootjans, J., Leenaerts, I., Degeest, G., Reekmans, G., Coomans, C., & David, G. 2001, "Characterization of syntenin, a syndecan-binding PDZ protein, as a component of cell adhesion sites and microfilaments", *Mol.Biol.Cell*, vol. 12, no. 2, pp. 339-350.

Zimmermann, P., Zhang, Z., Degeest, G., Mortier, E., Leenaerts, I., Coomans, C., Schulz, J., N'Kuli, F., Courtoy, P. J., & David, G. 2005, "Syndecan recycling [corrected] is controlled by syntenin-PIP2 interaction and Arf6", *Dev.Cell*, vol. 9, no. 3, pp. 377-388.